DEPOSITIONAL ENVIRONMENTS OF THE LATE CRETACEOUS (MAASTRICHTIAN) DINOSAUR-BEARING PRINCE CREEK FORMATION: COLVILLE RIVER REGION, NORTH SLOPE, ALASKA

Presented to the Faculty

of the University of Alaska Fairbanks

In Partial Fulfillment of the Requirements

for the Degree of

DOCTOR OF PHILOSOPHY

By

Peter Paul Flaig, B.S., M.S.

Fairbanks, Alaska

May 2010

DEPOSITIONAL ENVIRONMENTS OF THE LATE CRETACEOUS (MAASTRICHTIAN) DINOSAUR-BEARING PRINCE CREEK FORMATION: COLVILLE RIVER REGION, NORTH SLOPE, ALASKA

By

Peter Paul Flaig

RECOMMENDED:

Advisory Committee Chair

Chair, Department of Geology and Geophysics

APPROVED:

Dean, College of Natural Sciences and Mathematics

Dean of the Graduate School

April 20, 2010

Date

Abstract

The Prince Creek Formation contains first-order meandering trunk channels, second-order meandering distributary channels, third-order fixed anastomosed(?) distributary channels, crevasse splays, levees, lakes, ponds, swamps, paleosols, and ashfall deposits. Trampling by dinosaurs is common. Most deposition occurred on crevasse splay-complexes adjacent to trunk channels. Rhythmically-repeating coarse-to fine-grained couplets in inclined heterolithic stratification suggest tidal-influence in channels.

Cumulative to compound soils similar to *Entisols*, *Inceptisols*, and potential acid sulfate soils formed on levees, point bars, crevasse splays, and on the margins of lakes and swamps. Frequent overbank flooding is evidenced by silt and sand dispersed throughout paleosol profiles and fluctuations with depth in several molecular ratios. Drab colors, organics, siderite, depletion coatings, and zoned peds indicate waterlogged, anoxic conditions while ferruginous and manganiferous features, insect and worm burrows, and rare illuvial clay coatings and infillings suggest drying and oxidation of some soils. Repeated wetting and drying is tied to fluctuating river discharge. Marine influence is evidenced by jarosite, pyrite, and gypsum which become increasingly common up-section near the contact with the shallow-marine Schrader Bluff Formation.

Recovered biota include Peridinioid dinocysts; algae; projectates; *Wodehouseia edmontonicola*; pollen from lowland trees, shrubs and herbs; *Bisaccates*; fern and moss spores; and fungal hyphae and indicates that all strata are Early Maastrichtian and that

sediments become progressively younger from measured section NKT in the south to measured section LBB in the north. $^{40}Ar/^{39}Ar$ analysis of a tuff returned an age of 69.2 ± 0.5 Ma in the Sling Point outcrop belt.

World-class dinosaur bonebeds are encased in muddy overbank alluvium overlying floodplains. No concentration of bone was found in channels. Bonebeds are laterally extensive except where truncated by distributaries. At the Sling Pont, Liscomb, and Byers bonebeds alluvium encasing bone exhibits a bipartite division of flow and a massive mudstone facies containing flow-parallel plant fragments that "float" in a mud matrix suggesting deposition by fine-grained hyperconcentrated flows.

Exceptional floods driven by seasonal snowmelt in the Brooks Range increased suspended sediment concentrations, generating hyperconcentrated overbank flows that killed and buried scores of juvenile dinosaurs occupying this high-latitude coastal plain. This unique killing mechanism likely resulted from fluctuating discharge tied to seasonality brought about by the near polar latitude of northern Alaska in the Late Cretaceous.

Table of Contents

Page

List of Figures

List of Tables

List of Appendices

Acknowledgments

I graciously thank the National Science Foundation Office of Polar Programs for grants OPP-425636 to Paul McCarthy and OPP-424594 to Anthony Fiorillo that funded this majority of this project. Thank you Paul McCarthy and Tony Fiorillo for believing in me and trusting me with this big project. It was SO MUCH FUN (he says wagging his tail as he guns the 30HP Mercury)!! Thank you Paul for the wonderful conversations, for the friendship, and for teaching me all that I now know about soils and paleosols, which is SO much more then when I started. Thank you Tony for the dinosaurs, I've loved those bizarre creatures since I was a kid and I can't believe how lucky I am to have seen what I've seen. Thanks to David LePain and Paul Layer for agreeing to be on my committee, for passing on excellent advice and much needed constructive criticism, and for reading my rambling e-mails. Thank you Dolores van der Kolk, my best friend and everything else...for everything... What would I have ever done without you?? HOW MUCH FUN DID WE HAVE! WOOOOHOOOOO! Thanks Larry for the two cabins, man were those GREAT! We sure do miss them! Oh, and thanks for grabbing our mail...in fact...I bet you're still grabbing our mail.

Thanks to the Barrow Arctic Science Consortium (BASC), CH2M Hill (formerly Veco Polar Resources), Wrights Air, Air Logistics, Alaska Air Taxi, Evergreen Helicopters, and the support staff at Umiat, Alaska. Thank you Dolores van der Kolk, Thomas Adams, David Norton, Roland Gangloff, Douglas Hissom, Susi Tomsich, and

Jason Addison for your diligent assistance in the field...it definitely takes a team and we have a great one. Thank you David Houseknecht, Paul Decker, Marwan Wartes, Dick Garrard, and of course Charles "Gil" Mull for many enlightening discussions regarding the evolution of the Colville Basin and the Cretaceous stratigraphy of Alaska...is there anything that you haven't seen up there Gil?

Thank you BP America, Weatherford Laboratories, and Spectrum Petrographics for sample analyses. Thank you Don Triplehorn, Susana Salazar, Maciej Sliwinski, and Jeff Benowitz for assistance in the laboratory.

A big ol' big brother, son, uncle, buddy thank you to my family and friends, man did I need a support group and man did I have one! Everyone...c'mon to Austin, you are the reason we will always have a spare room.

And...Finally, thank you John Isbell- for showing me what it is to be a Sedimentologist.

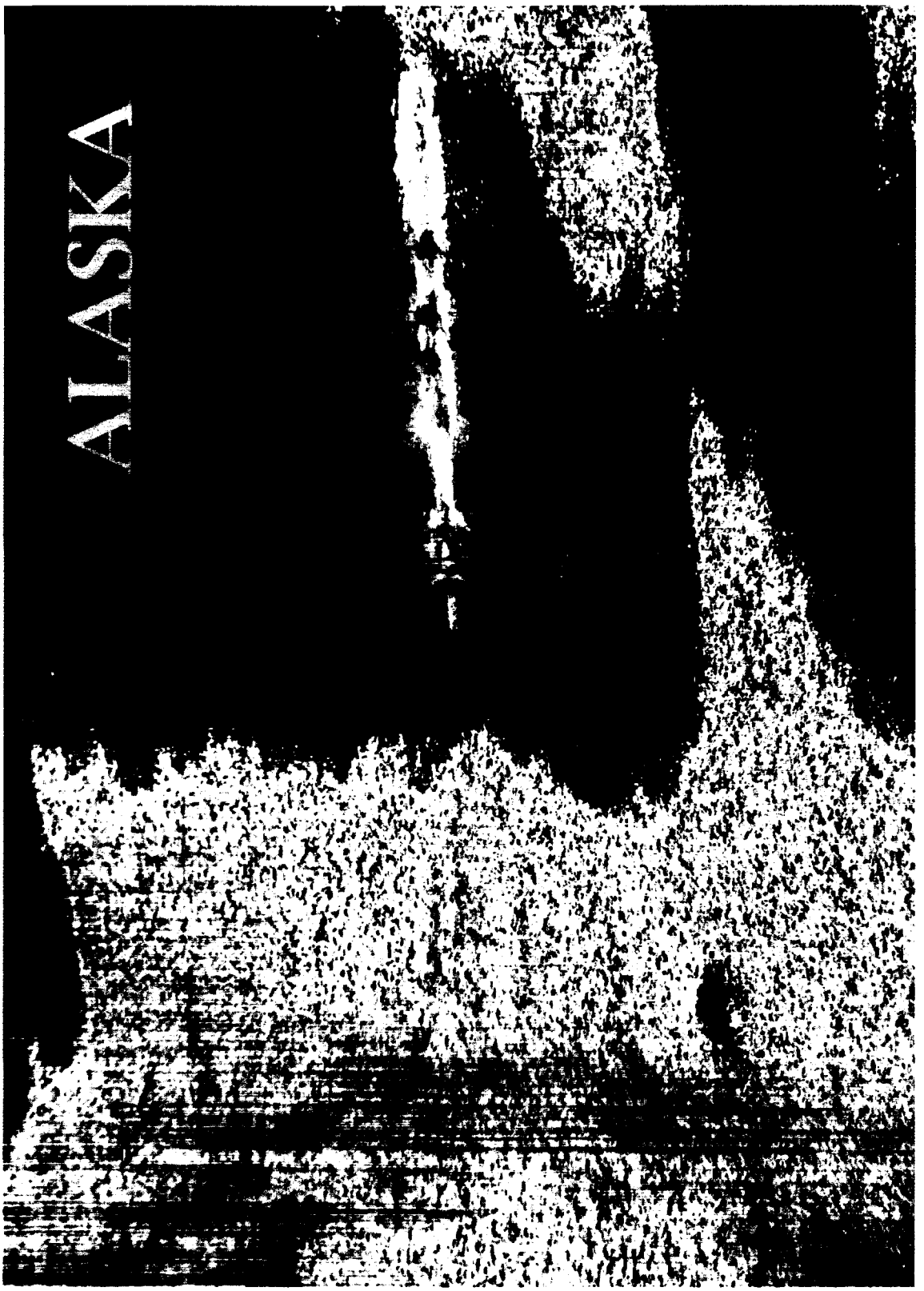
ALASKA

Chapter 1 Introduction

The Prince Creek Formation (Fm.) is a coastal plain succession (Roehler 1987, Mull et al. 2003; Fiorillo et al. 2009, 2010a, 2010b) deposited on the North Slope of Alaska at paleolatitudes as high as 82°-85° N (Brouwers et al. 1987, Witte et al. 1987, Besse and Courtillot 1991, Rich et al. 2002, Spicer and Herman 2010) under Cretaceous greenhouse conditions (Fischer 1981, Parrish et al. 1987, Spicer et al. 1992, Zakharov et al. 1999, Deconto et al. 2000, Spicer 2003, Nordt et al. 2003, Gallagher et al. 2008). The Prince Creek Formation has been of special interest to paleontologists for many years because it contains the densest concentrations of dinosaur bones of any high latitude location in the world (Rich et al., 1997; 2002, Fiorillo et al. 2010a, 2010b). This makes the Prince Creek Formation a rare example of a high-latitude coastal plain upon which Arctic dinosaurs lived and died.

Prior to this investigation, no collaborative paleontological and sedimentological study had been undertaken to generate a comprehensive depositional model for the Prince Creek Formation in the Colville River region. A depositional model for the Prince Creek Formation is very important to both paleontologists and sedimentologists because:

(1) The Prince Creek Fm. preserves within it paleoenvironmental clues necessary to help reconstruct an ancient Arctic dinosaur ecosystem during Cretaceous greenhouse conditions.

(2) Ancient Arctic environments such as this are intrinsically tied to ancient climate. We must study ancient climates to understand natural climate cycles and our current position in them (e.g. there is no modern analogue for warm temperatures under a polar light regime).

(3) A depositional model for this high-latitude Cretaceous coastal plain can be compared and contrasted to models of lower-latitude coastal plains along the Cretaceous Western Interior Seaway of North America and provide insights into the unique features of an arctic "greenhouse" environment.

(4) Oil and gas exploration on the North Slope will benefit from a refined depositional model of the Prince Creek Fm that includes revised facies descriptions, updated sandbody geometries, detailed alluvial architecture, and estimates of the preservation potential of facies. The Prince Creek Fm. can ultimately be used as an example for reservoir geometries expected in high-latitude coastal plain successions.

(5) Paleosols make up a significant portion of Prince Creek Fm. sediments (Fiorillo et al 2010a, 2010b). Analyzing these paleosols gives additional clues to climate, organisms, relief, hydrology, and marine influence on this ancient coastal plain.

(6) A study of Prince Creek Fm. biota can help identify flora and fauna typical of high-latitude Cretaceous floodplains and can help to constrain the age of sediments in northern Alaska. Identifying flora and fauna aids in the

reconstruction of an ancient high-latitude dinosaur ecosystem. Age constraint of sediments on the North Slope is challenging and additional data are welcomed.

(7) The depositional mechanism for emplacement of bonebeds in the Prince Creek Fm. has remained a mystery. A suitable explanation for the deposition and preservation of bonebeds almost exclusively within facies of the Prince Creek Fm. on the North Slope will help paleontologists understand the unique killing mechanism of these Arctic dinosaurs.

The objective of this dissertation is to examine the facies and alluvial architecture of the Prince Creek Formation in bluffs along the Colville, Kogosukruk and Kikiakrorak rivers of northern Alaska in order to: (1) produce a regional depositional model for the Prince Creek Formation in the Colville River region, (2) determine the type of alluvial system(s) responsible for sedimentation, (3) describe the paleosols of the Prince Creek Formation, (4) combine the paleopedological analysis with analysis of biota to identify floodplain pedogenic paleoenvironments and further constrain the age of Prince Creek sediments, (5) describe and correlate facies of the Prince Creek Fm. in bluffs that include the Sling Point, Byers, and Liscomb bonebeds in order to establish the environment(s) of bonebed deposition on the Cretaceous coastal plain, (6) report a new $^{40}Ar/^{39}Ar$ age from a tuff in the Sling Point outcrop belt, and (7) present a depositional model for the emplacement of bonebeds.

This dissertation is organized as a series of manuscripts that describe the unique characteristics of the Prince Creek Formation. Included in this dissertation are three first-authored manuscripts by Peter P. Flaig et al. Although each of the manuscripts includes co-authors, the majority of each manuscript was written by me and the majority of the data presented in each paper was collected by me. Each manuscript was written for publication in a specific journal. The manuscript entitled "A tidally-influenced, high-latitude coastal plain: The Late Cretaceous (Maastrichtian) Prince Creek Formation, North Slope, Alaska" (Chapter 2) is accepted for publication in the SEPM Special Publication: *From River to Rock Record: The Preservation of Fluvial Sediments and their Subsequent Interpretation*. The expected publication date is October, 2010. The manuscript entitled "Anatomy, evolution and paleoenvironmental interpretation of an ancient Arctic coastal plain: Integrated paleopedology and palynology from the Late Cretaceous (Maastrichtian) Prince Creek Formation, North Slope, Alaska, USA" (Chapter 3) will be submitted to the SEPM *Journal of Sedimentary Research* in 2010. The manuscript entitled "Muddy Hyperconcentrated Flows: Dinosaur Killer Crevasse Splays of the Cretaceous Arctic (Prince Creek Formation, northern Alaska)" (Chapter 4) will be submitted to the journal *Palaios* in 2010. A shortened version of this manuscript focusing entirely on sediments encasing the Sling Point, Liscomb, and Byers bonebeds will be submitted to the Geological Society of America journal *Geology* in late 2010 or early 2011. An additional section focusing on the taphonomy of the bonebeds will be incorporated into the final drafts of the *Palaios* and *Geology* manuscripts by Dr. Anthony Fiorillo and is not included in the version of the manuscript in this thesis.

Additional publications in which I am a co-author resulting from investigations in this Dissertation include:

Fiorillo, A.R., Tykoski, R.S., Currie, P.J., McCarthy, P.J., and Flaig, P.P., 2009, Description of two Troodon partial braincases from the Prince Creek Formation (Upper Cretaceous), North Slope, Alaska: Journal of Vertebrate Paleontology, v. 29, No. 1, p. 178-187.

Fiorillo, A.R., McCarthy, P.J., Flaig, P.P., Brandlen, E., Norton, D., Jacobs, L., Zippi, P. and Gangloff, R.A., 2010a, Paleontology and paleoenvironmental interpretation of the Kikak-Tegoseak dinosaur quarry, (Prince Creek Formation: Late Cretaceous), northern Alaska: A multi-disciplinary study of an ancient high-latitude, ceratopsian dinosaur bonebed, *in* Ryan, M.J., Chinner-Algeier, B.J., and Eberth, D.A., eds., New Perspectives on Horned Dinosaurs: The Royall Tyrell Museum Ceratopsian Symposium: Bloomington, IN, Indiana University Press, p. 456-477.

Fiorillo, A. R., McCarthy, P. J., and Flaig, P. P., 2010b, Taphonomic and sedimentologic interpretations of the dinosaur-bearing Upper Cretaceous Prince Creek Formation, Alaska: Insights from an ancient high-latitude terrestrial ecosystem: Palaeogeography, Palaeoclimatology, Palaeoecology, doi:10.1016/j.palaeo.2010.02.029.

Also, a publication for the Alaska Division of Geological and Geophysical Surveys that describes and interprets the Paleocene Prince Creek Fm. along the Toolik River is to be released in 2010:

Flaig, P. P., and van der Kolk, D. A., 2010, Depositional Environments of the Prince Creek Formation along the East Side of the Toolik River: Sagavanirktok Quadrangle, North Slope, Alaska: Alaska Division of Geological & Geophysical Surveys Preliminary Interpretive Report 2009-1, Preliminary Results of field Investigations in the Brooks Range Foothills and North Slope, Alaska.

REFERENCES

Besse, J., and Courtillot, V., 1991, Revised and synthetic apparent polar wander paths of the African, Eurasian, North American and Indian plates, and true polar wander since 200 Ma: Journal of Geophysical Research, v. 96, p. 4029-4050.

Brouwers, E.M., Clemens, W.A., Spicer, R.A., Ager, T.A., Carter, L.D., and Sliter, W.V., 1987, Dinosaurs on the North Slope, Alaska: High latitude, latest Cretaceous environments: Science, v. 25, p. 1608-1610.

Deconto, R.M., Brady, E.C., Bergengren, J., and Hay, W.W., 2000, Late Cretaceous climate, vegetation, and ocean interactions, *in* Huber, B.T., MacLeod, K.G., and Wing, S.L., eds. 2000, Warm Climates in Earth History: Cambridge University Press, Cambridge, UK, p. 275-296.

Fiorillo, A.R., Tykoski, R.S., Currie, P.J., McCarthy, P.J., and Flaig, P.P., 2009, Description of two Troodon partial braincases from the Prince Creek Formation (Upper Cretaceous), North Slope, Alaska: Journal of Vertebrate Paleontology, v. 29, No. 1, p. 178-187.

Fiorillo, A.R., McCarthy, P.J., Flaig, P.P., Brandlen, E., Norton, D., Jacobs, L., Zippi, P. and Gangloff, R.A., 2010a, Paleontology and paleoenvironmental interpretation of the Kikak-Tegoseak dinosaur quarry, (Prince Creek Formation: Late Cretaceous), northern Alaska: A multi-disciplinary study of an ancient high-latitude, ceratopsian dinosaur bonebed, *in* Ryan, M.J., Chinner-Algeier, B.J., and Eberth, D.A., eds., New Perspectives on Horned Dinosaurs: The Royall Tyrell Museum Ceratopsian Symposium: Bloomington, IN, Indiana University Press, p. 456-477.

Fiorillo, A. R., McCarthy, P. J., and Flaig, P. P., 2010b, Taphonomic and sedimentologic interpretations of the dinosaur-bearing Upper Cretaceous Prince Creek Formation, Alaska: Insights from an ancient high-latitude terrestrial ecosystem. Palaeogeography, Palaeoclimatology, Palaeoecology. doi:10.1016/j.palaeo.2010.02.029.

Fischer, A.G., 1981, Climatic oscillations in the biosphere, *in* Nitecki, M.H., ed., Biotic Crisis in Ecological and Evolutionary Time: New York, NY, Academic Press, p. 103-132.

Gallagher, S.J., Wagstaff, B.E., Baird, J.G., Wallace, M.W., and Li, C.L., 2008, Southern high latitude climate variability in the Late Cretaceous greenhouse world: Global and Planetary Change, v. 60, p. 351-364.

Mull, C.G., Houseknecht, D.W., and Bird, K.J., 2003, Revised Cretaceous and Tertiary stratigraphic nomenclature in the Colville Basin, northern Alaska: United States Geological Survey Professional Paper 1673, p. 1-51.

Nordt, L., Atchley, S., and Dworkin, S., 2003, Terrestrial evidence for two greenhouse events in the latest Cretaceous: GSA Today, v. 13, No. 12, p. 4-9.

Parrish, J.M., Parrish, J.T., Hutchison, J.H., and Spicer, R.A., 1987, Late Cretaceous vertebrate fossils from the North Slope of Alaska and implications for dinosaur ecology: Palaios, v. 2, p. 377-389.

Rich, T.H., Gangloff, R.A., and Hammer, W.R. 1997, Polar Dinosaurs, *in* Currie, P.J., and Padian K., eds., Encyclopedia of Dinosaurs: Academic Press, San Diego, California, p. 562-573.

Rich, T.H., Gangloff, R.A., and Hammer, W.H., 2002, Polar Dinosaurs: Science, v. 295, p. 979-980.

Roehler, H.W., 1987, Depositional environments of the coal-bearing and associated formations of Cretaceous age in the National Petroleum Reserve in Alaska: United States Geological Society Bulletin 1575, 16 p.

Spicer, R.A., 2003, Changing climate and biota, *in* Skelton, P., ed., The Cretaceous World: Cambridge, U.K., Cambridge University Press, p. 85-162.

Spicer, R.A., Parrish, J.T., and Grant, P.R., 1992, Evolution of vegetation and coal-forming environments in the Late Cretaceous of the North Slope of Alaska, *in* McCabe, P.J., and Parrish, J.T., eds., Controls on the Distribution and Quality of Cretaceous Coals: Geological Society of America Special Paper 267, p. 177-192.

Spicer, R.A., and Herman, A.B., 2010, the Late Cretaceous environment of the Arctic: A quantitative reassessment based on plant fossils: Palaeogeography, Palaeoclimatology, Palaeoecology, doi: 10.1016/j.palaeo.2010.02.025.

Witte, K.W., Stone, D.B., and Mull, C.G., 1987, Paleomagnetism, paleobotany, and paleogeography of the Cretaceous, North Slope, Alaska, *in* Tailleur, I., and Weimer, P., eds., Alaska North Slope Geology: The Pacific Section, Society of Economic Paleontologists and Mineralogists and the Alaska Geological Society, v. 1, p. 571-579.

Zakharov, Y.D., Boriskina, N.G., Ignatyev, A.V., Tanabe, K., Shigeta, Y., Popov, A.M., Afanasyeva, T.B., and Maeda, H., 1999, Paleotemperature curve for the Late Cretaceous of the northwestern circum-Pacific: Cretaceous Research, v. 20, p. 685-697.

Chapter 2 A tidally-influenced, high-latitude coastal plain: The Late Cretaceous (Maastrichtian) Prince Creek Formation North Slope, Alaska*

Peter P. Flaig, Paul J. McCarthy, and Anthony R. Fiorillo

*Flaig, P. P., McCarthy, P. J., and Fiorillo, A. R., 2009, A tidally-influenced, high-latitude coastal plain: the Late Cretaceous Prince Creek Formation, North Slope, Alaska. Submitted to the SEPM Special Publication "*From River to Rock Record: The Preservation of Fluvial Sediments and their Subsequent Interpretation*"

ABSTRACT

The Prince Creek Formation is a Late Cretaceous, dinosaur-bearing, high-latitude alluvial succession on a coastal plain that crops out along the Colville, Kogosukruk, and Kikiakrorak Rivers of northern Alaska. Studies that document the complex stratigraphy and alluvial architecture of high-latitude fluvial/alluvial systems deposited under greenhouse conditions are extremely rare. It is exceptionally uncommon to find extensive, accessible outcrops that also contain numerous Arctic dinosaur fossils; hence the Prince Creek Formation is not only of great significance to sedimentologists but also to paleontologists involved in reconstructing high-latitude dinosaur habitats.

Maastrichtian strata of the Prince Creek Formation record deposition on a tidally-influenced high-latitude coastal plain within (i) first-order meandering trunk channels, (ii) second-order meandering distributary channels, (iii) third-order fixed (anastomosed?) distributary channels, and (iv) floodplains. Conglomerate and medium-to coarse-grained multi-storey sandbodies are found exclusively within regionally restricted 13-17 m-thick fining-upward successions (FUS) that display inclined heterolithic stratification (IHS) capped by finer-grained, organic-rich facies. These relatively-thick FUS are interpreted as first-order meandering trunk channels. Thinner (2-6 m-thick), single-storey, heterolithic sheet-sandbodies composed predominantly of IHS and including abundant mud-filled channel plugs are the most frequently encountered channel-form. Trough cross-lamination at the base of the IHS records paleoflow at high-angles relative to the dip of the inclined beds, indicating that lateral accretion of point bars was the primary depositional mechanism. These single-storey sandbodies are interpreted as second-order

meandering distributary channels. Fine-grained, 1.5-3.0 m-thick, ripple cross-laminated ribbon sandbodies deposited primarily by vertical accretion above an arcuate erosion surface and containing only minor IHS are interpreted as third-order fixed (anastomosed?) distributary channels. Thinner (0.2-1.0 m-thick) current rippled sheet-sands and silts are interpreted as small-scale crevasse splays and levees. Organic-rich siltstone and mudstone, carbonaceous shale, coal, bentonite, and tuff, are interpreted as deposits of lakes, ponds, swamps, marshes, mires, paleosols, and ashfall on floodplains.

Heterolithic sheet sandstones deposited by small, sinuous meandering distributary channels typically appear lenticular along strike, commonly incise into pre-existing distributary channels, and interfinger with and incise into organic-rich floodplain facies. Fixed, ribbon-form (anastomosed?) distributaries either incise into meandering distributaries or into floodplain facies, with numerous ribbons typically preserved in tiers at the same stratigraphic level. Spatial relationships between channel types, and between channels and floodplain facies, indicate that the bulk of deposition took place on crevasse splay-complexes adjacent to trunk channels. Crevasse splay-complexes were constructed by the lateral migration of sinuous meandering distributaries and the vertical filling of fixed (anastomosed?) distributaries, with splay-complexes separated from each other by organic floodplain facies. Flow within meandering distributaries and fixed (anastomosed?) distributaries may have been contemporaneous. Alternatively, fixed (anastomosed?) distributaries may record the initial and/or waning stages of flow during splay-complex formation and/or abandonment.

IHS composed of rhythmically-repeating, coarse-to-fine couplets of current rippled sandstone or siltstone and mudstone is found within all three types of channels. The rhythmic and repetitive nature of these couplets together with relatively thick, muddy fine-grained members in couplets suggest that flow within channels was likely influenced by tidal effects.

Drab colors in fine-grained sediments, abundant carbonaceous plant material, and common siderite nodules and jarosite suggest widespread reducing conditions on poorly-drained floodplains influenced in more distal areas by marine waters. However, carbonaceous root-traces found ubiquitously within all distributary channels and most floodplain facies along with common Fe-oxide mottles indicate that the alluvial system likely experienced flashy, seasonal, or ephemeral flow and a fluctuating water table. The flashy nature of the alluvial system may have been driven by recurring episodes of vigorous seasonal snowmelt in the Brooks Range orogenic belt as a consequence of the high paleolatitude of northern Alaska in the Late Cretaceous.

INTRODUCTION

The Late Cretaceous (Maastrichtian) Prince Creek Formation is exposed semi-continuously in 20-50 m bluffs along the Colville, Kogosukruk, and Kikiakrorak Rivers in northern Alaska (Figs. 2.1, 2.2). Outcrop exposures of the Prince Creek Fm. have, to date, been primarily the focus of paleontological studies to examine and collect dinosaur specimens because the formation contains the richest concentration of dinosaur bones of any high latitude location in the world (Rich et al. 1997; 2002). Although rigorous documentation of vertebrate and plant fossils of the Prince Creek Fm. has resulted in ground-breaking discoveries regarding Alaskan dinosaurs and biota (e.g. Parrish et al. 1987; Parrish and Spicer 1988; Clemens and Nelms 1993; Fiorillo and Gangloff 2000; Gangloff et al. 2005; Fiorillo et al. 2009, 2010), and although a number of local sedimentologic studies have focused on areas near these vertebrate bonebeds (Phillips 1989, 2003; Brandlen 2008; Fiorillo et al. 2010), no comprehensive regional outcrop study has yet been undertaken. A comprehensive depositional model for the Prince Creek Fm. is required to: (1) place current and future paleontological discoveries in a regional paleoenvironmental and geomorphologic context within which a high-latitude, dinosaur ecosystem thrived during the Late Cretaceous, and (2) improve our understanding of facies relationships, sediment-body geometries, alluvial architecture, and vertical and lateral variations within a high-latitude, coastal plain succession.

The purpose of this paper, therefore, is to examine the facies and alluvial architecture of the Prince Creek Fm. in order to (1) document the various depositional environments, (2) determine the type of alluvial system(s) present, and (3) develop a

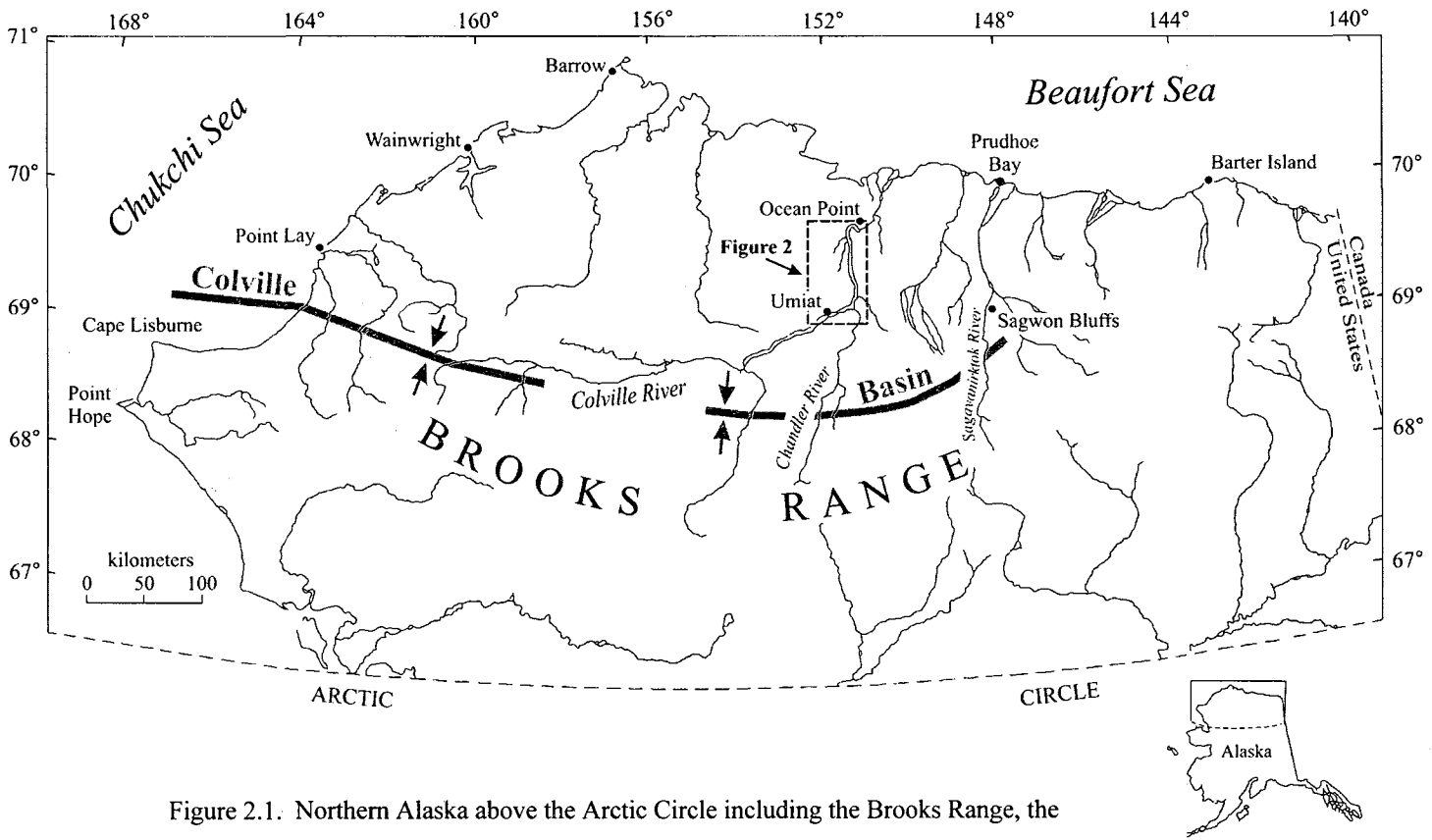

Figure 2.1. Northern Alaska above the Arctic Circle including the Brooks Range, the Colville Basin, and the location of the study area depicted in Figure 2 Modified from Fiorillo and Gangloff 2000, and Bird 2001).

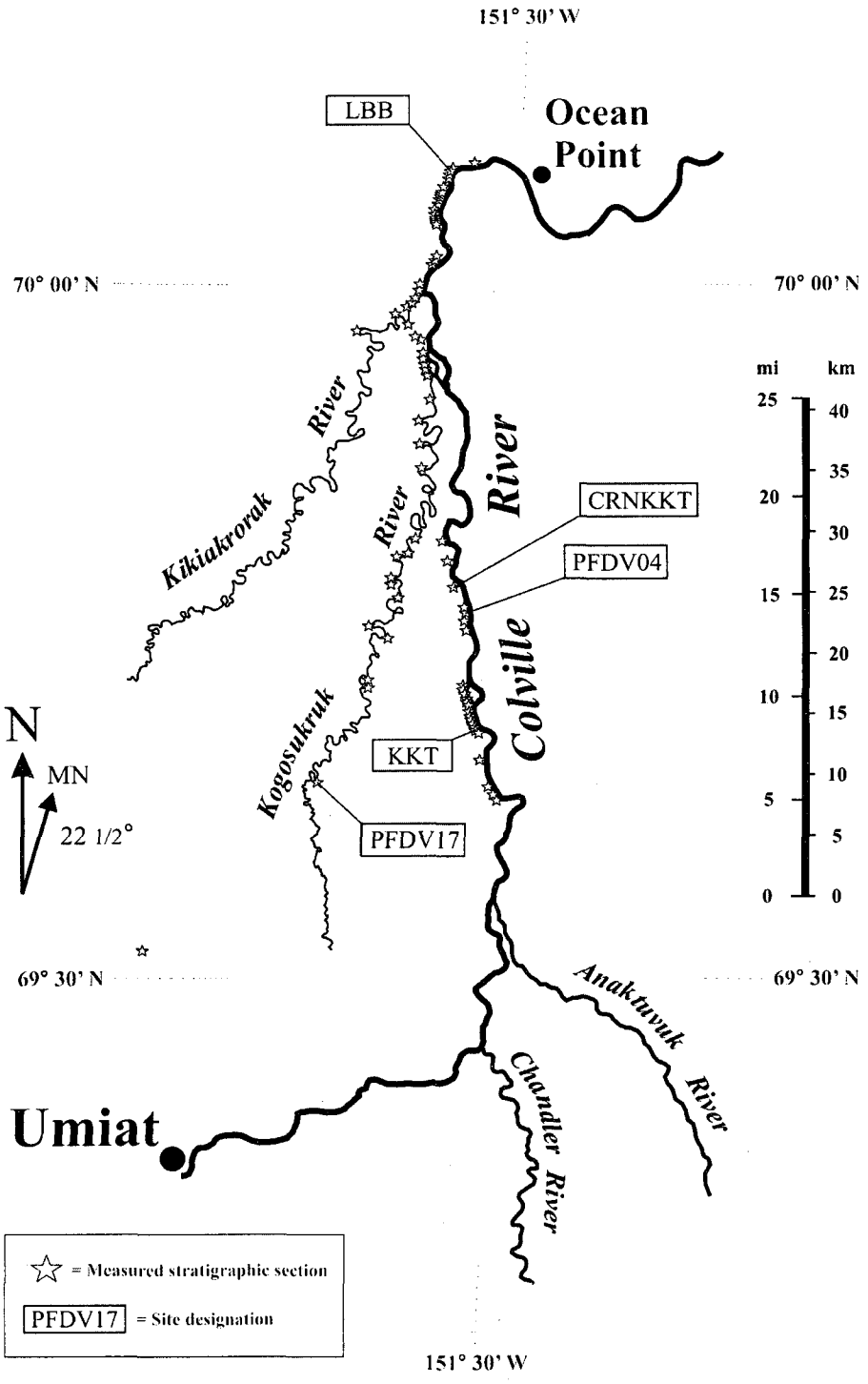

Figure 2.2. Study area including rivers, measured stratigraphic sections, and the location of sites discussed in the text. MN=magnetic north.

depositional model for the Prince Creek Fm. in the Colville River region during the Late Cretaceous.

GEOLOGIC SETTING AND PREVIOUS WORK

The Colville Basin is a foreland basin on the North Slope of Alaska (Fig. 2.1). Jurassic to Early Cretaceous subduction led to northward emplacement of allocthons and uplift of the Brooks Range orogenic belt (Moore et al. 1994). Additional crustal loading in the Aptian/Albian, driven by continued convergence, initiated lithospheric flexure and subsidence to the north of the Brooks Range producing the east-west trending Colville Basin (Moore et al. 1994; Cole et al. 1997). Uplift and erosion of the evolving mountain belt drove sediments from the west into the foredeep resulting in a predominantly axial basin fill (Molenaar 1985; Mull 1985; Moore et al. 1994; Mull et al. 2003; Decker 2007). Additional sediments entered the basin transversely from the south (Moore et al. 1994). The Colville Basin continued to fill throughout the Late Cretaceous and Tertiary, preserving in excess of 4,000 m of sediment in some locations (Molenaar et al. 1987).

The Prince Creek Fm. (Fig. 2.3) is a coastal plain succession composed of conglomerate, sandstone, siltstone, mudstone, carbonaceous shale, coal, bentonite, and tuff (Roehler 1987, Mull et al. 2003; Flores et al. 2007a, 2007b; Fiorillo et al. 2009, 2010). Deposits of the Prince Creek Fm. are the most proximal in a predominantly progradational, Late Cretaceous to Paleocene continental to marine succession that also includes shallow to marginal marine facies of the Schrader Bluff Fm., slope to deepwater

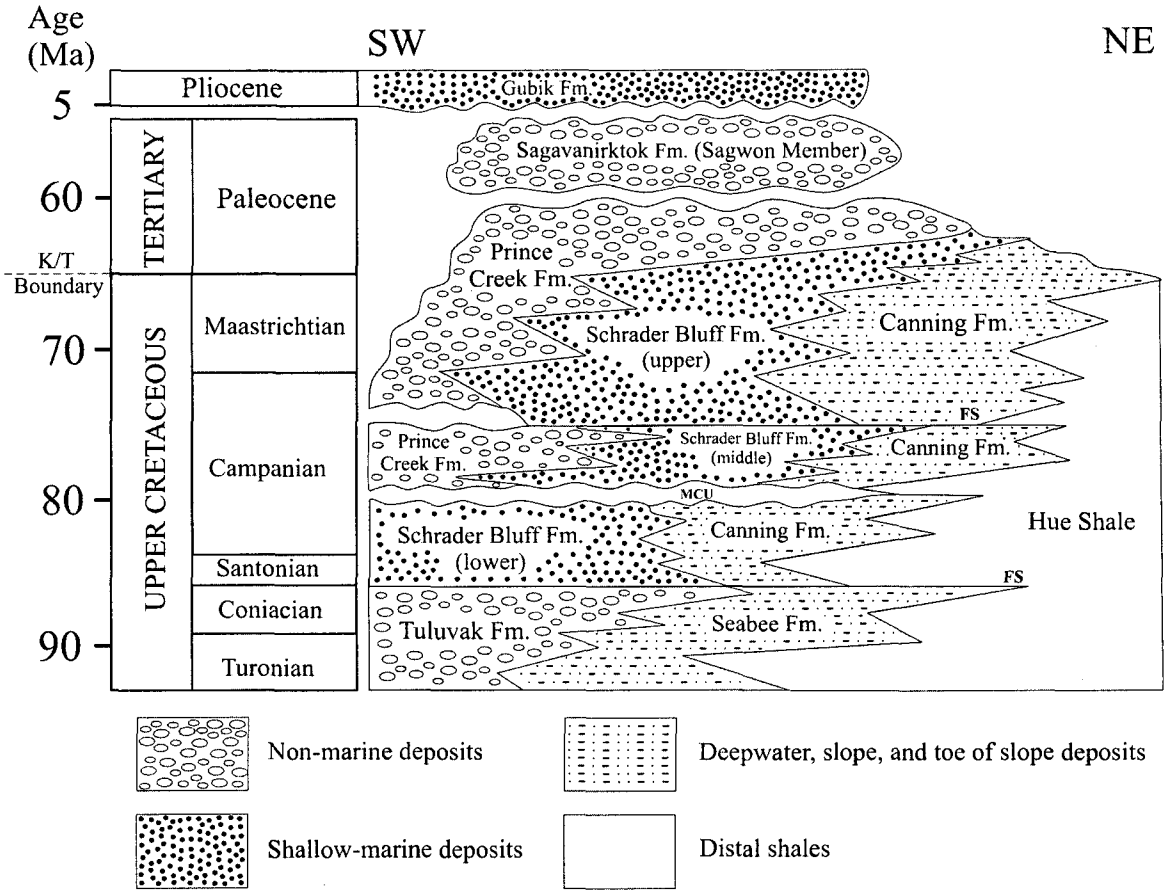

Figure 2.3. Generalized chronostratigraphic column for the central North Slope of Alaska. Abbreviations include: FS (flooding surface), MCU (mid-Campanian unconformity), and K/T, (Cretaceous/Tertiary boundary). Revised from Mull et al. (2003), Garrity et al. (2005), and Decker et al. (in press).

facies of the Canning Fm., and the distal Hue Shale (Fig. 2.3; Mull et al. 2003; Decker 2007). The Prince Creek Fm. was originally sub-divided into two clastic tongues: the Turonian-Coniacian Tuluvak Tongue, and the Campanian-Maastrichtian Kogosukruk Tongue (Gryc et al. 1951). Mull et al. (2003) revised this nomenclature by removing the Tuluvak Tongue from the Prince Creek Fm. and raising the Tuluvak to formation status. The Prince Creek Fm. is now redefined to include only the former Kogosukruk Tongue and Paleocene strata originally assigned to the Sagwon Member of the Sagavanirktok Fm. at Sagwon Bluffs (Figs 1, 3).

No surface exposure containing a complete succession of the Prince Creek Fm. exists (Mull et al. 2003), and the total thickness along the Colville River can only be estimated from outcrop studies at ~ 450 m (Detterman et al. 1963; Brosge et al. 1966). Strata along the Colville River have a gentle structural dip (3° or less) to the northeast and locally contain minor faults and folds. Estimates for depth of burial in the study area from downhole vitrinite reflectance profiles and sonic-porosity logs range from ~2000 to 6000 ft. (Burns et al. 2005).

The entire formation generally fines upward from a conglomeratic base (Flores et al. 2007b) to muddier, finer-grained facies at the top. In surface exposures along the Colville River near the confluence of the Chandler and Anaktuvuk Rivers (Fig 2.2), the base of the Prince Creek Fm. is erosional, with fluvial channel sandstones and conglomerates incised into shallow-marine sandstones of the lower Schrader Bluff Fm. (Mull et al. 2003; Flores et al. 2007b). Locally, this contact is interpreted as an

unconformity beneath an incised paleovalley (Flores et al. 2007a, 2007b) and correlates regionally with a submarine mass wasting and erosion surface (mid-Campanian unconformity of Decker 2007). At Ocean Point (Fig 2.2), the contact between the top of the Prince Creek Fm. and the overlying upper Schrader Bluff Fm. is transgressive between alluvial and interdistributary bay facies of the Prince Creek Fm. and shallow marine shoreface deposits of the upper Schrader Bluff Fm. (Phillips 2003). In our study area, the Prince Creek Fm. is truncated by Pliocene/Pleistocene shoreface sands of the shallow marine Gubik Fm. (Black 1964) or the Holocene unconformity.

Palynomorphs (Frederiksen et al. 1986, 1988, 2002; Frederiksen 1991; Frederiksen and McIntyre 2000; Flores et al. 2007b; Brandlen, 2008; Fiorillo et al. 2010, unpublished data), floral and faunal evidence (Parrish and Spicer 1988; Brouwers and de Deckker 1993), and K/Ar and $^{40}Ar/^{39}Ar$ analyses (Conrad et al. 1990; unpublished data) indicate that the age of the Prince Creek Fm. ranges from Campanian to Paleocene, however, all of the deposits in our study area are Early Maastrichtian (Flores et al. 2007b; Fiorillo et al. 2010, unpublished data).

There is no modern analogue for an ecosystem that experienced relatively warm temperatures under a polar light regime (Spicer 2003). The Late Cretaceous Arctic was nearly devoid of polar ice caps and supported luxuriant high-latitude forests (Spicer et al. 1992; Spicer 2003). Although the present latitude of strata in the study area is ~70^0 N, earlier work suggests that the Prince Creek Fm. may have been deposited at paleolatitudes as high as 67°-85° N (Brouwers et al. 1987; Witte et al. 1987; Besse and

Courtillot 1991; Rich et al. 2002). The Cretaceous was a time of global warmth (Parrish et al. 1987; Zakharov et al. 1999; Spicer et al. 1992; Deconto et al. 2000; Spicer 2003) during a greenhouse period in Earth's history (Fischer 1981; Nordt et al. 2003; Gallagher et al. 2008). Temperature estimates for the North Slope of Alaska during the Late Cretaceous (Maastrichtian) based on megaflora suggest that the warmest month mean was 10-12 °C with a coldest month mean of 2-4 °C (Brouwers et al. 1987). Overall, mean annual temperatures for the North Slope were likely ~5° C (Spicer and Parrish 1987; Parrish and Spicer 1988; Spicer 2003; Fiorillo et al. 2009, 2010). Mean annual precipitation is estimated at between 500 mm a^{-1} and 1500 mm a^{-1} (Spicer and Parrish 1990; Brandlen 2008). These estimates are in contrast to modern records (Haugen 1982; Spicer 2003) indicating a mean annual temperature of -12 °C at Prudhoe Bay and mean annual precipitation of 140 mm a^{-1} at Sagwon Bluffs (Fig. 2.1).

Characteristics of paleosols reveal that the coastal plain was wet with periods of (seasonal?) drying (Brandlen 2008; Fiorillo et al. 2009, 2010). Vegetation consisted mainly of deciduous conifers (*Taxodiaceae)*, pine (*Pinaceae*), horsetails (*Equisetites*), and ferns (*Omundaceae, Polipodiaceae, Cyantheaceae*) (Spicer and Parrish; 1987; Spicer 2003; Brandlen 2008; unpublished data). Abundant charcoal indicates that forest fires were common during periodic dry periods (Spicer and Parrish 1987; Spicer 2003). No evidence of cryoturbation or ground ice has been found in Late Cretaceous sediments or paleosols of the Prince Creek Fm.; however, growth rings and false rings in fossilized wood suggest that limited seasonal freezes probably occurred (Spicer et al. 1992; Spicer 2003). Elevations within the Brooks Range likely exceeded 1500 m, with mean annual

temperatures below 0^0 C at high elevations (Spicer 2003) that likely resulted in at least seasonal snow and ice (Spicer and Parrish 1990; Fiorillo et al. 2009).

METHODS

Fieldwork was conducted along the Colville, Kogosukruk, and Kikiakrorak rivers (Figs. 2.1, 2.2) during July and August 2005-2007. Site selection was limited to exposures from immediately south of the Kikak-Tegoseak dinosaur quarry to northeast of the Liscomb dinosaur quarry (KKT and LBB in Fig. 2.2) in order to avoid duplication of previous work on the Prince Creek Fm. (Phillips 2003; Flores et al. 2007b)

Sites were selected in order to obtain a representative sample of the regional stratigraphy and on the basis of accessibility of outcrop, complexity of alluvial architecture, observable flora and fauna, and regional geographic and stratigraphic relationships. 75 measured sections, including detailed descriptions of grain size, lithology, contacts, sedimentary structures, flora, fauna, and vertical and lateral facies relationships form the data set for this paper (Fig. 2.2). All exposures were photographed to generate photomosaics that were modified into interpretive line-drawings of alluvial architecture. Interpreted photomosaics were compared with measured sections, paleoflow orientations, and hand samples for consistency during architectural analysis and paleoenvironmental interpretation.

FACIES AND FACIES ASSOCIATIONS

Thirteen facies are defined on the basis of grain size, thickness, sedimentary structures, the nature of upper and lower contacts, and flora and fauna (Table 2.1). These thirteen facies define four facies associations (FA) on the basis of facies relationships and stacking patterns (Table 2.2, Fig. 2.4). Facies associations record sediment deposition within three distinct types of channels (FA-I, FA-II, FA-III) and on floodplains (FA-IV).

Facies Association I: Large Sinuous Channels

FA-I is an erosive-based, 13-17 m-thick succession that fines-upward from a basal conglomerate and medium-grained multi-storey sandbody through an interval of IHS into carbonaceous shale, coal, and mudstone (Fig. 2.5A). FA-I consists of a combination of facies that may include F-1, F-2a, F-3, F-6a, F-6b, F-7a, F-7b, F8, and F-9 (Tables 2.1, 2.2; Fig. 2.4).

At the base of each FUS in FA-I is a 0.2-0.5 m-thick conglomerate lag (F-1; Fig. 2.5B). The basal surface of the conglomerate is erosional with relief of up to 13 m or more. The succession fines upward from F-1 into a 7-9 m-thick, medium-grained, multi-storey sandbody (F-2a, Fig. 2.5A) containing cosets of trough cross-lamination with individual sets averaging 0.5 m thick (Fig. 2.5C). Sandbodies of FA-I are conspicuously devoid of root-traces and invertebrate fossils but contain convolute bedding (Fig. 2.5D), scour-and- fill structures, spherical mudstone balls, and coalified wood (Fig. 2.5E).

Table 2.1. Description and interpretation of the thirteen facies identified in the Prince Creek Formation, North Slope, Alaska

Facies		Thickness	Contacts	Physical Sedimentary Structures & Minerals	Flora / Fauna	Grain Size & Sediment Texture	Depositional Environment	Occurrence
F-1 Conglomerate		< 0.5 m	Basal Erosional Upper Gradational	Common Quartz/chert pebbles, cobbles, and boulders up to 30 cm long along longest axis, trough cross-laminations, mud/coal rip-up clasts	Common Carbonized or silicified wood fragments and plant fragments, wood impressions, silicified vertebrate bone fragments, coalified logs.	Clast-to matrix supported. Well-rounded pebble-to boulder-sized clasts of quartz, chert and minor quartzite rock fragments. Matrix of medium- to coarse-grained sub-rounded to sub-angular quartz & chert rich sand.	Channel thalweg highest-energy bedload transport deposit.	Found only at base of FA-I
F-2 Trough cross-laminated Medium-to fine-grained sandstone	**F-2a** Medium-grained	2.0-9.0 m	Basal Erosional to gradational Upper Gradational	Common Multi-storey trough cross-laminations, ripple cross-laminations, mud/coal rip-up clasts, mud-balls, siderite nodules, convolute bedding. Rare Cut and fill structures. Tuffaceous concretions, quartz/chert pebbles	Common Silicified/ carbonized wood/plant fragments, wood impressions, silicified vertebrate bone fragments. Rare Silicified/ coalified logs, tree stumps (max.dia. 18 cm). Vertebrate bone up to 0.5 m long	Medium-grained, moderately well-sorted sub-rounded to sub-angular quartz & chert rich sand.	3-D dunes deposited in channel thalweg on point bar toes.	FA-I above F-1
	F-2b Fine-grained	0.3-1.0 m	Basal Erosional to gradational Upper Gradational	Similar to F-2a but Trough cross-laminations are single-storey	Same as F-2a except no large vertebrate bone, logs, or stumps	Moderately well-sorted, sub-rounded to sub-angular quartz & chert rich fine-grained sand.	Same as F-2a but found in smaller channels	At base of FA-II and very rarely FA III

Table 2.1 cont. Description and interpretation of the thirteen facies identified in the Prince Creek Formation, North Slope, Alaska

F-3 Very-fine to fine-grained heterolithic ripple-cross-laminated sandstone, siltstone and mudstone	1.5-6.0 m	Basal Erosional Upper Sharp to gradational	Common Sand-mud or silt-mud couplets (IHS), ripples, reddish-orange mottles, siderite/carbonate concretions, jarosite. Paleoflow indicators at high angles to dip of inclined beds Rare Mud/coal rip-up clasts. Tuffaceous concretions	Common Roots (range from 5-30 cm-long and .02-2 cm-diameter). Carbonized wood and plant fragments, coalified/silicified logs (max. dia. 20 cm).	Alternating cm-to-dm scale couplets of fine-grained sand and silt/mud	Laterally-accreting point bars in meandering channel fill successions	Above F-2 in both FA-I and FA II and at the top of FA-III
F-4 Very-fine to fine-grained *ripple cross-laminated* to massive sandstone	0.05-3.0 m	Basal Erosional to gradational *or disturbed* Upper Sharp to gradational or disturbed	Common Ripples, reddish-orange mottles, siderite nodules *mud-drapes on ripples* Rare Soft sediment deformation, rip-up clasts, carbonate concretions, tuffaceous concretions, jarosite, burrows (<15 mm dia.)	Common Carbonized roots up to 30 cm long, Carbonized *wood and plant fragments.* Rare Silicified vertebrate bone and bone fragments, logs, clams, gastropods	Typically composed of homolithic very fine-grained sand. May contain glass *shards and may weather* white.	Anastomosed channel fill and small-scale crevasse splays	At base of FA-III and in FA-IV
F-5 Very-fine to fine-grained plane parallel-laminated sandstone/ siltstone	0.2-1.5 m	Basal Sharp to gradational Upper Sharp to gradational	Common Plane-parallel stratification. Primary current and parting lineation. Rare Ripples, jarosite	Common Carbonized wood and plant fragments	Alternating poorly-sorted very fine-grained sand and organic silt	Channel-proximal levees and sandy lakes	FA-IV

Table 2.1 cont. Description and interpretation of the thirteen facies identified in the Prince Creek Formation, North Slope, Alaska

F-6 Siltstone	**F-6a** Extremely rare to absent root-traces	0.6-5.0 m	Basal Sharp to gradational, Upper Sharp to gradational	Common Ripples Rare Siderite nodules, burrows (<15 mm dia.), jarosite, vivianite	Common Carbonized or silicified wood and plant fragments, coalified logs, Rare Clams, gastropods	Predominantly silt with interspersed clay sized particles and organic material	Deepest floodplain lakes (e.g. oxbow lakes) and large channel abandonment (point bar)	FA-IV and upper FA-I
	F-6b Common root-traces	0.1-8.0 m	Basal Sharp to gradational, Upper Sharp to gradational or disturbed	Common Reddish-orange mottles, siderite nodules, jarosite, vivianite Rare Ripples, tuffaceous concretions	Common Carbonaceous root traces, carbonized or silicified wood and plant fragments. Rare Silicified vertebrate bones and bone fragments, pelecypods, gastropods, amber, burrows	Similar to F-6a but includes both macroscopic and microscopic vertically-oriented, branching carbonaceous root-traces	Distal levees, distal crevasse splays, lake margins, paleosols	FA-IV and near top of FUS in FA-I and FA-II
F-7 Mudstone	**F-7a** Extremely rare to absent root-traces	0.5-2.0 m	Basal Sharp to gradational, or disturbed Upper Sharp to gradational or disturbed	Common Reddish-orange to-yellow mottles (to 10 cm diameter), jarosite, vivianite	Common Carbonized plant fragments Rare Clams, gastropods, burrows, bioturbation	Massive mudstone with interspersed organics	Shallow floodplain lakes/ponds and some channel abandonment successions (point bar)	FA-IV and near top of FUS in FA-I, FA-II, and FA-III
	F-7b Aggregated (blocky or platy), with common roots	0.5-4.0 m	Basal Sharp to gradational, or disturbed Upper Sharp to gradational or disturbed	Common Reddish-orange to-yellow mottles, siderite nodules, carbonate concretions Rare Tuffaceous concretions, jarosite	Common Roots (range from 1-20 cm-long and .01-.5cm-thick), carbonized plant fragments	Mudstone with a blocky/platy structure and interspersed organics	Paleosols	FA-IV and top of FUS in FA-I and FA-II

Table 2.1 cont. Description and interpretation of the thirteen facies identified in the Prince Creek Formation, North Slope, Alaska

F-8 Carbonaceous Shale	0.1-2.0 m	Basal Sharp to gradational, disturbed Upper Sharp to gradational	Common Jarosite	Common Carbonized wood and plant fragments, coalified logs. Rare amber	Clay with shale-partings.	Mires	FA-IV and near top of FUS in FA-I and FA II
F-9 Coal	0.1-0.8 m	Basal Sharp to gradational, Upper Sharp to gradational	Common Mud interbeds, jarosite	Common Carbonized wood and plant fragments, coalified logs	Composed entirely of carbonized plant fragments. Brittle with common vitreous luster.	Backswamps	FA-IV and near top of FUS in FA-I and FA-II
F-10 Tuff/Bentonite	0.05-0.3 m	Basal Sharp or disturbed Upper Sharp or disturbed	Lacks sedimentary structures. Basal contact is frequently disturbed.	Large roots up to 30 cm long and 5 cm diameter. May contain embedded carbonaceous plant or wood fragments	Massive. Composed of mix of unaltered/altered glass shards and clay. Weathers white or light green.	Ashfall deposits	FA-IV

Table 2.2. Description and interpretation of the four facies associations identified in the Prince Creek Formation.

Facies Association	Paleo-environment	Inclusive Facies	Diagnostic Features	Occurrence
FA-I	Large Sinuous Channel	F-1,F-2a, F-3, F-6a, F-6b, F-7a, F-7b, F8, F-9	13-17 m-thick fining-upward succession capped by organic shale, coal, or paleosol	Regionally-restricted FUS deposited within larger meandering channels
FA-II	Small Sinuous Channel	F-2b, F-3, F-6b, F-7a, F-7b, F-8, F-9	2 to 7-m-thick fining-upward succession. Lenticular sandbody containing inclined heterolithic stratification (IHS) indicative of lateral accretion. Abundant mud-filled abandoned channels. Often capped by thin (< 1m-thick) organic shale, coal, or paleosol.	Most common type of channel deposit. Deposited in small meandering channels. Often associated with FA-III. Interdigitates with FA-IV.
FA-III	Small Low-sinuosity Channel	F-2b, F-3, F-4, F-7a, F-7b, F-8	1 to 3-m-thick concave-up ribbon-form channel. IHS may occur within top 0.5 m. Deposits indicate primary vertical accretion and minor lateral accretion.	Frequent deposit of small fixed crevasse channels. May incise into FA-II or FA-IV.
FA-IV	Interbedded Floodplain Sand, Silt, and Mud	F-4, F-5, F-6a, F-6b, F-7a, F-7b, F-8, F-9, F-10	Variable thickness. Contains the bulk of the fine-grained sediments in the study area. Often found as laterally-extensive organic successions encasing FA-I, FA-II, and FA-III	Extremely common. Includes all overbank sedimentation, abandoned channel fill, and soil-forming environments

Figure 2.4 (Following 2 Pages). Idealized measured sections for the 4 facies associations of the Prince Creek Formation in the Colville River region. Facies Association-I (FA-I), Large Sinuous Channels; FA-II, Small Sinuous Channels; FA-III, Small Low-sinuosity Channels; and FA-IV, Interbedded Sandstone, Siltstone, and Mudstone. Detailed descriptions of individual facies and facies associations are given in Tables 2.1 and 2.2.

Key


Conglomerate

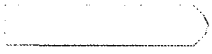
Sandstone


Siltstone


Mudstone


Carbonaceous Shale


Coal


Bentonite

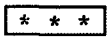
Tuff

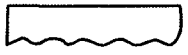
Erosional Contact

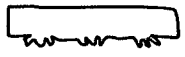
Trampled Contact


Trough Cross-lamination

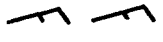
Ripple Cross-lamination

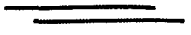
Horizontal Lamination


Convolute bedding

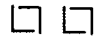
Blocky structure

Boulders

Cobbles

Pebbles

Coal rip-up-clasts

Mud rip-up-clasts

Mud balls


Root Traces


Leaf/Plant Fragments


Coalified/Silicified Log


Wood Impressions


Tree stump


Vertebrate bone


Vertebrate bone fragments


Invertebrates


Burrows

Siderite Concretions

Carbonate Concretions

Tuffaceous Concretions


Mottles

J Jarosite

P Pyrite

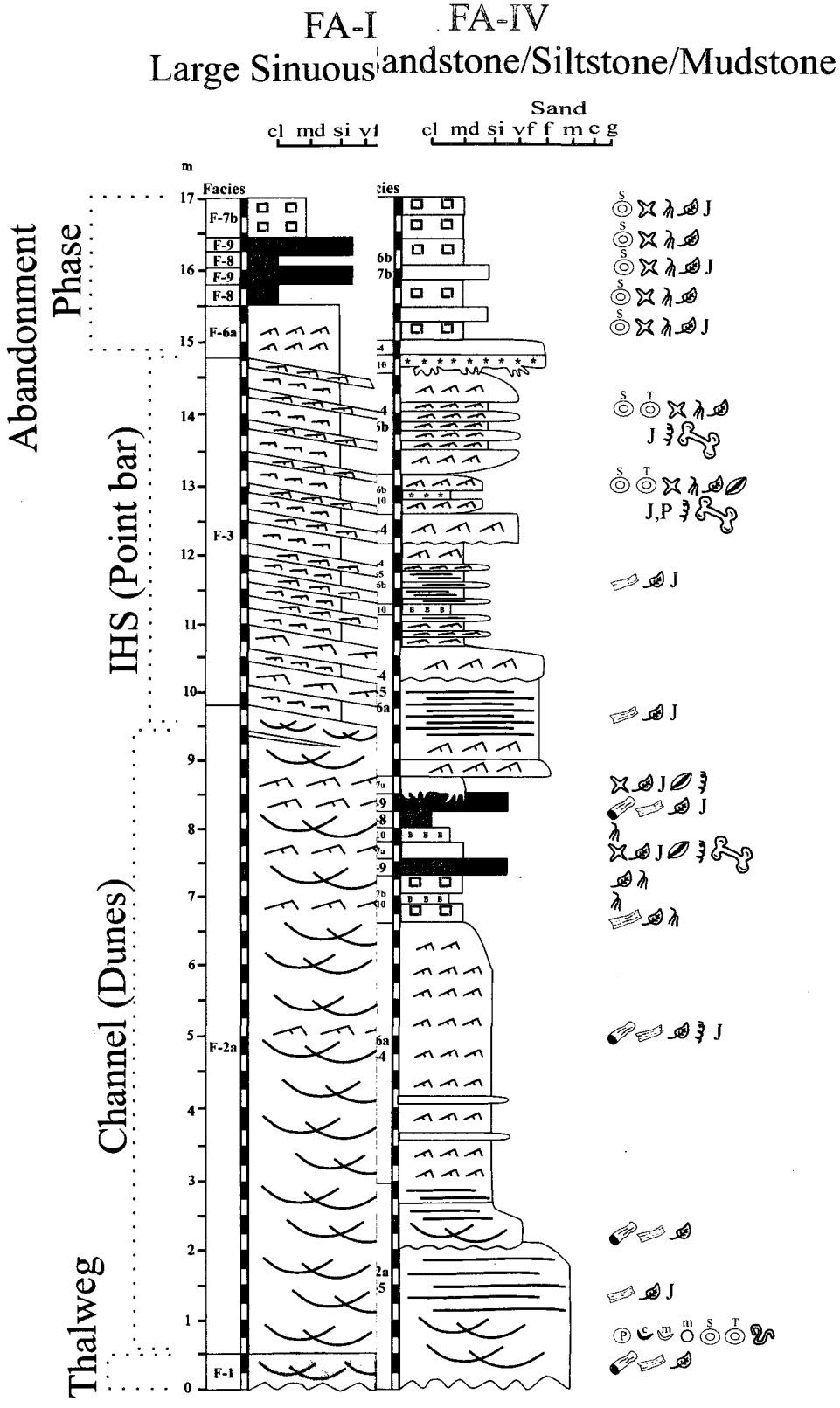
FA-I
FA-IV
Large Sinuous
andstone/Siltstone/Mudstone
Sand
cl md si vf
cl md si vf f m c g
m
Facies
F-7b
F-9
F-8
F-9
F-8
F-6a
F-3
F-2a
F-1
Abandonment Phase
IHS (Point bar)
Channel (Dunes)
Thalweg
J
J,P

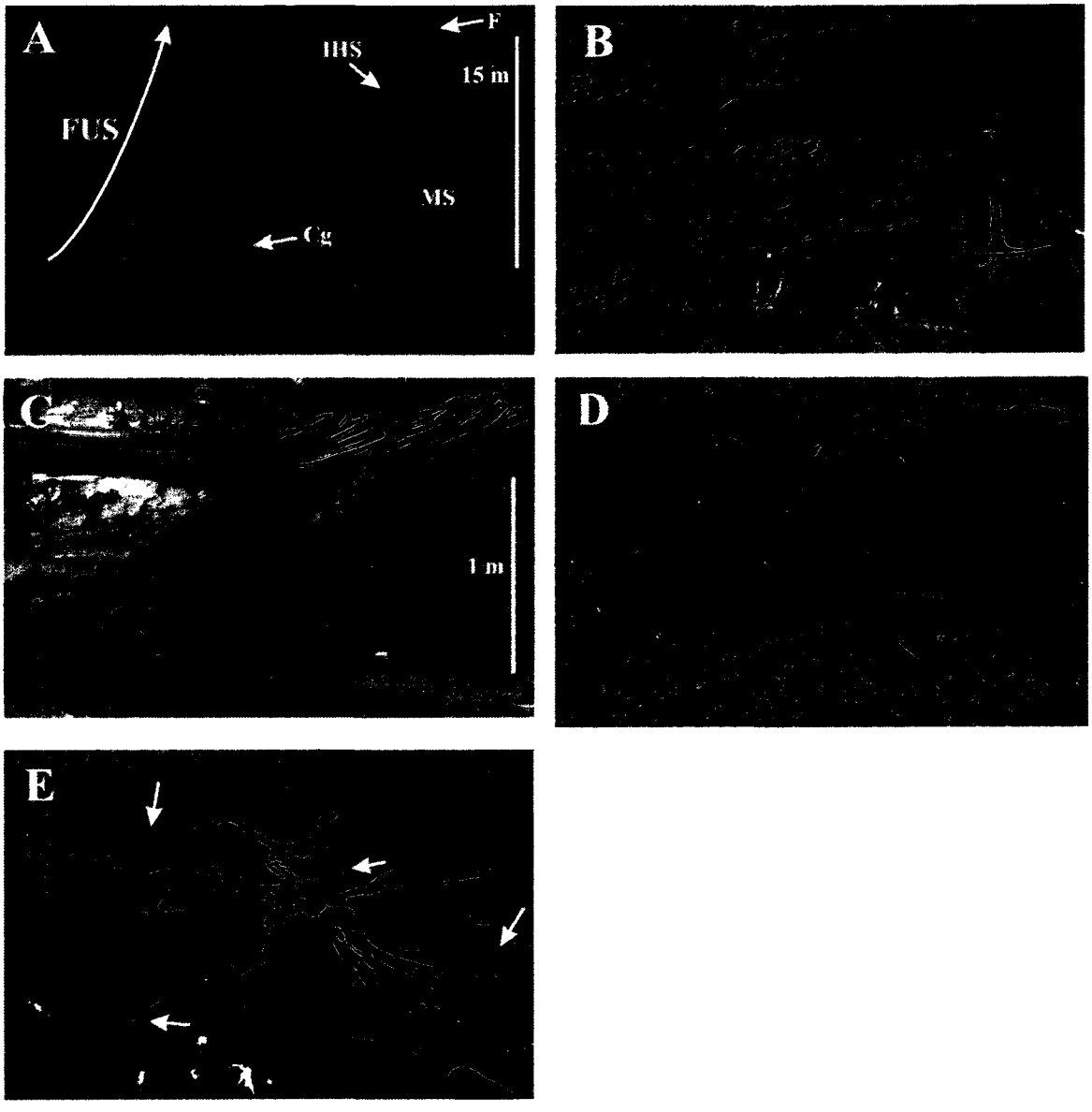

Figure 2.5. Facies, physical sedimentary structures, flora, and fauna typical of FA-I (Large Sinuous Channels). A) Complete fining-upward succession (FUS) including coarse-grained conglomeratic base (Cg), multi-storey medium-grained sandbody (MS), inclined heterolithic stratification (IHS), and fine-grained top (F); B) pebble-to-cobble conglomerate; C) cross-bed coset composed of 0.5 m-thick sets of trough cross-lamination; D) convolute bedding; and E) carbonized tree (18 cm diam.) with roots and (arrows) spherical mudstone balls Hammer is 30 cm long.

F-2a grades upward into 2-5 m of IHS (F-3; Fig. 2.5A). Inclined beds within the IHS dip at angles of 5-10° and tangentially onlap the top of F-2a (Fig. 2.5A). Paleoflow recorded from trough cross-laminations within the IHS is typically at a high angle to the dip direction of the inclined beds. The heterolithic succession passes gradationally upward into a 3-4 m-thick succession of finer-grained facies that typically includes ripple cross-laminated to massive rooted siltstone (F-6b), blocky, rooted mudstone (F-7b), carbonaceous shale (F-8), and coal (F-9).

Interpretation.-

The FUS of FA-I is interpreted as the channel thalweg and point bar deposits of large, sinuous, suspended-load meandering channels (*sensu* Allen 1964, 1965a, b, 1970; Schumm 1968, 1985; Leeder 1973; Elliott 1976; Smith 1987, 1988). Erosively based, fining upward successions containing basal lags, trough cross-laminated sandbodies, lateral accretion surfaces, and fine-grained upper facies are typical of meandering systems (Allen 1965a, 1970; Elliott 1976; Walker 1979; Nanson 1980; Ethridge et al. 1981; Smith 1987; Choi et al. 2004). Conglomerate lags on scoured surfaces in FUS are commonly interpreted as channel thalweg deposits (Allen 1964, 1965b, 1970; Nanson 1980; Plint 1983). Sets of trough cross-lamination record 3-D dune migration along the bed of the channel (Allen 1963, 1965b; Elliott 1976; Plint 1983; Choi et al. 2004). The multi-storey nature of the channel fill reflects scouring within the channel during flooding events and bar-form migration (Elliott 1976, Gibling 2006, McLaurin and Steel 2007).

IHS dipping normal, or at high angles to paleoflow is interpreted as lateral accretion surfaces on point bars that record the migration of the channel as it wandered across the floodplain (Allen 1963, 1965a; Elliott 1976; Collinson 1978; Nanson 1980; Thomas et al. 1987). Convolute bedding within sandbodies indicates high sedimentation rates with shearing of sediments by current drag while the sediments were still liquefied (Banks 1973). Scour-and-fill structures are interpreted as chute channels on point bars (Plint 1983). Spherical mudstone-balls form in channels with high suspended sediment concentrations by the erosion of both mud drapes on point bars and fine-grained channel margins (Baker et al. 1995; Dalrymple and Choi 2007). Large Sinuous Channels are interpreted as suspended load channels on the basis of relatively high concentrations of mud in the upper portion of FUS and thick mud drapes on point bar surfaces (Schumm 1968; Stewart 1983). Drifted logs, leaves, wood, and plant fragments are common in point bar sands (Allen 1965b). Finer-grained facies (F-6b, F-7a, F-7b, F-8, F-9) record vertical accretion at the top of point bars at shallow depths and low bed shear stresses (Allen 1965a, 1970; Elliott 1976; Nanson 1980). The absence of root traces within sandbodies and the IHS of FA-I suggest that these larger channels experienced continuous flow conditions which did not allow vegetation to root in these relatively deep channels.

Facies Association II: Small Sinuous Channels

FA-II is a 2.0-6.0 m-thick FUS composed predominantly of a single-storey, 1.5-5.0 m-thick sandbody dominated by IHS (Fig. 2.6A). FA-II contains a combination of facies which may include F-2b, F-3, F-6b, F-7a, F-7b, F-8, and F-9 (Tables 2.1, 2.2; Fig.2.4).

The base of FA-II is erosional with relief of up to 6.0 m (Figs. 2.6A, 2.6B, 2.6D) and there is no conglomerate above the basal erosion surface. Instead, fine-grained, trough cross-laminated sandstone (F-2b), 0.3-1.0 m-thick and commonly containing coalified wood and mudstone clasts, is typically found at the base (Figs. 2.6A, 2.6B, 2.6C). Crossbed set thicknesses average 0.2 m. The thickness of this cross-bedded sand is highly variable and it may be locally absent; however, where present it is thinner and finer-grained than the medium-grained sandbody (F2a) found near the base of Large Sinuous Channels (FA-I, Fig. 2.5A).

Lying gradationally above this sand or directly above the basal erosion surface is a 1.5-5.0 m-thick FUS succession of IHS (F-3; Figs. 2.6A, 2.6D). The inclined beds that make up the IHS generally appear to dip at higher angles (max. 20°) than the IHS in Large Sinuous Channels (FA-I) (max. 10°). Both the coarse and fine members of IHS couplets in FA-II contain abundant vertical to sub-horizontal root-traces up to 30 cm long and 2.0 cm in diameter (Figs. 2.6E, 2.6F). The IHS typically passes gradationally upward into a thin (< 0.5 m) succession of rooted mudstone (F-7b), carbonaceous shale (F-8), and coal (F-9). In many instances the entire IHS succession grades laterally into an

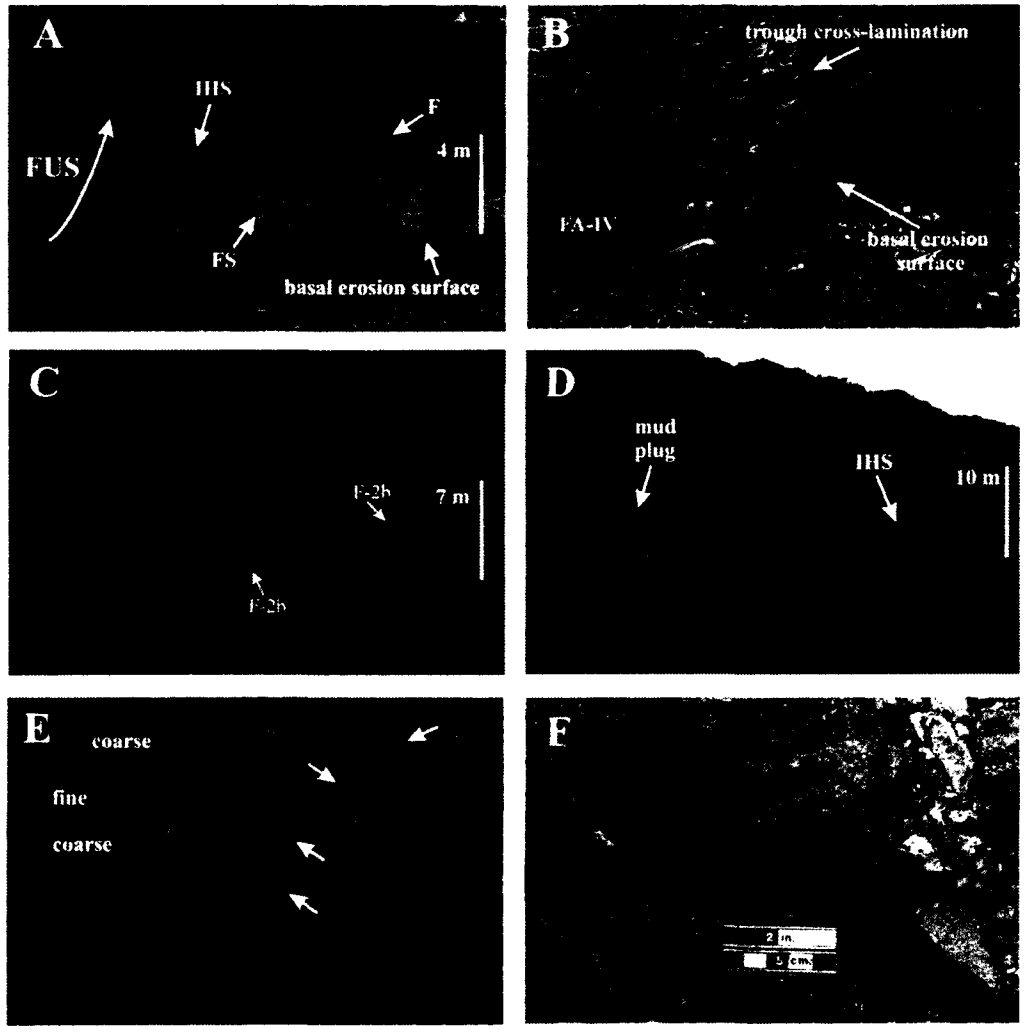

Figure 2.6. Facies, physical sedimentary structures, and flora typical of FA-II (Small Sinuous Channels). A) Complete fining-upward succession (FUS) including basal erosion surface, fine-grained sand base (FS), inclined heterolithic stratification (IHS), and fine-grained top (F); B) trough cross-lamination within a fine-grained sandbody in erosional contact with floodplain deposits of FA-IV; C) stacked channels with apparent dips in opposing directions, the stratigraphically lower channel contains coarse-members of inclined heterolithic stratification (IHS) that thicken down-dip and merge with trough cross-laminated sand (F-2b); D) IHS grading laterally into mud-filled channel plug; E) alternating coarse and fine members of IHS couplets containing vertical carbonized roots (arrows), and F) carbonized root 15 cm long and 0.5 cm in diameter exhibiting horizontal and vertical growth as well as branching. Pocket knife is 9 cm long.

asymmetrical, trough-shaped feature filled with rooted mudstone and siltstone overlying a concave-up erosion surface (Fig. 2.6D).

Interpretation.-

The FUS of FA-II is interpreted as point bar deposits of small, sinuous meandering channels. These channels also carried the majority of their sediment in suspension and are interpreted as suspended-load streams (Schumm 1968). Meandering is evidenced by prominent IHS with paleoflow orientations at high angles to the dip of inclined beds, indicating lateral accretion of channels (Allen 1963; Collinson 1978; Thomas et al. 1987). Fine-grained facies at the top of FA-II record vertical accretion at the top of point bars (F-6b, F-7a, F-7b, F-8, F-9). Asymmetrical, trough-shaped features filled with rooted and current-rippled organic-rich siltstone and mudstone are similar in geometry, lithology, and facies relationships to mud-filled abandoned channels formed during neck cutoff (Fisk 1944; Collinson 1978; Chevren 1978; Ethridge et al. 1981; Plint 1983). Mud-filled abandoned channels and laterally extensive point bar deposits are common in sinuous meandering systems (Allen 1965b; Schumm 1985; Miall 1985).

Facies Association III: Small Low-sinuosity Channels

FA-III is composed of a FUS that is thinner than the majority of FUS of

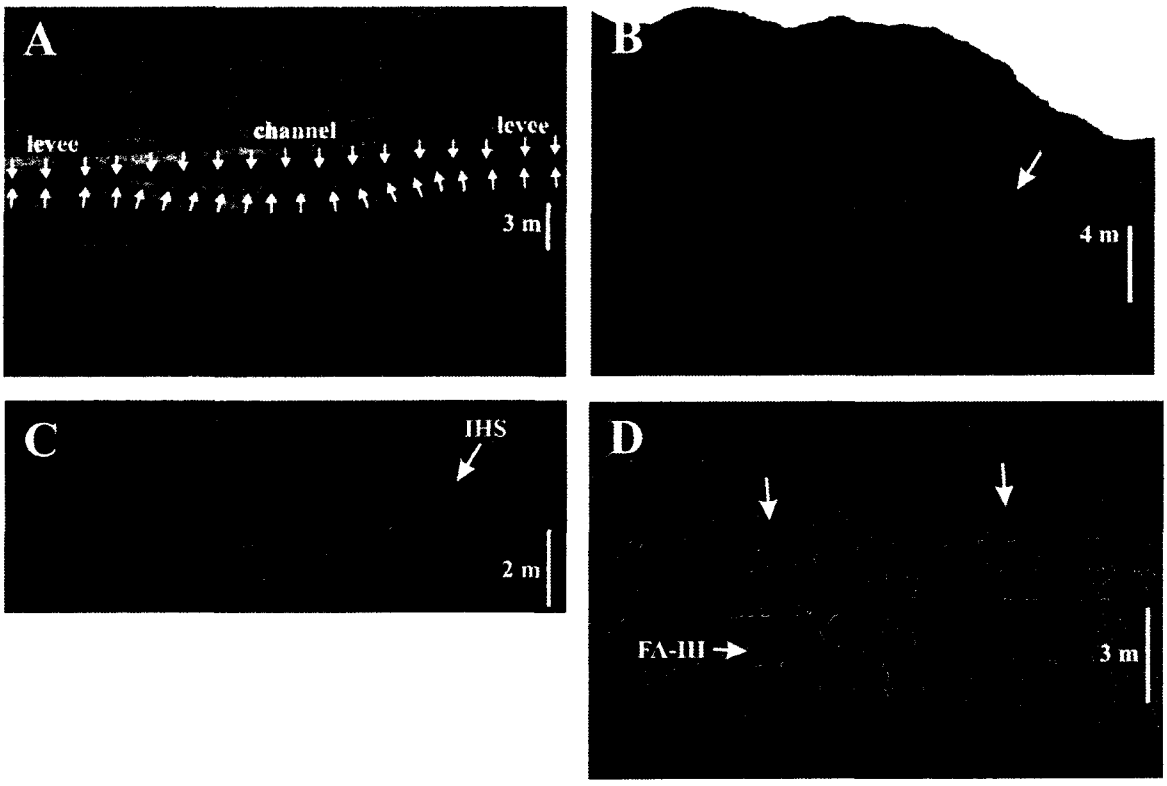

Figure 2.7. Facies and physical sedimentary structures typical of FA-III (Small Low-sinuosity Channels) A) channel-form (outlined by arrows) displaying arcuate shape and "wings" interpreted as channel-attached levees; B) channel (arrow) encased in floodplain facies of FA-IV; C) Small Low-sinuosity Channel (FA-III) including minor inclined heterolithic stratification (IHS) at the top of the channel-fill sequence incised into a Small Sinuous Channel of FA-II; and D) Small Low-sinuosity Channel (FA-III) containing two smaller channels (arrows) incised into the top of the channel-fill sequence, image also includes a Small Sinuous Channel (FA-II).

Small Sinuous Channels (FA-II) and considerably thinner than those of Large Sinuous Channels (FA-I). Small Low-sinuosity Channels of FA-III are dominated by a current rippled sandbody overlying an arcuate, concave-up erosional base. FA-III contains a limited number of facies including F-2b (extremely rare), F-3, F-4, F-7a, F-7b, and F-8 (Tables 2.1, 2.2; Fig. 2.4).

FA-III is composed predominantly of a single-storey, 1.5-3.0 m-thick, very-fine to fine-grained sandbody (F-4) that sits atop a concave-up basal erosion surface with relief of up to 3 m (Figs. 2.7A, 2.7B). Ripple cross-lamination is the primary sedimentary structure although, rarely, trough-cross laminated sand (F-2b) can be found between the current rippled sand (F-4) and the erosion surface. These sandbodies are ubiquitously rooted. IHS (F-3) is largely absent from the FUS and, where present, is found only at the top of the channel-fill (Fig. 2.7C). The sandbody of FA-III typically fines-upward into a thin layer of rooted, organic-rich mudstone (F-7b) and carbonaceous shale (F-8). At some locations "wings" composed of horizontally bedded, very fine-grained, ripple cross-laminated sandstone or siltstone < 0.5 m thick extend laterally from the uppermost portion of the channel-fill (Fig. 2.7A). Rarely, Small Low-sinuosity Channels of FA-III may be devoid of sand and, instead, are filled with rooted and/or ripple cross-laminated mudstone and tuff. In one case, two smaller channels were found to have scoured into the top of a larger channel-fill succession of FA-III (Fig. 2.7D).

Interpretation.-

FA-III is interpreted as a laterally-stable, ribbon sandbody (*sensu* Friend et al. 1979; Friend 1983) similar in facies and geometry to anastomosed channels (Smith 1976; Smith and Smith 1980; Smith and Putnam 1980; Knighton and Nanson 1993; Eberth and Miall 1991; Nadon 1994; Stouthamer 2001; Makaske 2001). Many of these channels are interpreted as (anastomosed?) crevasse channels that form part of larger splay complexes (Smith 1983; Fiorillo et al. 2010).

Most of FA-III is composed of a single, vertically-accreted sandbody that lacks predominant lateral accretion surfaces. The only evidence of lateral accretion is found near the top of the channel-fill sequence. Minor lateral accretion surfaces have been reported in channels interpreted as anastomosed (Kirschbaum and McCabe 1992; Törnqvist et al. 1993; Smith and Pêrez-Arlucea 1994; Makaske 2001; Abbado et al. 2005) suggesting that some lateral migration of anastomosed channels is possible (Thomas et al. 1987), however vertical accretion dominates over lateral accretion in anastomosing systems (Smith and Smith 1980; Smith 1983; Eberth and Miall 1991; Nadon 1994; Makaske 2001). The "wings" which extend laterally outward from the top of some of these ribbon channels are frequently described from channels interpreted as anastomosed (Smith and Smith 1980; Smith 1983; Eberth and Miall 1991; Kirschbaum and McCabe 1992; Nadon 1994; Kraus 1996). These "wings" are interpreted as levees which help to stabilize channels and prevent lateral migration (Kraus 1996; Nadon 1993, 1994; Makaske 2001; Heritage et al. 2001). Anastomosed channels remain largely "fixed" in position on the floodplain owing to low stream power, low gradients, and bank

stability resulting from abundant silt, mud and/or vegetation (Smith 1976; Kirschbaum and McCabe 1992; Törnqvist 1993; Törnqvist et al. 1993; Nadon 1994; Abbado et al. 2005; Guow and Barendsen 2007). Anastomosis is common in very low-gradient systems containing abundant fine-grained material and high concentrations of suspended load (Smith 1983; Smith et al. 1989).

Facies Association IV: Interbedded Sandstone, Siltstone, and Mudstone

FA-IV contains finer-grained facies which may include F-4, F-5, F-6a, F-6b, F-7a, F-7b, F-8, F-9, and F-10 (Tables 2.1, 2.2; Fig. 2.4). FA-IV lacks the coarser-grained facies of Large Sinuous Channels (FA-I) and Small Sinuous Channels (FA-II) and sedimentary structures indicative of high-energy environments. Sandbodies are typically < 2 m thick, non-channelized, sheet-like, ripple-cross-laminated or planar-laminated, and coarsen-upward or fine-upward or both (Figs. 2.8A, 2.8B). Contacts with underlying strata are erosive-to-gradational or disturbed, and lack significant relief. Burrows up to 15 mm in diameter are rare. Organic-rich sandstones and siltstones of FA-IV are found within a number of dinosaur quarries along the Colville River and contain abundant vertebrate bones and bone fragments (Phillips 2003; Fiorillo et al. 2009, 2010). Many of these sandstones and siltstones overlie finer-grained, organic-rich facies (Fig. 2.8B). Some sheet-like sandbodies, when traced laterally, are attached to the margins of channels (Fig. 2.8C). Mudstones (F7; Figs. 2.8B, 2.8D, 2.8E) commonly overlie and/or underlie sheet sandbodies of FA-IV (F4, F5, Fig. 2.8A).

Figure 2.8 (Following 2 Pages). Facies and physical sedimentary structures typical of FA-IV (Interbedded Sandstone, Siltstone, and Mudstone). A) Thin sheet sandstones interbedded with siltstone, carbonaceous shale and coal; B) coarsening-upward succession (CUS) showing sheet sandstone with abundant carbonaceous roots with jarosite halos (arrows) gradationally overlying interbedded siltstone, mudstone, and carbonaceous shale containing jarosite; C) sheet sandstone interpreted as a levee grading laterally into a Small Sinuous Channel (FA-II) containing inclined heterolithic stratification (IHS); D) drab-colored, cumulative, brown, gray, and black paleosols; E) carbonaceous root-traces (arrows) in paleosols.; F) clams (*Nucula* aff. *N. percrassa* Conrad) in ripple cross-laminated organic siltstone; G) olive-green to yellow bentonite layer above a rippled siltstone lacking root-traces; H) disturbed "punch-down" contact at the base of a sandstone containing convolute bedding (cb) and peat (now coal) "injected" upward into the sandbody likely as the result of trampling by dinosaurs; F) fine-grained Large Sinuous Channel (FA-I) plug containing rippled siltstone overlying planar-laminated fine-grained sandstone. Hammer is 30 cm long, Pocket knife is 9 cm long, pencil is

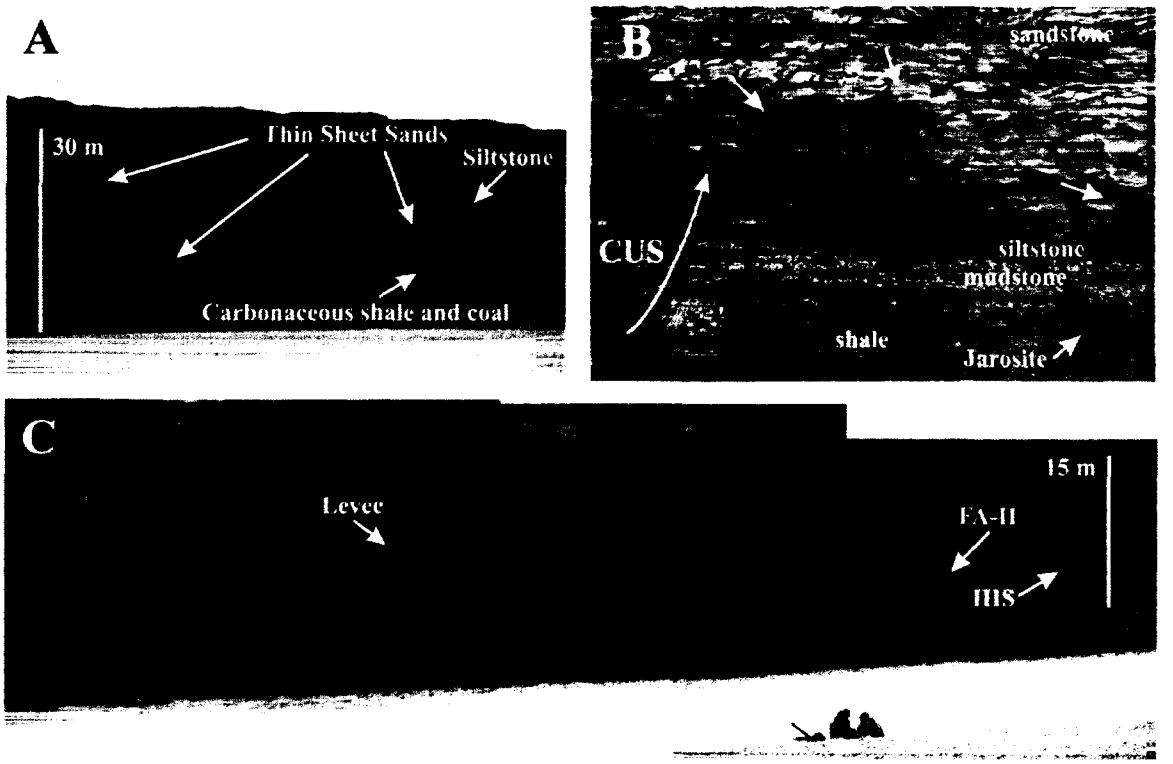
A
30 m
Thin Sheet Sands
Siltstone
Carbonaceous shale and coal
B
sandstone
CUS
siltstone
mudstone
shale
Jarosite
C
15 m
Levee
FA-II
IHS
D
E

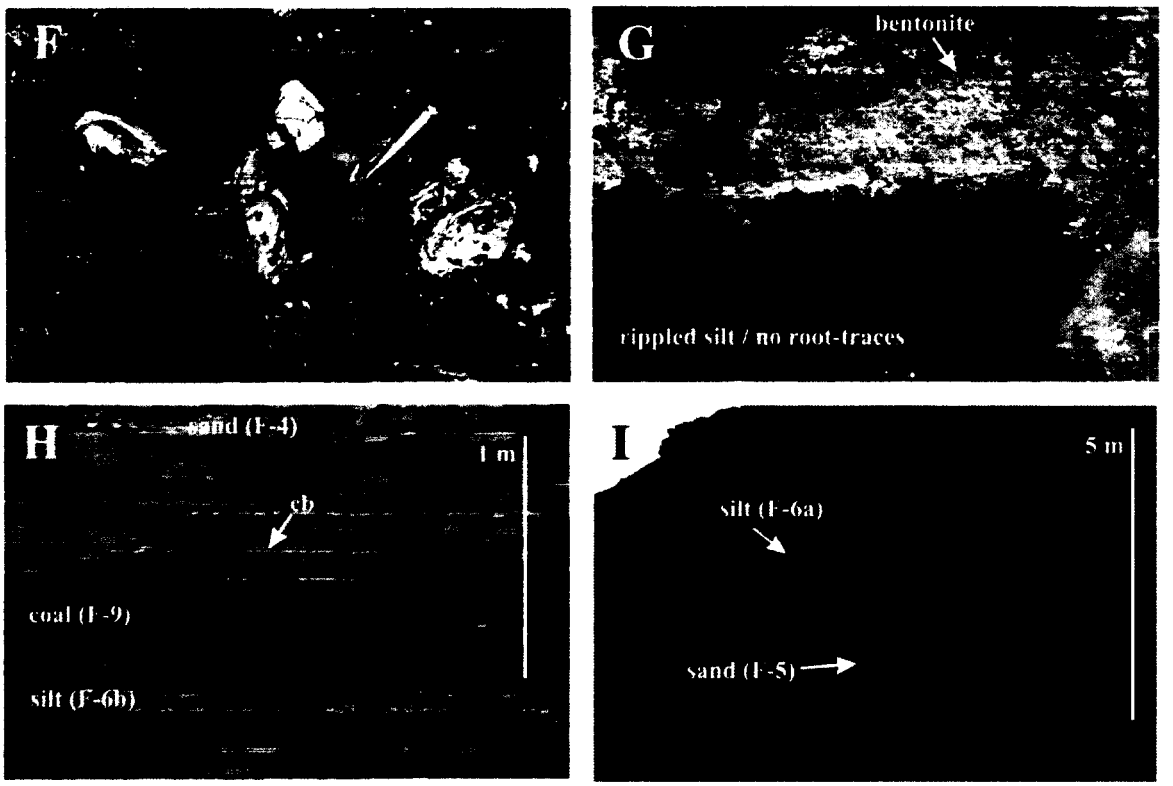

Figure 2.8 cont.

At some locations siltstones and mudstones (F6, F7) contain clams, gastropods, snails, and rare burrows up to 15 mm in diameter (Fig. 2.8F). Jarosite halos on roots, jarosite mottles, and bluish vivianite mottles become more common up-section. Organic-rich shales (F8; Fig. 2.8B) are common but true coals (always < 1 m thick) are rare (F9) (Fig. 2.8H). Disturbed basal contacts (Fig. 2.8H) and iron-oxide mottles are found in nearly all fine-grained facies. Thin (< 0.5 m) tuffs and bentonites (F10) may be locally interbedded with the other facies (Fig. 2.8G).

Interpretation.-

FA-IV is interpreted to represent floodplain deposition. Laterally extensive, thin, sheet-like, ripple cross-laminated or planar-laminated sandstones and siltstones with erosive-to-gradational or disturbed basal contacts, abundant root-traces, Fe-oxide mottles, and comminuted plant material overlying finer-grained organic facies such as carbonaceous shale, organic-rich mudstones or coal are interpreted as crevasse splays and channel-proximal levees (c.f. Coleman et al. 1964; Elliott 1974; Bridge 1984; Fielding 1984; Kraus 1987; Mjøs et al. 1993; Smith and Pêrez-Arlucea 1994; Changsong et al. 1995; Rajchl and Uličný 2005; Martín-Closas and Galtier 2005). Sandstones represent proximal splay deposits and/or higher flow-velocities while siltstones represent distal splay deposits and/or waning flow (e.g. Pêrez-Arlucea and Smith 1999; Rajchl and Uličný 2005). Similar deposits have also been attributed to levees (Allen 1965b; Fielding 1986; Pêrez-Arlucea and Smith 1999; Stouthamer 2001; Michaelsen et al. 2000),

although a levee interpretation is more convincing when thin, sheet-like sandstones and siltstones can be seen to thicken and grade laterally into channel deposits (e.g. Fig. 2.8C). Thin sheet sandstones with undulating or disturbed basal contacts (Fig. 2.8H) suggest that these surfaces may have been trampled by dinosaurs (e.g. La Porte and Behrensmeyer 1980; Loope 1986; Avanzini et al. 1997).

Lacustrine intervals in alluvial successions commonly comprise fine-grained sandstone, siltstone or mudstone that is often laminated or rippled (e.g. Fielding 1984; Astin 1990; Besley and Collinson 1991, Smith and Pêrez-Arlucea, 1994; McCarthy et al. 1999; Tanner 2000). FUS composed predominantly of 3-4 m of planar-laminated or current rippled siltstone (F-6) that lacks evidence of roots but contains carbonized plant fragments, carbonized wood, and unusually abundant coaly logs and overlies 3-5 m of fine-to medium-grained, planar-laminated (F-5) and trough-cross-laminated (F-2a) sandstone (Figs. 2.4, 2.8I) are interpreted as channel plugs of Large Sinuous Channels (FA-I) formed after neck cutoff (e.g. Lewis and Lewin 1983; Miall 1996; Pêrez-Arlucea and Smith 1999). Thinner packages of ripple cross-laminated and rarely rooted or burrowed siltstone and mudstone (typically < 1 m-thick) that may contain brackish-water clams (*Nucula* aff. *N. percrassa* Conrad; Fig 2.8F) along with indeterminate gastropods with spiral ornaments and indeterminate snails (pers. comm. Robert Blodgett) are interpreted as small lakes and ponds that occupied topographic lows on the floodplain (Pêrez-Arlucea and Smith 1999). Often these siltstones/mudstones exhibit disturbed (trampled) basal contacts.

Organic-rich mudstone, carbonaceous shale, and coal were deposited in swamps, marshes, and mires (c.f. Coleman et al. 1964; Tatsch, 1980; Smith and Smith 1980; Smith 1983; Flores 1984; Fielding 1984; Smith and Pêrez-Arlucea 1994; Fielding 1987a; Pêrez-Arlucea and Smith 1999). The presence of jarosite and vivianite indicate an oxygen-reduced, organic-rich environment (Postma 1977, Davies-Vollum 1999, Driese and Ober 2005) and may signal proximity to sulfate-rich marine/tidal waters (Wright 1986, Ufnar et al. 2001).

Carbonaceous root-traces are common in FA-IV, with the exception of the rippled siltstone (F-6) found within channel plugs, indicating that extensive vegetation was present on the floodplain. The abundance of carbonaceous plant material and siderite concretions suggests that many environments experienced anoxic or reducing conditions (Retallack 2001; Ashley et al. 2004; Johnson and Graham 2004).

Drab-colored, rooted siltstones and mudstones with common Fe-oxide mottles are interpreted as poorly drained paleosols (Fiorillo et al. 2010). Individual paleosol profiles are often difficult to discern in the field owing to frequent clastic influx and cumulative pedogenesis, and are similar to modern Inceptisols and Entisols (Fiorillo et al. 2009). Although drab colors and preserved organic matter suggest poorly drained conditions on floodplains, abundant rooted horizons and ferruginous features indicate periodically better-drained or possibly seasonally dry conditions (Smith et al. 1989; Nadon 1994; Ashley et al. 2004; Johnson and Graham 2004; Brandlen 2008; Fiorillo et al. 2009)

PALEOFLOW

Paleoflow orientations from channel-fills are useful for determining basin geometries and sources for ancient river systems (e.g. Barrett 1970; Vavra 1984; Isbell 1990; Collinson et al. 1994; Flaig 2005) and their dispersion can also assist in distinguishing the type of fluvial system responsible for deposition (Miall 1976; Collinson 1978; Bridge 1985).

A total of 68 paleoflow orientations were recorded from channel-fill deposits at 20 locations (Fig. 2.9). Measurements used to calculate mean paleoflow were restricted to trough cross-lamination on dune foresets in fine-to coarse-grained sandbodies. Paleocurrent orientations indicate that regional paleoflow within the Prince Creek Fm. varied from northwest to southeast. The overall vector mean for all paleoflow in the study area is 060°. This value is consistent with previously published data indicating regional paleoflow to the northeast (Phillips 2003; Mull et al. 2003), although our data also indicate a high degree of variability in flow direction. No convincing evidence for bi-directional flow was found in any facies.

ALLUVIAL ARCHITECTURE

Architectural analysis (*sensu*. Miall 1985) is a technique that is used to decipher the sequence of events responsible for the formation of alluvial successions and the nature of the system(s) responsible for their deposition (Eberth and Miall 1991; Wood 1989; Roberts 2007; McLaurin and Steel 2007). In this architectural analysis we

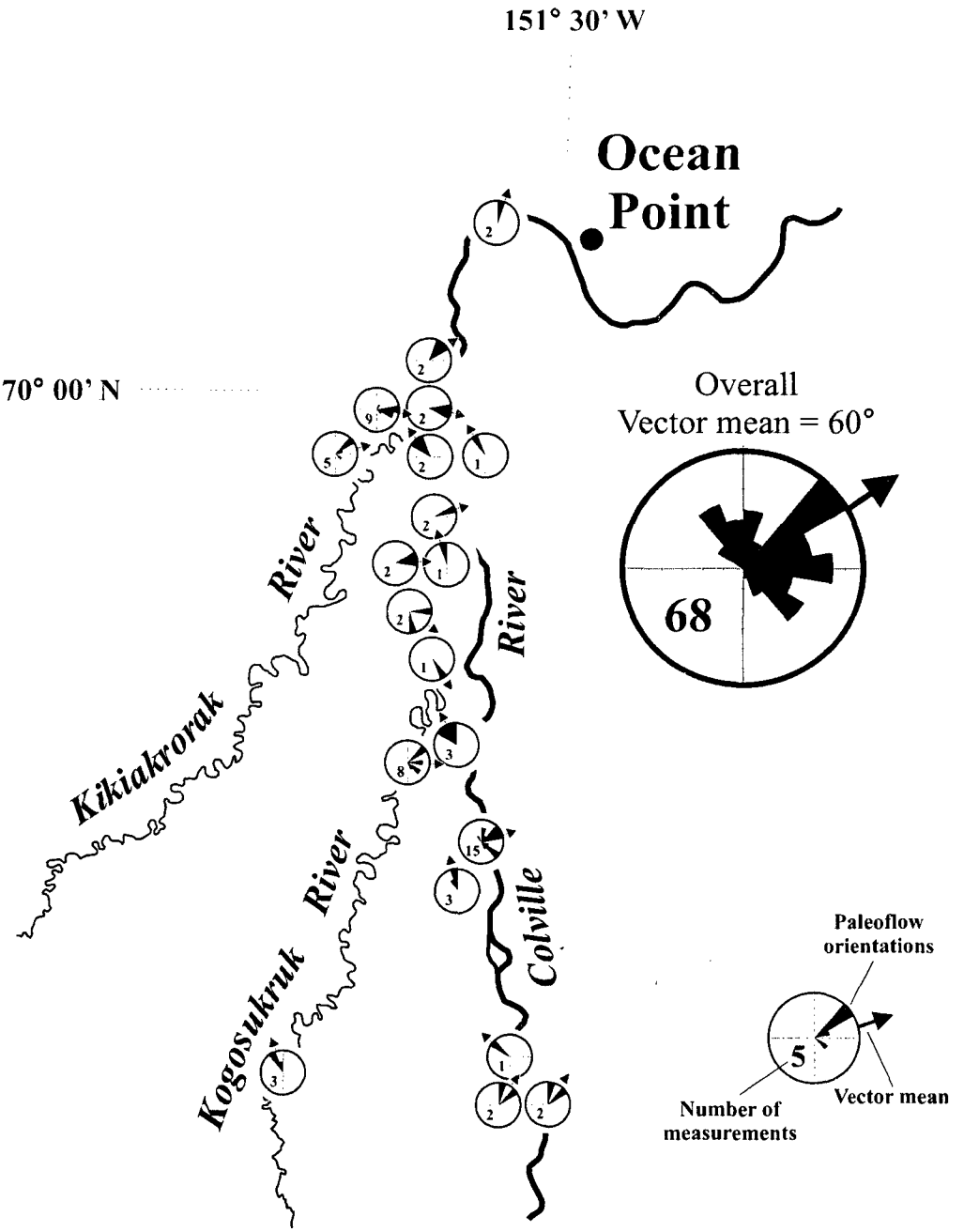

Figure 2.9. Paleocurrent orientations recorded from trough cross-laminations within channel thalwegs at 20 separate locations in the Prince Creek Formation along the Colville, Kogosukruk, and Kikiakrorak Rivers. Included in the diagram are paleoflow vector rose diagrams that include the number of measurements recorded and mean paleoflow at each location. The diagram also displays the overall vector mean of paleoflow in the study area.

integrate measured stratigraphic sections with interpreted line-drawings on photomosaics. We also identify genetic lateral and vertical relationships between sandbodies and between sandbodies and floodplain facies. Architectural components used in the architectural analysis include Facies Associations I, II, III, and IV. The analysis is divided into three sections with each section focusing on a specific channel-type (FA I, II, and III). Many photomosaics include channels of more than one type. The architecture of FA-IV (floodplains) is intimately linked to the other facies associations (channels) and is, therefore, incorporated into each section. Due to the vertical nature and inaccessibility of many of the bluffs, the dip direction of IHS discussed here is apparent dip rather than true dip. Outcrop trend and paleoflow are incorporated into each photomosaic to assist in interpretation.

Large Sinuous Channels (FA-I)

The alluvial architecture of Large Sinuous Channels (FA-I) is best observed at section PFDV-17 (Figs. 2.2, 2.10, 2.11). PFDV-17 was chosen for architectural analysis because both the basal conglomerate and the finer-grained organic-rich top of the FUS of FA-I are visible in outcrop. Section PFDV-17 also contains the largest clasts found in the study area (quartz boulders, longest axis = 30 cm).

Figure 2.10 is a 125 m-wide composite image showing a 28 m-thick vertical succession containing one 13 m-thick FUS of FA-I (Large Sinuous Channels), two laterally-extensive 2-4 m-thick FUS of FA-II (Small Sinuous Channels), and

Figure 2.10 (Following Page). Photomosaic and interpreted line-drawing at location PFDV-17 including outcrop trend, paleoflow orientations, and location of measured section PFDV-17 (see Fig. 2.11). Image contains one complete fining-upward succession (FUS) of FA-I (Large Sinuous Channel),two FUS of FA-II (Small Sinuous Channels), and interbedded floodplain deposits of FA-IV (Interbedded Sandstone, Siltstone and Mudstone). Abbreviations include: FA, facies association; IHS, inclined heterolithic stratification; and Lv/Sp, levee or splay. Arrows on image show apparent dip direction within IHS (point bars) and apparent direction of

H

Figure 2.11 (Following Page). Measured stratigraphic sections PFDV-17, PFDV-04, and KKT. Diagrams include paleoenvironmental interpretations. See Figure 4 for key to symbols. Detailed descriptions of individual facies and facies associations are given in Table 2.1 and Table 2.2.

FA IV
FA II
FA IV
FA-I
FA IV
(Swamp, Mire, Soil)
Swamp, Mire
Swamp, Mire
Splay
Mire, Lake
Splay
Swamp. Mire. Soil
Distal Splay
Swamp. Mire
Facies
Sand
clinoform
FDV-17
FA-II
FA-IV
FA-II
FA-IV
(Mire)
FA-II
FA-III
FA-II
FA-IV
FA-II
Swamp, Mire
Soils
Swamp, Mire
Soils and Mire
Facies
Sand
clinoform
FDV-44

FA-IV
FA-III
FA-IV
Splay, Levee
Pond
Splays, Levees
Splays, Levees
Pond, Mire
Splays, Levees
Marsh
Soils
Splays, Levees
Marsh
Splays, Levees
Facies
Sand
Silt
KKT

interdigitating facies of FA-IV. Section PFDV-17 (Fig. 2.11) was measured while walking up-section along the ridge on the left of the image in Figure 2.10; hence the entire FUS of FA-I, only one of the two FUS of FA-II (between 6.25-8.0 m) and a sampling of the interdigitating facies of FA-IV appears in the measured section. The erosion surface at the base of the conglomerate in the Large Sinuous Channel (FA-I), which exhibits 13 m of relief, is incised into an interval of stacked facies of FA-IV. Measurements recorded from trough cross-laminations in the medium-grained sandstone near the base of FA-I indicate that paleoflow in the large channel was directed obliquely out of the plane of the image at 343° which is approximately 060° to the northwest relative to the strike of the outcrop (045°/225°). The medium-grained sandbody grades upward into an interval of IHS, capped by an interval of siltstone, carbonaceous shale, coal, and rooted mudstone. The IHS is composed of decimeter-scale, coarse-to-fine couplets of sandstone and mudstone, with the muddy component at least equal in thickness, and sometimes thicker, than the sandy component. IHS containing sand and mud couplets of approximately equal thickness are also visible within the two Small Sinuous Channels (FA-II) in Figure 2.10. Depositional environments of FA-IV (Interbedded Sandstone, Siltstone, and Mudstone) in PFDV-17 include levees, crevasse splays, shallow lakes, swamps, mires, soils, and ashfall deposits. Thick mud-drapes on point bar surfaces (IHS) in Large Sinuous Channels (FA-I) and Small Sinuous Channels (FA-II) and the thick succession of fine-grained facies of FA-IV found stratigraphically above, below, and interfingering with channels suggest that these were suspended-load channels (Schumm 1981; Stewart 1983; Orton and Reading 1993).

At PFDV-17 initial deposition took place on the floodplain. A Small Sinuous Channel (FA-II) migrated into the area over the floodplain, depositing both levee and within-channel facies. The channel migrated out of the area and floodplain facies (FA-IV) replaced channel deposits. Paleoenvironments included crevasse splays, swamps, soils, and a 0.4 m thick ashfall deposit preserved in a small pond or mire. A second Small Sinuous Channel (FA-II) migrated through the region followed by another interval of floodplain deposition. The initial indication of a Large Sinuous Channel (FA-I) in the vicinity is evidenced by the appearance of a relatively thick levee or splay sandstone deposited on top of the floodplain deposits. This sandstone is only visible in the photomosaic and was not measured in section PFDV-17. Large channel incision into previously deposited levee and floodplain facies followed. Lateral migration of the channel is indicated by point bar deposits preserved as prominent IHS. Levees, crevasse splays, and organic-rich floodplain facies were deposited along the flanks of the channel. The entire succession was capped by a final episode of floodplain deposition after the large channel migrated out of the area.

Small Sinuous Channels (FA-II)

The alluvial architecture of Small Sinuous Channels (FA-II) is visible at many locations in the study area; however, diagnostic attributes of FA-II are exceptionally well exposed at sections PFDV-04 and CRNKKT (Figs. 2.2, 2.12, 2.13). Bluffs near PFDV-04 (Fig. 2.12) were chosen for architectural analysis because: (1) they are composed

Figure 2.12 (Following Page). Photomosaic and interpreted line-drawing at location PFDV-04 (Fig. 2.2) including outcrop trend, paleoflow orientations, and location of measured section PFDV-04 (Fig. 2.11). Image contains 8 Small Sinuous Channels (FA-II) along with associated mud-filled abandoned channels, one example of a Small Low-sinuosity Channel (FA-III), and Interbedded Sandstone, Siltstone, and Mudstone (FA-IV). Abbreviations include: FA, facies association; IHS, inclined heterolithic stratification; and Lv/Sp, levee or splay. Arrows on image show apparent dip direction within IHS (point bars) and apparent direction of channel migration See text for detailed interpretation.

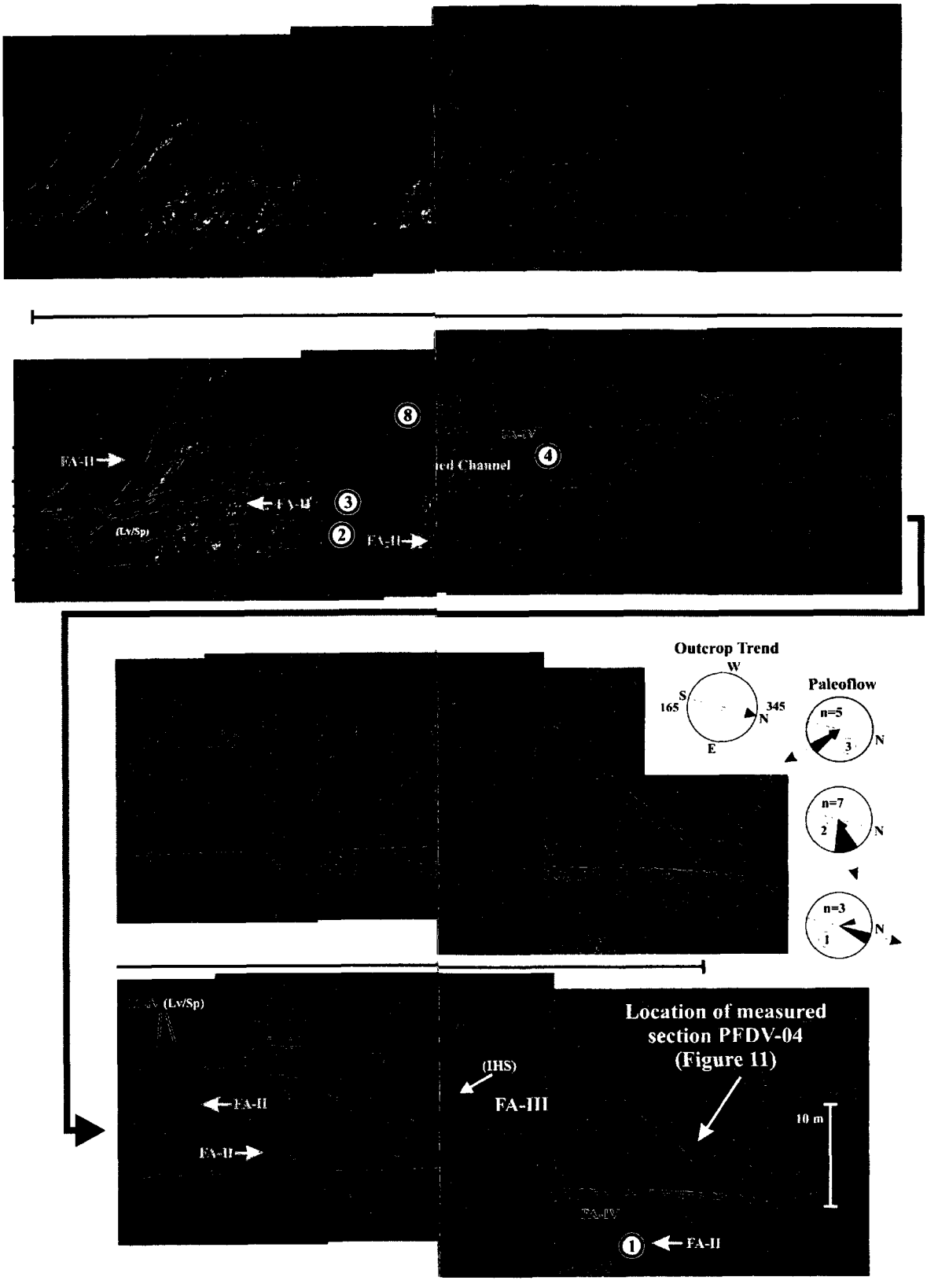
FA-II
(Lv/Sp)
FA-II
FA-II
8
4
3
2
Outcrop Trend
W
S
165
345
N
E
Paleoflow
n=5
N
3
n=7
2
N
n=3
1
N
(Lv/Sp)
FA-II
FA-II
(IHS)
FA-III
Location of measured section PFDV-04 (Figure 11)
10 m
FA-IV
1
FA-II

Figure 2.13 (Following Page). Photomosaic and interpreted line-drawing at location CRNKKT (Fig. 2.2) including outcrop trend. Overall paleoflow is inferred to be similar to Figure 2.12. Image contains 8 Small Sinuous Channels (FA-II) along with Interbedded Sandstone, Siltstone, and Mudstone (FA-IV). Abbreviations include: FA, facies association; IHS, inclined heterolithic stratification; and Lv/Sp, levee or splay. Arrows on image show apparent dip direction within IHS (point bars) and apparent direction of channel migration. See text for detailed interpretation.

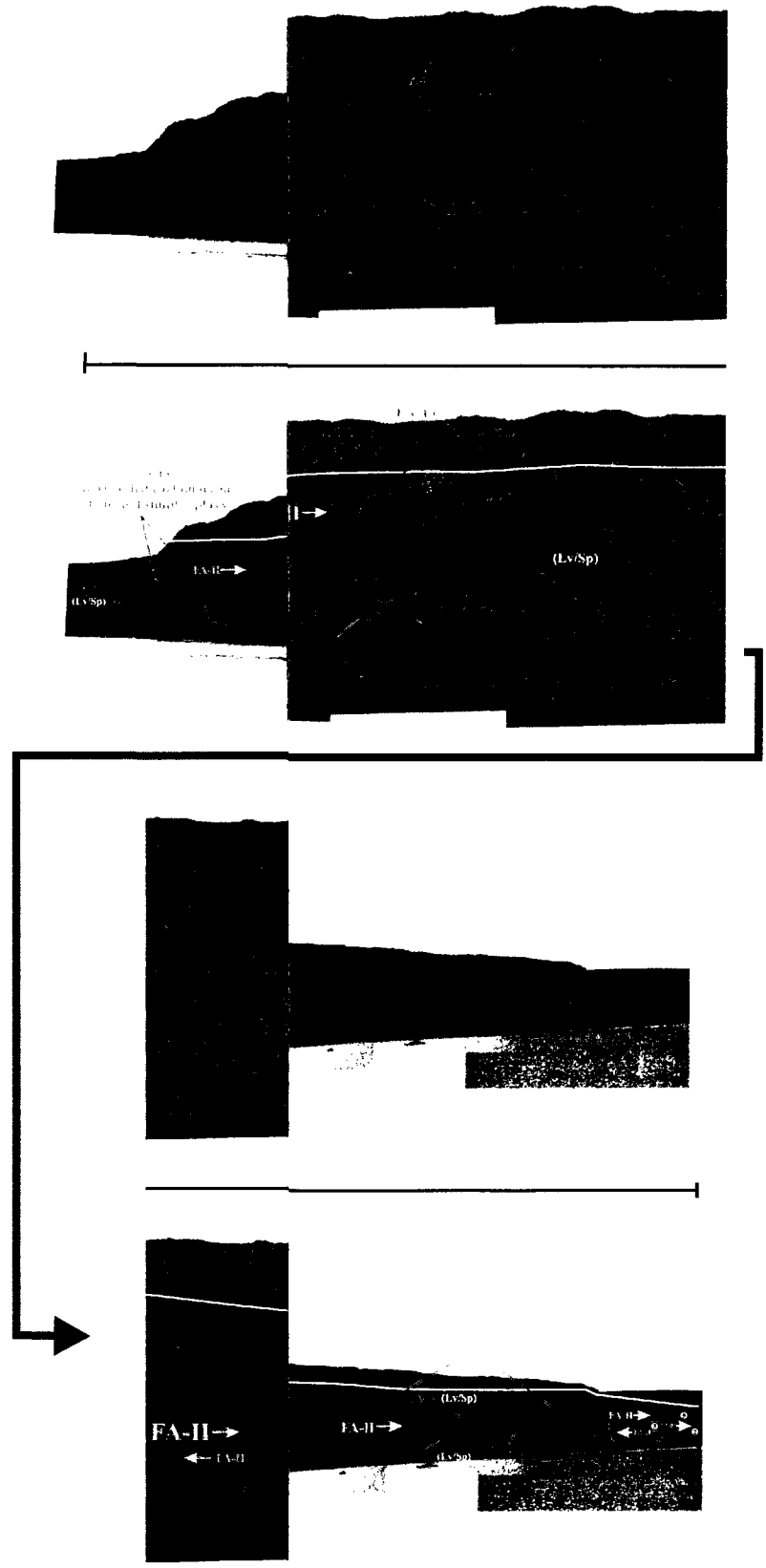
(Lv/Sp)
FA-II
(Lv/Sp)
FA-II
FA-II
FA-II
(Lv/Sp)
(Lv/Sp)

of a series of vertically stacked Small Sinuous Channels (FA-II) containing IHS with apparent dips which trend in opposing directions, (2) there are numerous mud-filled abandoned channels visible, (3) the exposure also contains a Small Low-sinuosity Channel (FA-III) incised into a Small Sinuous Channel (FA-II), and (4) a small drainage allowed access to the north for the measurement of section PFDV-04 (Fig. 2.11). An additional photomosaic of bluffs near section CRNKKT (Fig. 2.13) is included to illustrate more extensive lateral relationships between FA-II and FA-IV over a distance of 1.6 kilometers, approximately along strike of paleoflow.

Section PFDV-04.-

Figure 2.12 is a composite image that covers an area 400 m wide by 30 m high. A series of at least 8 vertically-stacked Small Sinuous Channels of FA-II, many containing mud-filled channel plugs, are visible in the photomosaic. Small Sinuous Channels (FA-II) interfinger with Interbedded Sandstone, Siltstone, and Mudstone (FA-IV). Floodplain facies were deposited on crevasse splays and levees; in lakes, ponds, marshes, and swamps; and include immature cumulative soils. Small Sinuous Channels (FA-II) in PFDV-04 are single-storey and vertically separated by 0.2-5.0 m-thick packages of floodplain facies (FA-IV) unless the stratigraphically higher channel erodes into the underlying channel. Also included on the right side of the image (Fig. 2.12) and in measured section PFDV-04 (Fig. 2.11) is a single Small Low-sinuosity Channel (FA-III) incised into a Small Sinuous Channel (FA-II). An additional mud- and tuff-filled Small

Low-sinuosity Channel (FA-III) located at the same stratigraphic level can be found 125 m to the north, out of the field of view.

The bluffs at PFDV-04 strike at 165°/345°. Paleocurrent orientations recorded from trough cross-laminations at the base of three separate Small Sinuous Channels (FA-II) in PFDV-04 (channels #1, #2, and #3, Fig. 2.12) indicate that mean paleoflow varied between 360°, 058°, and 136° at angles ranging from 15-75° relative to the apparent dip of the IHS and the strike of the bluffs. The mean resultant vector for paleoflow at PFDV-04 is 072°. Flow at high angles relative to the apparent dip of inclined surfaces within the IHS supports an interpretation of FA-II as remnants of laterally-accreting point-bars. The sinuous nature of these channels is evidenced by the opposing apparent dip of IHS within stacked channels in this succession (Gradzinski 1970; Stewart 1983, Smith 1987; Flores et al. 2009b) along with the abundance of mud-filled abandoned channels (Collinson 1978; Miall 1996). The sand-filled Small Low-sinuosity Channel (FA-III) at the right of the image (~15-17 m in section PFDV-04, Fig. 2.11) was filled mainly by vertical accretion, although minor IHS visible near the top of the channel (Fig. 2.7C) indicates that limited lateral migration of the channel likely occurred.

At PFDV-04, point bars deposited by lateral migration of Small Sinuous Channels (FA-II) alternate with highly organic floodplain facies (FA-IV). The migration direction of these sinuous channels was highly variable and abandonment of channels was common. Small Sinuous Channels (FA-II) either incise into pre-existing point bar deposits, or into floodplain deposits. The sand-filled Small Low-sinuosity Channel (FA-

III) incises into point bar deposits of a Small Sinuous Channel (FA-II, channel #3, Fig. 2.12) and is overlain by abandoned Small Sinuous Channels (FA-II, channels #6 and #7, Fig. 2.12), suggesting that the smaller, fixed channel was active after the point bars of the Small Sinuous Channel (FA-II, channel #3, Fig. 2.12) were deposited, but prior to new Small Sinuous Channel (FA-II) and floodplain (FA-IV) deposition.

Section CRNKKT.-

Figure 2.13 is a composite image of bluffs along the Colville River 2 kilometers to the north of PFDV-04 at location CRNKKT (Fig. 2.2) and covers an area 1600 m wide by 35 m high. The bluffs at CRNKKT strike at 155°/335°, similar to the strike of bluffs at PFDV-04. Figure 2.13 also includes a series of at least 8 vertically stacked Small Sinuous Channels (FA-II). Mud-filled channel-plugs are present but they are not as common as in Figure 2.12 and are omitted in the interpreted line-drawing for clarity. No paleoflow data were recorded at CRNKKT, however apparent dips of IHS and the close proximity of CRNKKT to PFDV-04 suggest that paleoflow was likely toward the east-northeast, similar to that recorded in channels at PFDV-04

Small Sinuous Channels (FA-II) in Figure 2.13 grade laterally from channelized deposits with erosional bases and prominent IHS into levees or splays with sharp to gradational basal contacts. Laterally-extensive sandbodies assume an overall lenticular shape. The Small Sinuous Channel (FA-II) designated "channel #2" is divided into two separate lobes by thinner levee deposits which are overlain by carbonaceous shale and

coal. This geometry suggests that two channels may have either been contemporaneous and separated by thin, interconnected levees, or they were successively deposited in close proximity to each other.

At CRNKKT, point bars of Small Sinuous Channels (FA-II) and associated levees and splays form lenticular deposits in a range of orientations oblique to channel axes. Small Sinuous Channels (FA-II) alternate with and pinch-out into floodplain facies that typically both overlie and underlie these channels. Small Sinuous Channels (FA-II) commonly erode into other, pre-existing Small Sinuous Channels (FA-II) and levee or splay deposits of FA-IV. Geometries suggest that multiple channels may have been active at the same time in close proximity to each other on the floodplain.

Small Low-sinuosity Channels (FA-III)

The alluvial architecture of Small Low-sinuosity Channels (FA-III) is best viewed at a location stratigraphically below and immediately to the south of the Kikak-Tegoseak dinosaur quarry (KKT in Fig. 2.2). This location was chosen for architectural analysis of FA-III because three, small, low-sinuosity ribbon-form sandbodies (FA-III) are exposed at the same stratigraphic level (Fig. 2.14). The bluffs in Figure 2.14 are vertical and no stratigraphic succession was measured there. However, section KKT located 200 m to the north of the bluffs with an interval from ~4.5-6.0 m containing a Small Low-sinuosity Channel (FA-III) is included for reference (Fig. 2.11). The interval from 15-17 m in section PFDV-04 (Fig. 2.11) provides an additional example of a Small Low-sinuosity

Figure 2.14 (Following Page). Photomosaic and interpreted line-drawing at location KKT (Fig. 2.2) including outcrop trend, paleoflow orientations, and location of measured section KKT (Fig. 2.11). Image contains three Small Low-sinuosity Channels (FA-III), two Small Sinuous Channels (FA-II), and Interbedded Sandstone, Siltstone, and Mudstone (FA-IV). Abbreviations include: FA, facies association; IHS, inclined heterolithic stratification; and Lv/Sp, levee or splay. Arrows on image show apparent dip direction within HIS (point bars) and apparent direction of channel migration. See text for detailed interpretation.

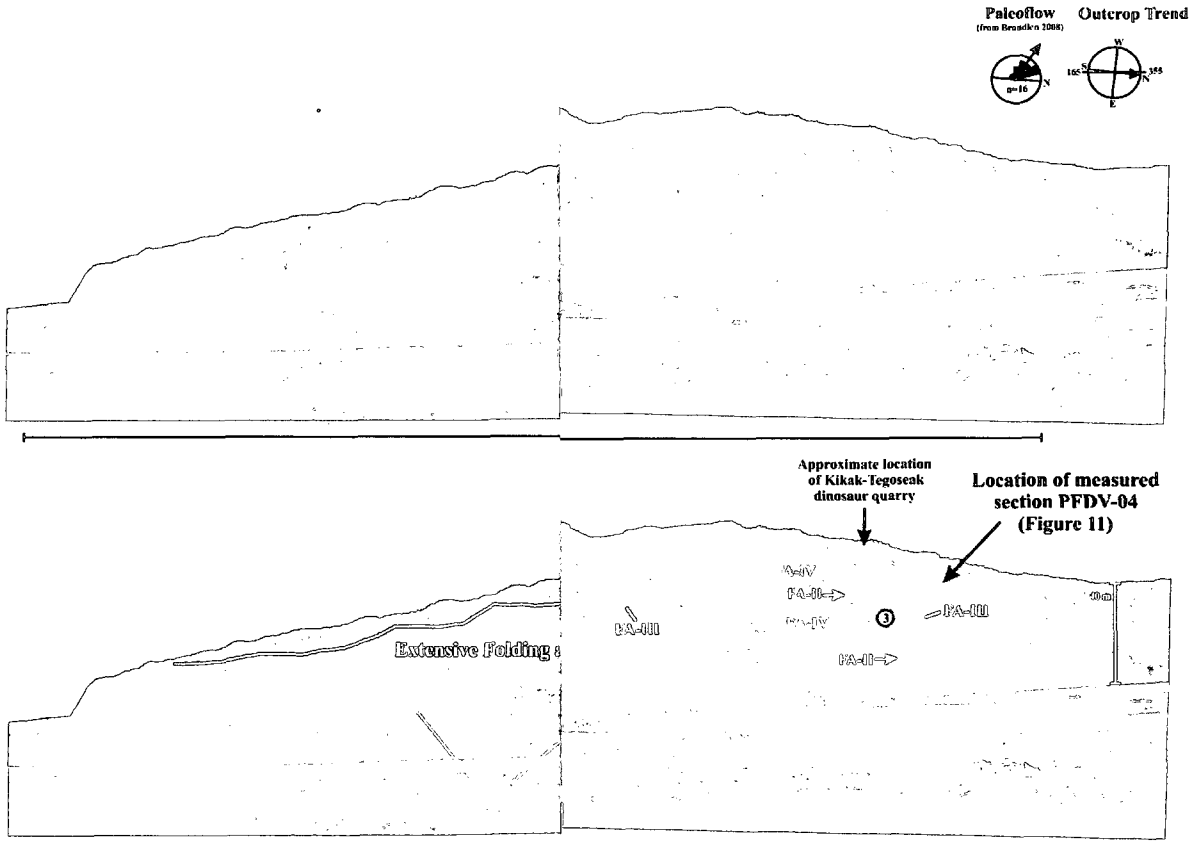
Paleoflow
(from Brandon 2008)
Outcrop Trend
W
N
E
n=16
165
355
Approximate location
of Kikak-Tegoseak
dinosaur quarry
Location of measured
section PFDV-04
(Figure 11)
FA-III
FA-II
FA-III
FA-II
Extensive Folding

Channel (FA-III). Details of depositional environments near the Kikak-Tegoseak dinosaur quarry can be found in Brandlen (2008) and Fiorillo et al. (2010).

Figure 2.16 covers an area 900 m-wide by 40 m-high. The bluffs at KKT visible in the photomosaic strike at 165°/355°. Paleoflow orientations taken from Brandlen (2008) (n=16) show the mean direction of paleoflow near the Kikak-Tegoseak dinosaur quarry is 298° , 057° to the west of the strike of the outcrop.

Most of the succession shown in Figure 2.14 is composed of Interbedded Sandstone, Siltstone, and Mudstone (FA-IV). The image includes two Small Sinuous Channels (FA-II), one near the base of the succession and one near the top. The stratigraphically lower of the two channels grades laterally to the south into a levee or splay that ultimately pinches out into organic-rich floodplain deposits. Also included in Figure 2.14 are three, ribbon-form Small Low-sinuosity Channels (FA-III). All three ribbon-form channels are sand-filled, located at the same stratigraphic position in the bluffs, and are incised into floodplain deposits (FA-IV).

Near KKT, most deposition occurred on floodplains. Small Sinuous Channels (FA-II) and associated levees and splays interfinger with and pinch out into floodplain facies. Small Low-sinuosity Channels (FA-III) near KKT incise into floodplain deposits (FA-IV). This is in contrast to the Small Low-sinuosity Channel (FA-III) at PFDV-04 in Figure 2.12 which incises into a Small Sinuous Channel (FA-II).

CHANNEL CHARACTERISTICS

Although a 2-D architectural analysis is useful in establishing typical genetic relationships between channels and floodplain facies it is also helpful to extract sandbody geometries. However, incomplete or inaccessible exposures of the Prince Creek Fm. did not always allow for quantitative estimates of channel geometries in the field, therefore, we use a series of methods (Schumm 1963, Ethridge and Schumm 1978, Gardner 1983, McLaurin and Steel 2007) to estimate channel depth, channel width, and sinuosity for each of the three channel-types in the Prince Creek Fm.

Channel Depth

Channel depths for Large Sinuous Channels (FA-I), Small Sinuous Channels (FA-II), and Small Low-sinuosity Channels (FA-III) in the Prince Creek Formation are estimated using two different techniques. Estimates of bankfull depth provided are minimum estimates due to compaction of sediments during burial (~2000-6000 ft. Burns et al. 2005). Other values (e.g. bankfull width) that incorporate channel depth into calculations should also be considered minimum values.

Initial calculations employ a series of field measurements taken from a number of different channels of each type. In complete FUS, bankfull depth was assumed to be the thickness of the succession from the base of the thalweg to the top of the point bar surface or channel-fill sequence (Ethridge and Schumm 1978, Gardner 1983). Outcrop measurements indicate that minimum flow depths for Large Sinuous Channels (FA-I,

n=2) range from 13-17 m with an average depth of 15 m. Flow depths for Small Sinuous Channels (FA-II, n=36) range from 2-6 m with an average depth of 4 m while flow depths for Small Low-sinuosity Channels (FA-III, n=5) range from 1.5-3.0 m with an average depth of 2.5 m. These results were compared to values obtained using the method of LeClair and Bridge (2001) in which the average crossbed set thickness serves as a proxy for flow depth by assuming that crossbed set thickness is equal to one-third dune height and that flow depth is six to ten times dune height. Using an average crossbed set thickness of 0.5 m for Large Sinuous Channels (FA-I) (which allows for the inclusion of measurements from incomplete FUS throughout the study area) a range of flow depths between 9 and 15 m was calculated. An average crossbed set thickness of 0.2 m for Small Sinuous Channels (FA-II) gives a range of flow depths between 3.5 and 6.0 m. Crossbeds are extremely rare in Small Low-sinuosity Channels (FA-III) and the thickness of crossbed sets was not recorded in these channels. Results for Large Sinuous Channels (FA-I) and Small Sinuous Channels (FA-II) from both methods are comparable. Therefore, ranges for average maximum bankfull depths of 9-17 m for Large Sinuous Channels (FA-I), 2-6 m for Small Sinuous Channels (FA-II), and 1.5-3.0 m for Small Low-sinuosity Channels (FA-III) were used in the following calculations to estimate channel width.

Channel Width

Outcrop exposures containing complete FUS of Large Sinuous Channels (FA-I) are rare and no exposure containing both channel margins was found. Because of the scarcity of laterally extensive exposures, widths for Large Sinuous Channels (FA-I) must be estimated. Additionally, most smaller channels and channel-plugs in the study area are in vertical bluffs that are either inaccessible or make quantitative measurement of channel-width challenging. Because of difficulties involved with direct measurement and incomplete exposures we use the empirical regression equation of Bridge and Mackey (1993) to estimate the width of channels:

$$w_c = 8.88 d_m^{1.82} \qquad \text{Equation \#1}$$

where w_c is equal to the bankfull channel width and d_m is equal to the mean bankfull depth. Mean bankfull depth is approximately equal to one-half the maximum bankfull depth (Bridge and Mackey 1993). Incorporating half the range of calculated maximum bankfull depths from the previous section into equation # 1 we obtain estimates for bankfull channel widths of 140-435 m for Large Sinuous Channels (FA-I), 10-65 m for Small Sinuous Channels (FA-II), and 5-19 m for Small Low-sinuosity Channels (FA-III). Using these results for channel width and the maximum bankfull depth from the previous section, width to thickness ratios (w/t) are estimated at: 15:1 to 25:1 for Large Sinuous Channels (FA-I), 4:1 to 11:1 for Small Sinuous Channels (FA-II), and 3:1 to 6:1 for Small Low-sinuosity Channels (FA-III). Following Gibling (2006), Large Sinuous Channels (FA-I) are classified as narrow sheets (range = 15:1 to 100:1),

Small Sinuous Channels (FA-II) are classified as broad ribbons (5:1-15:1), and Small Low-sinuosity Channels (FA-III) are classified as narrow ribbons (< 5:1).

Sinuosity

Schumm (1963) provides an empirical equation that can be used to estimate sinuosity based on the relationship between sinuosity and the ratio of channel width to channel depth:

$$sn = 3.5\ (W_b/D_{max})^{-0.27} \qquad \text{Equation \#2}$$

where W_b is equal to bankfull width and D_{max} is equal to maximum bankfull depth. By incorporating the calculated range of bankfull widths and bankfull depths into Equation #3, Schumm's equation yields sinuosities for Large Sinuous Channels (FA-I) ranging from 1.23 to 1.98 with an average sinuosity of 1.60, and sinuosities for Small Sinuous Channels (FA-II) from 1.37 to 3.0 with an average value of 2.19.

Channel sinuosity can also be estimated by examining overall paleoflow variation, where low dispersion of paleoflow suggests low sinuosity and a high dispersion suggests high sinuosity. Bridge et al. (2000) suggest that a relationship exists between the range of paleoflow orientations in a channel system and the sinuosity of the system. They provide two sinuosity equations that assume bends within channels can be represented as circular arcs or sine-generated curves:

$$sn = \Phi/\sin\Phi \qquad \text{(circular arc method)} \qquad \text{Equation \#3}$$

$sn = 4.84/ (4.84 - \Phi^2)$ (sine-generated curve method) Equation #4

where *sn* is equal to the sinuosity of the channel, and Φ is equal to one-half of the maximum paleocurrent range in radians. In order to obtain more accurate estimates for the sinuosity of individual channel-types in the Prince Creek Fm. Large Sinuous Channels (FA-I) were separated from Small Sinuous Channels (FA-II). In addition, because of the wide dispersion of paleocurrents for Small Sinuous Channels (FA-II), we limit the range to paleocurrents collected from the three stacked channels at PFDV-04. This minimizes the error that would occur by inadvertently including paleoflow from distributaries on both sides of a main channel. Instead, we limit the estimated sinuosity to a series of apparently sequential Small Sinuous Channels (FA-II) at a single location.

The range of paleocurrents recorded from trough cross-laminations in the thalwegs of Large Sinuous Channels (FA-I, n=21) is 190°. Taking one-half of the range (95°) in radians and incorporating it into equation #3 yields a sinuosity value of 1.66. Substitution in equation #4 yields a higher value of 2.31. The range of paleocurrents (n=15) for Small Sinuous Channels (FA-II) at PFDV-04 is 180°. Taking one-half of the range and incorporating it into equation #3 yields a sinuosity value of 1.57. Using equation #4 yields a higher value of 2.03.

All results indicate that both Large Sinuous Channels (FA-I) and Small Sinuous Channels (FA-II) should be classified as highly-sinuous channels (*sensu* Miall 1996). The relative lack of IHS (point bars) within Small Low-sinuosity Channels (FA-III) and

their consistent arcuate shape in outcrop suggests that they were most likely low-sinuosity channels.

DISCUSSION

Channel Hierarchy in the Prince Creek Formation

Channel-fill deposits of the Prince Creek Fm. are identified as FUS that include a combination of two or more of the following attributes: (1) a basal erosion surface, (2) IHS with flow directions at high angles relative to the dip of inclined surfaces indicating lateral accretion, and (3) a concave-up, arcuate geometry. Channels are ranked as *first-order*, *second-order* and *third-order* using a hierarchy based on (1) relative thicknesses of FUS, (2) facies character, (3) grain size, (4) sedimentary structures, (5) geometries, and (6) regional spatial relationships. Frequency relationships are inherent to a hierarchical classification (Catuneanu et al. 2009). First-order channels are expected to be the least frequent, second-order channels of a higher frequency, and third-order channels the most frequent. However, a difficulty arises when adapting a hierarchical scheme to ancient alluvial successions as preservation potential becomes a factor. This is in contrast to modern alluvial systems where channel geometries, channel-order, and channel frequency are evident in plan view (e.g. Fisk 1944; Morisawa 1985; Morisawa and Montgomery 1985; Roberts 1997; Morozova and Smith 2000; Olariu and Bhattacharya 2006). In the Prince Creek Fm., first-order channels appear less frequently than second- or third-order channels. However, second-order channels appear to be the most frequent

while third-order channels are of intermediate frequency. This is likely an artifact of the relatively poor preservation potential of third-order channels (see below) and we, therefore, choose to downplay apparent frequency in our hierarchical scheme.

First-order Channels.-

Large Sinuous Channels (FA-I) are the least frequently encountered in outcrop, exhibit FUS that are the thickest overall, contain the coarsest grain sizes in the region, and include sedimentary structures suggesting the highest flow velocities (Ethridge et al. 1981; Morisawa 1985; Morisawa and Montgomery 1985; Olariu and Bhattacharya 2006). Large Sinuous Channels (FA-I) of the Prince Creek Fm. are therefore interpreted as *first-order* meandering trunk channels. First-order trunk channels are composed of FUS that are > 13m-thick; at least twice the thickness of FUS found within second-order channels. First-order channels also contain basal pebble-to-boulder conglomerate and medium-grained sandbodies that exhibit the highest frequency of trough cross-lamination and convolute bedding. Sandbodies in first-order channels lack carbonaceous root traces suggesting greater depths and continuous flow. Conglomerate is noticeably absent in second- and third-order channels and no other channel type in the Prince Creek Fm. consistently contains grain sizes larger than fine-grained sand. Multi-storey sandbodies are also found exclusively within first-order channels. Large Sinuous Channel (FA-I) fills do not meet the requirements for incised valley fills (Gibling 2006) as their basal erosion surfaces are local phenomena and roughly scale to the depth of individual FUS.

Also FUS of Large Sinuous Channels (FA-I) are less than an order of magnitude greater than FUS of Small Sinuous Channels (FA-II).

Second-order Channels.-

Small Sinuous Channels (FA-II) have intermediate FUS thicknesses, intermediate grain sizes, and contain sedimentary structures suggesting intermediate or mixed flow velocities and are interpreted as *second-order* meandering distributary channels. FUS in second-order channels range in thickness from 1.5-5.0 m, thinner than first-order channels and generally thicker than third-order channels. Second-order channels also lack the conglomerate found in first-order channels, and all sandbodies are fine-grained and single-storey. Sedimentary structures include both trough cross-lamination and ripple cross-lamination; however ripple cross-lamination is most common. All second-order channels contain carbonaceous root-traces throughout, suggesting shallower depths than first-order channels and indicating possible fluctuating flow velocities and water depths within these channels.

Third-order Channels.-

Small Low-sinuosity Channels (FA-III) have the thinnest average FUS, the finest grain sizes, and sedimentary structures indicating the lowest average flow velocities of all channels and are interpreted as *third-order* fixed (anastomosed?) distributary channels.

FUS in third-order channels range in thickness from 1.5-3.0 m and have the thinnest average thickness of all channel types. Third-order channels lack the conglomerate of first-order channels and all sandbodies are single-storey and ubiquitously rooted. Ripple cross-lamination is the dominant sedimentary structure and trough cross-lamination is extremely rare. Third-order channels consistently lack the thick packages of IHS that dominate the deposits of first-order and second-order channels, suggesting that flow-velocities were generally lower than required for lateral channel migration.

Floodplains

Floodplains (FA-IV) of the Prince Creek Fm. were predominantly poorly drained and sporadically inundated with sediment. Large abandoned channels were present near trunk channels. Facies deposited in smaller abandoned channels, lakes, ponds, swamps, marshes, and mires are found interbedded with distributary channels, suggesting close spatial relationships between these environments. Crevasse splays frequently covered low areas with silt and sand. Bentonites and tuffs are preferentially preserved in lakes and ponds and are occasionally reworked into crevasse splays or preserved within fixed channels. Disturbed basal contacts are common in floodplain deposits, suggesting that dinosaurs occupied areas adjacent to major rivers and distributaries. Abundant root-traces indicate that vegetation grew in most environments on the floodplain.

Paleosols of the Prince Creek Fm. are cumulative, and poorly developed. Detailed descriptions, geochemistry, and mineralogy of paleosols near KKT (Fig. 2.2) are

presented elsewhere (Brandlen 2008; Fiorillo et al. 2009). Drab-colored fine-grained sediments, well-preserved carbonaceous plant material, and abundant siderite nodules suggest poorly drained conditions and shallow standing water typical of wetlands (Bown and Kraus 1987; Kraus 1987; Kraus and Bown 1988; Retallack 2001; Ashley et al. 2004; Rajchl and Uličný 2005). Jarosite, an oxidation product of pyrite (Kraus 1998, Davies-Vollum 1999, Krause and Hasiotis 2006), becomes more common up section in the Prince Creek Fm. as strata approach the contact with the shallow-marine shoreface successions of the Schrader Bluff Fm. The presence of jarosite may signal the intermixing of marine/tidal waters with pore fluids in floodplain sediments (Wright 1986, Ufnar et al. 2001, McCarthy and Plint 2003). Micromorphological features of paleosols include microscopic, ovoid elliptical burrows (up to 0.5 mm in diameter) attributed to insects and earthworms (McCarthy and Plint 2003), ferruginous void and grain coatings and nodules, mottled soil aggregates and depletion features as well as evidence of illuvial clay coatings in voids. These features suggest that floodplains were subjected to fluctuating drainage conditions, or perhaps seasonally dry conditions, with significant portions of the floodplain drying out for a period of time (McCarthy et al. 1998; Brandlen 2008; Fiorillo et al. 2009; Fiorillo et al. 2010).

The relatively thin coals in the study area may be the result of repeated episodes of sediment influx onto the floodplain during floods, retarding prolonged peat production (Flores 1984, Fielding 1987b; Spicer 2003; Fiorillo et al. 2010). Additionally, fluctuating groundwater-levels and periodic drying out of floodplain sediments (Spicer 2003; Fiorillo

et al. 2009, 2010) may also have limited peat production and preservation (Diessel 1992; van Asselen et al. 2009).

Crevasse Splays and Crevasse Splay Complexes

Crevasse splays are defined as sheet sandbodies that are lobate or elongate in plan view, lenticular or lens-shaped along strike, and interdigitate with finer-grained floodplain deposits (Fisk 1944; Coleman and Gagliano1964; Allen 1965b; Elliott 1974; Collinson 1978; Bridge 1984; Smith et al. 1989; Mjøs et al. 1993; Jorgensen and Fielding 1996; Morozova and Smith 2000). Some authors separate crevasse splays into two categories: (1) "small-scale" or simple crevasse splays and (2) large-scale composite crevasse splays or "crevasse splay complexes" (Elliott 1974; Fielding 1987a; Smith et al. 1989; Mjøs et al. 1993; Smith and Pêrez-Arlucea 1994). Smith et al. (1989) in their study of crevasse splays from the Cumberland Marshes point out that the development of crevasse splays on an alluvial plain is typically not an event but rather a complex evolutionary process. They identify three stages in the formation of splays adjacent to trunk channels. Stage I splays are the smallest, record initial crevassing of the trunk channel, and typically consist of a relatively thin, lobate, lenticular (along strike) sheet sandbody that lies directly on older floodplain sediments. In contrast, Stage II splays may be best described as "splay complexes" as they are larger, evolve from Stage I splays, and are composed of a network of active and abandoned channels. Stage III splays evolve from Stage II splays and exhibit lower channel densities than Stage II

splays. With additional flow velocity redirected through the crevasse channel, Stage III splays may capture the main flow of a channel during channel avulsion.

The Prince Creek Fm. contains Large Sinuous Channels (FA-I) which we classify as first-order meandering trunk channels (Figs. 2.6A, 2.12) and thin, laterally extensive, ripple cross-laminated sheet-like sandbodies (small-scale splays of FA-IV, Figs. 2.9A, 2.15) that we interpret as Stage I splays (Smith et al. 1989). In addition to these smaller Stage I or "small-scale" splays, second-order meandering distributaries and third-order fixed (anastomosed?) distributaries of the Prince Creek Fm. construct larger "splay complexes" adjacent to trunk channels, similar to Stage II splays described by Smith et al. (1989). Evidence in the Prince Creek Fm. for construction of these splay complexes includes: (1) meandering distributaries (FA-II) and fixed (anastomosed?) distributaries (FA-III) eroded into and encased in organic-rich floodplain deposits throughout the succession (Figs. 2.10, 2.12, 2.13, 2.14) indicating deposition of coarser-grained facies onto finer-grained floodplains; (2) distributary channels deposited as laterally-extensive sheets that commonly exhibit lenticular or lens-shaped geometries when viewed in orientations oblique to strike (Fig. 2.13) which are similar to geometries expected for crevasse splay lobes in cross section; (3) distributaries incised into sheet sandstones of FA-IV (Fig. 2.14) suggesting a common, genetic relationship between smaller channels and small-scale Stage I splays; (4) distributaries incised into pre-existing distributary channels (Figs. 2.7A, 2.7C, 2.12) which most likely record the reworking of splay complexes by distributary channels; and (5) tiers of fixed, ribbon-form distributaries (FA-

III) in close proximity to each other at the same stratigraphic level (Fig. 2.14) suggestive of anastomosed channels.

The geometries of sandbodies constructed by distributary channels of the Prince Creek Formation are similar to those found in numerous descriptions of crevasse splay complexes (Fisk 1944; Coleman and Gagliano1964; Fielding 1984; Fielding 1986; Smith et al. 1989; Jorgensen and Fielding 1996; Bristow et al. 1999; Pêrez-Arlucea and Smith 1999; Morozova and Smith 2000; Stouthamer 2001; Tooth 2005). Crevasse splays of the Prince Creek Fm. likely began as Stage I splays similar to those described by Smith et al. (1989). With increased discharge through the crevasse channel, Stage I splays evolved into Stage II crevasse splay-complexes through the formation of a series of fixed channels that incised into the Stage I splay in areas proximal to the trunk channel, and into floodplain deposits at more distal locations. The flow in these channels either did not achieve sufficient velocities for the channels to begin to wander on the fine-grained floodplain, or lateral migration was inhibited by vegetation such as peat (Smith 1976; Kirschbaum and McCabe 1992; Törnqvist 1993; Nadon 1994). However, as additional flow was diverted into the crevasse channel, and as flow velocities and sedimentation increased, channels on the splay complex began to wander, ultimately evolving into meandering channels. This change in channel-form may have been driven, in part, by peat compaction (Smith and Pêrez-Arlucea 2004; Rajchl and Uličný 2005; van Asselen et al. 2009). When subjected to a load, peat compacts (Tatsch 1980; Elliott 1985; Diessel 1992; Allen 1999; van Asselen et al. 2009). It has been suggested that peat compaction can play a role in shaping stratal geometries by controlling accommodation space and

inhibiting channel incision (Diessel 1992; Michaelsen et al. 2000; Smith and Pêrez-Arlucea 2004; Rajchl and Uličný 2005; van Asselen et al. 2009). As flow velocities and sedimentation rates in distributary channels on the crevasse splay complex increase, peat is compacted below the channel-fills and, ultimately, peat compaction ceases, which limits accommodation (Elliott 1985; van Asselen et al. 2009). This compacted peat layer inhibits vertical scouring at the base of the channel and promotes lateral migration (Smith and Pêrez-Arlucea 2004; van Asselen et al. 2009). Accretion within these channels transitions from predominantly vertical to principally lateral, producing sheet-like sandbodies with point bars and high width-to-depth ratios (Smith and Pêrez-Arlucea 2004; Rajchl and Uličný 2005; van Asselen et al. 2009). Lateral migration of the channel continues until the peat layer below the thalweg is breached or the channel is abandoned (Smith and Pêrez-Arlucea 2004). During this stage in the evolution of the crevasse splay complex both fixed and meandering distributary channels may have been active at different locations depending on flow velocities in distributary channels, local accommodation and the depth to the peat layer, and local substrate conditions (i.e. sand- or mud-rich). With additional discharge diverted through the crevasse channel an avulsion might have occurred (Morozova and Smith 2000; Stouthamer 2001). Alternatively, the main crevasse channel could have become plugged by sediment, forcing abandonment of the splay complex. In the event of rapid abandonment, meandering distributaries and/or fixed distributaries would fill with fine-grained sediment and floodplain facies would be deposited above the abandoned splay complex (e.g. Coleman and Gagliano 1964; Smith and Pêrez-Arlucea 1994, 2004; Pêrez-Arlucea and

Smith 1999; Morozova and Smith 2000). In the event of a slow abandonment, the cycle of deposition would reverse itself, driving the system back through the fixed (anastomosed?) splay complex, Stage I splay formation, and ultimately deposition of floodplain facies. In either scenario, the preservation potential for fixed (anastomosed?) distributaries may be lower than the preservation potential for meandering distributaries based on (1) their stratigraphic position below, or possibly adjacent to, higher-energy meandering distributaries on the splay-complex that could capture the bulk of the flow (Pêrez-Arlucea and Smith 1999), (2) their relatively narrow cross section and lack of lateral accretion (Smith and Pêrez-Arlucea 2004), or (3) in the case of a slow abandonment, their relatively shallow depths and increased height relative to the thalweg of the main channel and base level (Reading 1996; Bridge 2003; Kjemperud et al. 2008). The preservation potential for fixed (anastomosed?) distributaries is decreased further in the event of the reactivation of a formerly active crevasse channel with flow velocities and sedimentation rates sufficient to cause lateral migration and scouring of the splay-complex or avulsion (Smith et al. 1989; Morozova and Smith 2000; Stouthamer 2001; Smith and Pêrez-Arlucea 2004).

The exact reason for the crevassing of trunk channels in the Prince Creek Fm. is unknown, however high concentrations of suspended load along with abundant mud and volcanic ash in channels may have been a contributing factor. Seasonality brought about by the high-latitude (paleo-Arctic) setting (Spicer et al. 1992; Spicer 2003) may have driven snowmelt in the Brooks Range and triggered spring floods which subsequently carved splay channels.

Inclined Heterolithic Stratification in the Prince Creek Formation

IHS is defined as "large-scale, waterlain, lithologically heterogeneous siliciclastic sedimentary sequences whose constituent strata are inclined at an original depositional angle to the horizontal or paleohorizontal" (Thomas et al. 1987, p. 125). Typically, IHS is composed of a series of repeating sand-mud or silt-mud couplets inclined relative to a basal, horizontal erosion surface. Recognizing IHS in a sedimentary succession is important because the physical properties of the IHS can be used to identify the likely depositional environment. For example, paleoflow at high angles to the dip of the inclined beds indicates lateral accretion in point bars while paleoflow at low angles relative to the dip of inclined beds indicates downstream accretion in mid-channel bars or Gilbert-type deltas (Allen 1963; Stanley and Surdam 1978). IHS successions in the Prince Creek Fm. fine-upward (e.g. Fig 2.5A, 2.6A) and paleoflow is consistently at high angles to the dip of the inclined beds suggesting that IHS records lateral migration of point bars (Allen 1965a; Stanley and Surdam 1978; Thomas et al. 1987).

Although IHS has been recognized in purely fluvial environments (Stewart 1981; Jackson 1981; Arche 1983; Page et al. 2003), the majority of IHS is attributed to tidally-influenced settings (Thomas et al. 1987; Smith 1987, 1988; Nio and Yang 1991; Nakajo 1998; Rogers 1998; Changsong et al. 1995; Choi et al. 2004; Joeckel et al. 2005; Yang et al. 2007; Dalrymple and Choi 2007; Hovikoski et al. 2008). In fact the recognition of IHS has played a key role in the reinterpretation of some coastal plain successions as

tidally influenced (e.g. the McMurray Formation of Alberta: Mossop and Flach 1983; Flach and Mossop 1985; Crerar 2003; Crerar and Arnott 2007). On low-gradient coastal plains the tidal zone may reach tens to hundreds of kilometers inland with highly-sinuous meandering channels being common, especially in the landward reaches of tidal influence where tidal current speeds decrease (Dalrymple et al. 1992; Orton and Reading 1993; Eberth 1996; Crerar 2003; Dalrymple and Choi 2007). High levels of suspended sediment are common on delta-plains where high suspended sediment concentrations and thick mud drapes on point bars are driven in part by a low gradient and river/tidal interaction in the transition between the terrestrial and marine zones (Schumm 1968; Schumm and Kahn 1972; Smith 1987, 1988; Baker et al. 1995; Dalrymple and Choi 2007). Mud drapes on lateral accretion surfaces have been attributed to tidal influence in delta distributary channels (Smith 1987, 1988; Wood et al. 1988; Gastaldo et al. 1995; Changsong et al. 1995; Nakajo 1998; Rogers 1998; Makaske and Weerts 2005; Joeckel et al. 2005; Hovikoski et al. 2008). Although mud drapes do occur on point-bar surfaces in purely fluvial deposits (e.g. Jackson 1981), they are not as abundant or as thick as those deposited during slackwater periods in tidally-influenced deposits (Thomas et al. 1987; Wood et al. 1988; Dalrymple and Choi 2007). Rounded mud pebbles and fluid muds are also very common in this environment (Baker et al. 1995; Dalrymple and Choi 2007; Bhattacharya and MacEachern 2009). The bulk of the channels of the Prince Creek Fm. are classified as highly sinuous, transported a large percentage of their sediment as suspended load, and contain thick mud drapes on point bar surfaces (Fig. 2.15) and rounded mudstone pebbles (Fig.2.5E) similar to tidally-influenced channels.

Figure 2.15. Rhythmically-repeating centimeter to decimeter-scale sandstone-mudstone couplets on point bar deposits (IHS) common to the Prince Creek Formation. Sand-rich beds in image appear more resistant while clay-rich beds are more easily eroded.

IHS containing rhythmic-style repetition of coarse-to-fine couplets is present at some stratigraphic level in all three orders of channels (Figs. 2.5A, 2.6A, 2.7C) indicating that all three types of channels (including Small Low-sinuosity Channels of FA-III) migrated laterally during some period in their evolution (Smith 1987, 1988; Dalrymple and Choi 2007) and likely experienced tidal effects that affected deposition (Thomas et al. 1987; Smith 1987, 1988; Gastaldo et al. 1995; Makaske and Weerts 2005).

Faunal assemblages of the Prince Creek Fm. when encountered are extremely high dominance, low diversity and suggest biologically-stressed brackish water conditions (pers. comm. Robert Blodgett). Bioturbation of sediments is often low in tidally-influenced channels due to stressed environments characteristic of turbid, brackish water conditions (Dalrymple and Choi 2007). Bivalves and gastropods are most tolerant of these stressed conditions (MacEachern et al. 2005; Dalrymple and Choi 2007). Bioturbation is rare in channel deposits of the Prince Creek Fm. and bivalves and gastropods, although rare, are the most common invertebrates and are most likely responsible for bioturbation in channel sediments.

Although we recognize that the thickness of mud-drapes and other fine-grained laminae should be demonstrably cyclic in order to conclusively infer tidal influence on a system (Dalrymple and Choi 2007), we consider that the large relative thickness of mud drapes on point bar surfaces and the rhythmically-repetitive nature of the coarse-to-fine couplets in the IHS is such that tidal influence is the best explanation for prominent IHS in the Prince Creek Fm.

Depositional Model for the Prince Creek Formation

A depositional model for the Prince Creek Fm. in the Colville River region is presented in Figure 2.16. The figure includes a large, sinuous meandering trunk channel (FA-I) along with crevasse splays, crevasse splay-complexes, and associated floodplain deposits. Flow was directed from the southwest to the northeast and fluctuated seasonally(?). Tidal effects entered the system from the northeast. Levees (F-5) extend outward from the main channel. Abandoned channels, smaller lakes, ponds, mires, swamps and paleosols (FA-IV) are widespread on the floodplain (F-6a, F-6b, F-7a, F-7b, F-8, F-9, and F-10). Initially, a small crevasse channel is open and crevassing occurs as a small-scale crevasse splay (F-4, F-6b) or Stage I splay of Smith et al. (1989). As discharge and sediment influx through the crevasse channel increases, fixed (anastomosed?) channels (FA-III) form on the splay-complex and likely extend onto the distal floodplain. Floodplain facies are deposited adjacent to splay complexes. With additional discharge and sediment influx, peat compacts below distributary channels until maximum compaction is achieved, limiting accommodation space. Distributary channels begin to wander, and a meandering distributary channel (FA-II) replaces the fixed (anastomosed?) distributaries (FA-III) on the splay complex. With an additional increase in discharge through the crevasse channel an avulsion of the main channel would occur. Alternatively, if the crevasse channel is blocked and discharge decreases, fixed (anastomosed?) distributaries (FA-III) would reoccupy the splay complex and incise

Figure 2.16 (Following Page). Depositional model for the Prince Creek Formation in the Colville River region of Northern Alaska. Abbreviations and descriptions of facies and facies associations are included in Table 2.1 and Table 2.2.

Decreasing discharge and sediment influx through crevasse channel
Increasing discharge and sediment influx through crevasse channel
Avulsion
FA-IV
FA-II
FA-III
FA-I
F4-F6b
1.5 km
SW
NE
Seasonally(?) Fluctuating Flow
Tidal Influence

into previously deposited meandering distributaries (FA-II). With a further decrease in discharge a Stage I splay (small-scale splay of FA-IV) reoccupies a portion of the splay complex. If the crevasse channel is blocked completely, overbank sedimentation on floodplains and/or in interdistributary bays becomes the dominant mode of deposition.

Although the meandering distributary channels (FA-II) of the Prince Creek Fm. are classified as broad ribbons (Gibling 2006), in actuality point bar deposits of these systems create laterally extensive, asymmetrical, lenticular, heterolithic sheets that pinch out into floodplain deposits. These lenticular sheets may contain incised, fixed (anastomosed?) distributaries (FA-III) and are separated from each other by organic-rich floodplain facies (FA-IV) which may also be incised by tiers of fixed (anastomosed?) distributaries. Deposits of larger meandering trunk channels (FA-I) are rare, thicker, regionally restricted, and alternate with all other deposits in the area.

This depositional model is compatible with the findings of Phillips (2003) who suggests that the uppermost facies of the Prince Creek Fm. to the northeast of the study area at Ocean Point (Figs. 2.1, 2.2) were deposited in meandering distributaries and within interdistributary bays transgressed by shallow-marine deposits of the Schrader Bluff Fm. Interdistributary bay deposits increase in abundance up-section in the Prince Creek Fm. with brackish-water indicators such as clams, gastropods, jarosite, and vivianite becoming more common. The entire Prince Creek Fm. generally fines-upward from conglomeratic sands that fill incised valleys at the base (Flores et al. 2007a, 2007b) to finer-grained, interdistributary facies with brackish water indicators at the top

(Brouwers and de Deckker 1993; Phillips 2003). Tidally-influenced deposits would be expected on the muddy, low-gradient coastal plain during this period of base level rise culminating in an apparent marine transgression.

CONCLUSIONS

The Late Cretaceous (Maastrichtian) Prince Creek Formation in the Colville River Region of northern Alaska is an alluvial succession on a coastal plain containing (i) first-order, larger, sinuous meandering trunk channels, (ii) smaller, second-order, sinuous meandering distributary channels, (iii) third-order, fixed (anastomosed?) distributary channels and (iv) organic-rich floodplains.

First-order meandering trunk channels are regionally restricted, exhibit the thickest FUS, contain the largest clasts and coarsest grain sizes, exhibit an interval of IHS indicative of lateral accretion, display thick mud drapes on point bars, and include sedimentary structures that indicate the highest flow velocities in the region. Sandbodies within trunk channels are multi-storey and lack root-traces, also suggesting high flow velocity within relatively deep channels.

Second-order meandering distributary channels exhibit smaller FUS, lack conglomerates, and include sedimentary structures indicative of intermediate flow velocities. Meandering distributaries are single-storey and composed predominantly of

IHS with thick mud drapes (point bars) along with mud-filled abandoned channels common to sinuous channels.

Fixed (anastomosed?) distributaries display the smallest FUS, include sedimentary structures indicative of the lowest flow velocities, and lack prominent IHS, demonstrating that they were filled predominantly by vertical rather than lateral accretion.

Both meandering and fixed (anastomosed?) distributaries contain carbonaceous root-traces throughout the channel–fill succession suggesting shallower water-levels and/or fluctuating flow.

Abundant, thin sheet sandbodies are interpreted as crevasse splays and levees. Organic-rich siltstone and mudstone, carbonaceous shale, coal, bentonite, and tuff interpreted as abandoned channels, small lakes, ponds, swamps, marshes, mires, paleosols, and ashfall deposits.

Meandering distributaries typically appear lenticular along strike, erode into pre-existing distributary deposits, and interfinger with and incise into organic-rich floodplain facies. Fixed (anastomosed?) distributaries either incise into meandering distributary deposits or into organic-rich floodplain facies. Multiple fixed (anastomosed?) distributaries may be preserved in tiers at the same stratigraphic level. Spatial relationships between channels and floodplains indicate that the bulk of deposition in the Prince Creek Fm. occurred on crevasse splay-complexes adjacent to trunk channels. Splay-complexes were constructed above organic-rich floodplain deposits by the lateral

migration of meandering distributaries and the vertical filling of anastomosed distributaries. Flow within meandering and fixed (anastomosed?) distributaries may have been contemporaneous or, alternatively, fluctuating discharge through the main crevasse channel and peat compaction may have controlled the type of system dominating the splay-complex.

IHS is found in all three orders of channels. Thick mud drapes on point bars and the rhythmic and repetitive nature of the coarse-to-fine couplets in the IHS suggest that flow within channels was likely influenced by tidal effects. Common jarosite and vivianite also suggest an influx of marine waters at the distal end of the system.

Drab colors in paleosols and fine-grained sediments, abundant carbonized plant material, and common siderite nodules suggest that floodplains were wet and reducing conditions were widespread. However, carbonaceous root traces throughout most fine-grained facies and within all distributary channels along with Fe-oxide mottles and illuvial clay coatings in paleosols, indicate that the alluvial system likely experienced flashy, seasonal, or ephemeral flow and a fluctuating water table. The flashy nature of this arctic alluvial system may have been driven by seasonal snowmelt in the evolving Brooks Range orogenic belt as a consequence of the high paleolatitude of the Prince Creek Fm. near the end of the Cretaceous Period.

ACKNOWLEDGMENTS

This research is part of the doctoral dissertation of Peter P. Flaig. This project was funded through the National Science Foundation Office of Polar Programs grants OPP-425636 to McCarthy and OPP-424594 to Fiorillo. Additional funding was provided by the Geist Fund at the University of Alaska Museum of the North, the Alaska Geologic Society, the University of Alaska-Fairbanks Graduate School Fellowship Program, the Geological Society of America, the Evolving Earth Foundation, and BP America. Logistical support was provided by the Barrow Arctic Science consortium (BASC), CH2M Hill (formerly Veco Polar Resources), Wrights Air, Air Logistics, Alaska Air Taxi, Evergreen Helicopters, and the support staff at Umiat, Alaska. We thank Dolores van der Kolk, Thomas Adams, David Norton, Roland Gangloff, Douglas Hissom, Susi Tomsich, and Jason Addison, for their diligent assistance in the field. We also thank David Houseknecht, Paul Decker, Marwan Wartes, and Charles "Gil" Mull for enlightening discussions regarding the evolution of the Colville Basin and the Cretaceous stratigraphy of Alaska. This manuscript benefitted greatly from insightful and helpful reviews by Guy Plint and Gary Hampson.

REFERENCES

Abbado, D., Slingerland, R., and Smith, N.D., 2005, Origin of anastomosis in the upper Columbia River, British Columbia: Special Publication of the International Association of Sedimentologists, No. 35, p. 3-15.

Allen, J.R.L., 1963, The classification of cross-stratified units with notes on their origin: Sedimentology, v. 2, p. 93-114.

Allen, J.R.L., 1964, Studies in fluvitile sedimentation: Six cyclothems from the lower Old Red Sandstone, Anglo-Welsh Basin: Sedimentology, v. 3, p. 163-198.

Allen, J.R.L., 1965a, Fining upward cycles in alluvial successions: Geological Journal, v. 4, p. 229-246.

Allen, J.R.L., 1965b, A review of the origin and characteristics of recent alluvial sediments: Sedimentology, v. 5, p. 89-191.

Allen, J.R.L., 1970, Studies in fluvitile sedimentation; a comparison of fining-upwards cyclothems, with special reference to coarse-member composition and interpretation: Journal of Sedimentary Petrology, v. 40, p. 299-323.

Allen, J.R.L., 1999, Geological impacts on coastal wetland landscapes: some general effects of sediment autocompaction in the Holocene of northwest Europe: The Holocene, v. 9, No. 1, p. 1-12.

Arche, A., 1983, Coarse-grained meander lobe deposits in the Jarma River, Madrid, Spain, *in* Collinson, J.D., and Lewin, J., eds., Modern and Ancient Fluvial Systems: International Association of Sedimentologists Special Publication 6, p. 313-321.

Ashley, G.M., Maitima Mworia, J., Musya, A.M., Owens, R.B., Driese, S.G., Hover, V.C., Renaut, R.W., Gowan, M.F., Mathai, S., and Blatt, S.H. 2004, Sedimentation and recent history of a freshwater wetland in a semi-arid environment: Lobi Swamp, Kenya, East Africa: Sedimentology, v. 55, p. 1301-1321.

Astin, T.R., 1990, The Devonian lacustrine sediments of Orkney, Scotland; Implications for climate cyclicity, basin structure, and maturation history: Journal of the Geological Society of London, v. 147, p. 141–151.

Avanzini, M., Frisa, S., van den Driessche, K., Keppens, E., 1997, A dinosaur tracksite in An Early Liassic tidal flat in Northern Italy: Paleoenvironmental reconstruction from sedimentology and geochemistry: Palaios v. 12, p. 538-551.

Baker, E.K., Harris, P.T., Keene, J.B., and Short, S.A., 1995, Patterns of sedimentation in the macrotidal Fly River delta, Papua New Guinea, *in* Flemming, B.W., and Bartholomä, A., eds., Tidal Signatures in Modern and Ancient Sediments: Special Publication of the International Association of Sedimentologists, v. 24, p. 193-211.

Banks, N.L., 1973, The origin and significance of some downcurrent-dipping cross-stratified sets: Journal of Sedimentary Petrology, v. 43, No. 2, p. 423-427.

Barrett, P.J., 1970, Paleocurrent analysis of the mainly fluvitile Permian and Triassic Beacon rocks, Beardmore Glacier area, Antarctica: Journal of Sedimentary Petrology, v. 40, No.1, p. 395-411.

Besly, B.M., and Collinson, J.D., 1991, Volcanic and tectonic controls of lacustrine and alluvial sedimentation in the Stephanian coal-bearing sequence of the Malpas–Sort basin, Catlonian Pyrenees: Sedimentology, v. 38, No. 1, p. 3–26.

Besse, J., and Courtillot, V., 1991, Revised and synthetic apparent polar wander paths of the African, Eurasian, North American and Indian plates, and true polar wander since 200 Ma: Journal of Geophysical Research, v. 96, p. 4029-4050.

Bhattacharya, J.P., and MacEachern, J.A., 2009, Hyperpycnal rivers and prodeltaic shelves in the Cretaceous Seaway of North America: Journal of Sedimentary Research, v. 79, p. 184-209.

Bird, K.J., 2001, Alaska—A twenty-first-century petroleum province, *in* Downey, M.W., Threet, J.C., and Morgan, W.A., eds., Petroleum provinces of the twenty-first century: American Association of Petroleum Geologists Memoir 74, p. 137–165.

Black, R.F., 1964, Gubik Formation of Quaternary age in northern Alaska: US Geological Survey Professional Paper 302-C, p. 59–91.

Bown, T.M. and Kraus, M.J. 1987, Integration of channel and floodplain suites I. Developmental sequence and lateral relations of alluvial paleosols: Journal of Sedimentary Petrology, v. 57, p. 587-601.

Brandlen, E., 2008, Paleoenvironmental reconstruction of the Late Cretaceous (Maastrichtian) Prince Creek Formation, near the Kikak-Tegoseak dinosaur quarry, North Slope, Alaska: Unpublished Master's Thesis, University of Alaska-Fairbanks, Fairbanks, Alaska, 225 p.

Bridge, J.S., 1984, Large scale facies sequences in alluvial overbank environments: Journal of Sedimentary Petrology, v. 54, No. 2, p. 583-588.

Bridge, J.S., 1985, Paleochannel patterns inferred from alluvial deposits; a critical evaluation: Journal of Sedimentary Petrology, v. 55, No, 4, p. 579-589.

Bridge, J.S., 2003, Rivers and Floodplains, Forms, Processes, and Sedimentary Record: Malden, MA, Blackwell Science Ltd., 491 p.

Bridge, J.S., and Mackey, S.D., 1993. A theoretical study of fluvial sandbody dimensions, *in* Flint, S.S., and Bryant, I.D. eds., The geologic modeling of hydrocarbon reservoirs and outcrop analogues: International Association of Sedimentologists Special Publication 15, p. 213–236.

Bridge, J.S., Guillermo, A.J., and Georgieff, S.M., 2000, Geometry, lithofacies, and spatial distribution of Cretaceous fluvial sandstone bodies, San Jorge Basin, Argentina: Outcrop analog for the hydrocarbon-bearing Chubut Group: Journal of Sedimentary Research, v. 70, No. 2, p. 341-359.

Bristow, C.S., Skelly, R.L., and Ethridge, F.G., 1999, Crevasse splays from the rapidly aggrading, sand bed, braided, Niobrara River, Nebraska: effect of base level rise: Sedimentology, v. 46, p. 1029-1047.

Brosge, W.P., Whimington, C.L., and Morris, R.H., 1966, Geology of the Umiat-Maybe Creek region, Alaska: Geological Survey Professional Paper 303-H, p. 548-570.

Brouwers, E.M., Clemens, W.A., Spicer, R.A., Ager, T.A., Carter, L.D., and Sliter, W.V., 1987, Dinosaurs on the North Slope, Alaska: High latitude, latest Cretaceous environments: Science, v. 25, p. 1608-1610.

Brouwers, E.M., and de Deckker, P., 1993, Late Maastrichtian and Danian ostracod faunas from northern Alaska: Reconstructions of environment and paleogeography: Palios, v. 8, p. 140-154.

Burns, W.M., Hayba, D.O., Rowan, E.L., and Houseknecht, D.W., 2005, Estimating the amount of eroded section in a partially exhumed basin from geophysical well logs: an example from the North Slope, United States Geological Survey Special Paper 1732-D, p. 1-18.

Catuneanu, O., Abreu, V., Bhattacharya, J.P., Blum, M.D., Dalrymple, R.W., Eriksson, P.G., Fielding, C.R., Fisher, W.L., Galloway, W.E., Gibling, M.R., Giles, K.A., Holbrook, J.M., Jordan, R., Kendall, C.G.St.C., Macurda, B., Martinsen, O.J., Miall, A.D., Neal, J.E., Nummendal, D., Pomar, L., Posamentier, H.W., Pratt, B.R., Sarg, J.F., Shanley, K.W., Steel, R.J., Strasser, A., Tucker, M.E., and Winker, C., 2009, Towards the standardization of sequence stratigraphy: Earth Science Reviews, v. 92, p. 1-33.

Changsong, L., Sitian, L., and Zhen, L., 1995, Facies architecture, stratigraphic sequences, and coal occurrences in the Late Carboniferous and Early Permian delta complexes of the North Huabei Basin, China, *in* Oti, M.N., and Potsma, G.P., eds., Geology of Deltas: A.A. Balkema, Netherlands p. 125-138.

Chevren, V.B., 1978, Fluvial and deltaic facies in the Sentinel Butte Formation, central Williston Basin: Journal of Sedimentary Petrology, v. 48, No. 1, p.159-170.

Choi, K.S., Dalrymple, R.W., Seung, S.C., and Seong-Pil, K., 2004, Sedimentology of modern inclined heterolithic stratification (IHS) in the macrotidal Han River Delta, Korea: Journal of Sedimentary Research, v. 74, No. 5, p. 677-689.

Clemens, W.A., and Nelms, L.G., 1993, Paleoecological implications of Alaskan terrestrial vertebrate fauna in latest Cretaceous time at high paleolatitudes: Geology, v. 21, p. 503–506.

Cole, F., Bird, K.J., Toro, J., Roure, F., O'Sullivan, P.B., Pawlewicz, M., and Howell, D.G., 1997, An integrated model for the tectonic development of the frontal Brooks Range and Colville Basin 250 km west of the Trans-Alaska Crustal Transect: Journal of Geophysical Research, v. 102, No. B9, p. 20,685–20,708.

Coleman, J.M., and Gagliano, S.M., 1964, Cyclic sedimentation in the Mississippi River deltaic plain: Transactions - Gulf Coast Association of Geological Societies, v. 14, p. 67-80.

Coleman, J.M., Gagliano, S.M., and Webb, G.E., 1964, Minor sedimentary structures in a prograding distributary: Marine Geology, v. 1, No. 3, p. 240-258.

Collinson, J.D., 1978, Vertical sequence and sand body shape in alluvial sequences, *in* Miall, A.D., ed., Fluvial Sedimentology: Canadian Society of Petroleum Geologists Memoir 5, p. 577–587.

Collinson, J.W., Isbell, J.L., Elliot, D.H., Miller, M.F., and Miller, J.M.G., 1994, Permian- Triassic Transantarctic basin, *in* Veevers, J.J., and Powell, C.M., eds., Permian-Triassic Pangean basins and foldbelts along the Panthalassan margin of Gondwanaland: Geological Society of America Memoir 184, p. 173–222.

Conrad, J.E., McKee, E.H. and Turrin, B.D., 1990, Age of tephra beds at the Ocean Point Dinosaur Locality, North Slope, Alaska, based on K-Ar and $^{40}Ar/^{39}Ar$ Analyses: United States Geological Survey Bulletin 1990-C, p. 1–12.

Crerar, E.E., 2003, Sedimentology and stratigraphic evolution of a tidally-influenced marginal-marine complex: the Lower Cretaceous McMurray Formation, Athabasca oil sands deposit, northeastern Alberta: Unpublished Master's Thesis, University of Ottawa, Ottawa, ON, Canada, 309 p.

Crerar, E.E., and Arnott, R.W.C., 2007, Facies distribution and stratigraphic architecture of the Lower Cretaceous McMurray Formation, Lewis Property, northeastern Alberta: Bulletin of Canadian Petroleum Geology, v. 55, No. 2, p. 99-124.

Dalrymple, R.W., Zaitlin, B.A., and Boyd, R., 1992, Estuarine facies models: Conceptual, basis, and stratigraphic applications: Journal of Sedimentary Petrology, v. 62, No. 6, p. 1130-1146.

Dalrymple, R.W., and Choi, K., 2007, Morphologic and facies trends through the fluvial-marine transition in tide-dominated depositional systems: A schematic framework for environmental and sequence-stratigraphic interpretation: Earth Science Reviews, v. 81, p. 135-174.

Davies-Vollum, K.,1999, The formation of beds underlying carbonaceous shales as Aquic paleosols: examples from the Bighorn Basin of Wyoming: International Journal of Coal Geology, v. 41, p. 239-255.

Decker, P. L., 2007, Brookian Sequence stratigraphic correlations, Umiat Field to Milne Point Field, west-central North Slope, Alaska: Preliminary Interpretive Report 2007-2, Alaska Department of Natural Resources, Fairbanks, Alaska, 21 p., 1 map.

Decker, P.L., LePain, D.L., Wartes, M.A., Gillis, R.J., Mongrain, J.R., Kirkham, R.A., and Schellenbaum, D.P., (in press), Sedimentology, stratigraphy, and subsurface expression of Upper Cretaceous strata in the Sagavanirktok River area, east central North Slope, Alaska, *in* Wartes, M.W., and Decker, P.L., eds., Preliminary results of recent geologic field investigations in the Brooks Range foothills and North Slope, Alaska: Alaska Division of Geologic & Geophysical Surveys Preliminary Interpretive Report 2009-1C, 3 sheets.

Deconto, R.M., Brady, E.C., Bergengren, J., and Hay, W.W., 2000, Late Cretaceous climate, vegetation, and ocean interactions, *in* Huber, B.T., MacLeod, K.G., and Wing, S.L., 2000, Warm Climates in Earth History: Cambridge University Press, Cambridge, UK, p. 275-296.

Detterman, R.L., Bickel, R.S., and Gryk, G., 1963, Geology of the Chandler River region, Alaska: United States Geological Society Special Paper 303-E, p. 223-324.

Diessel, C.F.K., 1992, Coal-bearing depositional systems: Berlin, Springer-Verlag, 721 p.

Driese, S.G., and Ober, E.G., 2005, Paleopedologic and paleohydrologic records of precipitation seasonality from Early Pennsylvanian "underclay" paleosols, U.S.A: Journal of Sedimentary Research, v. 75, p.997-1010.

Eberth, D.A., and Miall, A.D., 1991, Stratigraphy, sedimentology, and evolution of a vertebrate-bearing braided to anastomosed fluvial system, Cutler Formation (Permian-Pennsylvanian), north-central New Mexico: Sedimentary Geology, v. 72, p. 225-252.

Eberth, D.A., 1996, Origin and significance of mud-filled incised valleys (Upper Cretaceous) in southern Alberta, Canada: Sedimentology, v. 43, p. 459-477.

Elliott, T., 1974, Interdistributary bay sequences and their genesis: Sedimentology, v. 21, p. 611-622.

Elliott, T., 1976, The morphology, magnitude, and regime of a Carboniferous fluvial-distributary channel: Journal of Sedimentary Petrology, v. 46, No. 1, p. 70-76.

Elliott, R.E., 1985, Quantification of peat to coal compaction stages, based especially on the phenomena in the East Pennine Coalfield, England: Proceedings of the Yorkshire Geological Society, v. 45, part 3, p. 163-172.

Ethridge, F.G., and Schumm, S.A., 1978, Reconstructing paleochannel morphologic and flow characteristics; methodology, limitations and assessment: Memoir – Canadian Society of Petroleum Geologists, No.5, p.703-721.

Ethridge, F.G., Jackson, T.J., and Youngberg, A.D., 1981, Floodbasin sequence of a fine-grained meander belt subsystem: The coal-bearing Lower Wasatch and Upper Fort Union Formations, southern Powder River Basin, Wyoming, *in* Ethridge, F.G., and Flores, R.M. eds., Recent and ancient nonmarine depositional environments; models for exploration: Special Publication of the Society of Economic Paleontologists and Mineralogists, v. 31, p.191-209.

Fielding, C.R., 1984, Upper delta plain lacustrine and fluviolacustrine facies from the Westphalian of the Durham coalfield, NE England: Sedimentology, v. 31, p. 547-567.

Fielding, C.R., 1986, Fluvial channel and overbank deposits from the Westphalian of the Durham coalfield, NE England: Sedimentology, v. 33, p. 119-140.

Fielding, C.R., 1987a, Lower delta-plain interdistributary deposits; an example from the Westphalian of the Lancashire Coalfield, northwestern England: Geological Journal, v. 22, No. 2, p. 151-162.

Fielding, C. R., 1987b, Coal deposition models for deltaic and alluvial plain sequences: Geology, v. 15, No. 7, p. 661-664.

Fiorillo, A.R., and Gangloff, R.A, 2000, Theropod teeth from the Prince Creek Formation (Cretaceous) of northern Alaska, with speculations on arctic dinosaur paleoecology: Journal of Vertebrate Paleontology, v. 20, p 675–682.

Fiorillo, A.R., Tykoski, R.S., Currie, P.J., McCarthy, P.J., and Flaig, P.P., 2009, Description of two Troodon partial braincases from the Prince Creek Formation (Upper Cretaceous), North Slope, Alaska: Journal of Vertebrate Paleontology, v. 29, No. 1, p. 178-187.

Fiorillo, A.R., McCarthy, P.J., Flaig, P.P., Brandlen, E., Norton, D., Jacobs, L., Zippi, P. and Gangloff, R.A., 2010, Paleontology and paleoenvironmental interpretation of the Kikak-Tegoseak dinosaur quarry, (Prince Creek Formation: Late Cretaceous), northern Alaska: A multi-disciplinary study of an ancient high-latitude, ceratopsian dinosaur bonebed, *in* Ryan, M.J., Chinner-Algeier, B.J., and Eberth, D.A., eds., New Perspectives on Horned Dinosaurs: The Royall Tyrell Museum Ceratopsian Symposium: Bloomington, IN, Indiana University Press, p. 456-477.

Fischer, A.G., 1981, Climatic oscillations in the biosphere, *in* Nitecki, M.H., ed., Biotic Crisis in Ecological and Evolutionary Time: New York, NY, Academic Press, p. 103-132.

Fisk, H.N., 1944, Geological investigation of the alluvial valley of the lower Mississippi River: Tulsa Geological Society Digest, v. 15, 78 p.

Flach, P.D., and Mossop, G.D., 1985, Depositional environments of the Lower Cretaceous McMurray Formation, Athabasca Oil Sands, Alberta: The American Association of Petroleum Geologists Bulletin, v. 69, No. 8, p. 1195-1207.

Flaig, P.P., 2005, Changing fluvial style across the Permian-Triassic boundary: Beardmore Glacier Region, Central Transantarctic Mountains, Antarctica: Unpublished Master's Thesis, University of Wisconsin-Milwaukee, Milwaukee, Wisconsin, 288 p.

Flores, R.M., 1984, Comparative analysis of coal accumulation in Cretaceous alluvial deposits, southern United States Rocky Mountain basins: Canadian Society of Petroleum Geologists Memoir, v. 9, p. 373-385.

Flores, R.M., Stricker, G.D., Decker, P.L., and Myers, M.D., 2007a, Sentinel Hill Core Test 1: facies descriptions and stratigraphic reinterpretations of the Prince Creek and Schrader Bluff Formations, North Slope, Alaska: United States Geological Survey Professional Paper 1747, 31 p.

Flores, R.M., Myers, M.D., Houseknecht, D.W., Stricker, G.D., Brizzolara, D.W., Ryherd, T.J., and Takahashi, K.I., 2007b, Stratigraphy and facies of Cretaceous Schrader Bluff and Prince Creek Formations in Colville River Bluffs, North Slope, Alaska: United States Geological Survey Professional Paper 1748, 52 p.

Frederiksen, N.O, 1991, Pollen zonation and correlation of Maastrichtian marine beds and associated strata, Ocean Point dinosaur locality, North Slope, Alaska: United States Geological Survey Bulletin 1990-E, 24 p.

Frederiksen, N.O., Ager, T.A., and Edwards, L.E., 1986, Comment on "Early Tertiary marine fossils from northern Alaska: Implications for Arctic Ocean paleogeography and faunal evolution": Geology, v. 14, p. 802-803.

Frederiksen, N.O., Ager, T.A., and Edwards, L.E., 1988, Palynology of Maastrichtian and Paleocene rocks, lower Colville River region, North Slope, Alaska: Canadian Journal of Earth Sciences, v. 25, p. 512-527.

Frederiksen, N.O., and McIntyre, D.J., 2000, Palynomorph biostratigraphy of mid(?) Campanian to upper Maastrichtian strata along the Colville River, North Slope of Alaska: United States Geological Survey Open-File Report 00-493, 36 p.

Frederiksen, N.O., McIntyre, D.J., and Sheehan, T.P., 2002, Palynological dating of some Upper Cretaceous to Eocene outcrop and well samples from the region extending from the easternmost part of NPRA in Alaska to the western part of ANWR, North Slope of Alaska: U.S. Geological Survey Open-File Report 02-405, 37 p.

Friend, P.F., Slater, M.J., and Willimas, R.C., 1979, Vertical and lateral buildings of river sandstone bodies, Ebro Basin, Spain: Journal of the Geological Society of London, v. 136, p. 39-46.

Friend, P.F., 1983, Towards the field classification of alluvial architecture or sequence, *in* Collinson, J.D., and Lewin, J., Modern and Ancient Fluvial Systems: International Association of Sedimentologists Special Publication 6, p. 345-354.

Gallagher, S.J., Wagstaff, B.E., Baird, J.G., Wallace, M.W., and Li, C.L., 2008, Southern high latitude climate variability in the Late Cretaceous greenhouse world: Global and Planetary Change, v. 60, p. 351-364.

Gangloff, R.A., Fiorillo, A.R., and Norton, D.W., 2005, The first Pachycephalosaurine (Dinosauria) from the Paleo-Arctic and its paleogeographic implications: Journal of Paleontology, v. 79, p 997–1001.

Gardner, T.W., 1983, Paleohydrology and paleogeomorphology of a Carboniferous, meandering, fluvial sandstone: Journal of Sedimentary Petrology, v. 53, No. 3, p. 991-1005.

Gastaldo, R.A., Allen, G.P., and Huc, A.-Y., 1995, The tidal character of fluvial sediments of the modern Markham River Delta, Kalimantan, Indonesia, *in* Flemming, B.W., and Bartholomä, A., eds., Tidal Signatures in Modern and Ancient Sediments: Special Publication of the International Association of Sedimentologists, v. 24, p. 171-181.

Garrity, C. P., Houseknecht, D.W., Bird, K.J., Potter, C.J., Moore, T.E., Nelson, P.H., and Schenk, C.J., 2005, U.S. Geological Survey 2005 oil and gas resource assessment of the central North Slope, Alaska: Play maps and results: U.S. Geological Survey Open-File Report 2005-1182, 29 p.

Gibling, M.R., 2006, Width and thickness of fluvial channel bodies and valley fills in the geological record: a literature compilation and classification: Journal of Sedimentary Research, v. 76, p.731-770.

Gradziński, R., 1970, Sedimentation of dinosaur-bearing Upper Cretaceous deposits of the Nemegt Basin, Gobi Desert: Palaeontologica Polonica, v. 21, p. 147-229.

Gryc, G., Patton, W.W., and Payne, T.G., 1951, Present stratigraphic nomenclature of northern Alaska: Journal of the Washington Academy of Sciences, v. 41, No. 5, p. 159-167.

Guow, M.J.P., and Berendsen, H.J.A., 2007, Variability of channel-belt dimensions and the consequences for alluvial architecture: observations from the Holocene Rhine-Muse Delta (the Netherlands) and Lower Mississippi Valley (U.S.A.): Journal of Sedimentary Research, v. 77, p. 124-138.

Haugen, R.K., 1982, Climate of remote areas in north-central Alaska, 1975-1979 summary, *in* US Army Cold Regions Research and Engineering Laboratory Report 82-35, p. 1-114.

Heritage, G.L, Charlton, M.E., and Regan, S.O., 2001, Morphological classification of fluvial environments: An investigation of the continuum of channel types: Journal of Geology, v. 109, p. 21-33.

Hovikoski, J., Räsänen, M., Gingras, M., Ranzi, A., and Melo, J., 2008, Tidal and seasonal controls in the formation of Late Miocene inclined heterolithic stratification deposits, western Amazonian foreland basin: Sedimentology, v. 55, p. 499-530.

Isbell, J.L., 1990. Fluvial sedimentology and basin analyses of the Permian Fairchild and Buckley formations, Beardmore Glacier region, and the Weller Coal Measures, Southern Victoria Land, Antarctica [Ph.D. thesis]: Department of Geological Sciences, The Ohio State University, Columbus, OH, 347 p.

Jackson, R.G., 1981, Sedimentology of muddy fine-grained channel deposits in meandering streams of the American middle west: Journal of Sedimentary Petrology, v. 51, p. 1169-1192.

Joeckel, R.M., Ludvigson, G.A., Witzke, B.J., Kvale, E.P., Phillips, P.L., Brenner, R.L., Thomas, S.G., and Howard, L.M., 2005, Paleogeography and fluvial to estuarine architecture of the Dakota Formation, (Cretaceous, Albian) eastern Nebraska, USA, *in* Blum, M.D., Mariott, S.B., and Leclair, S.F., eds., Fluvial Sedimentology VII: Special Publication of the International association of Sedimentologists, v. 35, p. 453-480.

Johnson, C.L., and Graham, S.A. 2004, Cycles in perilacustrine facies of Late Mesozoic rift basin, southeastern Mongolia: Journal of Sedimentary Research, v.74, p. 786-804.

Jorgensen, P.J., and Fielding, C.R., 1996, Facies architecture of alluvial floodbasin deposits: Three-dimensional data from the Upper Triassic Callide Coal Measures of east–central Queensland, Australia: Sedimentology, v. 43, p. 479-495.

Kirschbaum, M.A., and McCabe, P.J., 1992, Controls on the accumulation of coal and on the development of anastomosed fluvial systems in the Cretaceous Dakota Formation of southern Utah: Sedimentology, v. 39, p. 581-598.

Kjemperud, A.V., Schomacker, E.R., and Cross, T.A., 2008, Architecture and stratigraphy of alluvial deposits, Morrison Formation (Upper Jurassic), Utah: American Association of Petroleum Geologists Bulletin, v. 92, No. 8, p. 1055-1076.

Knighton, A.D., and Nanson, G.C., 1993, Anastomosis and the continuum of channel pattern: Earth Surface Processes and Landforms, v. 18, p. 613-625.

Kraus, M.J. 1987, Integration of channel and floodplain suites, II. Vertical relations of alluvial Paleosols: Journal of Sedimentary Petrology, v. 57, p. 602-617.

Kraus, M.J., 1996, Avulsion deposits in lower Eocene alluvial rocks, Bighorn Basin, Wyoming: Journal of Sedimentary Research, v. 66, No. 2, p. 354–363.

Kraus, M.J., 1998, Development of potential acid sulfate paleosols in Paleocene floodplains, Bighorn Basin, Wyoming, USA: Paleogeography, Paleoclimatology, Paleoecology, v. 144, p. 203-224.

Kraus, M.J., and Bown, T.M., 1988, Pedofacies analysis: a new approach to reconstructing ancient fluvial sequences: Geological Society of America, Special Paper v. 216, p. 143-152.

Kraus, M.J., and Hasiotis, S.T., 2006, Significance of different methods of rhizolith preservation to interpreting paleoenvironmental and paleohydrologic settings: Examples from Paleogene paleosols, Bighorn Basin, Wyoming, U.S.A.: Journal of Sedimentary Research, v. 76, p. 633-646.

La Porte, L.F., and Behrensmeyer, A.K., 1980, Tracks and substrate reworking by terrestrial vertebrates in quaternary sediment of Kenya: Journal of Sedimentary Petrology, v. 50, No. 4, p. 1337-1346.

Leclair, S.F., and Bridge, J.S., 2001, Quantitative interpretation of sedimentary structures formed by river dunes: Journal of Sedimentary Research, v. 71, p. 713-716.

Leeder, M.R., 1973, Fluviatile fining-upwards cycles and the magnitude of paleochannels: Geological Magazine, v. 110, No. 3, p. 265-276.

Lewis, G.W., and Lewin, J., 1983, Alluvial cutoffs in Wales and the Borderlands, *in* Collinson, J.D., and Lewin, J., eds., Modern and Ancient Fluvial Systems: Special Publication of the International Association of Sedimentologists 6, p. 145-154.

Loope, D.B., 1986, Recognizing and utilizing vertebrate tracks in cross section: Cenozoic hoofprints from Nebraska, Palaios, v. 1, p. 141-151.

MacEachern, J.A., Pemberton, S.G., Bann, K.L., and Gingras, M.K., 2005, Departures from the archetypal ichnofacies: Effective recognition of physico-chemical stresses in the rock record, *in* MacEachern, J.A., Bann, K.L., Pemberton, S.G., and Gingras, M.K. eds., Applied Ichnology: SEPM Short Course Notes, v. 52, p. 65-93.

Makaske, B., 2001, Anastomosing rivers: A review of their classification, origin and sedimentary products: Earth-Science Reviews, v. 53, p. 149–196.

Makaske, B., and Weerts, H.J.T., 2005, Muddy lateral accretion and low stream power in a sub-recent confined channel belt, Rhine-Meuse delta, central Netherlands: Sedimentology, v. 52, p. 651-668.

Martín-Closas, C., and Galtier, J., 2005, Plant taphonomy and paleoecology of Late Pennsylvanian intramontane wetlands in the Graissessac-Lode`ve Basin (Languedoc, France): Palios, v. 20, p. 249-265.

McCarthy, P.J., Martini, I.P., and Leckie, D.A., 1998, Use of micromorphology for interpretation of complex alluvial paleosols: examples from the Mill Creek Formation (Albian), southwestern Alberta, Canada: Palaeogeography, Palaeoclimatology, Palaeoecology, v. 143, p. 87-110.

McCarthy, P.J., Faccini, U.F., and Plint, G., 1999, Evolution of an ancient coastal plain: paleosols, interfluves and alluvial architecture in a sequence stratigraphic framework, Cenomanian Dunvegan Formation, NE British Columbia, Canada: Sedimentology, v. 46, p. 861-891.

McCarthy, P.J., and Plint, A.G., 2003, Spatial variability of paleosols across Cretaceous interfluves in the Dunvegan Formation, NE British Columbia, Canada: paleohydrological, paleogeomorphological, and stratigraphic implications: Sedimentology, v. 50, p. 1187-1220.

McLaurin, B.T., and Steel, R.J., 2007, Architecture and origin of an amalgamated fluvial sheet sand, lower Castlegate Formation, Book Cliffs, Utah: Sedimentary Geology, v. 197, p. 291-311.

Miall, A.D., 1976, Paleocurrent and paleohydrologic analysis of some vertical profiles through a Cretaceous braided stream deposit, Banks Island, Arctic Canada: Sedimentology, v. 23, p. 459-483.

Miall, A.D., 1985, Architectural-element analysis: A new method of facies analysis applied to fluvial deposits: Earth Science Reviews, v. 22, p. 261-308.

Miall, A.D., 1996, The geology of fluvial deposits; sedimentary facies, basin analysis, and petroleum geology: Berlin, Springer-Verlag, 582 p.

Michaelsen, P., Henderson, R.A., Crosdale, P.J., and Mikkelsen, S.O., 2000, Facies architecture and depositional dynamics of the Upper Permian Rangal Coal Measures, Bowen Basin Australia: Journal of Sedimentary Research, v. 70, No. 4, p. 879-895.

Mjøs, R., Walderhaug, O., and Prestholm, E., 1993, Crevasse splay sandstone geometries in the Middle Jurassic Ravenscar Group of Yorkshire, UK, *in* Marzo, M., and Puigdefabregas, C., eds., Alluvial Sedimentation: Special Publication of the International Association of Sedimentologists, v. 17, p. 167-184.

Molenaar, C.M., 1985, Subsurface correlations and depositional history of the Nanushuk Group and related strata, North Slope, Alaska, *in* Huffman, A.C., ed., Geology of the Nanushuk Group and Related Rocks, North Slope, Alaska: United States Geological Survey Bulletin 1614, p. 37-60

Molenaar, C.M., Bird, K.J., and Kirk, A.R., 1987, Cretaceous and Tertiary stratigraphy of northeastern Alaska, *in* Tailleur, I.L., and Weimer, P., eds., Alaskan North Slope Geology: Society of Economic Paleontologists and Mineralogists, Pacific Section, Book 50, v. 1, p. 513–528.

Moore, T.E., Wallace, W.K., Bird, K.J., Karl, S.M., Mull, C.G., and Dillon, J.T., 1994, Geology of northern Alaska, *in* Plafker, G, and Berg, H.C., eds., The Geology of Alaska: Geological Society of America, The Geology of North America, Boulder, Colorado, v. G-1, p. 49-140.

Morisawa, M., 1985, Topologic properties of delta distributary networks, *in* Michael, W.J., ed., Models in Geomorphology: Winchester, Massachusetts, Allen & Unwin, p.239–268.

Morisowa. M., and Montgomery, W., 1985, Delta distributary networks: some quantitative aspects, *in* Kumar, A., ed., Facets of Geomorphology: Allahabad, India, Thinker's Library, p. 106-121.

Morozova, G.S., and Smith, N.D., 2000, Holocene avulsion styles and sedimentation patterns of the Saskatchewan River, Cumberland Marshes, Canada: Sedimentary Geology, v. 130, p. 81-105.

Mossop, G.D., and Flach, P.D., 1983, Deep channel sedimentation in the Lower Cretaceous McMurray Formation, Athabasca oil sands, Alberta: Sedimentology, v. 30, p. 493-509.

Mull, C.G., 1985, Cretaceous tectonics, depositional cycles, and the Nanushuk Group, Brooks Range and Arctic Slope, Alaska, *in* Huffman, A.C. Jr., ed., Geology of the Nanushuk Group and related rocks, North Slope, Alaska: United States Geological Survey Bulletin 1614, p. 7-36.

Mull, C.G., Houseknecht, D.W., and Bird, K.J., 2003, Revised Cretaceous and Tertiary stratigraphic nomenclature in the Colville Basin, northern Alaska: United States Geological Survey Professional Paper 1673, p. 1-51.

Nadon, G.C., 1993, The association of anastomosed fluvial deposits and dinosaur tracks, eggs, and nests: Implications for the interpretation of floodplain environments and a possible survival strategy for Ornithopods: Palaios, v. 8, p. 31-44.

Nadon, G.C., 1994, The genesis and recognition of anastomosed fluvial deposits: Data from the St. Mary River Formation, southwestern Alberta, Canada: Journal of Sedimentary Research, v. B64, No. 4, p. 451-463.

Nakajo, T., 1998, Tidal influences on distributary-channel sedimentation of the Tertiary delta in the Taishu Group, Tsushima Islands, southwestern Japan: Journal of Geosciences, Osaka City University, v. 41, p. 37-46.

Nanson, G.C., 1980, Point bar and floodplain formation of the meandering Beatton River, northeastern British Columbia: Sedimentology, v. 27, p. 3-29.

Nio, S.D., and Yang, C.S., 1991, Diagnostic attributes of clastic tidal deposits: a review, *in* Smith D.G., Reinson, G.E., Zaitlin, B.A., and Rahmani, R.A., eds., Clastic Tidal Sedimentology: Canadian Society of Petroleum Geologists Memoir No. 16, p. 3-28.

Nordt, L., Atchley, S., and Dworkin, S., 2003, Terrestrial evidence for two greenhouse events in the latest Cretaceous: GSA Today, v. 13, No. 12, p. 4-9.

Olariu, C., an Bhattacharya, J.P., 2006, Terminal distributary channels and delta front architecture of river-dominated delta systems: Journal of Sedimentary Research, v. 76, p. 212-233.

Orton, G.J., and Reading, H.G., 1993, Variability in deltaic processes in terms of sediment supply with particular emphasis on grain size: Sedimentology, v. 40, p. 475-512.

Page, K.J., Nanson, G.C., and Frazier, P.S., 2003, Floodplain formation and sediment stratigraphy resulting from oblique accretion on the Murrumbidgee River, Australia: Journal of Sedimentary Research, v. 73, No. 1, p. 5-14.

Parrish, J.M., Parrish, J.T., Hutchison, J.H., and Spicer, R.A., 1987, Late Cretaceous vertebrate fossils from the North Slope of Alaska and implications for dinosaur ecology: Palaios, v. 2, p. 377-389.

Parrish, J.T., and Spicer, R.A., 1988, Late Cretaceous terrestrial vegetation: A near-polar temperature curve: Geology, v. 16, p. 22-25.

Pêrez-Arlucea, M., and Smith, N. D., 1999, Depositional pattern following the 1870's avulsion of the Saskatchewan River (Cumberland Marshes, Saskatchewan, Canada): Journal of Sedimentary research, v. 69, No. 1, p. 62-73.

Phillips, R.L., 1989, Summary of late Cretaceous environments near Ocean Point, North Slope, Alaska: Geological studies in Alaska by the United States Geological Survey: United States Government Printing Office, Washington D.C., p. 101-106.

Phillips, R.L., 2003, Depositional environments and processes in Upper Cretaceous nonmarine and marine sediments, Ocean Point dinosaur locality, North Slope, Alaska: Cretaceous Research, v. 24, p. 499-523.

Plint, A.G., 1983, Sandy fluvial point-bar sediments from the Middle Eocene of Dorset, England, *in* Collinson, J.D., and Lewin, J., eds., Modern and Ancient Fluvial Systems: Special Publication of the International Association of Sedimentologists 6, p. 355-368.

Postma, D., 1977, The occurrence and chemical composition of recent Fe-rich mixed carbonates in a river bog: Journal of sedimentary Petrology, v. 47, No. 3, p. 1089-1098.

Rajchl, M., and Uličný, D., 2005, Depositional record of an avulsive fluvial system controlled by peat compaction (Neogene, Most Basin, Czech Republic): Sedimentology, v. 52, p. 601-625.

Reading, H.G., 1996, Sedimentary Environments, Processes, Facies, and Stratigraphy: Malden, MA, Blackwell Science Ltd., 688 p.

Retallack, G.J., 2001, Soils of the past: an introduction to paleopedology: London, Blackwell Science, 404 p.

Rich, T.H., Gangloff, R.A., and Hammer, W.R., 1997, Polar dinosaurs, *in* Currie, P.J. and Padian, K., eds., Encyclopedia of Dinosaurs: San Diego, Academic Press, p. 562-573.

Rich, T.H., Gangloff, R.A., and Hammer, W.H., 2002, Polar Dinosaurs: Science, v. 295, p. 979-980.

Roberts, H.H., 1997, Dynamic changes of the Holocene Mississippi River delta plain: the Delta cycle: Journal of Coastal Research, v. 13, No. 3, p. 605-627.

Roberts, E.M., 2007, Facies architecture and depositional environments of the Upper Cretaceous Kaiparowits Formation, southern Utah: Sedimentary Geology, v. 197, p. 207-233.

Roehler, H.W., 1987, Depositional environments of the coal-bearing and associated formations of Cretaceous age in the National Petroleum Reserve in Alaska: United States Geological Society Bulletin 1575,16 p.

Rogers, R.R., 1998, Sequence analysis of the Upper Cretaceous Two Medicine and Judith River Formations, Montana: Nonmarine response to the Claggett and Bearpaw marine cycles: Journal of Sedimentary Research, v. 68, No. 4, p. 615-631.

Schumm, S.A., 1963, Sinuosity of alluvial rivers on the Great Plains: Geological Society of America Bulletin, v. 74, p. 1089-1100.

Schumm, S.A., 1968, Speculations concerning paleohydrologic controls of terrestrial sedimentation: Geological Society of America Bulletin, v. 79, p. 1573-1588.

Schumm, S.A., 1981, Evolution and response of the fluvial system, sedimentologic implications, *in* Ethridge, F.G. and Flores, R.M., eds., Recent and ancient nonmarine depositional environments: Society of Economic Paleontologists and Mineralogists Special Publication, n. 31, p. 19-29.

Schumm, S.A., 1985, Patterns of alluvial rivers: Annual Reviews of Earth and Planetary Sciences, v. 13, p. 5-27.

Schumm, S.A., and Kahn, H.R., 1972, Experimental study of channel patterns: Geological Society of America Bulletin, v. 83, p.1755-1770.

Smith, D.G., 1976, Effect of vegetation on lateral migration of anastomosed channels of a glacial meltwater river: Geological Society of America Bulletin, v. 87, p. 857-860.

Smith, D.G., 1983, Anastomosed fluvial deposits: modern examples from Western Canada, *in* Collinson, J.D., and Lewin, J., eds., Modern and Ancient Fluvial Systems: Special Publication of the International Association of Sedimentologists 6, p. 155-168.

Smith, D.G., 1987, Meandering river point bar lithofacies models: modern and ancient examples compared, *in* Ethridge, F.G., Flores, R.M., Harvey, M.D., and Weaver, J.N., eds., Recent Developments in Fluvial Sedimentology: Special Publication, Society of Economic Paleontologists and Mineralogists, v.39, p. 83-91.

Smith, D.G., 1988, Modern point bar deposits analogous to the Athabasca Oil Sands, Alberta, Canada, *in* de Boer, P.L., van Gelder, A., and Nio, S.D., eds., Tide-influenced Sedimentary Environments and Facies: Dordrecht, D. Reidel, p. 417-432.

Smith, D.G., and Smith, N.D., 1980, Sedimentation in anastomosed river systems: examples from alluvial valleys near Banff, Alberta: Journal of Sedimentary Petrology, v. 50, No. 1, p. 157-164.

Smith, D.G., and Putnam, P.E., 1980, Anastomosed river deposits: Modern and ancient examples in Alberta, Canada: Canadian Journal of Earth Sciences, v. 17, p. 1396-1406.

Smith, N.D., Cross, T.A., Dufficy, J.P., and Clough, S.R., 1989, Anatomy of an avulsion: Sedimentology, v. 36, p. 1-23.

Smith, N.D., and Pêrez-Arlucea, M., 1994, Fine-grained splay deposition in the avulsion belt of the Lower Saskatchewan River, Canada: Journal of Sedimentary Research, v. 64, No. 2, p. 159-168.

Smith, N.D., and Pêrez-Arlucea, M., 2004, Effects of peat on the shapes of alluvial channels: examples from the Cumberland Marshes, Saskatchewan, Canada: Geomorphology, v. 61, p. 323-335.

Spicer, R.A., 2003, Changing climate and biota, *in* Skelton, P., ed., The Cretaceous World: Cambridge, U.K., Cambridge University Press, p. 85-162.

Spicer, R.A., and Parrish, J.T., 1987, Plant megafossils, vertebrate remains, and paleoclimate of the Kogosukruk Tongue (Late Cretaceous), North Slope, Alaska: U. S. Geological Survey Circular, Report: C 0998, p. 47-48.

Spicer, R.A., and Parrish, J., 1990, Late Cretaceous-early Tertiary paleoclimates of northern high latitudes: a quantitative view: Journal of the Geological Society, London, v. 147, No. 6, p. 329-341.

Spicer, R.A., Parrish, J.T., and Grant, P.R., 1992, Evolution of vegetation and coal-forming environments in the Late Cretaceous of the North Slope of Alaska, *in* McCabe, P.J., and Parrish, J.T., eds., Controls on the Distribution and Quality of Cretaceous Coals: Geological Society of America Special Paper 267, p. 177-192.

Stanley, K.O., and Surdam, R.C., 1978, Sedimentation on the front of Eocene Gilbert-type deltas, Washake Basin, Wyoming: Journal of Sedimentary Petrology, v. 48, No. 2, p. 557-573.

Stewart, D.J., 1981, A meander-belt sandstone of the Lower Cretaceous of southern England: Sedimentology, v. 28, p. 1-20.

Stewart, D.J., 1983, Possible suspended-load channel deposits from the Wealden Group (Lower Cretaceous) of southern England, *in* Collinson, J.D., and Lewin, J., eds., Modern and Ancient Fluvial Systems: Special Publication of the International Association of Sedimentologists 6, p. 369-384.

Stouthamer, E., 2001, Sedimentary products of avulsions in the Holocene Rhine-Meuse Delta, The Netherlands: Sedimentary Geology, v. 145, p. 73-92.

Tanner, L.H., 2000, Palustrine–lacustrine and alluvial facies of the (Norian) Owl Rock Formation, (Chinile Group), Four Corners region, southwestern U.S.A.; Implications for Late Triassic paleoclimate: Journal of Sedimentary Research, v. 70, No. 6, p. 1,280–1,289.

Tatsch, J.H., 1980, Coal deposits: Sudsbury, Massachusetts, Tatsch Associates, 590 p.

Thomas, R.G., Smith, D.G., Wood, J.M., Visser, J., Calverley-Range, E.A., and Koster, E.H., 1987, Inclined heterolithic stratification- Terminology, description, interpretation, and significance: Sedimentary Geology, v. 53, p. 123-179.

Tooth, S., 2005, Splay formation along the lower reaches of ephemeral rivers on the northern plains of arid central Australia: Journal of Sedimentary Research, v. 75, p. 636-649.

Törnqvist, T.E., 1993, Holocene alternation of meandering and anastomosing fluvial systems in the Rhine-Meuse Delta (central Netherlands) controlled by sea level rise and subsoil erodability: Journal of Sedimentary Petrology, v. 63, No. 4, p. 683-693.

Törnqvist, T.E., van Ree, M.H.M, and Faessen, E.L.J.H., 1993, Longitudinal facies architectural changes of a Middle Holocene anastomosing distributary system (Rhine-Meuse Delta, central Netherlands), *in* Fielding, C.R., ed., Current Research in Fluvial Sedimentology: Sedimentary Geology, v. 85, p. 203-219.

Ufnar, D.F., González, L.A., Ludvigson, G.A., Brenner, R.L., and Witzke, B.J., 2001, Stratigraphic implications of meteoric sphaerosiderite $\delta^{18}O$ values in paleosols of the Cretaceous (Albian) Boulder Creek Formation, N.E. British Columbia foothills, Canada: Journal of Sedimentary Research, v. 71, p. 1017-1028.

van Asselen, S., Stouthammer, E., and van Asch, Th.W.J., 2009, Effects of peat compaction on delta evolution: a review on processes, responses, measuring, and modeling: Earth-Science Reviews, v. 92, p. 35-51.

Vavra, C. L., 1984, Provenance and alteration of the Triassic Fremow and Falla Formations, Central Transantarctic Mountains, Antarctica: Report - Institute of Polar Studies, v. 87, 98 p.

Walker, R.G. (ed.), 1979, Facies Models: Geological Association of Canada, 211 p.

Witte, K.W., Stone, D.B., and Mull, C.G., 1987, Paleomagnetism, paleobotany, and paleogeography of the Cretaceous, North Slope, Alaska, *in* Tailleur, I., and Weimer, P., eds., Alaska North Slope Geology: The Pacific Section, Society of Economic Paleontologists and Mineralogists and the Alaska Geological Society, v. 1, p. 571-579.

Wood, J.M., Thomas, R.G., and Visser, J., 1988, Fluvial processes and vertebrate taphonomy: The Upper Cretaceous Judith River Formation, south-central Dinosaur Provincial Park, Alberta, Canada: Paleogeography, Paleoclimatology, Paleoecology v. 66, p. 127-143.

Wood, J.M., 1989, Alluvial architecture of the Upper Cretaceous Judith River Formation, Dinosaur Provincial Park, Alberta, Canada: Bulletin of Canadian Petroleum Geology, v. 37, No. 2, p. 169-181.

Wright, V.P., 1986, Pyrite formation and the drowning of a paleosol: Geological Journal, v. 21, p. 139-149.

Yang, B., Dalrymple, R.W., Gingras, M.K., Seungshoo, C., and Lee, H., 2007, Up-estuary variation of sedimentary facies and ichnocoenosis in an open-mouthed, macrotidal, mixed energy estuary, Gosmo Bay, Korea: Journal of Sedimentary Research, v. 77, p. 757-771.

Zakharov, Y.D., Boriskina, N.G., Ignatyev, A.V., Tanabe, K., Shigeta, Y., Popov, A.M., Afanasyeva, T.B., and Maeda, H., 1999, Paleotemperature curve for the Late Cretaceous of the northwestern circum-Pacific: Cretaceous Research, v. 20, p. 685-697.

Chapter 3 Anatomy, evolution and paleoenvironmental interpretation of an ancient Arctic coastal plain: Integrated paleopedology and palynology from the Late Cretaceous (Maastrichtian) Prince Creek Formation, North Slope, Alaska, USA*

Peter P. Flaig, Paul J. McCarthy, and Anthony R. Fiorillo

*Flaig, P. P., McCarthy, P. J., and Fiorillo, A. R., 2010, Anatomy, evolution, and paleoenvironmental interpretation of an ancient Arctic coastal plain: Integrated paleopedology and palynology from the Late Cretaceous (Maastrichtian) Prince Creek Formation, North Slope, Alaska, USA. Prepared for submission to the SEPM *Journal of Sedimentary Research*

ABSTRACT

The Cretaceous (Early Maastrichtian), dinosaur-bearing Prince Creek Formation exposed along the Colville River in northern Alaska records high-latitude, alluvial sedimentation and soil formation on a low-lying, low gradient, muddy coastal plain during a greenhouse phase in Earth history. This study combines outcrop observations, micromorphology, geochemistry, and biota analyses of paleosols from the Prince Creek Fm. in order to reconstruct local paleoenvironments of weakly developed, high-latitude floodplain soils, some of which experienced marine influence.

Sediments of the Prince Creek Fm. include quartz and chert-rich sandstone channels, and floodplains containing organic-rich siltstone and mudstone, carbonaceous shale, coal and ashfall deposits. Vertically stacked horizons of blocky-to-platy, drab-colored mudstone and siltstone with carbonaceous root-traces and mottled aggregates separated by sandy intervals indicate that the development of compound and cumulative, weakly-developed soils on floodplains alternated with overbank alluviation and deposition in distributary channels on crevasse splay complexes and channels on floodplains . Soil formation occurred on levees, point bars, crevasse splays and along the margins of floodplain lakes, ponds, and swamps.

Soil-forming processes were repeatedly interrupted by alluviation and waterlogging, with additions of sediment likely added on top of soil profiles by flooding of nearby distributary channels. Alluviation is evidenced by thin (<0.5 m) sand and silt horizons dispersed throughout soil profiles, along with common pedorelicts, papules, and

fluctuations with depth in a variety of molecular ratios (e.g. Ti/Zr, Ba/Sr, Fe/Al, Al/Si, and Al/(Na+K+Ca+Mg)).

Abundant carbonaceous organic matter and root-traces, Fe-oxide depletion coatings, and zoned peds (soil aggregates with an outermost Fe-depleted zone, darker-colored, Fe-rich matrix, and lighter-colored Fe-poor center) suggest waterlogging, anoxia and gleying. In contrast, Fe-oxide mottles, ferruginous and manganiferous segregations, insect and worm burrows, and rare illuvial clay coatings suggest recurring oxidation and drying out of some soils. Trampling of sediments by dinosaurs is common. Jarosite mottles and halos surrounding rhizoliths, and rare pyrite and gypsum found in some distal soils imply a marine influence on pedogenesis that becomes increasingly common up-section.

Biota including Peridinioid dinocysts, brackish and freshwater algae, fungal hyphae, fern and moss spores, projectates, age-diagnostic *Wodehouseia edmontonicola*, hinterland *bisaccate* pollen and pollen from lowland trees, shrubs, and herbs indicate an Early Maastrichtian age for all sediments in the study area. The assemblage also demonstrates that although all sediments are Early Maastrichtian, strata become progressively younger from measured section NKT in the south to measured section LBB in the north. The integration of biota analyses with paleopedology can provide clues to regional biomass, paleo-relief, clastic input from channels, and the location of paleosol profiles relative to the paleo-coastline.

Paleosols of the Prince Creek Fm. are similar to modern aquic subgroups of Entisols and Inceptisols, and in more distal locations potential acid sulfate soils. A reconstruction of pedogenic processes suggests that soils were influenced by seasonally(?) fluctuating water levels and, in distal areas, a marine influence. These results offer a unique glimpse into soil-forming processes on paleo-Arctic Cretaceous floodplains governed by a near polar light, temperature, and precipitation regime upon which dinosaurs thrived.

INTRODUCTION

Studies of high-latitude paleosols developed under greenhouse conditions are extremely rare (e.g. Retallack and Alonso-Zarza 1998, Retallack 1999, Ufnar et al. 2004, Sheldon 2006, Brandlen 2008; Fiorillo et al. 2010a), and seldom include marine-influenced pedogenesis. Alluvial paleosols of the Prince Creek Formation (Fm.) formed on a tidally-influenced, high-latitude coastal plain adjacent to meandering and anastomosed (?) channels during the Cretaceous greenhouse (Flaig et al. 2010) and offer insight into soil-forming processes that occurred under a polar light, precipitation and temperature regime.

Macroscopic and microscopic characteristics of modern soils are commonly used to identify soil-forming processes and their relationship to environmental conditions (Soil Survey Staff 1999). In many ancient alluvial successions paleosols represent a significant portion of the observable facies (Leckie et al. 1989, Retallack et al. 1999,

Retallack and Krull 1999, McCarthy and Plint 2003, Flaig 2005). By comparing paleosol characteristics with modern soils we gain valuable insight into ancient environmental conditions including paleohydrology and paleotopography (e.g. Besly and Fielding 1989, Kraus and Aslan 1993, McCarthy and Plint 2003, Fiorillo et al. 2010a), the extent and degree of clastic influx onto the floodplain (Kraus 1986, Aslan and Autin 1999, Kemp and Zárate 2000), and proximity to paleo-shorelines (Driese et al. 1992, Ufnar et al. 2001, Álvaro et al. 2003). Paleosol geochemistry can also significantly improve paleoenvironmental interpretations in some circumstances (Leckie et al. 1989, Driese et al. 1992, Moore et al. 1992, Sheldon et al. 2002, McCarthy and Plint 2003, Kahman and Driese 2008). Pollen/biota assemblages preserved within paleosols provide an additional tool for interpreting ancient environments, constraining ancient climates, and assessing the age of sediments (e.g. Askin 1990, Askin et al. 1991, Falcon-Lang et al. 2004, Fiorillo et al. 2010a). Ultimately the integration of paleopedology, geochemistry, and pollen/biota analyses may be the best method for resolving pedogenic paleoenvironments from paleosol profiles (e.g. Alley et al. 1986, Jackson et al. 1999, Wu et al. 2002).

The purpose of this paper is to describe the paleosols of the Prince Creek Fm. using a combination of field observations, soil micromorphology, and soil geochemistry. These data are combined with biofacies established through biota analyses to reconstruct the ancient arctic environment on this high-latitude, tidally-influenced alluvial plain of Cretaceous northern Alaska. Insights gained through interpretations of these paleosols formed under greenhouse conditions in this ancient Arctic setting provide a detailed picture of Earth's high-latitude environments on a warmer Earth.

GEOLOGIC SETTING

The Colville Basin is a foreland basin on the North Slope of Alaska (Fig. 3.1). Jurassic to Early Cretaceous subduction in southern Alaska led to the northward emplacement of allocthons and uplift of the Brooks Range orogenic belt (Moore et al. 1994). Lithospheric loading during the Aptian/Albian initiated subsidence to the north of the Brooks Range, creating the east-west trending Colville Basin (Moore et al. 1994; Cole et al. 1997). Uplift and erosion drove sediments from the west into the foredeep throughout the Late Cretaceous and into the Tertiary, filling the basin both axially and transversely (Molenaar 1985, Mull 1985, Molenaar et al. 1987, Moore et al. 1994, Mull et al. 2003, Decker 2007).

The Prince Creek Fm. (Fig. 3.2) is a high-latitude coastal plain succession composed predominantly of alluvial conglomerate, sandstone, siltstone, mudstone, carbonaceous shale, coal, bentonite and tuff (Roehler 1987, Mull et al. 2003; Fiorillo et al. 2009, 2010a, 2010b, Flaig et al. 2010). The Prince Creek Fm. contains the most proximal sediments in a Late Cretaceous to Paleocene, continental to marine succession that includes the shallow marine Schrader Bluff Fm. and the slope to deepwater Canning Fm. and Hue Shale (Fig. 3.2).

Strata are exposed semi-continuously for approximately 60 km in bluffs along the Colville, Kogosukruk and Kikiakrorak Rivers (Fig. 3.1). The total thickness of the Prince Creek Fm. in outcrop along the Colville River is ~450 m (Detterman et al. 1963; Brosge et al. 1966, Mull et al. 2003). Strata dip gently (3° or less) to the northeast and locally

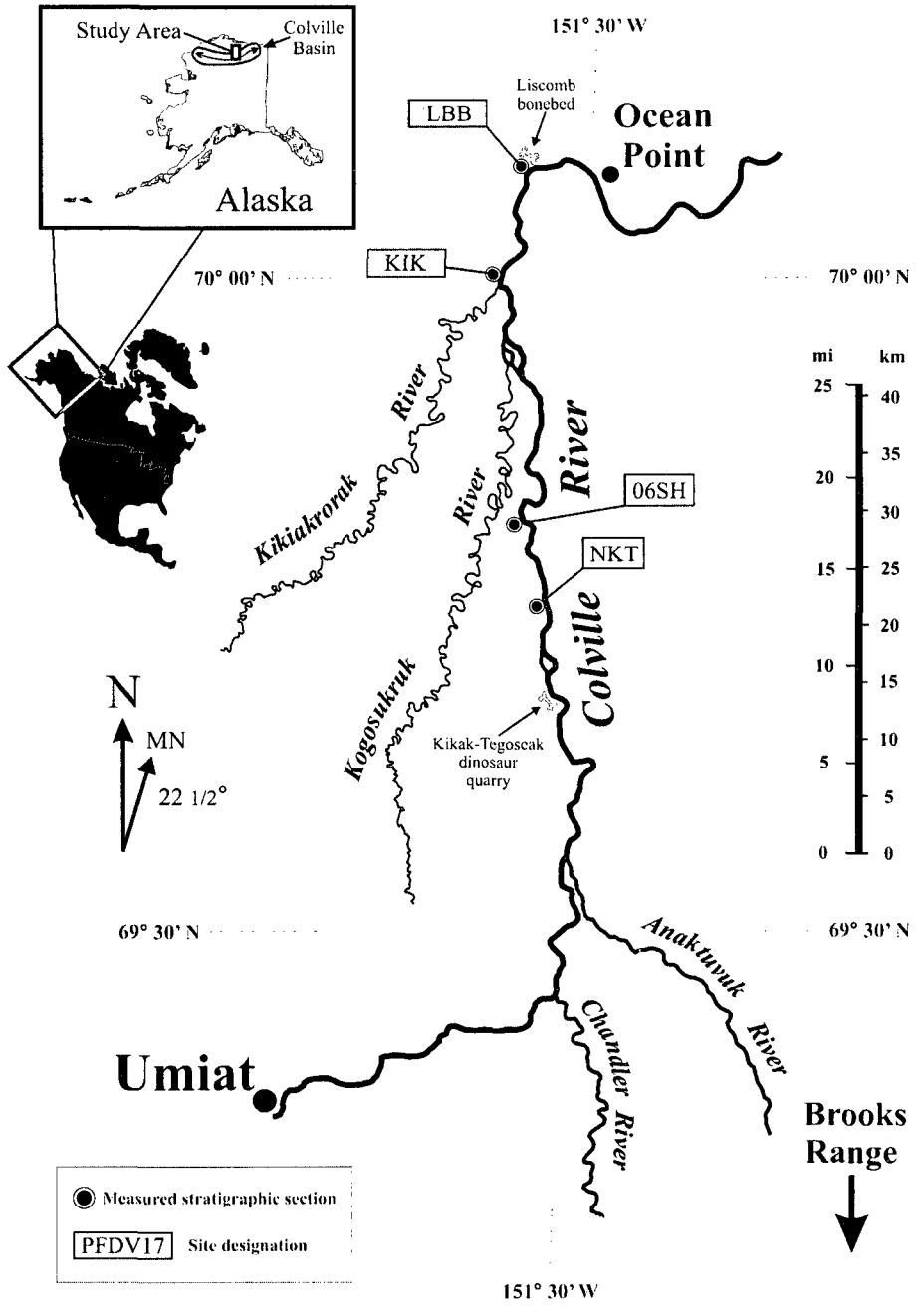

Figure 3.1. Study area along the Colville River, North Slope of Alaska including locations of the Kikak-Tegoseak dinosaur quarry, the Liscomb dinosaur quarry, Ocean Point, and the four measured stratigraphic successions described in this study (NKT, 06SH, KRM, LBB). Locations of all 75 measured sections along the Colville, Kogosukruk, and Kikiakrorak Rivers can be found in Flaig et al. 2010 (Figure 1). MN=magnetic north.

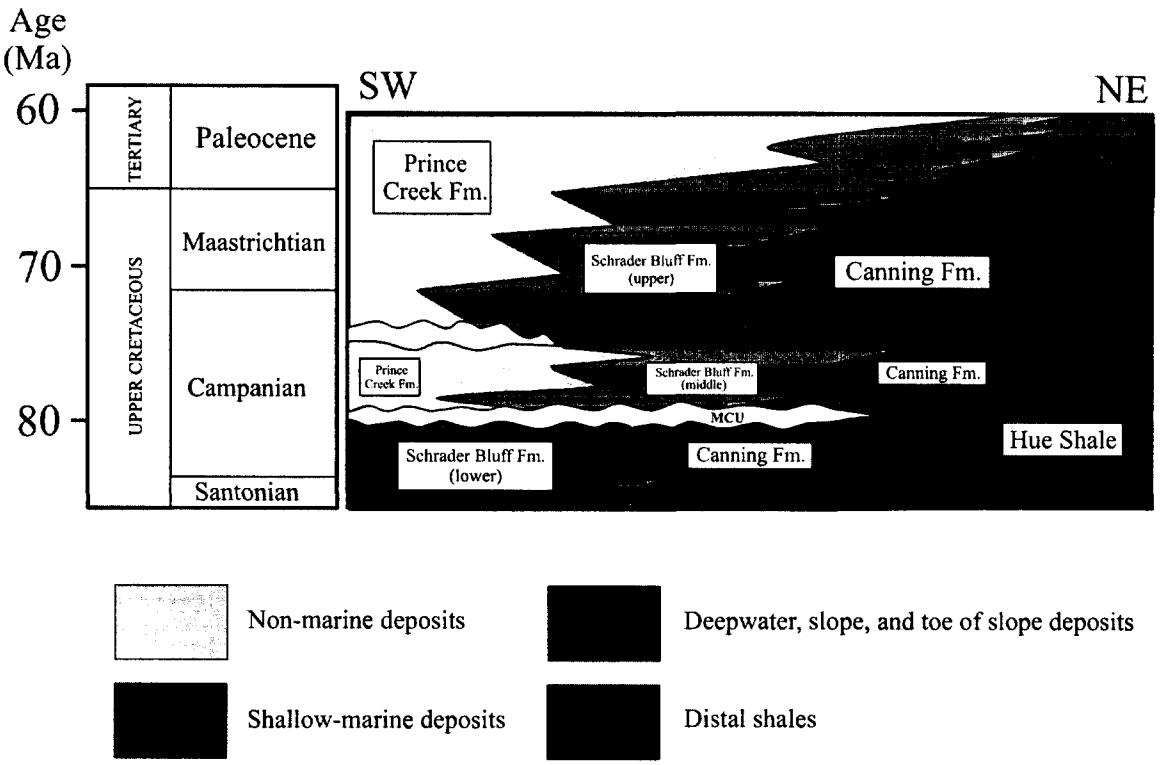

Figure 3.2. Generalized chronostratigraphic column for the central North Slope, Alaska. MCU=mid-Campanian unconformity. Revised from Mull et al. (2003), Garrity et al. (2005), and Decker et al. 2009.

contain minor faults and folds. The entire formation generally fines upward from a conglomeratic base (Flores et al. 2007b) to finer-grained facies at the top (Phillips 2003, Flaig et al. 2010). Exposures of the Prince Creek Fm. along the Colville River near the confluence of the Colville, Anaktuvuk, and Chandler Rivers (Fig. 3.1) contain basal fluvial sandstones and conglomerates incised into shallow-marine sandstones of the lower Schrader Bluff Fm. (Mull et al. 2003; Flores et al. 2007b). This contact is interpreted as an incised paleovalley (Flores et al. 2007a, 2007b). Approximately 60 km to the north, near Ocean Point (Fig. 3.1), the contact between the top of the Prince Creek Fm. and the overlying upper Schrader Bluff Fm. is transgressive between alluvial and interdistributary bay facies of the Prince Creek Fm. and shoreface deposits of the upper Schrader Bluff Fm. (Phillips 2003).

Estimates for depth of burial for the Prince Creek Fm. along the Colville River calculated from downhole vitrinite reflectance profiles and sonic-porosity logs range from 2000 to 6000 ft. (Burns et al. 2005). Vitrinite-reflectance values (n=4, average .3825; Robinson 1989, Johnson and Howell, 1996), suggest a maximum burial temperature of 48° C (Barker et al. 1986).

Palynomorph assemblages (Frederiksen et al. 1986, 1988, 2002; Frederiksen 1991; Frederiksen and McIntyre 2000; Flores et al. 2007b; Brandlen, 2008; Fiorillo et al. 2010a), floral and faunal evidence (Parrish and Spicer 1988; Brouwers and de Deckker 1993), and geochronological analyses (Conrad et al. 1990) indicate that the age of the Prince Creek Fm. ranges from Campanian to Paleocene. Recent work (Brandlen 2008,

Fiorillo et al. 2010a, Flaig et al. 2010) along with data presented in this paper demonstrate that all of the deposits in our study area are Early Maastrichtian.

The Prince Creek Fm. was likely deposited at paleolatitudes of 82°-85° N (Brouwers et al. 1987; Witte et al. 1987; Besse and Courtillot 1991; Rich et al. 2002, Spicer and Herman 2010). Temperature estimates for Cretaceous (Maastrichtian) northern Alaska based on megaflora indicate mean annual temperatures (MAT) of ~5° C (Spicer and Parrish 1987; Parrish and Spicer 1988; Spicer 2003; Fiorillo et al. 2009, 2010a) with a warmest month mean temperature (WMMT) of 10-12 ° C and a coldest month mean temperature (CMMT) of 2-4 ° C (Brouwers et al. 1987, Tomsich et al. 2010). No evidence of cryoturbation or ground ice is found in the Prince Creek Fm. (Fiorillo et al. 2010a), although false rings in fossil wood indicate that at least periodic freezes were likely (Spicer et al. 1992; Spicer 2003). Elevations in the nearby Brooks Range probably exceeded 1500 m with MAT below 0^0 C (Spicer 2003) suggesting that higher elevations may have supported snow and ice fields (Spicer and Parrish 1990; Fiorillo et al. 2009, Fiorillo et al. 2010b). Mean annual precipitation (MAP) is estimated at 500-1500 mm a^{-1} (Spicer and Parrish 1990; Brandlen 2008), however, the presence of abundant charcoal suggests that forest fires were common during periodic dry periods (Spicer and Parrish 1987; Spicer 2003).

Dinosaur body fossils (Fig. 3.3), including large and small theropods, a hypsilophodontid, a pachycephalosaur, ceratopsians and hadrosaurs have been excavated from bonebeds of the Prince Creek Fm. along the Colville River (Fiorillo et al. 2009;

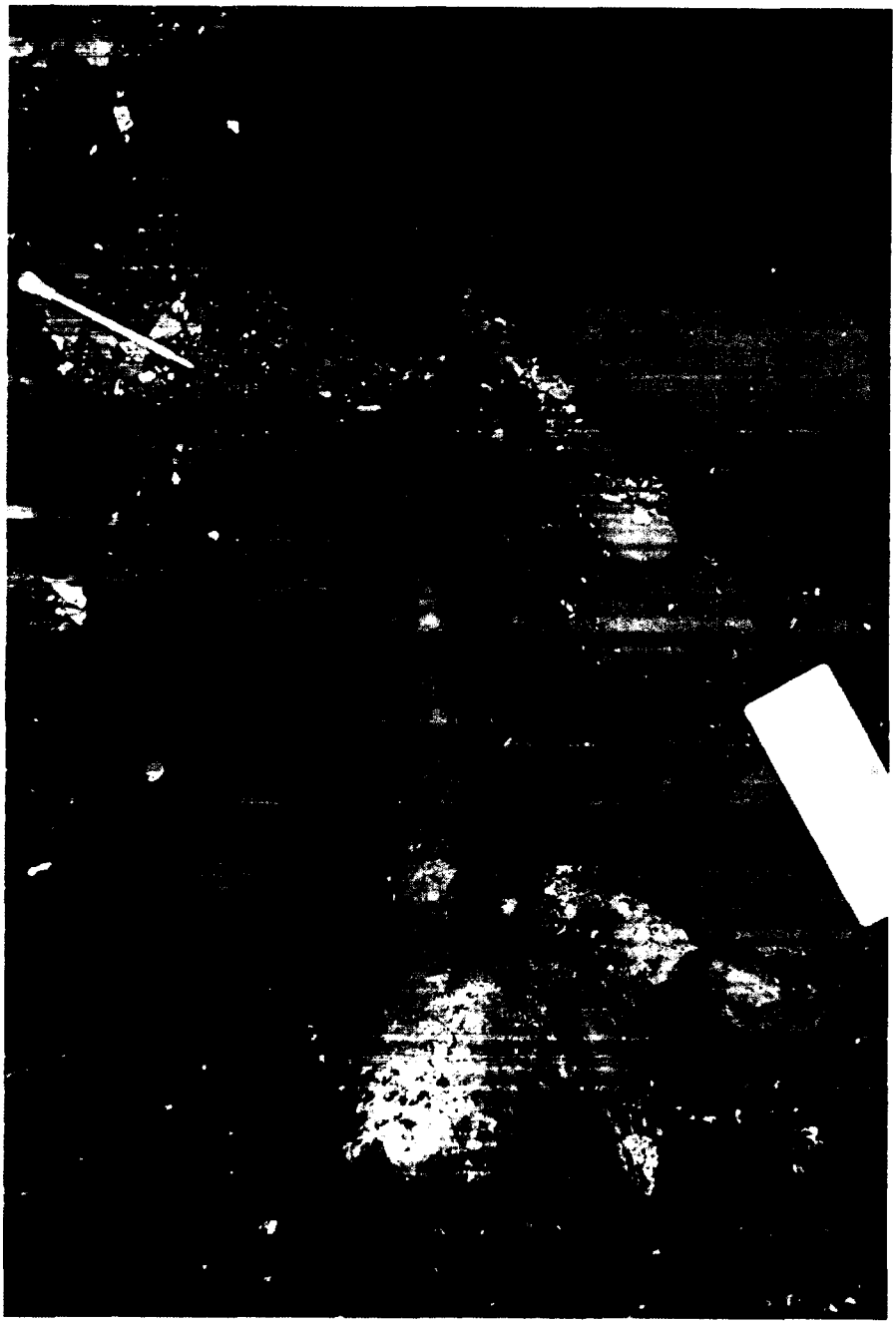

Figure 3.3. Concentration of juvenile duck-billed dinosaur limb bones from the Liscomb Bonebed, one of several dinosaur bonebeds found in the Prince Creek Formation exposures along the Colville River.

Fiorillo et al. 2010b). Cretaceous dinosaur remains from the Prince Creek Fm. indicate that non-avian dinosaurs thrived under the profound seasonality and light regime of the Cretaceous Arctic (Clemens and Nelms 1993, Fiorillo et al. 2009).

METHODS

75 sections were measured during the summers of 2005-2007 from near the Kikak-Tegoseak bonebed to just east of the Liscomb bonebed near Ocean Point (Fig. 3.1). Four sites (NKT, 06SH, KIK, and LBB) were selected for paleosol study based on accessibility of outcrop and abundance of facies containing paleopedological features (Figs. 3.1, 3.4). Macroscopic features including grain size, ped structure, sedimentary structures, mottles, nodules, roots, flora, and fauna were described in detail. Paleosol colors were determined using Munsell color charts (Munsell Colour, 1984) on damp sediments in fresh outcrop. Bulk and *in situ* samples were collected at 15-30 cm intervals from representative paleosols and all samples were subsequently air-dried. *In situ* samples were impregnated with epoxy resin and petrographic thin-sections were prepared by Spectrum Petrographics, Vancouver, WA. Grain sizes in thin sections, mineralogy, and micromorphological features were examined with an Olympus BH-2 petrographic microscope (2x-40x magnification) under plane- and cross-polarized light. Micromorphological descriptions of paleosols (Table 3.1, 3.2) follow the terminology of Bullock et al. (1985). Major oxide geochemistry in paleosol profiles was determined using a PANalytical Axios wavelength-dispersive X-ray fluorescence (XRF)

Figure 3.4 (Following 2 Pages). Measured stratigraphic sections NKT, 06SH, KRM, and LBB. Diagrams include facies association interpretations and the stratigraphic locations of *Paleosol 1* through *Paleosol 9* detailed in Figures 9-17. SSC=Small Sinuous Channels, SLSC=Small Low Sinuosity Channels, and ISSM=Interbedded Sandstone, Siltstone, and Mudstone. See Figure 3.1 for geographic location of measured sections and Figure 3.5 for outcrop examples of each facies association.

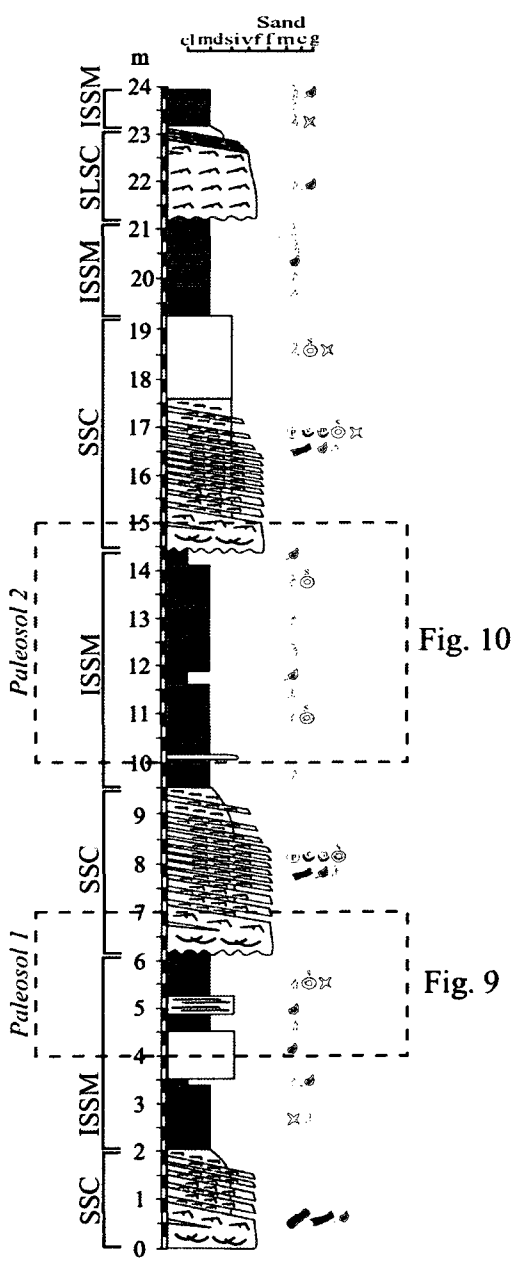

Fig. 10

Fig. 9

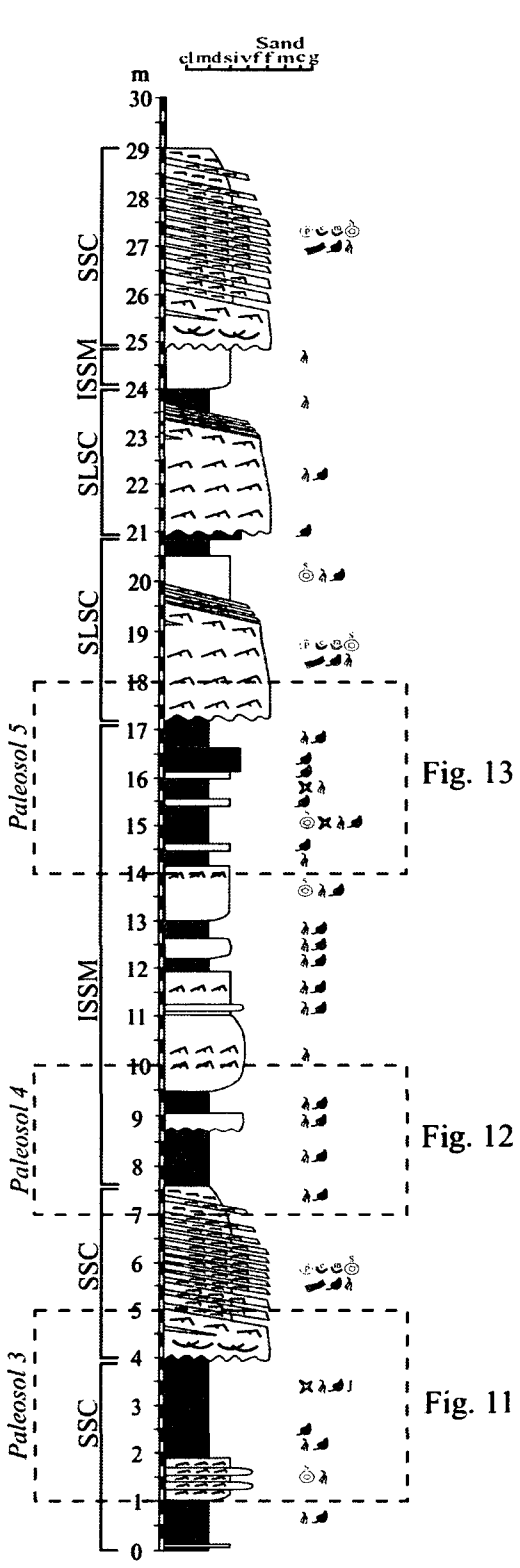

Fig. 13

Fig. 12

Fig. 11

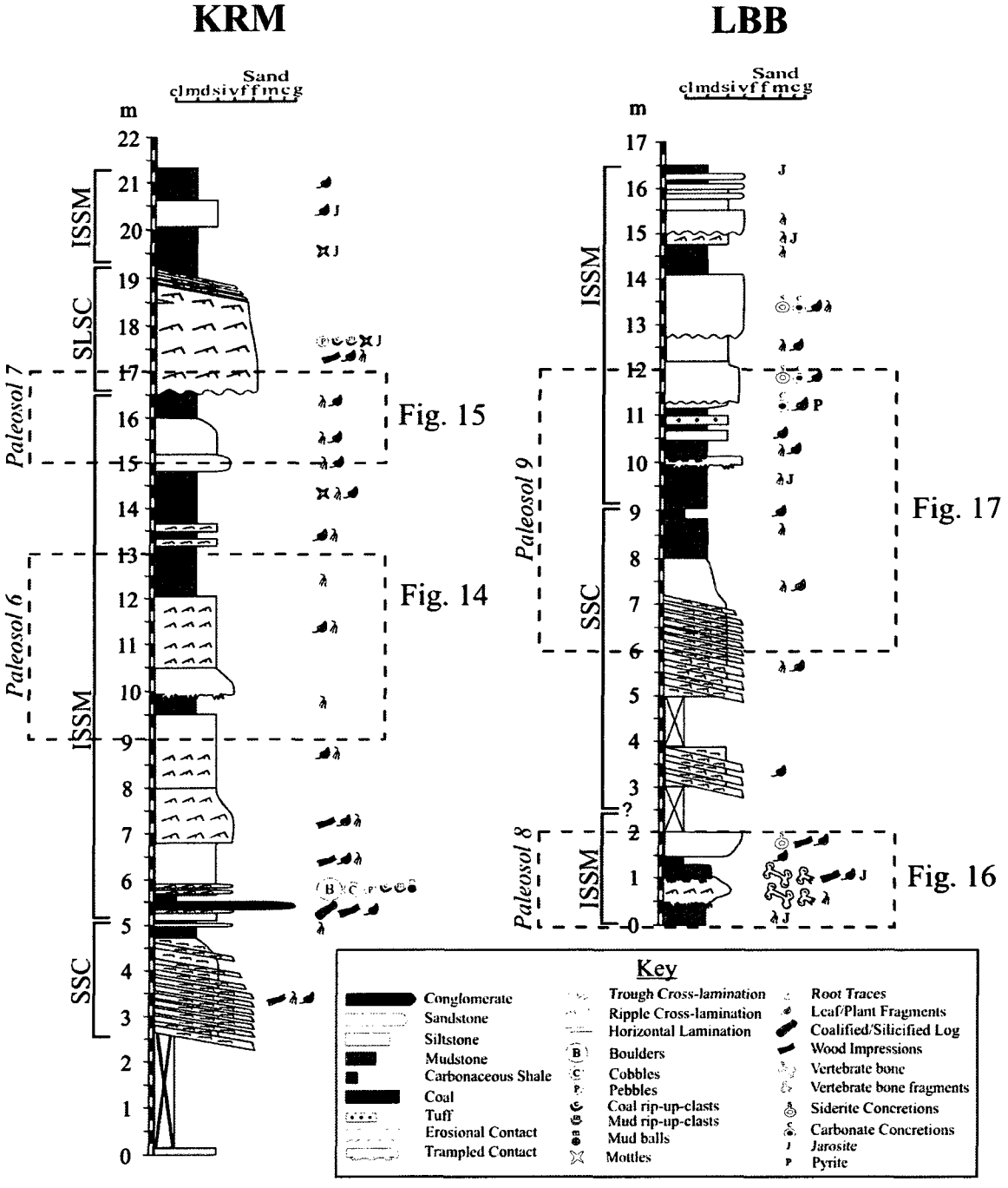

Figure 3.4 cont.

Table 3.1. Micromorphological features described from paleosols of the Prince Creek Formation

Feature	Description	Size	Interpretation
Physical Features			
Peds	Soil aggregates separated by natural surfaces of weakness. Blocky, platy, and channel microstructures are common.	0.25-4.0 cm avg. 1-2 cm	Blocky, platy structures indicate weakly-developed soils, repeated wetting and drying (Retallack 2001, McCarthy et al. 2003)
Voids	Includes channels, chambers, planes, vughs, packing voids.	variable	Actions of roots, organisms, packing (Brewer 1964, McCarthy et al. 2003)
Birefringence fabric (b-fabric)	Speckled, monostriated, porostriated, and bioturbated fabrics are common. Speckled and bioturbated fabrics randomly distributed throughout matrix. Monostriated and porostriated fabrics are sub-parallel and found adjacent to voids or microlaminae.	variable 50 μm-500 μm	Speckled fabrics develop from suspension settling and flocculation of clays. (McCarthy and Plint 2003)Striated fabrics develop through realignment of clays during wetting and drying (Brewer 1964)
Microlaminations	Sub-parallel laminations recognized by subtle color or grain size changes. Commonly penetrated by carbonaceous roots.	0.1-1.5 mm thick	Deposition and compaction of sediments
Ferruginous Features			
Depletion coatings	Zone along the surface of ped where iron, manganese, and clay has been removed.	< 0.75 mm thick	Fe-oxides mobilized and removed from ped and void margins (Bullock et al 1985, Richardson and Daniels 1993).
Zoned peds	Soil aggregates with an outermost depletion coating, darker-colored Fe-rich matrix, and lighter-colored Fe-poor center.	< 2 cm long	Result from gleization and repeated wetting and drying (Veneman et al. 1976, Richardson and Daniels 1993)
Ferruginous void coatings and infillings	Typic (regular in thickness over length) void coatings and dense void infillings. Can occur as hypocoatings (coatings adjoining but not on the surface of a channel) or quasicoatings (coatings related to the surfaces of voids but not immediately adjoining them). Rarely interlayered with microlaminated clay infillings.	< 250 μm	Segregation of Fe-oxides in voids during repeated wetting and drying cycles (Fanning and Fanning 1989)
Fe-oxide mottles and nodules	Reddish-orange mottles. Compound or compound impregnative discreet, typic to amiboidal reddish-orange iron-oxide nodules. May nucleate from organics.	mottles up to 2 cm long nodules 50 μm-2 mm	Segregation of Fe-oxides in matrix during repeated wetting and drying cycles (Fanning and Fanning 1989)

Table 3.1 cont. Micromorphological features described from paleosols of the Prince Creek Formation

Manganiferous Features			
Manganese-oxide nodules	Black, typic to amiboidal strongly impregnated nodules.	0.25-1.0 mm	Segregation of Mn-oxides during repeated episodes of wetting and drying (Fanning and Fanning 1989)
Textural Features			
Clay coatings and infillings	Microlaminated, typic, grey to yellowish-orange clays coating pore and void margins or partially to completely filling pores and voids. Continuous to discontinuous and crescentic. Rare ferruginous hypocoatings or quasicoatings.	< 50 μm	Translocation of clays during repeated episodes of wetting and drying (McCarthy and Plint 2003; Ufnar et al. 2005)
Grain coatings	Microlaminated clay surrounding framework grains.	avg. 15 μm thick	Shrink-swell or short term transport (McCarthy and Plint 2003
Clay intercalations	Elongate, undulating yellowish-grey clay inclusions interspersed throughout the matrix unrelated to voids.	< 1.5 mm long	Pedogenic incorporation of former clay coatings and infillings into the matrix (McCarthy and Plint 2003)
Pedorelicts	Sub-rounded soil aggregates, rarely composed of reddish-orange clay or silty clay. Common depletion coatings.	< 2 mm long	Short distance transport of peds under low energies (McCarthy and Plint 2003)
Papules	Reddish-brown sub-rounded clay-rich particles.	0.25-1.0 mm long	Pedoturbation and/or short-term transport (McCarthy and Plint 2003)
Biological Features			
Burrows	Ovoid to elliptical tubules with sharp to slightly irregular pale-yellow to orange clay boundaries, commonly contain a dark circular central mass. Also evidenced by disrupted groundmass with semi-elliptical orientation of clays and organics	avg. 0.5 mm diameter	Attributed to insects and/or earthworms. Suggests prolonged surface stability (Hasiotis 2002, McCarthy and Plint 2003, Hembree and Hasiotis 2007).
Carbonaceous root traces	Carbonaceous, sub-vertical organics in voids that taper downward, rarely branch, and often disturb or perforate microlaminae.	Up to 5 mm long & 0.5 mm wide	Root-zones. Carbonaceous preservation suggests poorly-drained, reducing conditions (Retallack 1997, Kraus and Hasiotis 2006).
Organic fragments and organic-rich stringers	Amorphous to subrounded opaque to black fragments, commonly with preserved cellular structure. Opaque to black stringers rarely with preserved cellular structure separated by up to 1 mm of muddy matrix and irregular contacts.	Fragments 0.25-2 mm long & 0.25 mm thick. Stringers < 0.25 mm thick	Carbonaceous plant fragments, preservation suggests poor drainage (Kraus 1998, Davies-Vollum and Wing 1998)

Table 3.1 cont. Micromorphological features described from paleosols of the Prince Creek Formation

Bone fragments	Brownish-tan sub-angular to sub-rounded bone fragments with preserved cellular structure.	< 1.0 mm long	Comminuted dinosaur bone
Minerals			
Sphaerosiderite	Reddish-orange circular, geodic masses that disrupt groundmass. Concentric to halo morphology. Commonly exhibit ferruginous coatings or hypocoatings .	0.1-0.5 mm diameter	Forms under saturated, organic-rich, reducing conditions (Browne and Kingston 1993, Ludvigson et al. 1998, McCarthy and Plint 1998). Suggests freshwater (Curtis and Coleman 1986)
Jarosite	Yellowish mottles and rare yellow coatings in voids or yellow coatings surrounding organic fragments.	mottles < 2 cm long coatings < 50 μm	Oxidation product of pyrite. Indicates available marine sulfate (Kraus 1998, Fanning and Fanning 1989, Davies-Vollum 1999)
Pyrite	Framboids and polyframboids.	<0.15 mm	Mixing of marine waters with pore fluids in paleosols (Wright 1986, Madsen and Jensen 1988)
Gypsum	Radiating, euhedral crystals.	< 0.2 mm	Oxidation of pyrite (Wright 1986, Kraus 1998, Fanning et al. 2010).
Volcanic glass shards	Angular to sub-angular glass laths or subrounded glass spherules. Spherules recognized by bubble junctions.	<0.2 mm	Ashfall (Retallack 1983, 1997, Hembree and Hasiotis 2007)

Table 3.2. Diagnostic features of microfacies of the Prince Creek Formation

Microfacies	Description	Diagnostic Features
Microfacies 1 Figs. 6A, 6B, 6C	Quartz and chert-rich sandstone	Common quartz (30-40%), chert (30-40%), biotite (10-15%), muscovite, feldspar, sedimentary rock fragments (< 5%) Rare yellow-orange clay coatings and grain coatings, amiboidal and strongly impregnated Mn-oxide and Fe-oxide nodules, pedorelicts and papules up to 1 mm long, Sub-rounded organic fragments
Microfacies 2 Figs. 6D	Laminated quartzose sandstone and siltstone or mudstone	Common quartz (40-50%), chert (20-30%), mica (biotite and muscovite 20-30%), feldspar and sedimentary rock fragments (< 5%), dark-brown to black silt and mud laminations up to 3 mm thick, amorphous subrounded opaque organic particles up to 2 mm long, organic-rich stringers < 1 mm thick along microlaminae Rare Mn-oxide and Fe-oxide nodules, clay infillings, clay coatings, grain coatings, reddish-orange papules up to 1 mm long
Microfacies 3 Figs. 6E, 6F, 6G, 6H	Massive to microlaminated mudstone	Common up to 40% silt, relict volcanic glass shards, clay infillings, grain coatings, reddish-orange papules up to 0.5 mm long, subrounded to amorphous organics < 0.5 mm along longest axis, sub-vertical carbonaceous root traces Rare bioturbation, ferruginous void coatings, Fe-oxide and Mn-oxide nodules, radiating euhedral gypsum crystals up to 0.2 mm long exclusively at LBB
Microfacies 4 Figs. 7A, 7B	Organic-rich mudstone	Common abundant organics (> 5%) as parallel to sub-parallel stringers< 0.25 mm thick with irregular contacts separated by up to 1 mm of muddy matrix, carbonaceous root traces, relict volcanic glass shards, microfacies is most common at the top of paleosol profiles Rare clay infillings, bioturbation, Fe-oxide and Mn-oxide nodules, ferruginous void coatings, reddish-brown papules up to 0.5 mm long, jarosite, pyrite framboids up to 0.15 mm in diameter exclusively at LBB

Table 3.2 cont.. Diagnostic features of microfacies of the Prince Creek Formation

Microfacies 5 Figs. 7C, 7D	Mudstone containing zoned peds	Common Zoned peds commonly containing multiple iron depletion zones appearing as a series of lighter-colored, grey or tan concentric rings radiating outward from a central light-colored zone and alternating with darker-colored matrix, Fe-oxide nodules, ferruginous void coatings, clay infillings and clay coatings, clays interlayered with ferruginous coatings, relict volcanic glass shards Rare Mn-oxide nodules
Microfacies 6 Figs. 7E, 7F	Bioturbated mudstone	Common ovoid, elliptical burrows with sharp to slightly irregular pale-yellow to orange clay boundaries filled with mudstone similar to matrix; viewed in cross-section tubules contain a dark, circular central mass; disrupted groundmass with semi-elliptical orientation of clay particles and organics, Fe-oxide and Mn-oxide nodules, ferruginous void coatings, relict volcanic glass shards
Microfacies 7 Figs. 7G, 7H	Mudstone with illuvial clay	Common > 5% of voids filled with pale-yellow to yellowish-orange typic, microlaminated, crescentic clay infillings or coatings partially or completely filling voids, interlayered ferruginous coatings, ferruginous hypocoatings or quasicoatings, simple clay intercalations, relict volcanic glass shards Rare impregnated Fe-oxide or Mn-oxide nodules
Microfacies 8 Figs. 8A, 8B	Mudstone with iron-oxide segregations	Common > 5% Fe-oxide segregations (ferruginous nodules and mottles, ferruginous grain coatings, ferruginous void coatings, and ferruginous infillings); discreet, typic to amiboidal, reddish or reddish-orange Fe-oxide nodules strongly impregnated within the groundmass; compound, or compound impregnative nodules and mottles; typic ferruginous void coatings and dense void infillings, black amiboidal Mn-oxide nodules, relict volcanic glass shards Rare ferruginous segregations nucleating from organics, reddish-orange papules up to 0.5 mm long, sphaerosiderite
Microfacies 9 Figs. 8C, 8D	Mudstone with sphaerosiderite	Common > 5% sphaerosiderite spherules up to 0.5 mm in diameter occurring as reddish-orange circular geodic masses, typically with a concentric to halo morphology, ferruginous coatings or hypocoatings on sphaerosiderite spherules, Fe-oxide and Mn-oxide nodules, ferruginous void coatings, bioturbation, relict volcanic glass shards

Table 3.2 cont. Diagnostic features of microfacies of the Prince Creek Formation

Microfacies 10 Figs. 8E, 8F 6H	Mudstone with abundant papules and/or pedorelicts	Common > 5% papules and/or pedorelicts composed of reddish-brown to reddish-orange clay or silty clay contrasting with the matrix, subrounded papules up to 1 mm long (longest axis), subrounded pedorelicts up to 2 mm long (longest axis), subrounded, opaque organic fragments and stringers, relict volcanic glass shards Rare Fe-oxide and Mn-oxide nodules, ferruginous void coatings, bioturbation, radiating euhedral gypsum crystals exclusively at LBB
Microfacies 11 Figs. 8G, 8H	Mudstone with comminuted bone and plant fragments	Common angular to sub-rounded comminuted carbonaceous plant fragments and dinosaur bone fragments aligned sub-parallel to one another encased in a muddy matrix

spectrometer on powdered whole-rock samples at the Advanced Instrumentation Laboratory at the University of Alaska, Fairbanks. Total organic carbon (TOC) was determined by Weatherford Laboratories, Shenandoah, Texas. Samples were pulverized, sieved, and reacted with concentrated HCl to dissolve carbonates. Samples were dried and combusted in a LECO model C230 combustion furnace. Carbon dioxide generated by the combustion of organic matter was quantified using an infrared detector to determine TOC. Quantitative bioanalyses of bulk samples from selected soil horizons was provided by Sue Matthews at Palynological Laboratory Services with results interpreted by Steve Lowe at BP America.

SEDIMENTOLOGY

Fluvial Channels

Detailed descriptions of the facies and alluvial architecture of the Prince Creek Fm. are presented elsewhere (Flaig et al. 2010). The Prince Creek Fm. contains three distinct channel-forms. Large sinuous channels (LSC, Fig. 3.5A) contain erosionally based, 13.0-17.0 m-thick, fining-upward successions (FUS) with a basal conglomerate and a medium- to fine-grained multi-storey sandbody that lacks root traces and fines-upward into an interval of inclined heterolithic stratification (IHS) and 3-4 m of finer-grained organic-rich sediments. IHS composed of rhythmically repeating sand and mud couplets indicates tidal influence in channels (Flaig et al. 2010). Large sinuous channels

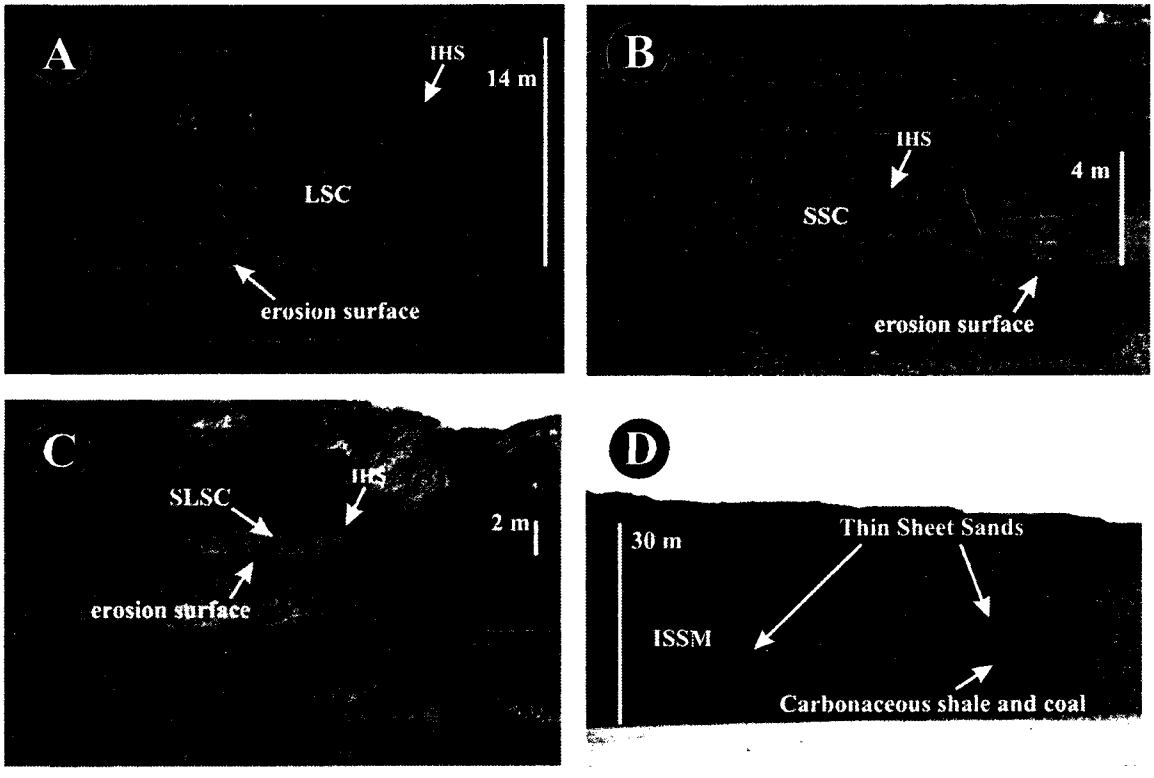

Figure 3.5. Facies associations of the Prince Creek Formation including (A) Large Sinuous Channels (LSC), (B) Small Sinuous Channels (SSC), (C) Small Low Sinuosity Channels (SLSC), and (D) Interbedded Sandstone, Siltstone, and Mudstone (ISSM), IHS=Inclined Heterolithic Stratification.

are interpreted as tidally-influenced, suspended-load meandering trunk channels (Flaig et al. 2010).

Small sinuous channels (SSC, Fig. 3.5B) are not as thick (2.0-6.0 m) and are composed predominantly of a single-storey, fine-grained sandbody dominated by IHS, and all sediments within them contain vertical to sub-horizontal root traces. Small sinuous channels occur as laterally extensive heterolithic sheets encased in organic-rich floodplain fines that appear lenticular along strike. These heterolithic sandbodies commonly grade laterally into asymmetrical, trough-shaped features filled with rooted mudstone and siltstone overlying a concave-up erosion surface. Small sinuous channels are interpreted as tidally influenced meandering distributary channels within crevasse splay-complexes (Flaig et al. 2010).

Small low-sinuosity channels (SLSC, Fig. 3.4C) are composed primarily of a 1.5-3.0 m-thick, very-fine to fine-grained, single-storey, current rippled, ubiquitously rooted sandbody that sits atop an arcuate, concave-up basal erosion surface. IHS is largely absent in these channels and, where present, is only found at the top of the channel-fill. Wings of horizontally bedded, ripple cross-laminated sandstone or siltstone commonly extend laterally from the uppermost portion of the channel-fill along channel margins. Numerous small, low-sinuosity channels are typically found in tiers at the same stratigraphic level either incised into small sinuous channels or into floodplain facies. Small low-sinuosity channels are interpreted as tidally influenced, laterally stable ribbon sandbodies (anastomosed channels?) within crevasse splay-complexes (Flaig et al. 2010).

Floodplains

Fine-grained facies predominate within the Prince Creek Fm. Fine-grained sheet-like sandstones and siltstones < 2 m thick (ISSM, Fig. 3.4D) are typically ripple-cross-laminated, coarsen-upward and/or fine-upward, and are interbedded with fine-grained, organic-rich facies. Some of these sandstones and siltstones contain dinosaur bone (Fig. 3.3) and bone fragments (Phillips 2003; Fiorillo et al. 2009, 2010a, 2010b, Flaig et al. 2010). Others, when viewed in cross-section, are connected to the margins of channels with mudstones overlying and/or underlying them. Small sheet-like sandstones and siltstones are interpreted as crevasse splays and levees (Flaig et al. 2010). FUS composed of 3-4 m of planar-laminated or current-rippled siltstone overlying 3-5 m of fine-to medium-grained, planar-laminated and trough-cross-laminated sandstone are interpreted as channel plugs of large sinuous channels. Thinner packages (< 1 m-thick) of ripple cross-laminated and, rarely, rooted or burrowed siltstone and mudstone that may contain brackish-water clams (*Nucula* aff. *N. percrassa* Conrad, pers. comm. Robert Blodgett) and indeterminate gastropods are interpreted as small floodplain lakes and ponds (Flaig et al. 2010). Organic-rich mudstone, carbonaceous shale, and coal record deposition in swamps. Although organic-rich shales are extremely common, true coals are rare and typically < 1 m thick. Drab-colored, ubiquitously rooted, and typically mottled siltstones and mudstones are interpreted as paleosols (Brandlen 2008, Fiorillo et al. 2010a, 2010b, Flaig et al. 2010). Thin (< 1 m thick) tuffs and bentonites are locally interbedded with other fine-grained facies. Irregular, undulating basal contacts, likely the result of trampling by dinosaurs (Flaig et al. 2010) are common in all finer-grained facies.

Taken together, channel and floodplain sediments exposed in the Prince Creek Fm. along the Colville River suggest deposition on a low-lying, tidally-influenced coastal plain comprised of larger, regionally restricted, meandering trunk channels; smaller, high- and low-sinuosity distributary channels that form parts of crevasse splay complexes; and extensive, vegetated floodplains (Flaig et al. 2010).

PALEOSOL MICROFACIES

Eleven microfacies are defined on the basis of lithology and micromorphology in the Prince Creek Fm (Tables 3.1, 3.2). Photomicrographs including distinguishing characteristics of each microfacies are provided in Figs. 3.6, 3.7, and 3.8. Vertical trends in microfacies define paleosol profiles in the Prince Creek Fm. (Figs. 3.9-3.17).

PALEOSOL DESCRIPTIONS

Nine representative paleosol profiles from four locations along the Colville River (NKT, 06SH, KRM, LBB; Figs. 3.1, 3.4) are described in detail (Figs.3.9-3.17). Paleosol morphologies are identified as compound, compound truncated or cumulative following the definitions outlined by Kraus (1999).

Figure 3.6 (Following Page). Representative microfacies and micromorphological features of the Prince Creek Formation including (A) *Microfacies 1*: lithic-rich quartzose sandstone; (B) impregnated manganese nodule in quartzose sandstone; (C) opaque organic fragment with preserved cellular structure; (D) *Microfacies 2*: laminated quartzose sandstone and siltstone and/or mudstone; (E) *Microfacies 3*: massive to microlaminated mudstone; (F) matrix containing abundant relict volcanic glass, arrows point to bubble junctions between glass shards (G) tapering and branching carbonaceous root-trace in organic-rich mudstone, rt=root; (H) euhedral gypsum crystals in *Microfacies 3* at measured section LBB.

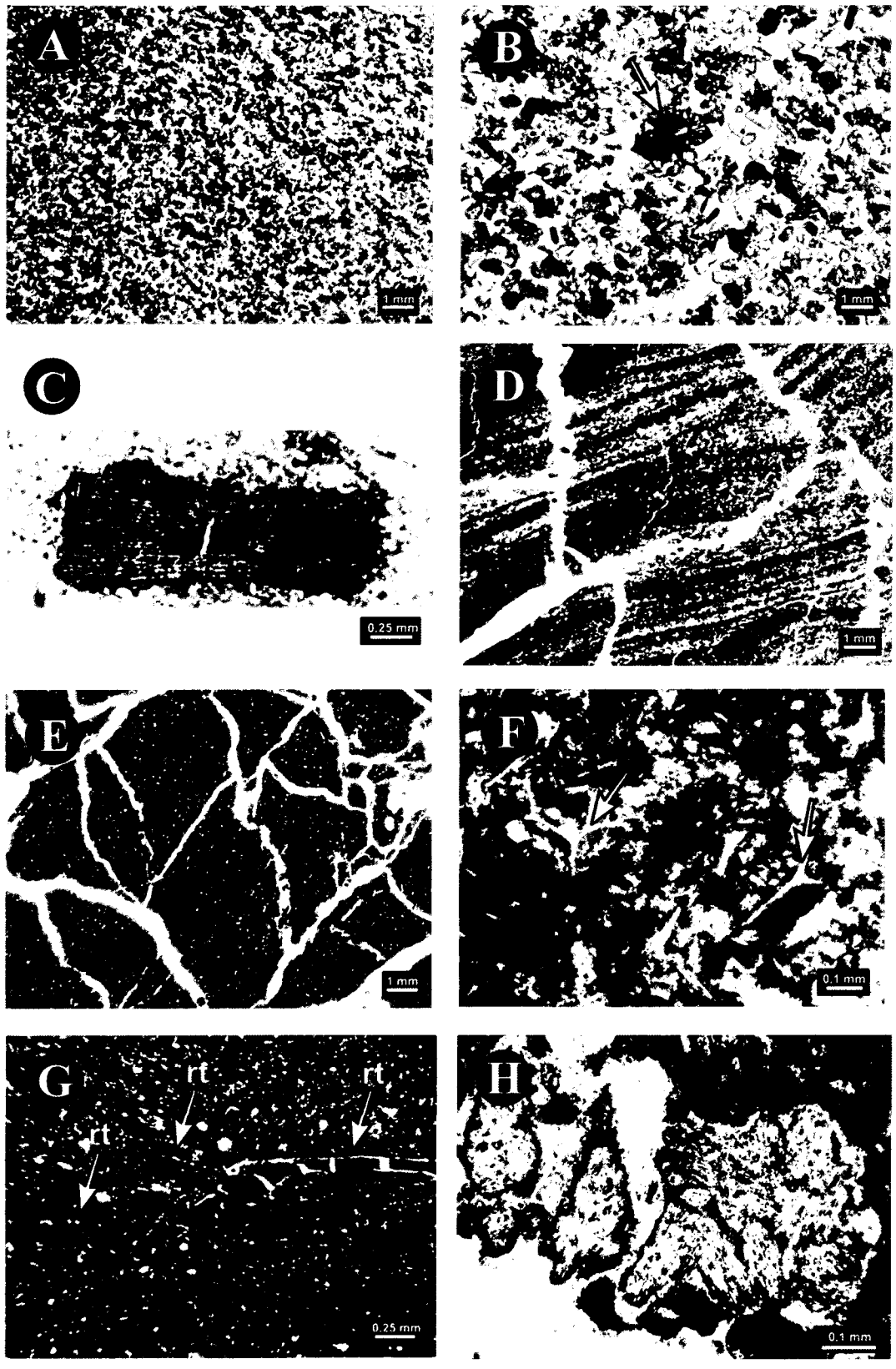
A
1 mm
B
1 mm
C
0.25 mm
D
1 mm
E
1 mm
F
0.1 mm
G
rt
rt
rt
0.25 mm
H
0.1 mm

Figure 3.7 (Following Page). Representative microfacies and micromorphological features of the Prince Creek Formation including (A) *Microfacies 4*: organic-rich mudstone; (B) pyrite framboids in *Microfacies 4* at measured section LBB; (C) *Microfacies 5*: mudstone containing zoned peds; (D) close-up of zoning in peds of *Microfacies 5* including central gley zone (gl) Fe-rich zone, and Fe-poor depletion coating (depl); (E) *Microfacies 6*: bioturbated mudstone bu=burrow; (F) close-up of semi-elliptical burrow with dark circular central mass (arrow) and clay margins (cl) (G) *Microfacies 7*: mudstone with illuvial clay coatings, cly=clay; (H) close-up of crescentic clay infillings in a void.

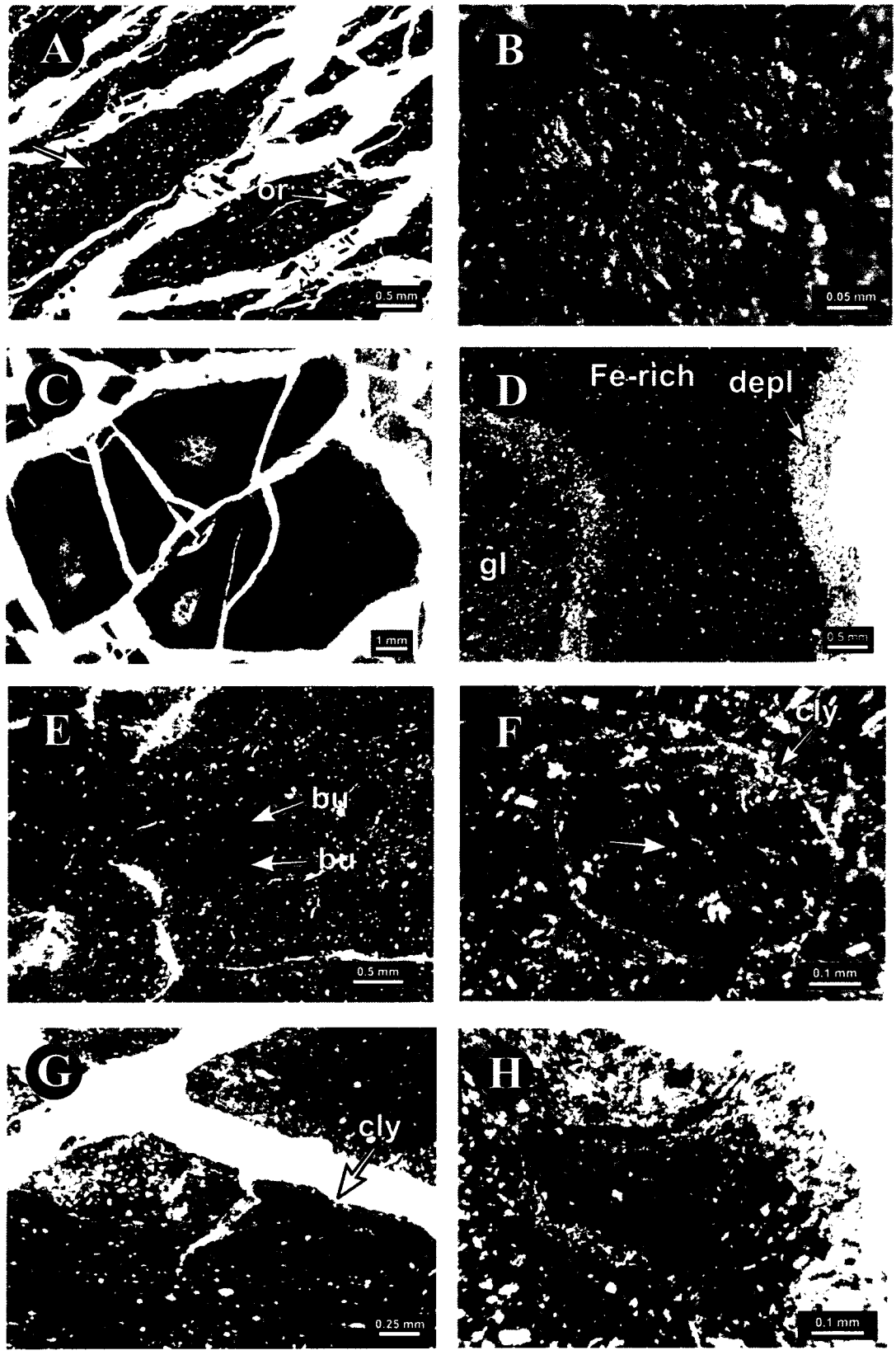
A
or
0.5 mm
B
0.05 mm
C
1 mm
D
Fe-rich
depl
gl
0.5 mm
E
bu
bu
0.5 mm
F
cly
0.1 mm
G
cly
0.25 mm
H
0.1 mm

Figure 3.8 (Following Page). Representative microfacies and micromorphological features of the Prince Creek Formation including (A) *Microfacies 8*: mudstone with iron-oxide segregations, Fe=iron; (B) reddish-orange ferruginous void coatings in *Microfacies 8*, Fe=iron; (C) *Microfacies 9*: mudstone with micro-sphaerosiderite, sd=siderite; (D) close-up of sphaerosiderite concretion showing concentric morphology, sd=siderite; (E) *Microfacies 10*: mudstone with abundant papules and/or pedorelicts, pap=papule (F) papule (pap) and pedorelict (pr) including depletion coating on pedorelict (depl); (G) *Microfacies 11*: mudstone with comminuted bone and plant fragments, or=organic matter; (H) dinosaur bone-fragment in *Microfacies 11*, db=dinosaur bone.

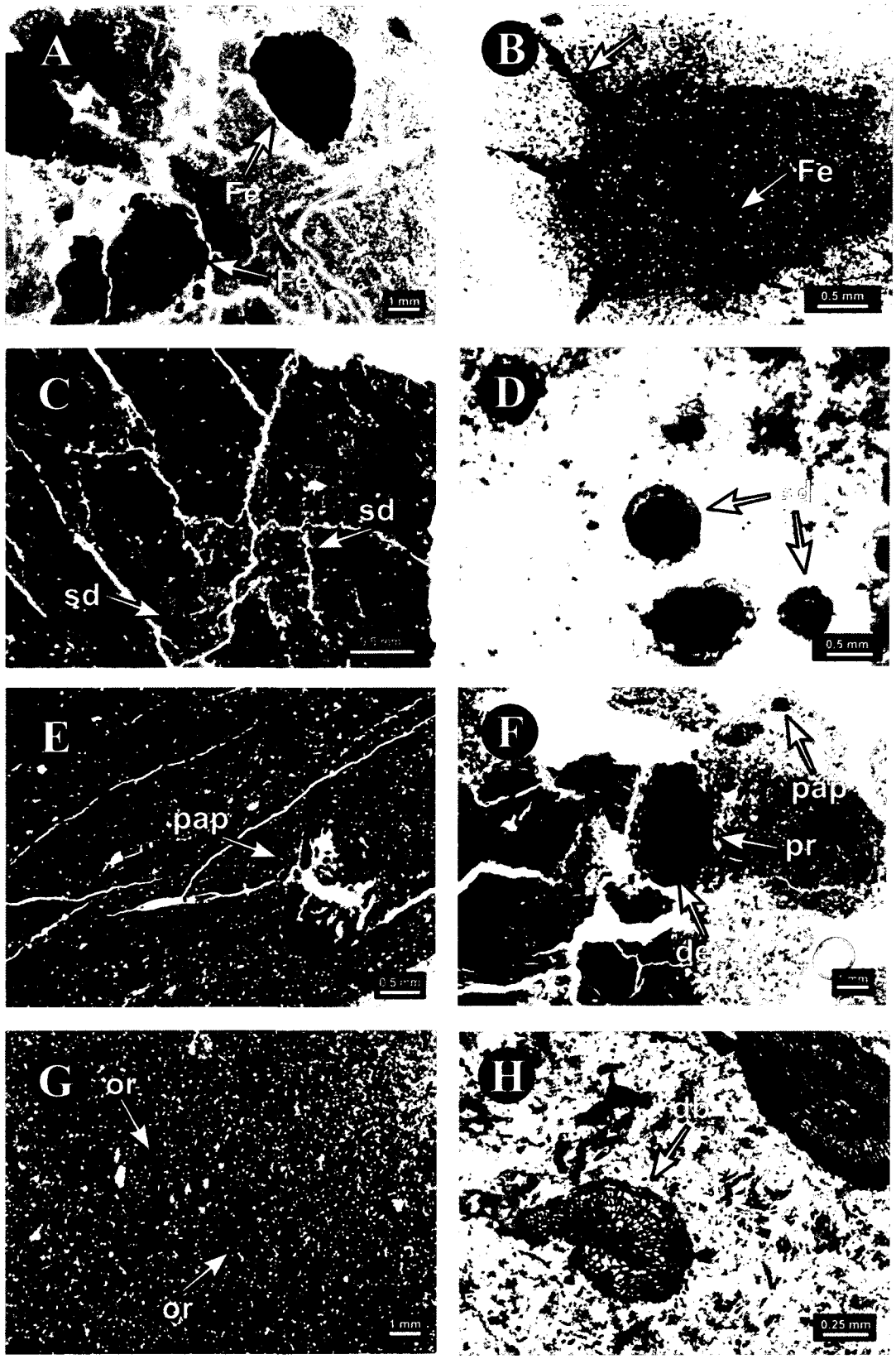
A
Fe
Fe
1 mm
B
Fe
0.5 mm
C
sd
sd
D
sd
0.5 mm
E
pap
F
pap
pr
de
G
or
or
1 mm
H
dt
0.25 mm

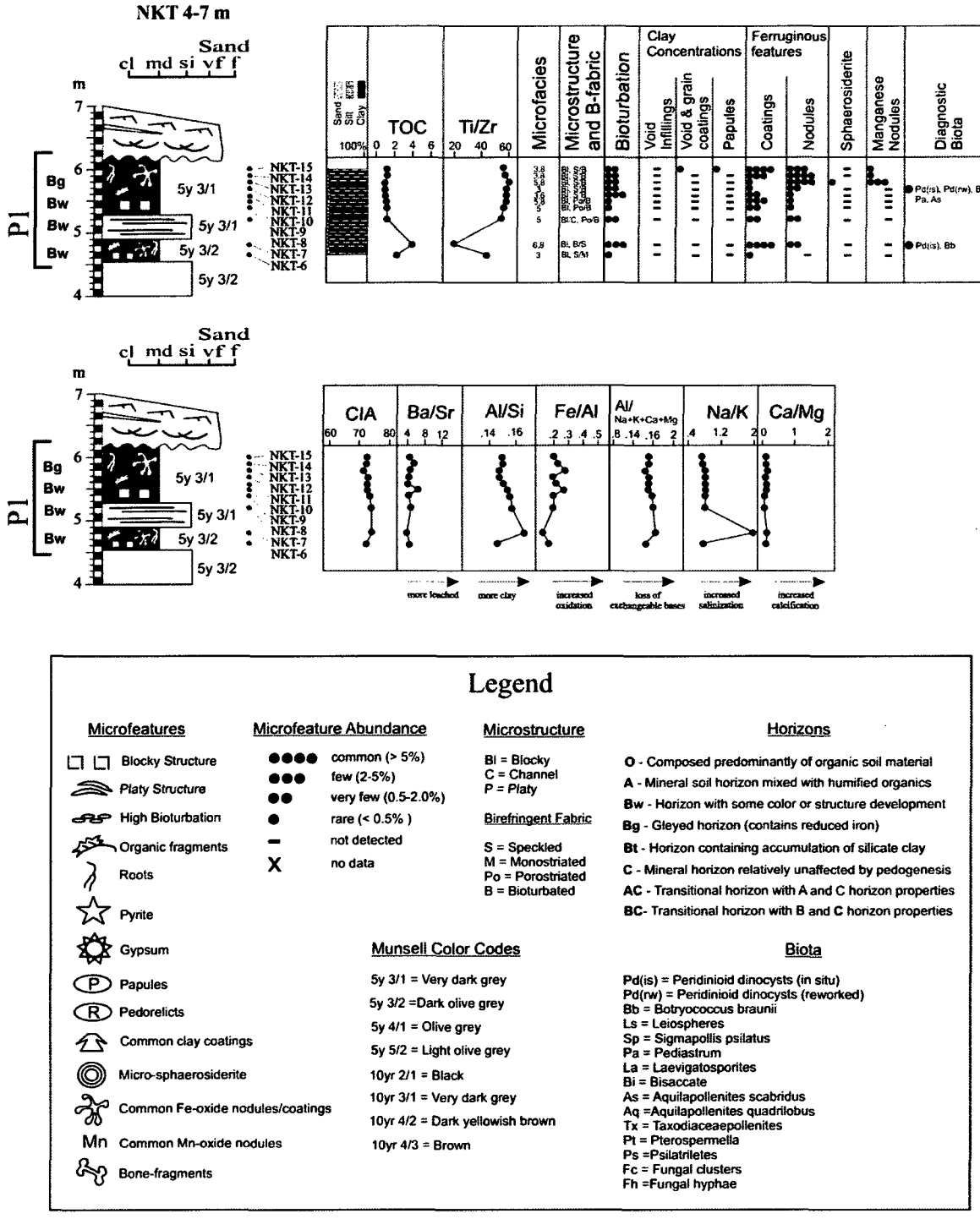

Figure 3.9. Detailed microstratigraphic log for *Paleosol 1* at location NKT (4-7 m) including legend for figures 3.9-3.17. For geographic and stratigraphic location see Figures 3.1 and 3.4. TOC=Total Organic Carbon, CIA=Chemical Index of Alteration.

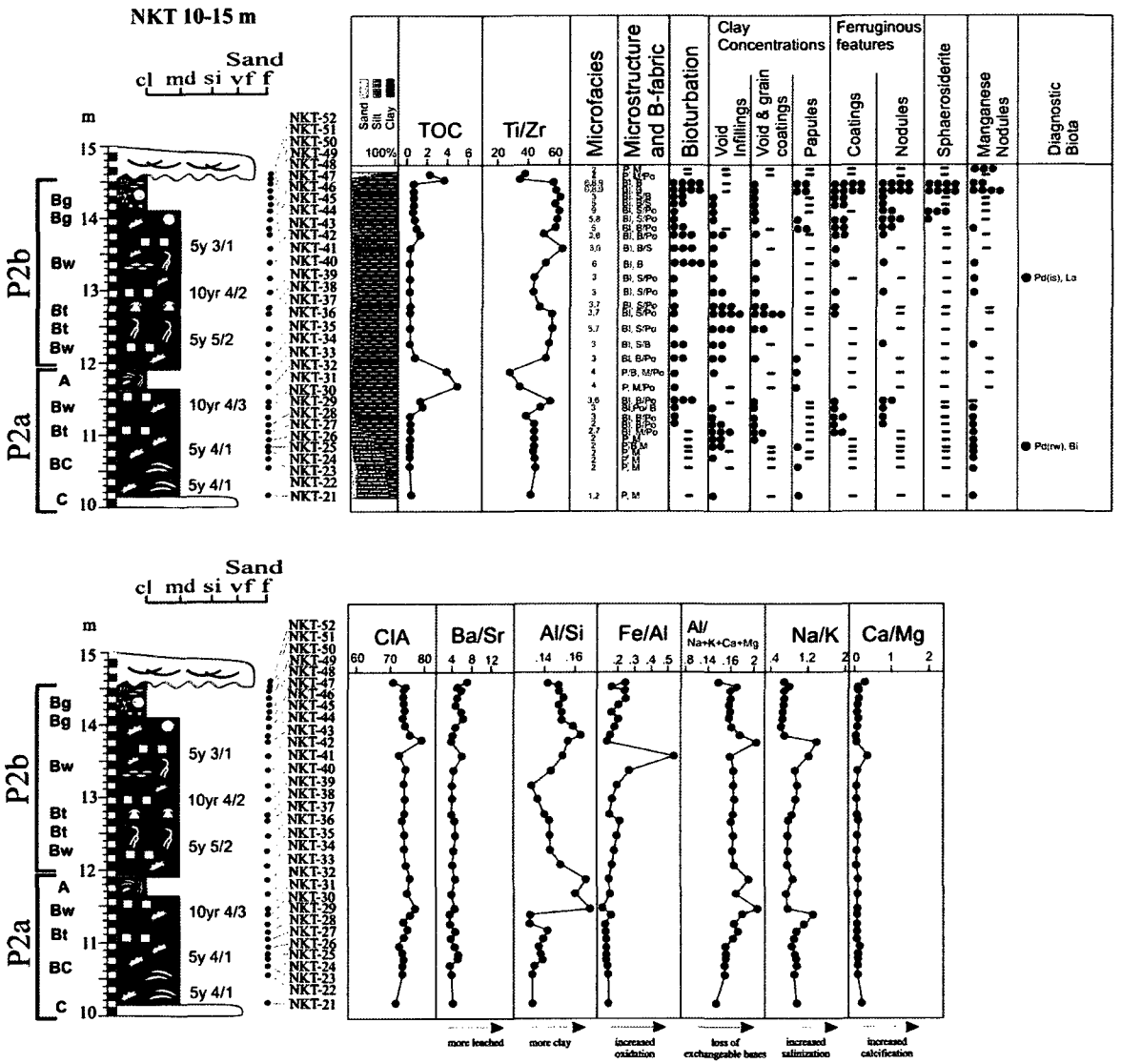

Figure 3.10. Detailed microstratigraphic log for *Paleosol 2a* and *Paleosol 2b* at location NKT (10-15 m). See Figure 3.9 for legend. For geographic and stratigraphic location see Figures 3.1 and 3.4. TOC=Total Organic Carbon, CIA=Chemical Index of Alteration.

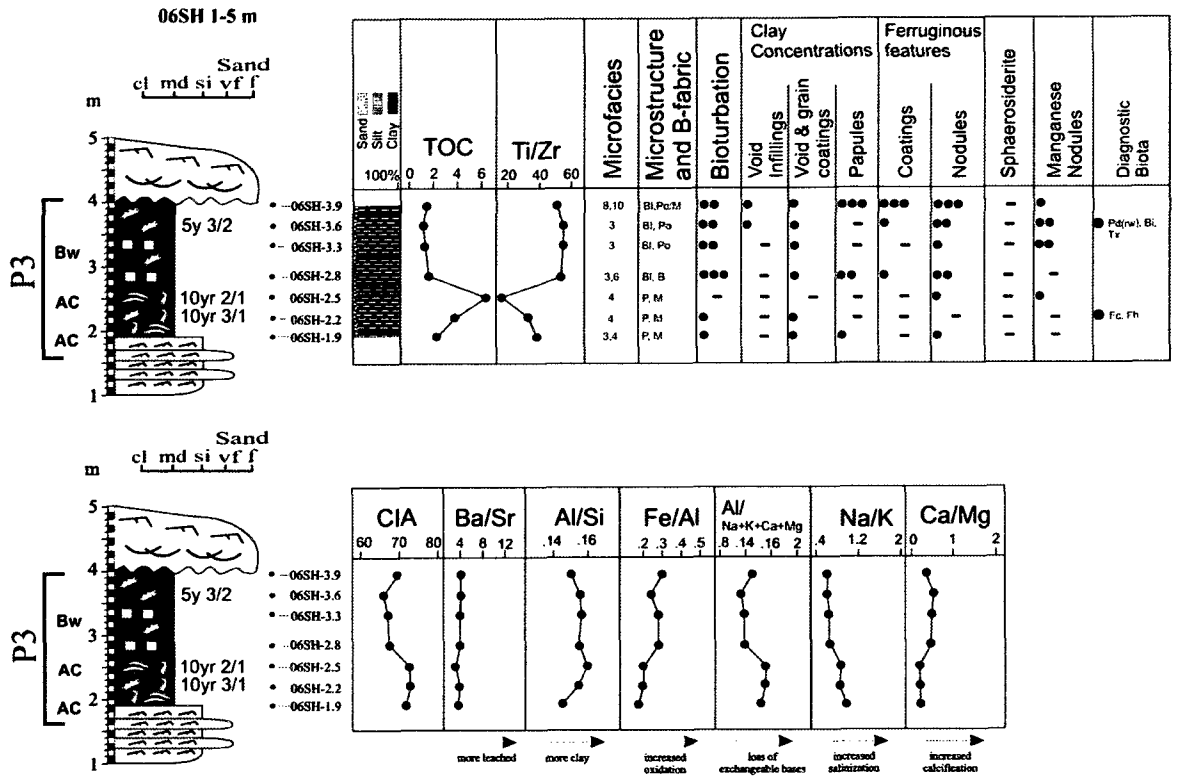

Figure 3.11. Detailed microstratigraphic log for *Paleosol 3* at location 06SH (1-5 m). See Figure 3.9 for legend. For geographic and stratigraphic location see Figures 3.1 and 3.4. TOC=Total Organic Carbon, CIA=Chemical Index of Alteration.

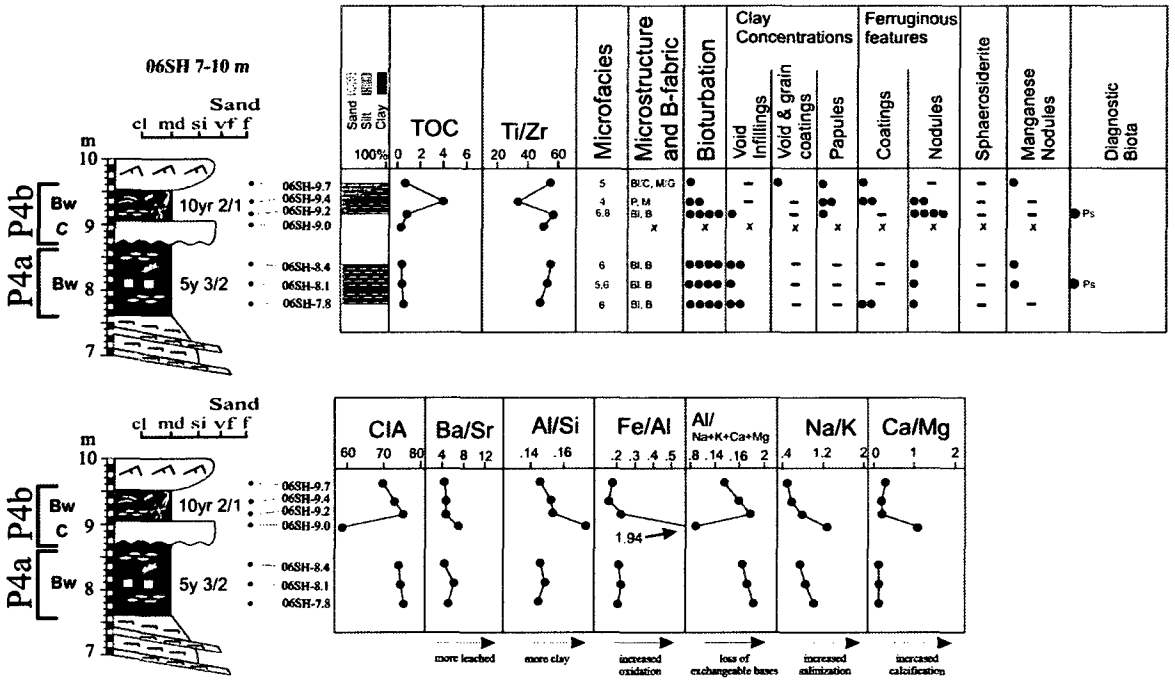

Figure 3.12. Detailed microstratigraphic log for *Paleosol 4a* and *Paleosol 4b* at location 06SH (7-10 m). See Figure 3.9 for legend. For geographic and stratigraphic location see Figures 3.1 and 3.4. TOC=Total Organic Carbon, CIA=Chemical Index of Alteration.

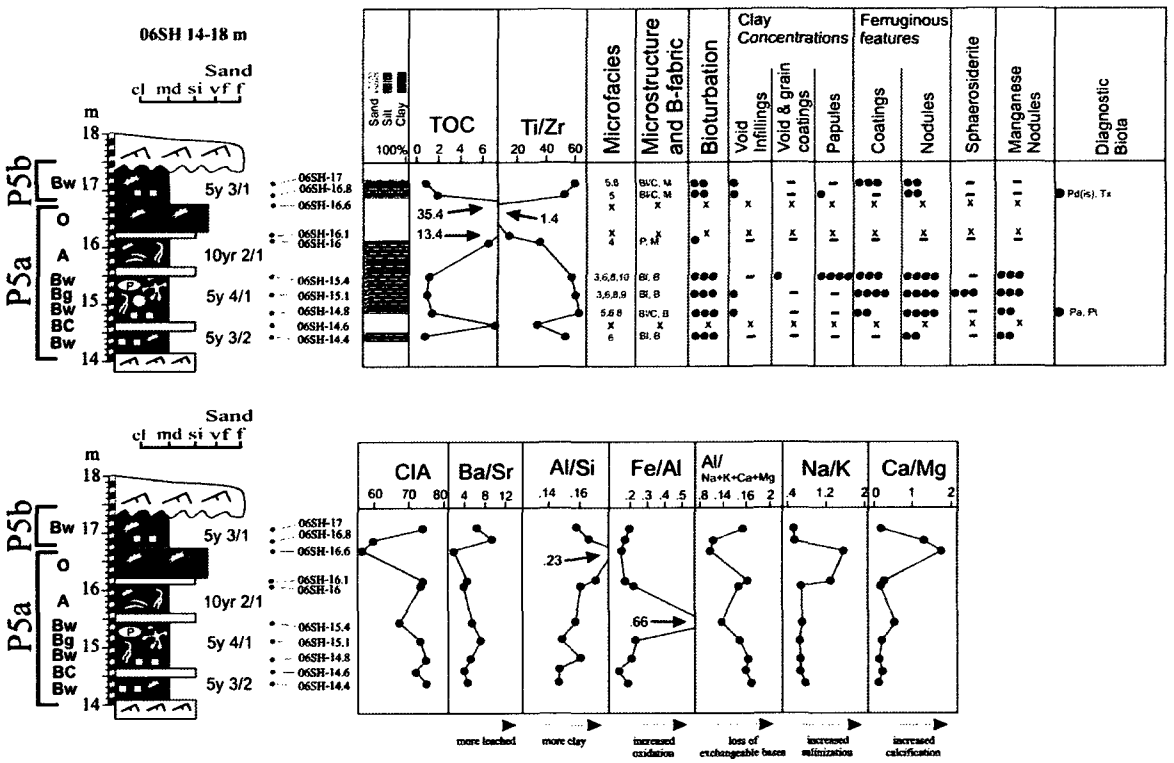

Figure 3.13. Detailed microstratigraphic log for *Paleosol 5a* and *Paleosol 5b* at location 06SH (14-18 m). See Figure 3.9 for legend. For geographic and stratigraphic location see Figures 3.1 and 3.4. TOC=Total Organic Carbon, CIA=Chemical Index of Alteration.

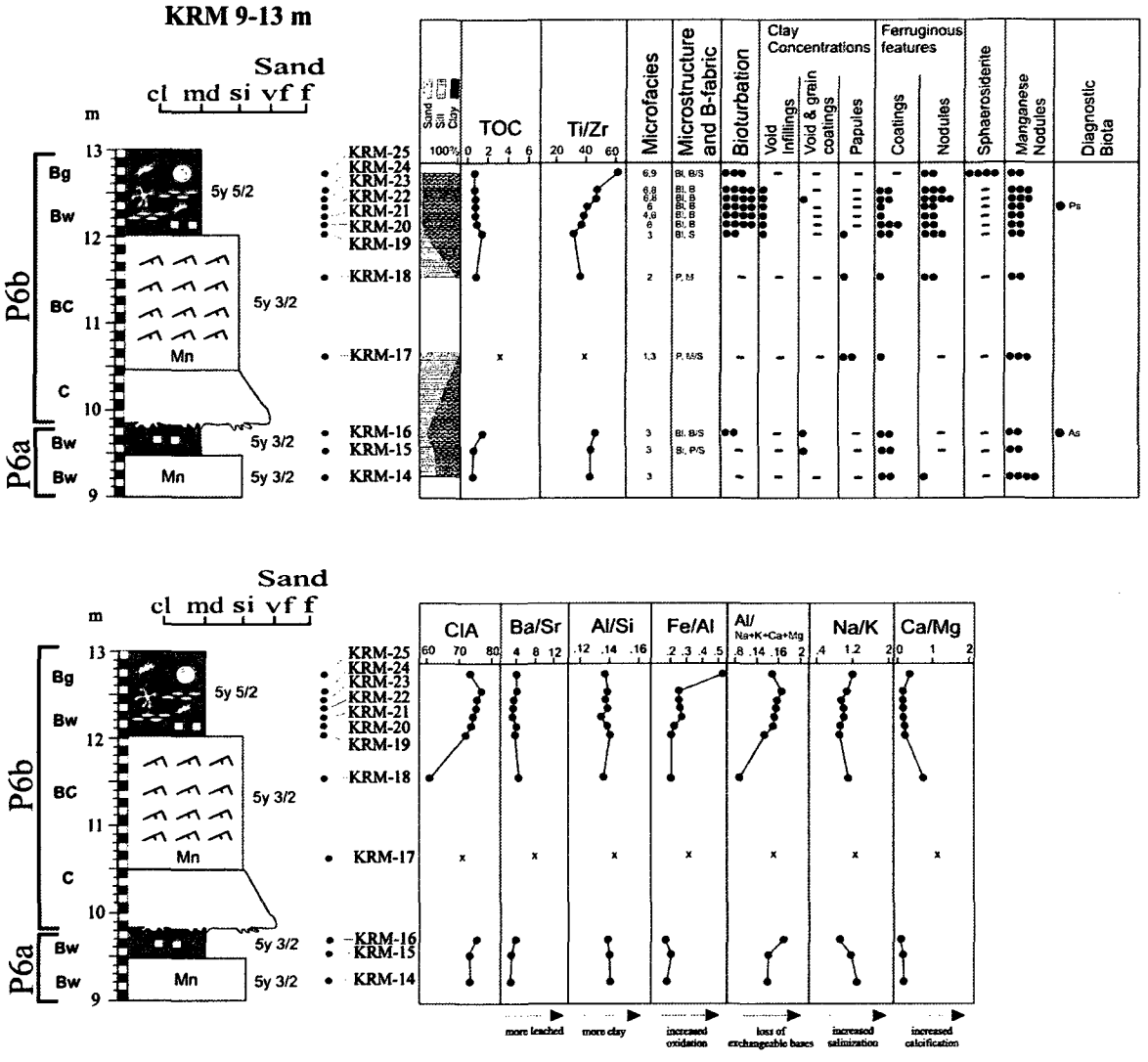

Figure 3.14. Detailed microstratigraphic log for *Paleosol 6a* and *Paleosol 6b* at location KRM (9-13 m). See Figure 3.9 for legend. For geographic and stratigraphic location see Figures 3.1 and 3.4. TOC=Total Organic Carbon, CIA=Chemical Index of Alteration.

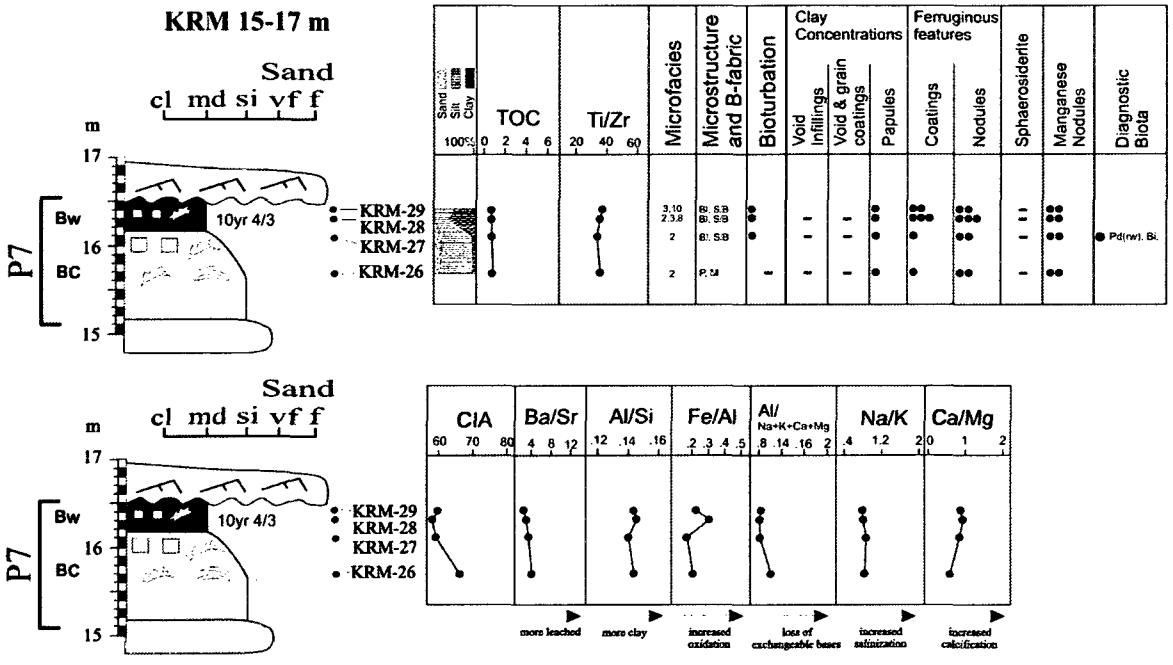

Figure 3.15. Detailed microstratigraphic log for *Paleosol 7* at location KRM (15-17 m). See Figure 3.9 for legend. For geographic and stratigraphic location see Figures 3.1 and 3.4. TOC=Total Organic Carbon, CIA=Chemical Index of Alteration.

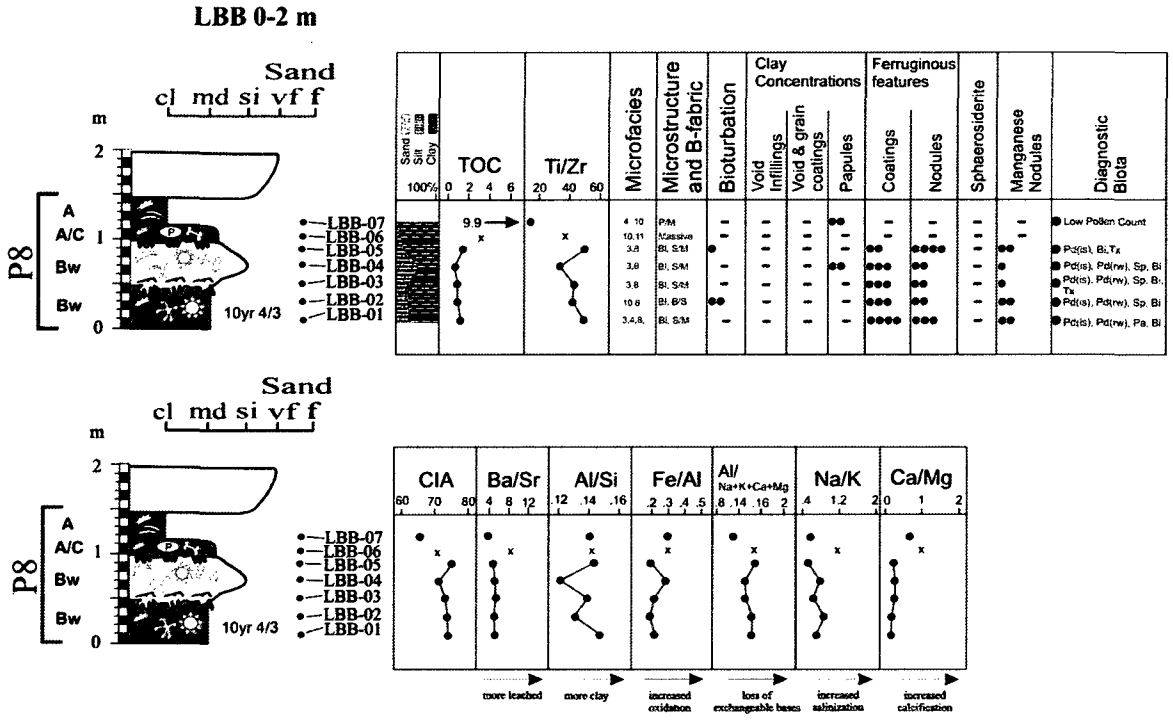

Figure 3.16. Detailed microstratigraphic log for *Paleosol 8* at location LBB (0-2 m). See Figure 3.9 for legend. For geographic and stratigraphic location see Figures 3.1 and 3.4.

TOC=Total Organic Carbon, CIA=Chemical Index of Alteration.

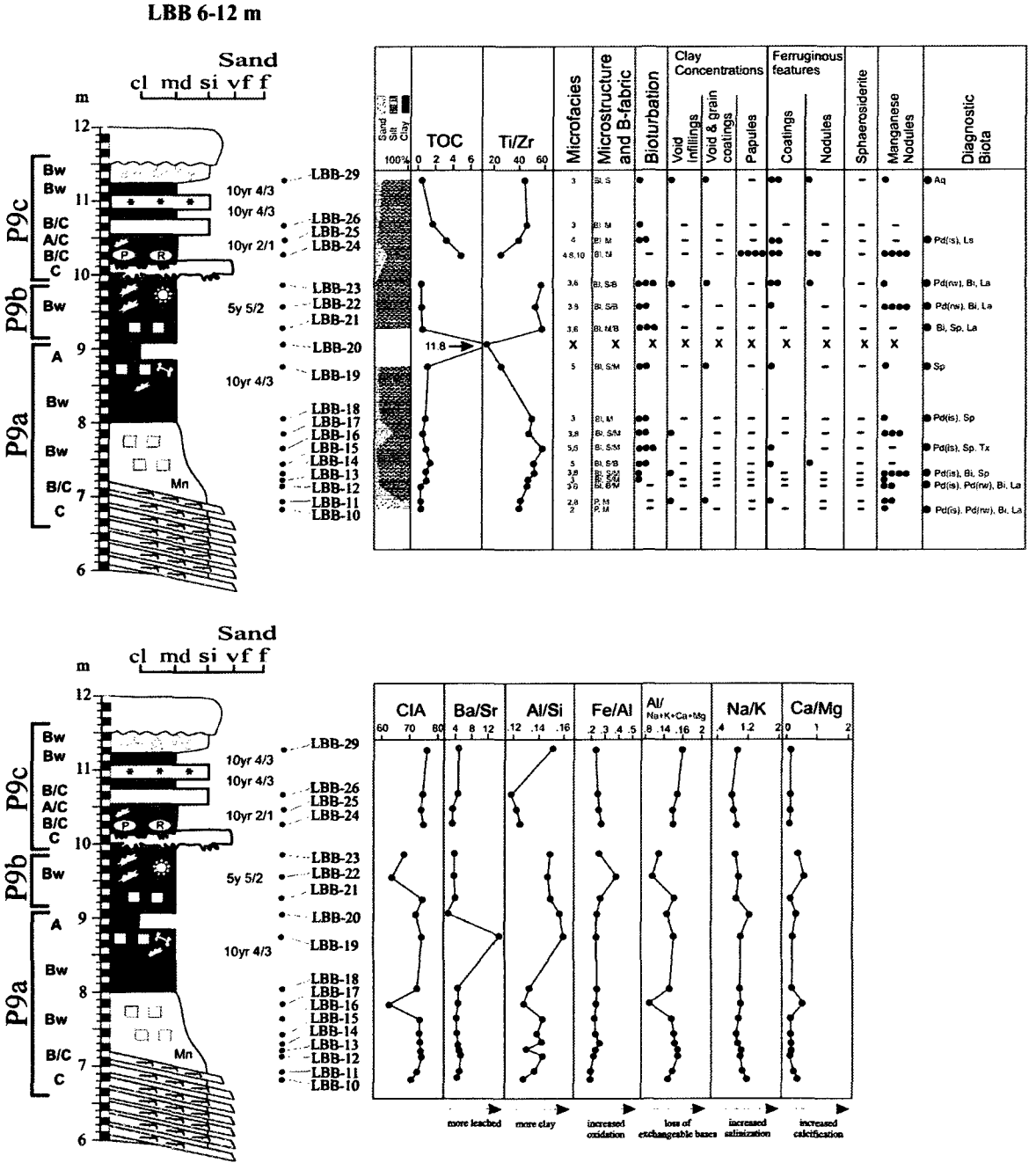

Figure 3.17. Detailed microstratigraphic log for *Paleosol 9a*, *Paleosol 9b*, and *Paleosol 9c* at location LBB (6-12 m). See Figure 3.9 for legend. For geographic and stratigraphic location see Figures 3.1 and 3.4. TOC=Total Organic Carbon, CIA=Chemical Index of Alteration.

Paleosols at North Kikak Tegoseak (NKT)

Paleosol-1 (NKT 4-7 m; Fig. 3.4). -

Paleosol 1 (P1) is a 2.2 m-thick compound paleosol (Fig.3.9). At the base is a 50 cm-thick, massive, dark olive grey (5Y 3/2) siltstone containing plant fragments (microfacies 3). The siltstone is overlain by 40 cm of dark olive grey (5Y 3/2) blocky mudstone that contains very fine carbonaceous root-traces (microfacies 6, 8). Above this is a 30 cm-thick, very dark grey (5Y 3/1) organic-rich laminated siltstone also containing plant fragments (microfacies 5). The paleosol is capped by a 120 cm-thick, very dark grey (5Y 3/1) blocky mudstone with dark-brown mottles, carbonaceous root traces, and siderite nodules up to 2 cm in diameter. (microfacies 3, 5, 6, 8) The upper surface of P1is truncated by the basal erosion surface of a small sinuous channel (Figs. 3.4, 3.5).

Paleosol-2 (NKT 10-15 m; Fig. 3.4).-

Paleosol 2 (P2) is a 4.5 m-thick cumulative paleosol that is sub-divided into two soil-forming successions, *Paleosol 2a* (P2a) and *Paleosol 2b* (P2b) (Fig. 3.10).

At the base of P2a is a 10 cm–thick silty-sandstone (microfacies 1, 2). Above this sandstone is a 30 cm-thick dark-grey (5Y 4/1) platy mudstone (microfacies 2). The mudstone contains fine carbonaceous root-traces and a thin (2-3 cm) hardened zone cemented by siderite near the top. Overlying this cemented zone is an 80 cm-thick dark-grey (5Y 4/1) platy to blocky mudstone containing abundant fine carbonaceous root

traces (microfacies 2, 7). Above this is an additional 40 cm of brown (10YR 4/3) blocky mudstone with abundant carbonaceous root traces (microfacies3, 6). This mudstone grades upward into a 20 cm-thick carbonaceous shale containing abundant carbonaceous plant fragments and root traces that project downwards into the underlying mudstone (microfacies 4).

At the base of P2b is an 80 cm-thick, light olive-grey (5Y 5/2) blocky mudstone containing abundant carbonaceous root traces (microfacies 3, 5, 7). Overlying this mudstone is 70 cm of dark yellowish-brown (10YR 4/2) blocky mudstone with few very fine carbonaceous root traces (microfacies 3, 7). Above this is an 80 cm-thick, very dark grey (5Y 3/1) blocky mudstone containing siderite nodules up to 2 cm in diameter and rare, very fine carbonaceous root traces (microfacies 3, 5, 6, 8, 9). P2b is capped by 20 cm of carbonaceous shale containing abundant plant fragments (microfacies 3, 4, 5, 6, 8, 9). The upper surface of P2b is truncated by the basal erosion surface of a small sinuous channel (Figs. 3.4, 3.5).

Paleosols at Sentinel Hill

Paleosol-3 (06SH 1-5 m; Fig. 3.4).-

Paleosol 3(P3) is a 2.25 m-thick cumulative paleosol (Fig. 3.11). The base of P3 is located at the top of an interval of decimeter-scale interbeds of very-fine sandstone and siltstone. The siltstone and sandstone contain abundant fine carbonaceous

root traces and siderite concretions up to 2 cm in diameter. Overlying this interbedded sandstone and siltstone is a very dark grey (10YR 3/1) platy mudstone containing very fine carbonaceous root traces and carbonaceous plant fragments (microfacies 3, 4). The grey mudstone grades upward into 25 cm of platy, black (10YR 2/1) organic-rich mudstone with carbonaceous plant fragments (microfacies 4). Lying above this mudstone is 130 cm of dark olive grey (5Y 3/2) blocky mudstone (microfacies 3, 6, 8, 10). The mudstone contains abundant plant fragments and carbonaceous root traces, with some root traces surrounded by 5 mm-thick jarosite halos. Reddish-orange mottles are common. P3 is truncated by the basal erosion surface of a small sinuous channel (Figs. 3.4, 3.5).

Paleosol-4 (06SH 7-10 m; Fig. 3.4).-

Paleosol 4 (P4) is a 2 m-thick compound truncated paleosol that is sub-divided into two soil-forming successions (Fig. 3.12) *Paleosol 4a* (P4a) and *Paleosol 4b* (P4b). P4a is a 110 cm-thick dark olive grey (5Y 3/2) blocky mudstone (microfacies 5, 6) found at the top of the small sinuous channel-fill succession that truncates *Paleosol 3*. The mudstone contains very-fine carbonaceous root traces and carbonaceous plant fragments.

At the base of P4b is a 25 cm-thick very fine yellowish-brown sandstone with a basal erosion surface that truncates the top of P4a. The sandstone contains abundant carbonaceous root traces and carbonaceous plant fragments. The paleosol

succession is capped by a black (10YR 2/1) blocky-to-platy organic-rich mudstone containing abundant carbonized plant fragments and very fine root traces (microfacies 4, 5, 6, 8). Lying gradationally above P4b is 150 cm of very fine-grained, ripple cross-laminated sandstone containing abundant carbonaceous root-traces (Fig. 3.4).

Paleosol-5 (06SH 14-18 m; Fig. 3.4).-

Paleosol 5 (P5) is a 3.25 m-thick compound paleosol that is sub-divided into two soil-forming successions (Fig. 3.13) *Paleosol 5a* (P5a) and *Paleosol 5b* (P5b). P5a lies sharply above a 110 cm-thick ripple cross-laminated siltstone (Fig. 3.4) containing carbonaceous root traces, plant fragments, and siderite nodules up to 2 cm in diameter. At the base of P5a is a dark olive grey (5Y 3/2) blocky mudstone containing common very fine carbonaceous root traces (microfacies 6). Above this mudstone is 10 cm of organic-rich siltstone with abundant carbonaceous plant fragments. Overlying the siltstone is 75 cm of blocky olive-grey (5Y 4/1) mudstone containing abundant plant fragments, very fine, carbonaceous root traces, siderite concretions up to 2 cm in diameter, and reddish-orange mottles (microfacies 3, 5, 6, 8, 9, 10). Above this mudstone is another 10 cm of organic-rich siltstone with abundant carbonaceous plant fragments. Overlying this siltstone is 50 cm of black (10YR 2/1), platy, organic-rich mudstone with rare yellowish-orange mottles and very-fine carbonaceous root-traces (microfacies 4). Above this mudstone is an additional 10 cm of organic-rich siltstone containing abundant carbonaceous plant fragments that grades upward into 50 cm of coal.

P5b is a 60 cm-thick very dark grey (5Y 3/1) blocky mudstone containing abundant very fine carbonaceous root traces and carbonaceous plant fragments (microfacies 5, 8). P5b is truncated by the basal erosion surface of a small low-sinuosity channel.

Paleosols at Kikiakrorak River Mouth (KRM)

Paleosol-6 (KRM 9-13 m; Fig. 3.4).-

Paleosol 6 (P6) is 4.0 m-thick compound paleosol that is sub-divided into two soil-forming successions (Fig. 3.14) *Paleosol 6a* (P6a) and *Paleosol 6b* (P6b). The base of P6a is contained within the top of a 175 cm-thick ripple cross-laminated to massive dark olive grey (5Y 3/2) siltstone (microfacies 3) that fines-upward from a very fine-grained, ripple cross-laminated sandstone with a sharp base containing carbonaceous roots, plant fragments, and carbonaceous wood. The top of the siltstone contains current-ripples, carbonaceous root traces, and carbonaceous plant fragments. Overlying the siltstone is 90 cm of dark olive grey (5Y 3/2) blocky mudstone containing very fine carbonaceous root traces (microfacies 3).

At the base of P6b is 70 cm of massive, very fine-grained sandstone with an irregular basal contact. Lying gradationally above the sand is a 160 cm-thick ripple cross-laminated to massive, dark olive grey (5Y 3/2) siltstone (microfacies 1, 2, 3). The top of the siltstone contains current-ripples, carbonaceous root-traces, and carbonaceous plant

fragments. Overlying this siltstone is 90 cm of light olive grey (5Y 5/2) blocky mudstone containing very-fine carbonaceous root-traces (microfacies 3, 4, 6, 8, 9).

Paleosol-7 (KRM 15-17 m; Fig. 3.4).-

Paleosol 7(P7) is a 1.25 m-thick compound paleosol (Fig. 3.15). The base of P7 is a siltstone that lies gradationally above a yellowish-brown, 60 cm-thick sandstone containing carbonaceous roots and plant fragments. The uppermost portion of the siltstone has a platy structure and contains carbonaceous root traces and carbonaceous plant fragments (microfacies 2). Lying gradationally above this siltstone is a brown (10YR 4/3) blocky mudstone that also contains carbonaceous root traces and carbonaceous plant fragments (microfacies 2, 3, 8, 10). P7 is truncated by the basal erosion surface of a small low-sinuosity channel (Figs. 3.4, 3.5)

Paleosols at Liscomb Bonebed (LBB)

Paleosol-8 (LBB 0-2 m; Fig. 3.4).-

Paleosol 8 (P8) is a 1.5 m-thick cumulative paleosol (Fig. 3.16). Strata below the base of *Paleosol 8* are scree-covered and inaccessible. At the base of P8 is a 50 cm-thick brown (10YR 4/3) blocky mudstone (microfacies 3, 4, 8, 10). The mudstone contains abundant carbonaceous root traces with jarosite halos. Gradationally overlying the brown mudstone is a 50 cm-thick siltstone to mudstone (microfacies 3, 8). The contact between

the siltstone and the underlying mudstone is highly irregular, suggesting trampling by dinosaurs (La Porte and Behrensmeyer 1980, Loope 1986, Avanzini et al. 1997, Flaig et al. 2010). At locations where the contact is less disrupted, the base of the siltstone contains ripple cross-laminations. The siltstone also contains semi-articulated, juvenile *Hadrosaur* bone, bone fragments, and carbonaceous root traces. Overlying the siltstone is a 20 cm-thick massive mudstone containing abundant carbonaceous plant fragments, carbonaceous wood fragments, jarosite mottles, and additional semi-articulated juvenile *Hadrosaur* bone and bone fragments (microfacies 10, 11). The contact between the mudstone and the underlying siltstone is also irregular. The paleosol is capped by 30 cm of carbonaceous shale containing abundant plant fragments (microfacies 4, 10). Lying gradationally above P8 is a very fine-grained massive sandbody containing siderite nodules up to 2 cm in diameter, and carbonaceous wood and plant fragments (Fig. 3.4).

Paleosol-9 (LBB 6-12 m; Fig. 3.4).-

Paleosol 9 (P9) is a 4.25 m-thick compound paleosol that is sub-divided into three soil-forming successions (Fig. 3.17) *Paleosol 9a* (P9a), *Paleosol 9b* (P9b), and *Paleosol 9c* (P9c). At the base of P9a is a 75 cm-thick massive to blocky siltstone that grades upward from sandstone and siltstone couplets within IHS at the top of a small sinuous channel-fill succession (Figs 3.4, 3.5). The blocky siltstone contains carbonaceous root traces and carbonaceous plant fragments (microfacies 2, 3, 5, 6, 8). Overlying this siltstone is 80 cm of brown (10YR 4/3) blocky mudstone containing very fine

carbonaceous root traces (microfacies 5). The brown mudstone is overlain by 25 cm of carbonaceous shale with abundant plant fragments.

P9b is a 90 cm-thick light olive grey (5Y 5/2) blocky mudstone containing carbonaceous root traces, with some root-traces exhibiting jarosite halos up to 5 mm thick (microfacies 3, 6, 8).

At the base of P9c is a 10 cm-thick grayish-yellow, very-fine sandstone. The contact between the sandstone and the underlying mudstone of P9b is irregular. Overlying the sandstone is 40 cm of black (10yr 2/1) blocky mudstone containing carbonaceous root traces and carbonaceous plant fragments (microfacies 4, 8, 10). The contact between the mudstone and the underlying sandstone is also irregular. Above this mudstone is 20 cm of organic-rich siltstone with abundant carbonaceous plant fragments (microfacies 3). Overlying this siltstone is a thin, (10 cm) brown (10YR 4/3) mudstone. A 20 cm-thick whitish-grey tuff overlies the brown mudstone. The contact between the tuff and the mudstone is sharp. Above the tuff is a second 10 cm-thick brown (10YR 4/3) mudstone that grades upward into an organic-rich siltstone. The paleosol succession is capped by 30 cm of organic-rich siltstone (microfacies 3). The siltstone contains carbonaceous plant fragments, rare pyrite nodules, and calcite concretions up to 30 cm wide (longest axis). P9c is erosionally truncated by 100 cm of massive very fine-grained sandstone containing carbonaceous plant fragments, siderite nodules up to 20 cm diameter, and calcite concretions (Fig. 3.4).

GEOCHEMISTRY

Geochemical investigations of paleosol profiles using molecular ratios from whole rock geochemical data, to assess parent material uniformity and identify weathering trends, are commonplace (e.g. Retallack 2001, Ashley and Driese 2000, McCarthy and Plint 2003). Geochemical data are plotted as ratio to element concentration plots (Fig. 3.18) and molecular ratio vs. depth plots adjacent to graphic paleosol logs (P1-P9, Figs. 3.9-3.17). Total organic carbon vs. depth is also plotted on Figs. 3.9-3.17.

Ratio to Element Concentration Plots

Ti and Zr are resistant to weathering (relatively immobile) and are residually enriched during pedogenesis (Ashley and Driese 2000, Driese et al. 2000, McCarthy and Plint 2003). Parent material uniformity was evaluated using crossplots of Zr/(Zr/Ti) and Ti/(Ti/Zr) (e.g. Driese et al. 2000, McCarthy and Plint 2003, Stiles et al. 2003). Slopes of Zr/(Zr/Ti) and Ti/(Ti/Zr) plots (Fig. 3.18) indicate that all of the studied paleosols were likely derived from similar parent material and that the source of this parent material was consistent over time. Most compositional differences are attributed to the formation of paleosols from similar source material but as lateral facies equivalents (*c.f.* McCarthy and Plint 2003).

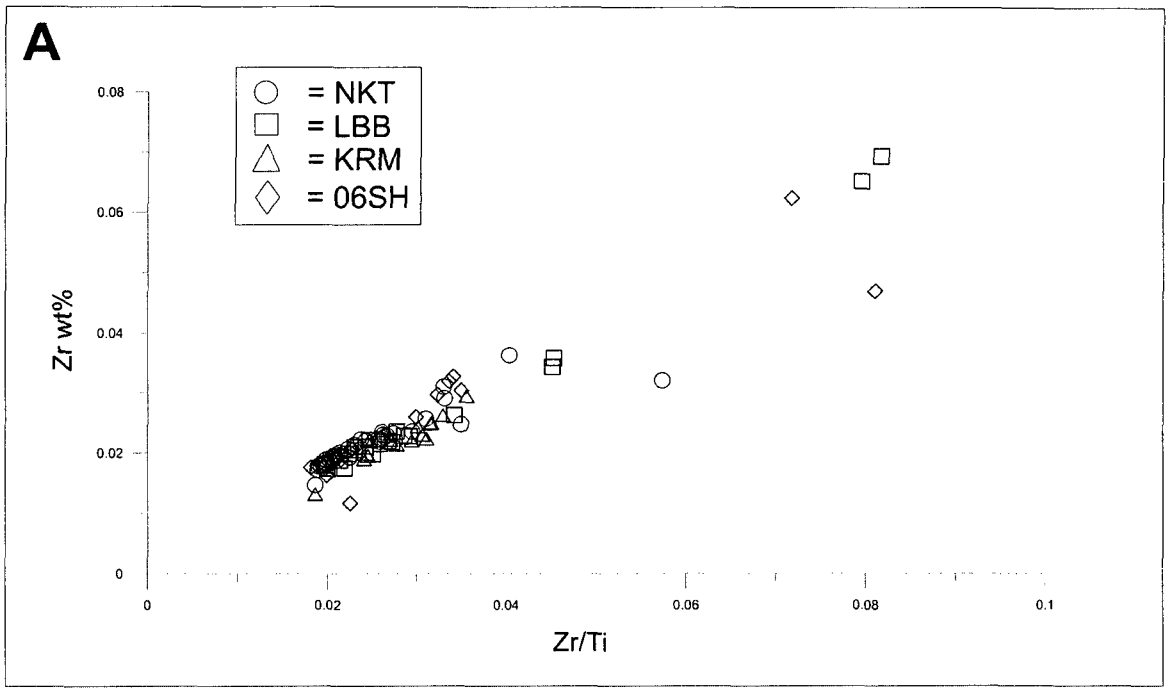

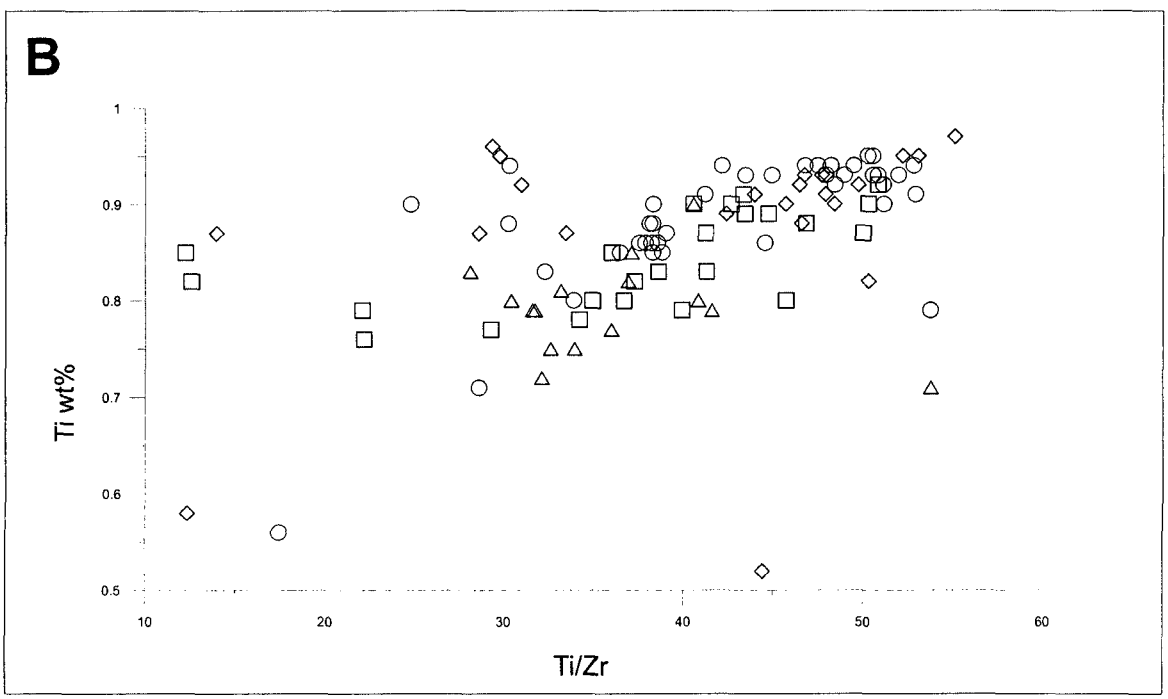

Figure 3.18. Ratio to element concentration plots for Ti and Zr. (A) wt% Zr vs. Zr/T and (B) wt% Ti vs. Ti/Zr.

Molecular Ratios

Because Ti and Zr tend to accumulate as weathering progresses, parent material uniformity in paleosol profiles can be assessed by analyzing the molecular ratio of Ti/Zr vs. depth (Law et al. 1991, Ashley and Driese 2000, Driese et al. 2000, McCarthy and Plint 2003). A gradual change in Ti/Zr vs. depth is expected for uniform parent materials in paleosol profiles (Birkeland 1999, McCarthy and Plint 2003). In paleosols of the Prince Creek Fm. Ti/Zr does not change gradually with depth but instead reflects excursions (e.g. 14.6 m in P5a, 9.3 m in P9b) that suggest recurring influxes of new alluvium onto the floodplains (McCarthy and Plint 2003).

The chemical index of alteration (CIA), which is a measure of the degree of weathering and the alteration of feldspars to clay (Nesbitt and Young 1982), is relatively high (60-80, mean=71), suggesting that the majority of the alluvium in the Prince Creek Fm. was derived from previously weathered material.

The ratio of Ba/Sr is an index of leaching and free drainage in paleosols (Retallack 2001, Ashley and Driese 2000) and although some paleosols may exhibit leaching (e.g. P7), fluctuations in Ba/Sr with depth coupled with similar inflections in the CIA in most of the paleosols (e.g. 9.0 m in P4b, 8.7 m in P9a) suggests that additions of alluvium generally control variations in these ratios (McCarthy and Plint, 2003).

Although the ratio of Al/Si, an indicator of clay abundance, is often related to weathering in soil profiles (Retallack 2001, Ashley and Driese 2000), the ratio of Al/Si in these paleosols is probably controlled by a combination of clay illuviation and sediment

influx. Some paleosol profiles display positive excursions in the Al/Si ratio that correlate with clay-rich Bt horizons (e.g. P2a, P2b). Other paleosols exhibit fluctuations that correspond to grain-size changes, suggesting that the ratio is strongly controlled by the mud/sand ratio of the deposited alluvium (e.g. P8, P9a, P9c; McCarthy et al. 1997; McCarthy and Plint 2003).

The ratio of Fe/Al reflects oxidation of soil profiles (Ashley and Driese 2000). Fe/Al ratios demonstrate an overall upward increase in some paleosol profiles (e.g. P3), indicating that oxidizing conditions were more common near the top of soil profiles. However, fluctuations with depth in Fe/Al are also controlled by sediment influx, with positive excursions corresponding to the introduction of Fe-rich alluvium into the profile (e.g. 9.0 m in P4b, 15.4 m in P5a).

The ratio of Al/(Na+K+Ca+Mg), an indicator of the loss of exchangeable bases and the extent of hydrolysis (Ashley and Driese 2000; Hamer et al. 2007), remains constant or increases upward in most paleosol profiles. Fluctuations within paleosol profiles again correspond well with sediment grain size changes suggesting that these ratios are highly influenced by sediment influx (e.g. 9.0 m in P4b, 15.4 m in P5a)..

The ratio of Na/K, an index of salinization and aridity in soils is typically low (< 1) as is the ratio of Ca/Mg (typically < 1), an index of calcification.

TOC in these paleosols ranges from 0.2 % to 35. 4 %. TOC either increases gradually with depth (e.g. P6b, P9c) or fluctuates with depth (e.g. P5) in most soil profiles. The highest TOC occurs in coal, carbonaceous shale, olive-grey to black

mudstone, and in siltstone and mudstone stratigraphically above and below these horizons. Increasing TOC with depth is attributed to anoxia and gleying (Krull and Retallack 2000). Anomalously high TOC measurements reflect abundant organic matter preserved under anoxic conditions (e.g. P5) or may record the former tops of soil profiles (e.g. P2a) that were subsequently buried and incorporated into compound or cumulative soils (Krull and Retallack 2000, Driese et al. 2008).

BIOTA AND AGE OF SEDIMENTS

Biota collected from 29 horizons within the nine paleosol profiles reveals a high abundance, high diversity assemblage (Tables 3.3-3.6). The biota includes: (1) *in-situ* and reworked Peridinioid dinocysts and Acritarchs; (2) brackish and freshwater algae such as *Botryococcus braunii, Pedisatrum, Sigmapollis psilatus,* and *Pterospermella*; (3) projectate pollen including *Aquilapollenites quadrilobus*, *Aquilapollenites aucellatus*, *Aquilapollenites scabridus*, and *Azonia cribrata*; (4) *Wodehouseia edmontonicola*; (5) pollen from lowland trees, shrubs, and herbs dominated by *Cranwellia*, *Reticulatasporites*, *Perinopollenites*, and *Taxodiaceaepollenites*; (6) *Bisaccate* pollen; (7) fern and moss spores dominated by *Deltoidospora*, *Laevigatosporites*, *Lycopodiumsporites*, *Osmundacidites*, and *Psilatriletes*; and (8) fungal hyphae.

The age of the Prince Creek Fm. in the study area is based on the presence or absence of Cretaceous marker species of known chronostratigraphic significance

Table 3.3. Biota total counts for paleosol horizons at measured section NKT. For geographic and stratigraphic location see Figures 3.1 and 3.4.

| | MARINE | | | | | | | | | | | | | | | | | | | | BRACKISH-FRESHWATER | | | | | | | | | | | | | | | | | | |

Table 3.4. Biota total counts for paleosol horizons at measured section 06SH. For geographic and stratigraphic location see Figures 3.1 and 3.4.

| | MARINE | | | | | | | | | | | | | | | | | | | | | | BRACKISH-FRESHWATER | | | | | | | | | | | | | | | | | | |

Table 3.5. Biota total counts for paleosol horizons at measured section KRM. For geographic and stratigraphic location see Figures 3.1 and 3.4.

| | MARINE | | | | | | | | | BRACKISH-FRESHWATER | | | | | | | | | | | EXOTIC | | | | | | | | | | |

Table 3.6. Biota total counts for paleosol horizons at measured section LBB. For geographic and stratigraphic location see Figures 3.1 and 3.4.

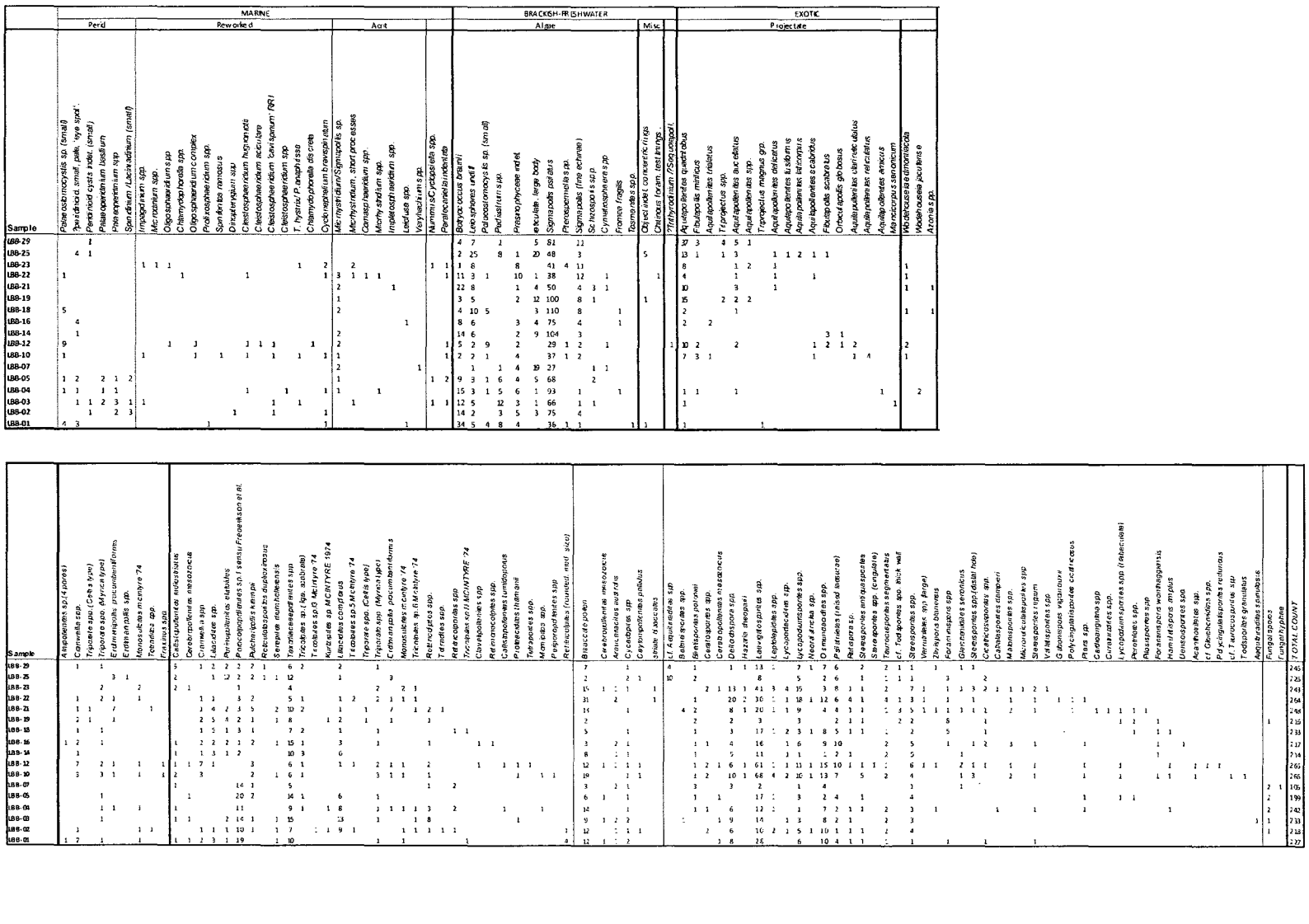

(Frederiksen 1991; Frederiksen and McIntyre 2000; Frederiksen et al. 1996, 1998, 2002; BP unpublished data). No definitive Campanian-restricted chronostratigraphic markers were found within paleosols. Additionally, the highly diagnostic Late Maastrichtian *Wodehouseia spinata* assemblage zone recorded in some North Slope wells and by Frederiksen (1991) in strata to the north of Ocean Point (Fig. 3.1) is conspicuously absent in the pollen assemblage. Instead, all samples contain a slightly older assemblage that includes the key Early Maastrichtian biota markers *Wodehouseia edmontonicola, Aquilapollenites aucellatus, Aquilapollenites quadrilobus* and *Azonia cribrata.* Therefore, the overall assemblage indicates that strata of the Prince Creek Fm. exposed in Colville River bluffs along a transect from measured section NKT in the south (N 69° 45.068' , W 151° 30.873') to measured section LBB in the north (N 70° 5.082' , W 151° 33.1') are all Early Maastrichtian in age. Biota also demonstrates that the southernmost measured section (NKT) contains the oldest sediments, with strata becoming progressively younger along the Colville River to measured section LBB in the north.

INTERPRETATION OF RESULTS

Pedogenic Processes on Floodplains

The platy to blocky structure of pedogenically modified siltstones and mudstones in the study area indicates that soils are weakly-developed and that pedogenic structures formed through repeated wetting and drying (McCarthy et al. 1998, 2003; Retallack 2001). Weak soil development likely resulted from soil-forming processes that were

frequently interrupted by an influx of alluvium (McCarthy 2002, Hamer et al. 2007) and waterlogging (Fastovsky and Mcsweeney 1991).

Evidence for alluviation (*sensu* Fanning and Fanning 1989) includes thin (< 20 cm) layers of silt and sand dispersed throughout most paleosol profiles (e.g. P4b, P5a, P9c, Figs. 3.12, 3.13, 3.17), common pedorelicts and papules (e.g. 15.4 m in P5a, 1.1 m in P8, 10.2 m in P9c) (Mcsweeney and Fastovsky 1987, McCarthy 2002, McCarthy and Plint 2003), and fluctuations with depth in the molecular ratios of Ti/Zr, Ba/Sr, Al/Si, Fe/Al, and Al/Bases Al/(Na+K+Ca+Mg) (e.g. P8).

Microlaminated clay coatings and clay infillings (Figs. 3.7G, 3.7H) form during the translocation of illuvial clay through the soil profile and require episodic wetting and drying of the soil (McCarthy and Plint 2003; Ufnar et al. 2005, Fiorillo et al. 2010a). The relative rarity of clay coatings and infillings suggest unstable floodplains frequently inundated with sediment, or alternatively, copious poorly drained floodplains, a condition unfavorable for extensive translocation of clays (McCarthy et al. 1999, Ufnar et al. 2005, Ufnar 2007).

Most paleosols exhibit drab colors that include shades of olive (5Y 4/1), gray (10YR 3/1), black (10YR 2/1) or brown (10YR 4/3). Drab colors in paleosols indicate predominantly poor paleo-drainage (Fanning and Fanning 1989, Fastovsky and Mcsweeney 1991, Davies-Vollum 1999, McCarthy and Plint 2003, Kraus and Hasiotis 2006) and may also reflect active reducing conditions during burial gleying (Fanning and Fanning 1989, Retallack 1991). Common carbonaceous shales (Fig. 3.19A) along with an

Figure 3.19 (Following Page). Characteristics typical of Prince Creek Formation paleosols including (A) carbonaceous shale (SH) bentonite (B) and ripple cross-laminated organic-rich siltstone (SLT) with iron-oxide mottles (m_{fe}); (B) carbonaceous root-traces (rt) in silty mudstone; (C) contact between a very-fine grained sandstone (SS) and grey blocky mudstone (MS) including wood fragments (wd), plant fragments (pl), jarosite (j), siderite nodules (sd), and iron staining (Fe); (D) very-fine grained ripple cross-laminated sandstone with jarosite halos (j) surrounding carbonaceous root-traces (rt); (E) close-up of iron-oxide mottles (m_{fe}) in grey mudstone; (F) Macroscopic siderite spherules in laminated sandstone and siltstone. Hammer is 30 cm long, pocket knife is 9 cm long.

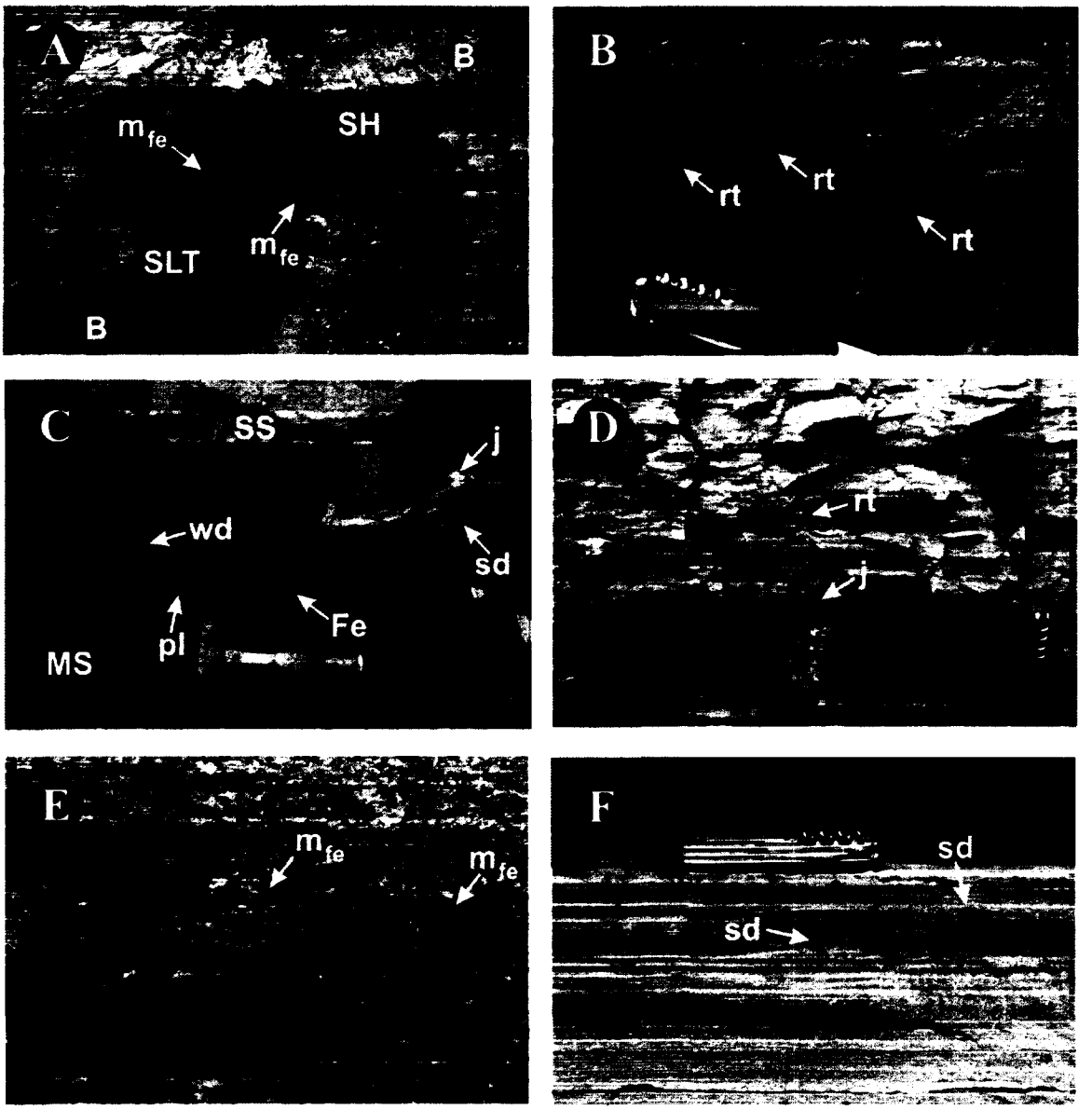
A
B
SH
m_{fe}
m_{fe}
SLT
B
B
rt
rt
rt
C
SS
j
wd
sd
pl
Fe
MS
D
rt
j
E
m_{fe}
m_{fe}
F
sd
sd

abundance of carbonaceous organic material indicates rapid burial of organic material (Fanning and Fanning 1989, Retallack 2001, Kraus and Hasiotis 2006) and widespread anoxia (Kraus 1998, Davies-Vollum and Wing 1998). Vertical to sub-horizontal root-traces preserved as carbonaceous strands in paleosols (Fig. 3.19B) occur under poorly-drained, reducing conditions (Retallack 1997, Kraus and Hasiotis 2006). Siderite (Figs. 3.19C, 3.19D, 3.19F, e.g. 14.4 m in P2b, Fig 3.10), is an additional indicator of saturated, anoxic conditions in a poorly-drained, organic-rich environment (Postma 1977, Bullock et al. 1985, Browne and Kingston 1993, Ludvigson et al. 1998, Retallack 2001, Driese and Ober 2005, Ufnar et al. 2005).

Depletion features (Figs. 3.7D, 3.8F) such as these are the result of episodic waterlogging and anoxia during which Fe-oxides are reduced and preferentially removed from ped and void margins (Bullock et al. 1985, Richardson and Daniels 1993, Fiorillo et al. 2010a). Zoned peds (Fig. 3.7C) are likely the result of gleization. Gleization involves the reduction of iron, diffusion of iron within the soil profile, and leaching of iron from the soil profile (Fanning and Fanning 1989). Under gley conditions a central, low-chroma, iron-depleted zone of variable thickness forms in peds (Richardson and Daniels 1993). Iron is diffused outward into the surrounding matrix producing a higher-chroma intermediate zone (Veneman et al. 1976). Simultaneously, a depletion coating forms on the ped surface. Reducing conditions are arrested before the process creates an extensively iron-depleted ped of uniformly low-chroma. Not only do zoned peds require prolonged anaerobic conditions in order to form, but they may indicate a water table that was very near the surface (Richardson and Daniels 1993). Repeated episodes of wetting

and drying in these paleosols (e.g. P5a, P5b, P9a) may be responsible for zoned peds that exhibit concentric rings of alternating low and high chroma matrix (Fig 3.7C).

In contrast to evidence for anoxia and waterlogging, abundant reddish-orange ferruginous mottles in otherwise drab-colored paleosols (Figs. 3.19A, 3.19C, 19E, e.g. P1, P2b, P5a, Figs. 3.9, 3.10, 3.13) suggest oxidation and drying-out of some soil horizons (Veneman et al. 1976, Fanning and Fanning 1989). Fe-oxide and Mn-oxide segregations including mottles, nodules, and void coatings (Figs. 3.8A, 3.8B) are the result of redistribution and *in situ* precipitation of iron and manganese from solution as the soil becomes oxidized (e.g. Veneman et al. 1976, Gasparatos et al. 2005, Fiorillo et al. 2010a). Manganese is reduced at a higher redox potential than iron, while iron is oxidized at a lower redox potential, therefore abundant Mn-oxide segregations and rare Fe-oxide segregations may indicate shorter periods of saturation followed by drying and oxidation (e.g. P9a) while abundant Fe-oxide segregations and rare Mn-oxide segregations suggest longer periods of saturation followed by oxidation (e.g. P8) (Veneman et al. 1976). In some paleosol profiles as the abundance of Mn-oxide segregations decreases the incidence of zoned peds increases (e.g. P1, P2, P5, P9a). This inverse relationship may result from longer periods of saturation, leaching, and removal of the bulk of the Mn from the profile (Veneman et al. 1976). In paleosols of the Prince Creek Fm., Fe-oxide and Mn-oxide nodules, ferruginous void coatings, and ferruginous void infillings are common in peds and pedorelicts that also contain Fe-depleted zones. Zones of Fe-depletion and ferruginous and manganiferous segregations typically occur together in periodically waterlogged soils (Bullock et al. 1985). This genetic relationship

occurs, under conditions of free drainage, from the redistribution of iron during episodes of wetting and reduction followed by drying and oxidation (Bullock et al. 1985, McCarthy and Plint 2003, Gasparatos et al. 2005). Because Fe-rich mottles consistently occur within drab-colored soils it is likely that soils either remained saturated for most of the time, but experienced fluctuating groundwater levels with episodes of both reduction and oxidation (Bown and Kraus 1986, Leckie et al. 1989, Turner 1993, Kraus and Aslan 1993, McCarthy and Plint 1998) or, alternatively, soils dried out periodically or seasonally (Fastovsky and Mcsweeney 1991, Fiorillo et al. 2010a, 2010b). Drab colors may have been enhanced by burial gleization (Fanning and Fanning 1989, Retallack 1991).

Bioturbation in these soils (Figs. 3.7E, 3.7F) is attributed to insects and/or earthworms and also suggests prolonged surface stability in paleosols containing these features (e.g. P2b, P4a, P6b) (Hasiotis 2002, McCarthy and Plint 2003, Hembree and Hasiotis 2007).

Microscopic pyrite framboids and polyframboids are found exclusively at measured section LBB (Figs. 3.1, 3.17, P9c), located stratigraphically higher in the Prince Creek Fm., as strata approach the contact with shallow-marine facies of the Schrader Bluff Fm. (Fig. 3.2). Pyrite forms in soils as iron interacts with sulfate (Sweeney and Kaplan 1973, Fitzpatrick 1984, Wright 1986, Ufnar et al. 2005). Sulfate is more abundant in marine waters than in freshwater settings (Retallack 1997, Kraus 1998) and the presence of pyrite likely signals the mixing of marine waters with pore fluids in

paleosols found in poorly drained coastal plain settings (Pons and van Breeman 1981, Wright 1986, Madsen and Jensen 1988, Vanstone 1991, Dent and Pons 1995, Ufnar et al. 2001). Pyrite is a common component of tidally influenced marsh soils that also contain abundant organic matter (Pons and van Breeman 1981, Lin et al. 1995, Dharmasri et al. 2004). The presence of pyrite at the distal end of the coastal plain (section LBB; Figs.3.7, 3.17) suggests that these soils may have experienced conditions similar to present day saline to brackish marsh soils (Hussein and Rabenhorst 1999, Fanning et al. 2010) and that these paleosols may be best classified as potential acid sulfate soils (Pons and van Breeman 1981, Ritsema and Groenberg 1993, Lin et al. 1995, Dent and Pons 1995, Kraus 1998).

Although pyrite is relatively rare in the Prince Creek Fm., jarosite, an oxidation product of pyrite (Kraus 1998, Davies-Vollum 1999, Ashley et al. 2004, Kraus and Hasiotis 2006) is more common (Figs. 3.4, 3.19C), especially in stratigraphically higher and younger sediments. The presence of jarosite (Fig. 3.19D) indicates former accumulations of pyrite and available marine sulfate (Fanning and Fanning 1989, Davies-Vollum 1999, Driese and Ober 2005).

Radiating euhedral gypsum crystals (Fig. 3.6H) are found exclusively at measured section LBB (Fig. 3.1, 3.16, 3.17, P8 & P9). Although gypsum is common in soils of arid regions (e.g. Wanas and Abu El-Hassan 2006) gypsum also forms through the oxidation of pyrite as calcium ions combine with sulfate ions (Wright 1986, Jafarzadeh and Burnhan 1992, Kraus 1998, Fanning et al. 2010). Because the molecular ratios of

Na/K and Ca/Mg in Prince Creek Fm. paleosols are low, the occurrence of gypsum likely indicates the presence of oxidized pyrite rather than arid conditions (Wright 1986, Vanstone 1991, Fanning et al. 2010).

Paleosols that contain pyrite, jarosite, and gypsum consistently lack sphaerosiderite (e.g. P8, P9). Siderite (Figs. 3.19C, 3.19D, 3.19F) is an additional indicator of saturated, anoxic conditions in a poorly-drained, organic-rich environment (Postma 1977, Bullock et al. 1985, Browne and Kingston 1993, Ludvigson et al. 1998, Retallack 2001, Driese and Ober 2005, Ufnar et al. 2005). Siderite precipitation occurs under saturated, organic-rich, reducing conditions (Postma 1977, Bullock et al. 1985, Browne and Kingston 1993, Ludvigson et al. 1998, McCarthy and Plint 1998, Retallack 2001, McCarthy and Plint 2003, Ashley et al. 2004, Driese and Ober 2005, Ufnar et al. 2005). Because siderite is unstable in soils with high-sulfate pore waters (Postma 1982, Browne and Kingston 2006) sphaerosiderite preferentially precipitated at locations with lower dissolved sulfur concentrations dominated by freshwater (e.g. P2b, P6b) (Curtis and Coleman 1986), while pyrite, jarosite, and gypsum record pedogenesis closer to a source of sulfate such as marine waters (e.g. P8, P9) (Postma 1982, Kraus 1998).

Biofacies

The assignment of palynofacies/biofacies based on the character and distribution of biota within lithofacies has proven valuable for reinforcing and enhancing paleoenvironmental interpretations (Oboh-Ikuenobe et al. 2005, Quattrocchio et al. 2006,

Steve Lowe personal comm.). Palynological/biological analyses (Tables 3.3-3.6) allowed us to identify six discrete biofacies (Table 3.7) based on diagnostic biota which strongly suggest deposition within specific floodplain environments (pers. comm. Steve Lowe). The primary biota used to characterize each biofacies is described below.

Lacustrine Biofacies.-

The Lacustrine biofacies is defined by an abundance of freshwater green algae, chiefly *Pedisatrum*. The predominance of green algae such as *Pedisatrum* suggests deposition in a standing body of fresh-water such as an oxbow lake, small floodplain lake, or pond.

Floodplain Paleosol Biofacies.-

The Floodplain Paleosol biofacies is interpreted to primarily record pedogenic processes and is dominated by fungal hyphae and clusters of brown fungal spheres. These fungi are significantly less abundant or absent in other palynofacies. An additional identifying characteristic of the Floodplain Paleosol biofacies is the absence or rarity of aquatic indicators such as *Pedisatrum* (algae).

Swamp Biofacies.-

The Swamp biofacies is characterized by an abundance peak of one specific pollen or spore species, which completely dominates the assemblage (e.g. *Psilatriletes* (ferns), sample KRM-22, Table 3.5). The dominant pollen type reflects the response of local vegetation to hydrological factors, light regime, and interspecies competition. Pollen abundance peaks suggest proximity to a specific, localized vegetation with the pollen assemblage relatively unaffected by allochthonous palynomorph sources. Swamp assemblages generally lack fluvial indicators such as bisaccate (conifer) pollen and marine indicators such as Peridinioid dinocysts and Acritarchs.

Fluvial Biofacies.-

The Fluvial biofacies is dominated by *bisaccate* (conifer) pollen which is considered allochthonous (e.g. hinterland pollen, pers. comm. Steve Lowe) when compared with the predominant lowland pollen assemblage. The Fluvial biofacies also contains reworked dinocysts (dinocysts too old to be considered *in situ*). Pollen assemblages containing high concentrations of *bisaccate* pollen and reworked dinocysts were likely deposited close to active channels on point bars, channel proximal levees, and proximal splays.

Overbank Biofacies.-

The Overbank biofacies is also dominated by fluvial palynomorphs such as *bisaccate* (conifer) pollen and reworked dinocysts, however, in addition to these fluvial indicators the Overbank assemblage contains a high diversity of Lower Delta Plain forms (see below) including *in situ* Peridiniod dinocysts. Pollen attributed to lacustrine environments and paleosols (e.g. *Pedisatrum* and fungal hyphae) are also common in Overbank assemblages. A mixture of pollen from multiple sources suggests that the depositional mechanism was most likely overbank sheet-floods or crevasse splays extending outward over levees and point bars and onto highly diverse floodplain environments.

Undifferentiated Lower Delta Plain Biofacies.-

The Undifferentiated Lower Delta Plain palynofacies is characterized by an abundance of algal forms; predominantly *Sigmapollis psilatus* and *Botryococcus* along with a rich and varied pollen assemblage typically dominated by *Taxodiaceaepollenites* (lowland trees). The occurrence of abundant, *in situ* Peridinioid dinocysts differentiates this palynofacies from most others and suggests some tidal influence or episodic storm surge activity. Depositional environments include swamps or lakes; however the pollen assemblage is not diagnostic enough to solely attribute the palynofacies to one of those specific depositional environments.

Pedogenic Environments of Prince Creek Paleosols

By combining facies trends, paleosol micromorphology, geochemistry, and biofacies interpretations, pedogenic paleoenvironments can be established for *Paleosols 1-9* (Table 3.8, Fig. 3.20). The location of a paleosol within the overall stratigraphy, pedogenic characteristics including macrofeatures and micromorphology and geochemical trends drive paleoenvironmental interpretations while biological analyses are used to reinforce or amend these interpretations.

Lake Margin Soils.-

Paleosol 5a and 5b (Fig. 3.13) are interpreted to have developed on the margin of a floodplain lake. Lake margin soils such as these lack clay coatings or infillings and contain zoned peds interspersed throughout the profile. TOC and bioturbation fluctuate between high and low values. Ferruginous features and Mn-oxide nodules are common. Zoned peds, high TOC, and lower bioturbation in some horizons suggest waterlogged conditions (e.g. 16.7-17 m in P5b) while ferruginous and manganiferous segregations and higher bioturbation in other horizons indicate dryer conditions (e.g. 14.7-15.5 m in P5a).

Table 3.7. Biofacies identified in the Prince Creek Formation

Biofacies	**Diagnostic Biota**	**Environment**
Lacustrine	Abundance of freshwater green algae, chiefly *Pedisatrum.*	oxbow lake, small lake, pond
Swamp	Abundance peak of one specific pollen or spore species that dominates the assemblage (e.g. *Psilatriletes*). Rare allochthonous palynomorphs. Lacks *bisaccate* pollen, Peridinioid dinocysts, and Acritarchs.	swamp
Fluvial	Dominated by allocthonous *bisaccate* (Coniferous) pollen and reworked dinocysts too old to be considered *in situ.*	point bar, levee, proximal splay
Floodplain Paleosol	Dominated by fungal hyphae and clusters of brown fungal spheres. Absence or rarity of aquatic indicators (e.g. *Pedisatrum.*)	exclusively pedogenesis
Overbank	Dominated by *bisaccate* pollen and reworked dinocysts. Also contains a high diversity of Lower Delta Plain forms (*in situ* Peridiniod dinocysts), Lacustrine forms (*Pedisatrum*) and Floodplain Paleosol forms (fungal hyphae)	overbank sheet-floods or crevasse splays above levees, point bars and highly diverse floodplains
Undifferentiated Lower Delta Plain	Abundant *in situ* Peridinioid dinocysts and abundant algal forms (e.g. *Sigmapollis psilatus* and *Botryococcus).* Also contains and a rich and varied pollen assemblage dominated by *Taxodium* (Swamp Cypress)	lower delta plain swamps, lower delta plain lakes (non diagnostic)

Table 3.8. Paleoenvironmental summary for all sample horizons

		Sample[1]	Diagnostic Biota[2]	Background Average[3] (total count)	Sample[4] (total count)	Positive Deviation[5]	Biofacies[6]	Pedogenic Paleoenvironment
P7	KRM	KRM-27	*Bisaccate*	9	18	100%	Fluvial	Levee
			Peridinioid dinocysts (reworked)	Abundant				
P6b	KRM	KRM-22	*Psilatriletes*	55	101	84%	Swamp/Mire	Swamp Margin
P6a	KRM	KRM-16	*Aquilapollenites scabridus*	41	115	180%	Swamp/Mire	
P5b	06SH	06SH-16.8	Peridinioid dinocysts *(in situ)*	Abundant			Undiff. Lower Delta Plain	Lake Margin
			Taxodiaceaepollenites	23	35	52%		
P5a	06SH	06SH-14.8	*Pterospermella*	6	19	217%	Lacustrine	
			Pediastrum	14	29	107%		
P4b	06SH	06SH-9.2	*Psilatriletes*	43	68	58%	Swamp/Mire	Swamp Margin
P4a	06SH	06SH-8.1	*Psilatriletes*	43	105	144%	Swamp/Mire	
P3	06SH	06SH-3.6	*Bisaccate*	8	21	163%	Fluvial	Crevasse Splay
			Peridinioid dinocysts (reworked)	Abundant				
			Taxodiaceaepollenites	23	44	91%		
		06SH-2.2	Fungal clusters	Abundant			Floodplain Paleosol	
			Fungal hyphae	Abundant				
P2b	NKT	NKT-40	Peridinioid dinocysts *(in situ)*	Present			Undiff. Lower Delta Plain	Point Bar
			Laevigatosporites	27	35	30%		
P2a	NKT	NKT-25	Peridinioid dinocysts (reworked)	Abundant			Fluvial	
			Bisaccate	18	45	150%		
P1	NKT	NKT-12	Peridinioid dinocysts *(in situ)*	Present			Overbank/ Swamp/Mire/ Lower Delta Plain	Swamp Margin
			Peridinioid dinocysts (reworked)	Present				
			Bisaccate	Abundant				
			Pediastrum	4	8	100%		
			Aquilapollenites scabridus	7	17	143%		
		NKT-7	Peridinioid dinocysts *(in situ)*	Present			Undiff. Lower Delta Plain	
			Botryococcus braunii	37	90	143%		

1. Sample name
2. Type of diagnostic biota found to be above the background average in the sample (Matthews and Lowe pers. comm.).
3. Background average is the arithmatic mean for all samples containing the diagnostic biota in a measured section
4. Total count of diagnostic biota found in sample
5. Deviation from the background average given as percent above the arithmatic mean
6. Biofacies interpretation based on criteria described in the text

Table 3.8 cont. Paleoenvironmental summary for all sample horizons

		Sample[1]	Diagnostic Biota[2]	Background Average[3] (total count)	Sample[4] (total count)	Positive Deviation[5]	Biofacies[6]	Pedogenic Paleonvironment
P9c	LBB	LBB-29	*Aquilapollenites quadrilobus*	9	37	311%	Swamp/Mire	Swamp Margin
		LBB-25	Peridinioid dinocysts *(in situ)*	Present			Undiff. Lower Delta Plain	
			Leiospheres	6	25	317%		
P9b		LBB-23	Peridinioid dinocysts (reworked)	Abundant			Fluvial	Distal Crevasse Splay
			Bisaccate	10	15	50%		
			Laevigatosporites	22	41	86%		
		LBB-22	Peridinioid dinocysts (reworked)	Present			Fluvial	
			Bisaccate	10	31	210%		
			Laevigatosporites	22	30	36%		
		LBB-21	*Bisaccate*	10	13	30%	Overbank	
			Sigmapollis psilatus	Abundant				
			Laevigatosporites	Abundant				
P9a		LBB-19	Interpretation Partly Based on Adjacent Facies				Undiff. Lower Delta Plain	Undifferentiated Lower Delta Plain (Lake Margin)
			Sigmapollis psilatus	63	100	59%		
		LBB-18	Peridinioid dinocysts *(in situ)*	Present			Undiff. Lower Delta Plain	
			Sigmapollis psilatus	63	110	75%		
		LBB-16	Peridinioid dinocysts *(in situ)*	Present			Undiff. Lower Delta Plain	
			Sigmapollis psilatus	63	75	19%		
			Taxodiaceaepollenites	9	15	67%		
		LBB-14	Peridinioid dinocysts *(in situ)*	Present			Overbank/Lacustrine/ Lower Delta Plain	
			Sigmapollis psilatus	63	104	65%		
			Bisaccate	Present				
		LBB-12	Peridinioid dinocysts *(in situ)*	Abundant			*Overbank/Lower Delta Plain*	
			Peridinioid dinocysts (reworked)	Abundant				
			Bisaccate	10	12	20%		
			Laevigatosporites	22	61	177%		
		LBB-10	Peridinioid dinocysts *(in situ)*	Present			Overbank/Lower Delta Plain	
			Peridinioid dinocysts (reworked)	Abundant				
			Bisaccate	10	19	90%		
			Laevigatosporites	22	68	209%		
P8		LBB-07	Low Pollen Count - Interpretation Based on Adjacent Facies				Undiff. Lower Delta Plain	Undifferentiated Lower Delta Plain (Lake Margin) or *(Channel Margin)*
		LBB-05	Peridinioid dinocysts *(in situ)*	Abundant			Undiff. Lower Delta Plain	
			Taxodiaceaepollenites	9	14	56%		
			Botryococcus braunii	63	68	8%		
		LBB-04	Peridinioid dinocysts *(in situ)*	Abundant			Overbank/Lacustrine/ Lower Delta Plain	
			Peridinioid dinocysts (reworked)	Present				
			Sigmapollis psilatus	63	93	48%		
			Bisaccate	10	14	40%		
		LBB-03	Peridinioid dinocysts *(in situ)*	Abundant			Overbank/Lacustrine/ Lower Delta Plain	
			Peridinioid dinocysts (reworked)	Present				
			Pediastrum	6	12	100%		
			Taxodiaceaepollenites	9	15	67%		
			Bisaccate	Present				
		LBB-02	Peridinioid dinocysts *(in situ)*	Abundant			Overbank/Lacustrine/ Lower Delta Plain	
			Peridinioid dinocysts (reworked)	Present				
			Bisaccate	10	12	20%		
			Sigmapollis psilatus	63	75	19%		
		LBB-01	Peridinioid dinocysts *(in situ)*	Abundant			Overbank/Lacustrine/ Lower Delta Plain	
			Peridinioid dinocysts (reworked)	Present				
			Pediastrum	6	8	33%		
			Bisaccate	10	12	20%		

1. Sample name
2. Type of diagnostic biota found to be above the background average in the sample (Matthews and Lowe pers. comm.).
3. Background average is the arithmatic mean for all samples containing the diagnostic biota in a measured section
4. Total count of diagnostic biota found in sample
5. Deviation from the background average given as percent above the arithmatic mean
6. Biofacies interpretation based on criteria described in the text

Figure 3.20 (Following Page). Summary diagram of pedogenic paleoenvironments of the Prince Creek Formation showing idealized macrofeatures, microfeatures, and biota for each soil type as well as the distribution of each paleosol across the Cretaceous coastal plain. Dinosaur footprints are found in all paleosol types and are excluded for clarity. Diagram is interpretive and no scale is implied. See Figure 9 for key to micrpmorphological features.

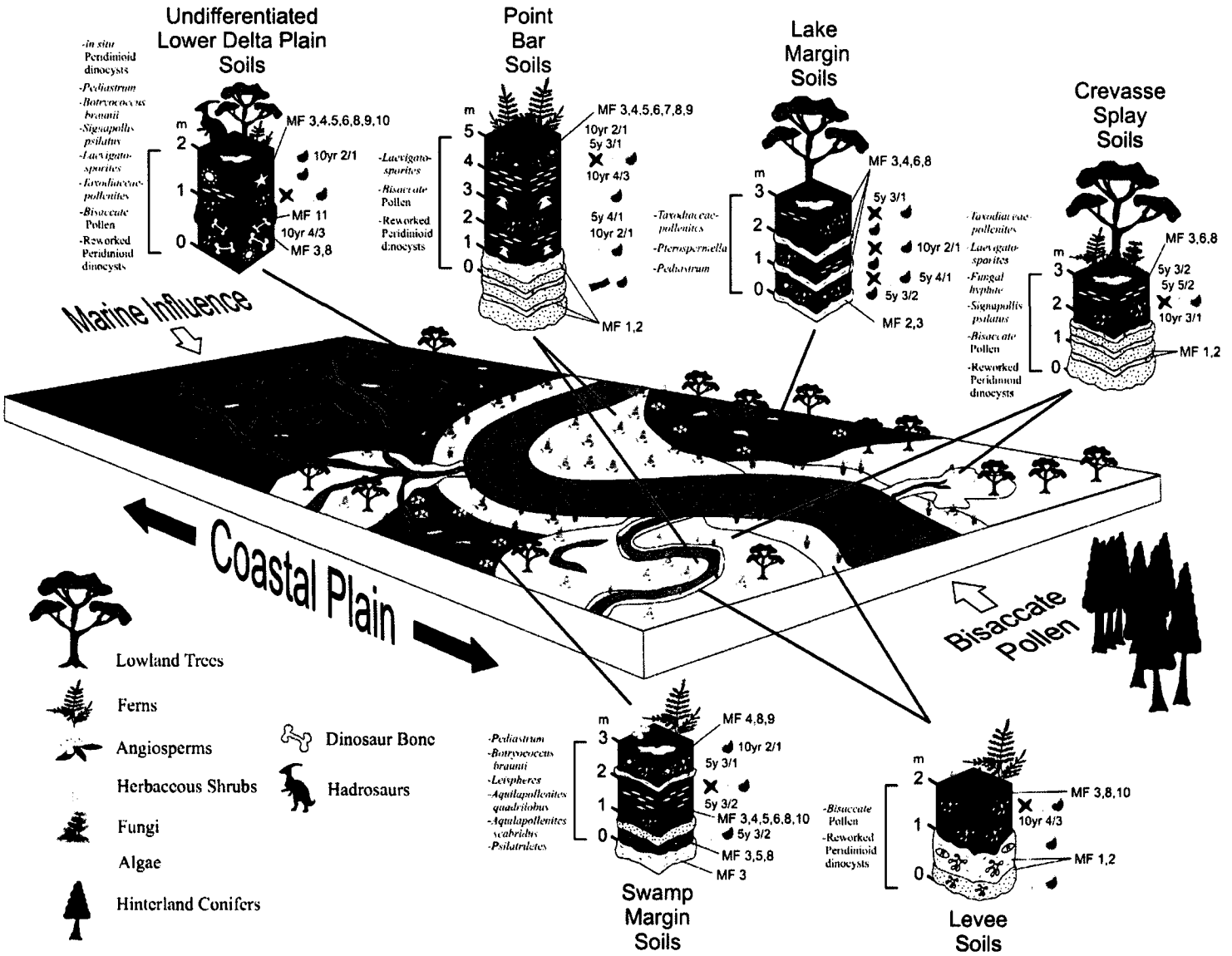
Undifferentiated Lower Delta Plain Soils
-in situ Peridinioid dinocysts
-Pediastrum
-Botryococcus braunii
-Signapollis psilatus
-Laevigato-sporites
-Taxodiaceae-pollenites
-Bisaccate Pollen
-Reworked Peridinioid dinocysts
m
2
1
0
MF 3,4,5,6,8,9,10
10yr 2/1
MF 11
10yr 4/3
MF 3,8
Point Bar Soils
-Laevigato-sporites
-Bisaccate Pollen
-Reworked Peridinioid dinocysts
m
5
4
3
2
1
0
MF 3,4,5,6,7,8,9
10yr 2/1
5y 3/1
10yr 4/3
5y 4/1
10yr 2/1
MF 1,2
Lake Margin Soils
-Taxodiaceae-pollenites
-Pterospermella
-Pediastrum
m
3
2
1
0
MF 3,4,6,8
5y 3/1
10yr 2/1
5y 4/1
5y 3/2
MF 2,3
Crevasse Splay Soils
-Taxodiaceae-pollenites
-Laevigato-sporites
-Fungal hyphae
-Signapollis psilatus
-Bisaccate Pollen
-Reworked Peridinioid dinocysts
m
3
2
1
0
MF 3,6,8
5y 3/2
5y 5/2
10yr 3/1
MF 1,2
Marine Influence
Coastal Plain
Bisaccate Pollen
Lowland Trees
Ferns
Angiosperms
Herbaceous Shrubs
Fungi
Algae
Hinterland Conifers
Dinosaur Bone
Hadrosaurs
-Pediastrum
-Botryococcus braunii
-Leiospheres
-Aquilapolleniles quadrilobus
-Aquilapollenites scabridus
-Psilatricolpites
m
3
2
1
0
MF 4,8,9
10yr 2/1
5y 3/1
5y 3/2
MF 3,4,5,6,8,10
5y 3/2
MF 3,5,8
MF 3
Swamp Margin Soils
-Bisaccate Pollen
-Reworked Peridinioid dinocysts
m
2
1
0
MF 3,8,10
10yr 4/3
MF 1,2
Levee Soils

Grain size variability coupled with fluctuations with depth in Ti/Zr, Ba/Sr, Al/Si and Fe/Al indicates common alluviation into the soils. Sphaerosiderite suggests a freshwater environment (e.g. 15.1 m in P5b). The assemblage for P5 is dominated by *Pediastrum* and *Pterospermella* (algae), and *Taxodiaceaepollenites* (lowland trees) along with rare *in situ* Peridinioid dinocysts indicating probable pedogenesis along a lake margin on the lower delta plain.

Swamp Margin Soils.-

Soils developed on the margins of swamps include P1, P4a, P4b, P6a, P6b, and P9c (Figs. 3.9, 3.12, 3.14, 3.17). These paleosols lack clay coatings and clay infillings, are typically organic-rich, and commonly contain zoned peds. TOC may increase with depth (e.g. 5.3-5.8 m in P1, 12-13 m in P6b, 7.8-8.4 m in P4a) suggesting waterlogging and gleization (Krull and Retallack 2000). These soils can exhibit moderate to high bioturbation (e.g. P6b) and may contain abundant Fe-oxide and Mn-oxide nodules (e.g. P1, P4b, P6b) suggesting periodic drying-out of swamp margins. In some of these soils Mn-oxide nodules are more common than Fe-oxide nodules suggesting shorter periods of saturation (9.0-9.5 m in P6a, 10.2 m in P9c). Interspersed coarser-grained sediments (P1, P4b, P9c), fluctuations with depth in Ba/Sr, Al/Si, and Al/(Na+K+Ca+Mg) (e.g. P4b, P9c), and abundant pedorelicts and papules (P9c) suggest repeated alluviation into paleosol profiles. An increase in ferruginous features, Fe-rich papules and pedorelicts, and an increase in Fe/Al correlating with grain-size changes indicate that additional Fe

may have been brought into swamp margin soils along with alluvium (e.g. 8.7-9.0 m in P4, 10.2 m in P9c). Some swamp margin soils exhibit an overall increase in Fe/Al near the top of the soil profile (e.g. P1, P6b) suggesting increased surface weathering. An increase in Al/(Na+K+Ca+Mg) down profile in P4 indicates increased hydrolysis. Irregular contacts suggest common trampling by dinosaurs (P6b, P9c). Pyrite, when present (P9c), suggests a brackish water environment while sphaerosiderite (P6b) suggests fresher water. In P1 the biota is dominated by *Aquilapollenites scabridus* (angiosperms), *Botryococcus braunii* and *Pediastrum* (algae), along with *in situ* and reworked Peridinioid dinocysts suggesting that this paleosol developed on the margin of a swamp on the lower delta plain. The biota of P4 dominated by *Psilatriletes* (ferns) indicates formation on the margin of a swamp while the overall stratigraphy suggests formation above a former point bar. Sphaerosiderite in P6b coupled with biota in P6a and P6b dominated by *Aquilapollenites scabridus* and *Psilatriletes* suggests paleosol development on the margin of a freshwater swamp. Pyrite in P9c coupled with a biota dominated by *Aquilapollenites quadrilobus* (angiosperms), *Leiospheres* (algae) and containing *in situ* Peridinioid dinocysts suggests pedogenesis on a brackish-water swamp margin on the lower delta plain. The preservation of a 20 cm tuff in P9c (11 m) likely occurred in standing water and lends credence to this interpretation (Huff et al. 1996, Königer and Stollhofen 2001).

Point Bar Soils.-

Point bar soils such as P2a and P2b (Fig. 3.10) exhibit moderate to high bioturbation throughout the bulk of the paleosol profile, with bioturbation becoming extremely common near the top of P2b. Sand and silt concentrations are highest at the base of P2a and decrease upward. Ferruginous features and Mn-oxides are found in isolated horizons, but become very common near the top of P2b, suggesting dryer conditions. P2a and P2b are rare examples of soils containing horizons with abundant clay coatings and infillings. Translocated clays (e.g. ~ 12.5 m in P2b), may correlate with relatively fixed molecular ratios, and suggest a stable soil-forming environment. Influx of new sediment into the profile is evidenced elsewhere by fluctuations in Ti/Zr, Ba/Sr, Al/Si and Fe/Al. The presence of sphaerosiderite near the top of P2b indicates a freshwater environment. The biota dominated by *Bisaccate* (conifer) pollen, *Laevigatosporites* (ferns), and *in situ* and reworked Peridinioid dinocysts, suggests a fluvial environment on the lower delta plain while the overall stratigraphy suggests that P2a and P2b formed above a point bar (Figs. 3.4, 3.10).

Levee Soils.-

P7 (Fig. 3.15) is a brown-colored, silty compound paleosol that lacks clay coatings and infillings. Fe-oxide nodules and coatings and Mn-oxide nodules are common. Zoned peds of *Microfacies 5* are notably absent. Al/(Na+K+Ca+Mg) suggests a loss of exchangeable bases with depth and Ba/Sr suggests leaching. Fluctuations in

Al/Si and Fe/Al suggest clastic influx into the paleosol profile. Brown-colored sediments, the absence of zoned peds, and common ferruginous features suggest drier conditions. The lack of bioturbation in P7 may indicate proximity to a sediment source as opposed to soil saturation and anoxia (Dashtgard et al. 2008). The biota of P7, dominated by *Bisaccate* pollen and reworked Peridinioid dinocysts, suggest a position on the floodplain close to a fluvial channel while the paleopedology and geochemistry indicates formation close to a sediment source on a raised, drier area of the floodplain such as a levee.

Crevasse Splay Soils.-

Soils interpreted to have developed on crevasse splays include P3 and P9b (Figs. 3.11, 3.17). These paleosols lack clay coatings and infillings and are moderately to highly bioturbated. A general trend of increasing ferruginous features and papules up-profile coupled with increasing Fe/Al upward in P3 suggests that the uppermost horizons experienced dryer conditions. Molecular ratios including CIA, Ti/Zr, Al/(Na+K+Ca+Mg), and Fe/Al fluctuate with depth suggesting frequent alluviation into the paleosol profiles. Mn-oxide nodules are common in both paleosols and Mn-oxide is more common that Fe-oxide in P9b, suggesting shorter periods of saturation in P9b. Zoned peds of *Microfacies 5* are not found in P3 or P5b, also suggesting drier conditions. The biota near the base of P3 contains abundant *fungal hyphae* suggesting that this horizon also primarily records soil-forming processes on a stable part of the floodplain.

The overall stratigraphy indicates that P3 initially formed on interbedded sand and silt interpreted as a distal crevasse splay. The biota dominated by *Bisaccate* pollen, fungal clusters, fungal hyphae, *Taxodiaceaepollenites* (lowland trees) and reworked Peridinioid dinocysts, indicates a dryer location on the floodplain near a source of fluvial clastics such as an elevated, distal splay. P9b is composed of coarser-grained material than is found at the top of P9a directly below it. Gypsum is common in P9b. The biota dominated by *Bisaccate* pollen, *Laevigatosporites* (ferns), *Sigmapollis psilatus* (algae) and reworked Peridinioid dinocysts indicates that P9b likely formed on fluvial overbank deposits. The overall stratigraphy, microfacies, and geochemistry suggest pedogenesis occurred on a distal crevasse splay while the presence of gypsum suggests proximity to marine waters during pedogenesis.

Undifferentiated Lower Delta Plain Soils.-

Undifferentiated lower delta plain soils including P8 and P9a (Figs. 3.16, 3.17) lack clay coatings and infillings. Grain size changes (e.g. P8) along with fluctuations with depth in the molecular ratios of Ti/Zr, Al/Si, Fe/Al, and Al/(Na+K+Ca+Mg) suggesting repeated clastic influx into the soil profiles. Ferruginous features are abundant in P8 while manganiferous nodules are abundant in P9a, suggesting shorter periods of saturation for P9a then P8. TOC exhibits an overall increase down profile in P8 also suggesting prolonged saturation. Bioturbation is higher in P9a than P8 suggesting greater surface stability at P9a (Hasiotis 2002, McCarthy and Plint 2003, Hembree and

Hasiotis 2007). Zoned peds are common in P9a (7.4-7.7 m) indicating repeated wetting and drying of the soil profile. These are the only soils in the study area containing dinosaur bone. The biota of P8 is dominated by *Bisaccate* (conifer) pollen; *Botryococcus braunii*, *Pediastrum*, and *Sigmapollis psilatus* (algae); *Taxodiaceaepollenites* (lowland trees) and includes both *in situ* and reworked Peridinioid dinocysts. Micromorphology, geochemistry, biofacies analysis, and the presence of gypsum (0.2 m in P8) indicates that pedogenesis likely occurred on the lower delta plain along a marine-influenced lake margin that experienced frequent sediment influx from overbank floods. The biota of P9a dominated by *Bisaccate* (conifer) pollen, *Laevigatosporites* (ferns), *Sigmapollis psilatus* (algae), *Taxodiaceaepollenites* (lowland trees) and including both *in situ* and reworked Peridinioid dinocysts suggests pedogenesis in an area of the lower delta plain that repeatedly received an influx of overbank alluvium. The overall stratigraphy for measured section LBB (Fig. 3.4) indicates that P9 formed on a point bar of a small sinuous distributary channel or on the margin of an abandoned distributary channel on the lower delta plain.

DISCUSSION

Paleoenvironmental Interpretations from Pedogenic Processes and Biofacies

The Prince Creek Fm. is a near-polar costal-plain succession deposited at latitudes as high as 82°-85° N (Brouwers et al. 1987; Witte et al. 1987; Besse and Courtillot 1991; Rich et al. 2002, Spicer and Herman 2010). Depositional environments include tidally-

influenced, suspended-load trunk channels, suspended-load distributary channels, crevasse splays, levees, lakes, ponds, and swamps on a low-relief, vegetated coastal plain with a high water table (Fiorillo et al., 2010; Flaig et al., 2010b). The distal parts of the depositional environment are interpreted as marine-influenced (Phillips 2003, Flaig et al. 2010). Previously published floral and faunal data suggests a cool, temperate, relatively wet climate (Parrish and Spicer 1988, Spicer and Parrish 1990, Spicer et al. 1992; Spicer 2003, Brandlen 2008; Fiorillo et al., 2010) with a MAT of 5-6° C, WMMT of 10-12° C, CMMT of 2-4 ° C, and MAP of 500-1500 mm a^{-1} (Brouwers et al. 1987, Parrish et al. 1987, Spicer and Parrish 1990, Brandlen 2008, Tomsich et al. 2010). Data also indicate a broad, low-gradient, water-saturated floodplain with herbaceous ground cover, subaquatic and emergent vegetation, and elevated salinities (Frederiksen et al. 1988, Brouwers and de Decker 1993). Root-traces in distributary channels indicate that streamflow was ephemeral, and perhaps fluctuated seasonally (Fiorillo et al. 2010a, Flaig et al. 2010). Plant communities occupied ephemeral channels and floodplains and flourished in wetlands and swamps that experienced fluctuating water levels and frequent alluviation (Phillips 2003, Fiorillo et al. 2010a, 2010b; Flaig et al. 2010). Vertebrate assemblages suggest that large dinosaur communities occupied these floodplains and may have been year-round inhabitants (Brouwers et al. 1987, Fiorillo et al. 2009, Fiorillo et al. 2010a, Fiorillo et al. in 2010b). Compound, compound truncated and cumulative soils developed under these conditions on the margins of lakes and swamps, and on point bars, levees, and crevasse splays alongside meandering and anastomosed(?) distributary channels (Brandlen 2008, Fiorillo et al. 2009, Fiorillo et al. 2010b Flaig et al. 2010).

Frequent alluviation into many of these soil profiles is evident from grain size changes (Fiorillo et al. 2010a, Flaig et al. 2010) and fluctuations with depth in molecular ratios.

Soils that developed in topographic lows along lake margins (P5a, P5b) and swamp margins (P1, P4a, P4b, P6a, P6b, P9c) exhibit evidence of waterlogging (e.g. drab colors, abundant carbonaceous material, sphaerosiderite) and of a water table very near the surface (zoned peds and organics). Most likely, lower-lying areas also experienced frequent inundation from flooding of distributary channels. Abundant shale and organic-rich siltstone suggest that at least some of these were palustrine environments (Ashley et al. 2004, Johnson and Graham 2004, Fiorillo et al. 2010a). Biota adjacent to swamps included algae (*Pediastrum, Botryococcus braunii, Leiospheres*), angiosperms (*Aquilapollenites quadrilobus, Aquilapollenites scabridus*) and ferns (*Psilatriletes*) while lakes were covered in algae (*Pediastrum, Pterospermella*) with lowland trees (*Taxodiaceaepollenites*) on their margins. These same, predominantly waterlogged soils also exhibit evidence of periodic drying-out (ferruginous and manganiferous segregations, zoned peds, horizons with high levels of bioturbation). Alternating episodes of wetting and drying in paleosols may result from fluctuating river discharge tied to seasonal snowmelt in the ancestral Brooks Range brought about by the high-latitude (paleo-Arctic) setting of the Prince Creek Formation (Spicer et al. 1992; Spicer 2003, Fiorillo et al. 2010a, 2010b, Flaig et al. 2010). Flooding of nearby distributary channels repeatedly brought fresh alluvium into soil profiles, inhibiting advanced soil development (Fiorillo et al. 2010a) resulting in immature soils similar to modern aquic suborders of Entisols and Inceptisols (Soil Survey Staff 1999, Hamer et al. 2007). Soil

development resumed on this alluvium and the recurring sequence of pedogenesis and alluviation produced widespread cumulative to compound soils (Fiorillo et al. 2010a). Soils similar to lake and swamp margin soils also formed on point bars of distributary channels (P2a, P2b). Point bar soils exhibit many of the same characteristics as lake and swamp margin soils but also contain well-developed clay coatings and clay infillings suggesting repeated episodes of wetting and dying but increased soil stability (Ufnar 2007) possibly reflecting their slightly raised position on the floodplain. Point bars supported fern communities (*Laevigatosporites*) while pollen from hinterland conifers (*bisaccate)* and older, reworked Peridinioid dinocysts were incorporated into soil profiles by distributary channels.

Levees of trunk channels and distributary channels were repeatedly breached, resulting in truncation of many soil profiles by crevasse splays (Fiorillo et al. 2010a, Flaig et al. 2010) and by distributary channels on crevasse splay complexes (Flaig et al. 2010). Levees, splays, and splay complexes were the high-ground on this low-lying, low-gradient coastal plain. Soil development and biota in these environments reflect drier, but still predominantly wet conditions. Drab colors dominate in crevasse splay soils (P3, P9a) and these soils also contain evidence of repeated wetting and drying (e.g. ferruginous and manganiferous features); however, the zoned peds found in lake margin, swamp margin, and point bar soils are absent in splay soils suggesting drier conditions on crevasse splays. Biota on splays included fungi (*fungal hyphae*) ferns (*Laevigatosporites*), lowland trees (*Taxodiaceaepollenites*), and algae (*Sigmapollis psilatus*). Hinterland conifer pollen (*bisaccate)* and reworked Peridinioid dinocysts are

also common in splay paleosols. Soils that developed on levees (P7) are browner in color, exhibit lower bioturbation, and contain biota assemblages dominated by hinterland conifers (*bisaccate)* and reworked Peridinioid dinocysts reflecting the driest conditions and highest clastic influx on the floodplain. Previous work suggests that levees could also support herbaceous shrubs and ferns (Brandlen 2008, Fiorillo et al. 2010a) and our data also indicate the presence of shrubs and ferns on levees.

Pedogenic processes in the most distal areas of the coastal plain occurred on the margins of lakes (P8) and the margins of distributary channels (P9a) in waterlogged, organic-rich, anoxic environments. Dinosaurs occupied these areas and their bones are preserved in these soils. Pyrite was incorporated into paleosols from sulfate-rich marine waters. These soils, similar to modern potential acid sulfate soils (Ritsema and Groenberg 1993, Lin et al. 1995, Dent and Pons 1995, Kraus 1998), developed prior to a transgression of the paleo-Arctic Ocean over the coastal plain (Phillips 2003, Flaig et al. 2010) and supported a rich and varied biota that included algae (*Botryococcus braunii*, *Pediastrum*, *Sigmapollis psilatus)*, ferns (*Laevigatosporites*) and lowland trees (*Taxodiaceaepollenites*). *Bisaccate* pollen and reworked Peridinioid dinocysts were brought to the far reaches of the coastal plain by distributary channels and were incorporated into soils during pedogenesis along with *in situ* Peridinioid dinocysts from marine waters.

Floodplain Evolution

Paleosols of the Prince Creek Formation are poorly developed, immature cumulative to compound soils. Pedogenesis was repeatedly interrupted by alluviation and waterlogging and does not reflect long-lasting, stable conditions on floodplains. Vertically stacked paleosol successions are separated from each other by distributary channels that either formed extensive crevasse splay complexes or incised directly into organic-rich floodplains (Flaig et al. 2010). Paleosol successions separated by splay deposits commonly include paleosols with different characteristics developed in diverse floodplain environments. The locations of channels on the coastal plain were determined by levee breaches, splay complex development, and channel avulsion (Bridge 1984, Flaig et al. 2010). This process is assumed to be "pseudo-random" and is driven by accommodation space (Bridge 1984, Smith et al. 1989, Aslan and Blum 1999). Paleosols of the Prince Creek Fm. developed in wet topographic lows between splay complexes, alongside channels on floodplains, and on crevasse splays and crevasse splay complexes. The type of paleosol that formed at a given location depended more on local accommodation space, the height of the local water table, and the proximity to splays and splay complexes than proximity to major channels and pedofacies relationships (Bown and Kraus 1986, Smith 1990). Because these soils developed from similar parent materials, it is likely that catenary relationships involving variations in topography and drainage related to landscape position and the height of the groundwater table controlled the characteristics of soils across the coastal plain (Wright 1992, McCarthy and Plint

2003). The youngest and most distal paleosols of the Prince Creek Fm. (P8, P9) formed under conditions of marine influence prior to a marine transgression on the coastal plain.

Integration of Paleosols and Biota

The integration of biota with paleosol macrofeatures, micromorphology, and geochemistry in Prince Creek Fm. paleosols is invaluable because these soils are weakly developed and can provide only limited information on local topography, climate, organisms, and parent material. In the case of the Prince Creek soils palynological/biological analysis can provide (1) an overview of the regional biota, (2) clues to changing relief and soil saturation during formation of compound and cumulative soils (e.g. fungal hyphae vs. freshwater algae), (3) evidence of clastic input from nearby channels during soil development (e.g. hinterland pollen and reworked pollen), and (4) a hint to position on the floodplain relative to the coastline (e.g. Acritarchs and *in situ* Peridinioid dinocysts).

CONCLUSIONS

Field observations, soil micromorphology, geochemistry, and biofacies demonstrate that a multifaceted approach to paleosol analysis can provide unparalleled detail when reconstructing ancient paleoenvironments from paleosol profiles.

Paleosols of the Prince Creek Fm. formed as stacked successions separated by distributary channels, crevasse splays, and crevasse splay complexes. Pedogenic paleoenvironments include point bars, levees, crevasse splays, and the margins of floodplain lakes, swamps, and mires. Trampling of sediments by dinosaurs was common. Weakly-developed cumulative to compound paleosols similar to modern aquic subgroups of *Entisols*, *Inceptisols*, and potential acid sulfate soils formed on a low-lying, muddy, frequently-wet lower delta-plain. Soil profiles experienced repeated alluviation from overbank flooding of nearby distributary channels as evidenced by thin layers of silt and sand dispersed throughout many paleosol profiles, common pedorelicts and papules, and fluctuations with depth in the molecular ratios of Ti/Zr, Ba/Sr, Fe/Al, Al/Si, and Al/(Na+K+Ca+Mg). Overbank floods also introduced additional Fe-oxide into some soil profiles.

Macroscopic and micromorphological features in these paleosols that suggest water-saturated, anoxic conditions include drab colors, carbonaceous organic material, carbonaceous root-traces, siderite, depletion coatings on ped surfaces, and zoned peds. In contrast, Fe-rich mottled soil aggregates, ferruginous and manganiferous nodules, ferruginous void and grain coatings, ferruginous void infillings, burrows, and rare illuvial clay coatings and clay infillings suggest oxidizing conditions and drying out of some soils. Repeated wetting and drying in paleosol profiles is likely the result of seasonal variations in light, temperature, and precipitation related to the high-paleolatitude of Alaska (82-85°) in the Late Cretaceous.

Marine influence on pedogenesis is evidenced by jarosite mottles, jarosite halos surrounding rhizoliths, microscopic pyrite, and euhedral gypsum. These features become increasingly evident to the north of the study area in stratigraphically higher facies near the contact with the overlying shallow-marine Schrader Bluff Formation.

Biota of the Prince Creek Fm. include Peridinioid dinocysts; brackish and freshwater algae; projectate pollen; age diagnostic *Wodehouseia edmontonicola*; pollen from lowland trees, shrubs and herbs; *Bisaccates*; fern and moss spores; and fungal hyphae. Biota indicate that all strata in the study area are Early Maastrichtian and that sediments become progressively younger from measured section NKT in the south to measured section LBB in the north. The integration of pollen/biota analyses with paleopedology in Prince Creek Fm. paleosols is invaluable because it provides an overview of the regional biota, clues to paleo-topography, evidence of clastic input from channels (e.g. influx of reworked dinocysts and hinterland pollen), and hints at the location of pedogenesis relative to the coastline.

ACKNOWLEDGMENTS

This project was funded through the National Science Foundation Office of Polar Programs grants OPP-425636 (to McCarthy) and #OPP-424594 (to Fiorillo). Additional funding was provided by the University of Alaska Museum of the North Geist Fund, Alaska Geologic Society, the University of Alaska-Fairbanks Graduate School Fellowship Program, the Geological Society of America, the Evolving Earth Foundation,

and BP America. Logistical support was provided by the Barrow Arctic Science consortium (BASC), CH2M Hill (formerly Veco Polar Resources), Wrights Air, Air Logistics, Alaska Air Taxi, Evergreen Helicopters, and the support staff at Umiat, Alaska. The authors thank BP America for biological analyses of paleosols and Weatherford Laboratories for total organic carbon analyses. We also thank Dolores van der Kolk, Thomas Adams, David Norton, Roland Gangloff, Douglas Hissom, Susan Tomsich, and Jason Addison for field assistance and Don Triplehorn, Susana Salazar, and Maciej Sliwinski for assistance in the laboratory. This manuscript benefitted greatly from reviews by _____ and _____.

REFERENCES

Alley, N.F., Valentine, K.W.G., and Fulton, R.J., 1986, Paleoclimatic implications of middle Wisconsinan pollen and a paleosol from the Purcell Trench, south central British Columbia: Canadian Journal of Earth Sciences, v. 23, No. 8, p. 1156-1168.

Álvaro, J. J., Van Vliet-Lanoë, B., Vennin, E., and Blanc-Valleron, M.M., 2003, Lower Cambrian paleosols from the Cantabrian Mountains (northern Spain): A comparison with Neogene-Quaternary estuarine analogues: sedimentary Geology, v. 163, p. 67-84.

Ashley, G.M., and Driese, S.G., 2000, Paleopedology and paleohydrology of a volcaniclastic paleosol interval, Implications for an early Pleistocene stratigraphy and paleoclimate record, Olduvai Gorge, Tanzania: Journal of Sedimentary Research, v. 70, No. 5, p. 1065-1080.

Ashley, G.M., Maitima Mworia, J., Musya, A.M., Owens, R.B., Driese, S.G., Hover, V.C., Renaut, R.W., Gowan, M.F., Mathai, S. and Blatt, S.H. 2004, Sedimentation and recent history of a freshwater wetland in a semi-arid environment: Lobi Swamp, Kenya, East Africa: Sedimentology, v. 55, p. 1301-1321.

Askin, R. A., 1990, Campanian to Paleocene spore and pollen assemblages of Seymour Island, Antarctica: Review of Paleobotany and Palynology, v. 65, p. 105-113.

Askin, R.A., Eliot, D.H., Stilwell, J.D., and Zintsmeister, W.J., 1991, Stratigraphy and paleontology of Campanian and Eocene sediments, Cockburn Island, Arctic Peninsula: Journal of South American Earth Sciences, v. 4, No. 1/2, p. 99-117.

Aslan, A., and Autin, W.J., 1999, Evolution of the Holocene Mississippi River floodplain, Ferriday, Louisiana: Insights on the origin of fine-grained floodplains: Journal of Sedimentary Research, V. 69, No. 4, p. 800-815.

Aslan A, and Blum M.D. 1999, Contrasting styles of Holocene avulsion, Texas Gulf Coastal Plain, USA., *in* Fluvial Sedimentology VI, Smith, N.D., and Rogers J. eds., Special Publication 28, International Association of Sedimentology: Blackwell Science, Oxford p. 193–209.

Avanzini, M., Frisa, S., van den Driessche, K., Keppens, E., 1997, A dinosaur tracksite in an Early Liassic tidal flat in Northern Italy: Paleoenvironmental reconstruction from sedimentology and geochemistry: Palaios v. 12, p. 538-551.

Barker, C.E., and Pawlewicz, M.J., 1986, The correlation of vitrinite reflectance with maximum paleotemperature in humic organic matter, *in* Buntebarth, G., and Stegena, L., eds., Paleogeothermics: New York, Springer-Verlag, p. 79–93.

Besly, B.M., and Fielding, C.R., 1989, Paleosols in Westphalian coal-bearing and red-bed sequences, central and northern England: Palaeogeography, Palaeoclimatology, Palaeoecology, v. 70, p. 303-330.

Besse, J., and Courtillot, V., 1991, Revised and synthetic apparent polar wander paths of the African, Eurasian, North American and Indian plates, and true polar wander since 200 Ma: Journal of Geophysical Research, v. 96, p. 4029-4050.

Birkeland, P.W., 1999, Soils and Geomorphology: Oxford University Press, Oxford, 433p.

Bown, T.M., and Kraus, M.J., 1986, Integration of channel and floodplain suites I: Developmental sequence and lateral relations of alluvial paleosols: Journal of Sedimentary Petrology, v. 7, No. 4, p.587-601.

Brandlen, E., 2008, Paleoenvironmental reconstruction of the Late Cretaceous (Maastrichtian) Prince Creek Formation, near the Kikak-Tegoseak dinosaur quarry, North Slope, Alaska: Unpublished Master's Thesis, University of Alaska-Fairbanks, Fairbanks, Alaska, 225 p.

Brewer, R., 1964, Fabric and Mineral analysis of Soils: John Wiley and Sons Inc., New York, 470 p.

Bridge, J.S., 1984, Large scale facies sequences in alluvial overbank environments: Journal of Sedimentary Petrology, v. 54, No. 2, p. 583-588.

Brosge, W.P., Whimington, C.L., and Morris, R.H., 1966, Geology of the Umiat-Maybe Creek region, Alaska: Geological Survey Professional Paper 303-H, p. 548-570.

Brouwers, E.M., Clemens, W.A., Spicer, R.A., Ager, T.A., Carter, L.D., and Sliter, W.V., 1987, Dinosaurs on the North Slope, Alaska: High latitude, latest Cretaceous environments: Science, v. 25, p. 1608-1610.

Brouwers, E.M., and de Deckker, P., 1993, Late Maastrichtian and Danian ostracod faunas from northern Alaska: Reconstructions of environment and paleogeography: Palios, v. 8, p. 140-154.

Browne, G.H., and Kingston, D.M., 1993, Early diagenetic spherulitic siderites from Pennsylvanian paleosols in the Boss Point Formation, Maritime Canada: Sedimentology, v. 40, p. 467-474.

Bullock, P., Fedoroff, N., Jorgerius, A., Stoops, G., and Tursina, T., 1985. Handbook for Soil Thin Section Description: Waine Research Publications, Mount Pleasant, U.K., 152 p.

Burns, W.M., Hayba, D.O., Rowan, E.L., and Houseknecht, D.W., 2005, Estimating the amount of eroded section in a partially exhumed basin from geophysical well logs: an example from the North Slope, United States Geological Survey Special Paper 1732-D, p. 1-18.

Clemens, W.A., and Nelms, L.G., 1993, Paleoecological implications of Alaskan terrestrial vertebrate fauna in latest Cretaceous time at high paleolatitudes: Geology, v. 21, p. 503–506.

Cole, F., Bird, K.J., Toro, J., Roure, F., O'Sullivan, P.B., Pawlewicz, M., and Howell, D.G., 1997, An integrated model for the tectonic development of the frontal Brooks Range and Colville Basin 250 km west of the Trans-Alaska Crustal Transect: Journal of Geophysical Research, v. 102, No. B9, p. 20,685–20,708.

Conrad, J.E., McKee, E.H. and Turrin, B.D., 1990, Age of tephra beds at the Ocean Point Dinosaur Locality, North Slope, Alaska, based on K-Ar and $^{40}Ar/^{39}Ar$ Analyses: United States Geological Survey Bulletin 1990-C, p. 1–12.

Curtis, C.D., and Coleman, M.L., 1986, Controls on the precipitation of early diagenetic calcite, dolomite, and siderite concretions in complex depositional sequences in Gautier, D.L. ed., Roles of organic matter in sediment diagenesis: Special Publication of the Society of Economic Paleontologists and Mineralogists, v. 38, p. 23-33.

Dashtgard, S., Gingras, M.K., and Pemberton, S.G., 2008, Grain-size controls on the occurrence of bioturbation: Palaeogeography, Palaeoclimatology, Palaeoecology, v. 257, p. 224-243.

Davies-Vollum, K. S., 1999, The formation of beds underlying carbonaceous shales as Aquic paleosols: examples from the Bighorn Basin of Wyoming: International Journal of Coal Geology, v. 41, p. 239-255.

Davies-Vollum, K.S., and Wing, S.L., 1998, Sedimentological, taphonomic, and climatic aspects of Eocene swamp deposits (Wildwood Formation, Bighorn Basin, Wyoming): Palaios, v. 13, No. 1, p. 28-40.

Decker, P.L., 2007, Brookian Sequence stratigraphic correlations, Umiat Field to Milne Point Field, west-central North Slope, Alaska: Preliminary Interpretive Report 2007-2, Alaska Department of Natural Resources, Fairbanks, Alaska, 21 p., 1 map.

Decker, P.L., LePain, D.L., Wartes, M.A., Gillis, R.J., Mongrain, J.R., Kirkham, R.A., and Schellenbaum, D.P., (2009), Sedimentology, stratigraphy, and subsurface expression of Upper Cretaceous strata in the Sagavanirktok River area, east central North Slope, Alaska, *in* Wartes, M.W., and Decker, P.L., eds., Preliminary results of recent geologic field investigations in the Brooks Range foothills and North Slope, Alaska: Alaska Division of Geologic & Geophysical Surveys Preliminary Interpretive Report 2009-1C, 3 sheets.

Dent, D.L., and Pons, L.J., 1995, A world perspective on acid sulphate soils: Geoderma, v. 67, p. 263-276.

Detterman, R.L., Bickel, R.S., and Gryk, G., 1963, Geology of the Chandler River region, Alaska: United States Geological Society Special Paper 303-E, p. 223-324.

Dharmasri, L.C., Hundall, W.H., and Ferrell, R.E. Jr., 2004, Pyrite formation in Louisiana coastal marshes: Scanning electron microscopy and x-ray diffraction evidence: Soil Science, v. 169, p. 624-631.

Driese, S.G., Mora, C.I., Cotter, E., and Foreman, J.L., 1992, Paleopedology and stable isotope chemistry of Late Silurian Vertic paleosols, Bloomsburg Formation, central Pennsylvania: Journal of Sedimentary Petrology, v. 62, No. 5, p. 825-841.

Driese, S.G., Mora, C.I., Stiles, C.A., Joeckel, R.M., and Nordt, L.C., 2000, Mass-balance reconstruction of a modern Vertisol: Implications for interpreting the geochemistry and burial alteration of paleo-Vertisols: Geoderma, v. 95, p. 179-204.

Driese, S.G., and Ober, E.G., 2005, Paleopedologic and paleohydrologic records of precipitation seasonality from Early Pennsylvanian "underclay" paleosols, U.S.A: Journal of Sedimentary Research, v. 75, p.997-1010.

Driese, S.G., Zheng-Hua, L., and McCay, L.D., 2008, Evidence for multiple, episodic, mid-Holocene Hypsithermal recorded in two soil profiles along an alluvial floodplain catena, southeastern Tennessee, USA: Quaternary Research, v. 69, p. 276–291.

Falcon-Lang, H.J., MacRae, R.A., and Csank, A.Z., 2004, Paleoecology of Late Cretaceous polar vegetation preserved in the Hansen Point Volcanics, NW Ellesmere Island, Canada: Palaeogeography, Palaeoclimatology, Palaeoecology, v. 212, p. 45-64.

Fanning, D. S., Rabenhorst, M. C., Balduff, D. M., Orr, R. S., and Zurheide, P. K., 2010, An acid sulfate perspective on landscape/seascape soil mineralogy in the U.S. Mid-Atlantic region: Geoderma, v. 154, p. 457-464.

Fanning, D.S., and Fanning, M.C.B., 1989, Soil morphology, genesis and classification: New York, John Wiley & Sons, 285 p.

Fastovsky, D. E., and McSweeney, K., 1987, Paleosols spanning the Cretaceous-Paleogene transition, eastern Montana and western North Dakota: Geological Society of America Bulletin, v. 99, p 66-77.

Fastovsky, D. E., and McSweeney, K., 1991, Paleocene paleosols of the petrified forests of Theodore Roosevelt National Park, North Dakota: A natural experiment in compound pedogenesis: Palaios, v. 6, p. 67-80.

Fiorillo, A.R., Tykoski, R.S., Currie, P.J., McCarthy, P.J., and Flaig, P.P., 2009, Description of two Troodon partial braincases from the Prince Creek Formation (Upper Cretaceous), North Slope, Alaska: Journal of Vertebrate Paleontology, v. 29, No. 1, p. 178-187.

Fiorillo, A.R., McCarthy, P.J., Flaig, P.P., Brandlen, E., Norton, D., Jacobs, L., Zippi, P. and Gangloff, R.A.,2010a, Paleontology and paleoenvironmental interpretation of the Kikak-Tegoseak dinosaur quarry, (Prince Creek Formation: Late Cretaceous), northern Alaska: A multi-disciplinary study of an ancient high-latitude, ceratopsian dinosaur bonebed, *in* Ryan, M.J., Chinner-Algeier, B.J., and Eberth, D.A., eds., New Perspectives on Horned Dinosaurs: The Royall Tyrell Museum Ceratopsian Symposium: Bloomington, IN, Indiana University Press, p. 456-477.

Fiorillo, A. R., McCarthy, P. J., and Flaig, P. P., 2010b, Taphonomic and sedimentologic interpretations of the dinosaur-bearing Upper Cretaceous Prince Creek Formation, Alaska: Insights from an ancient high-latitude terrestrial ecosystem. Palaeogeography, Palaeoclimatology, Palaeoecology, doi:10.1016/j.palaeo.2010.02.029.

Fitzpatrick, E. A., 1984, Micromorphology of Soils: Chapman and Hall Ltd., London, England, 433 p.

Flaig, P.P., 2005, Changing fluvial style across the Permian-Triassic boundary: Beardmore Glacier Region, Central Transantarctic Mountains, Antarctica: Unpublished Master's Thesis, University of Wisconsin-Milwaukee, Milwaukee, Wisconsin, 288 p.

Flaig, P. P., McCarthy, P. J., and Fiorillo, A. R., 2010, A tidally-influenced coastal plain: The Prince Creek Formation, North Slope, Alaska. SEPM Special Publication No. , From River to Rock Record: The Preservation of Fluvial Sediments and their Subsequent Interpretation, p.

Flores, R.M., Stricker, G.D., Decker, P.L., and Myers, M.D., 2007a, Sentinel Hill Core Test 1: facies descriptions and stratigraphic reinterpretations of the Prince Creek and Schrader Bluff Formations, North Slope, Alaska: United States Geological Survey Professional Paper 1747, 31 p.

Flores, R.M., Myers, M.D., Houseknecht, D.W., Stricker, G.D., Brizzolara, D.W., Ryherd, T.J., and Takahashi, K.I., 2007b, Stratigraphy and facies of Cretaceous Schrader Bluff and Prince Creek Formations in Colville River Bluffs, North Slope, Alaska: United States Geological Survey Professional Paper 1748, 52 p.

Frederiksen, N.O, 1991, Pollen zonation and correlation of Maastrichtian marine beds and associated strata, Ocean Point dinosaur locality, North Slope, Alaska: United States Geological Survey Bulletin 1990-E, 24 p.

Frederiksen, N.O., Ager, T.A., and Edwards, L.E., 1986, Comment on "Early Tertiary marine fossils from northern Alaska: Implications for Arctic Ocean paleogeography and faunal evolution": Geology, v. 14, p. 802-803.

Frederiksen, N.O., Ager, T.A., and Edwards, L.E., 1988, Palynology of Maastrichtian and Paleocene rocks, lower Colville River region, North Slope, Alaska: Canadian Journal of Earth Sciences, v. 25, p. 512-527.

Frederiksen, N. O., Sheehan, T. P., Ager, T. A., Collet, T. S., Fouch, T. D., Franczyk, K. J., and Johnson, M, 1996, Palynomorph biostratigraphy of Upper Cretaceous to Eocene samples from the Sagavanirktok Formation in its type region, North Slope of Alaska: U.S. Geological Survey Open-File Report 96-84, 44 p.

Frederiksen, N.O., Andrle, V.A.S., Sheehan, T.P., Ager, T.A., Collet, T.S., Fouch, T.D., Franczyk, K. J., and Johnson, M, 1998, Palynological dating of Upper Cretaceous to middle Eocene strata in the Sagavanirktok and Canning Formations, North Slope of Alaska: U.S. Geological Survey Open-File Report 98-471, 51p.

Frederiksen, N.O., and McIntyre, D.J., 2000, Palynomorph biostratigraphy of mid(?) Campanian to upper Maastrichtian strata along the Colville River, North Slope of Alaska: United States Geological Survey Open-File Report 00-493, 36 p.

Frederiksen, N.O., McIntyre, D.J., and Sheehan, T.P., 2002, Palynological dating of some Upper Cretaceous to Eocene outcrop and well samples from the region extending from the easternmost part of NPRA in Alaska to the western part of ANWR, North Slope of Alaska: U.S. Geological Survey Open-File Report 02-405, 37 p.

Garrity, C.P., Houseknecht, D.W., Bird, K.J., Potter, C.J., Moore, T.E., Nelson, P.H., and Schenk, C. J., 2005, U.S. Geological Survey 2005 oil and gas resource assessment of the central North Slope, Alaska: Play maps and results: U.S. Geological Survey Open-File Report 2005-1182, 29 p.

Gasparatos, D., Tarenidis, D., Haidouti, C., and Oikonomou, G., 2005, Microscopic structure of soil Fe-Mn nodules: Environmental implication: Environmental Chemistry Letters, v. 2, No. 4, p. 17-178.

Hamer, J.M.M., Sheldon, N.D., Nichols, G.J., and Collinson, M.E., 2007, Late Oligocene–Early Miocene paleosols of distal fluvial systems, Ebro Basin, Spain: Palaeogeography, Palaeoclimatology, Palaeoecology, v. 247, No. 3-4, p. 220-235.

Hasiotis, S.T. 2002, Continental Trace Fossils: SEPM Short Course Notes, No. 51, 132 p.

Hembree, D.I., and Hasiotis, S.T., 2007, Paleosols and ichnofossils of the White River Formation of Colorado: Insight into soil ecosystems of the North America midcontinent during the Eocene-Oligocene transition: Palaios, v. 22, p. 123-142.

Hussein, A.H., and Rabenhorst, M C., 1999, Modeling of sulfur sequestration in coastal marsh soils: Soil Science Society of America Journal, v. 63, p. 1954-1963.

Huff, W.D., Kolata, D.R., Bergström, S.M., and Zhang, Y.S., 1996, Large magnitude Middle Ordovician volcanic ash falls in North America and Europe: dimensions, emplacement and post –emplacement characteristics: Journal of Volcanology and Geothermal Research, v. 73, p. 285-301.

Jackson, L.E.Jr., Tarnocai, C., and Mott, R.J., 1999, A middle Pleistocene paleosol sequence from Dawson Range, central Yukon Territory: Géographie physique et Quaternaire, v. 53, No. 3, p. 313-322.

Jafarzadeh, A.A., and Burnham, C.P., 1992, Gypsum crystals in soils: Journal of Soil Science, v. 43, p. 409-420.

Johnson, M.J., and Howell, D.G., 1996, Thermal maturity of sedimentary basins in Alaska-An overview: United States Geological Survey Bulletin 2142, 9 p., 1 plate

Johnson, C.L. and Graham, S.A. 2004, Cycles of perilacustrine facies of Late Mesozoic rift basin, southeastern Mongolia: Journal of Sedimentary Research, v. 74, p. 786-804.

Kahman, J.A., and Driese, S.G., 2008, Paleopedology and geochemistry of Late Mississippian (Chesterian) Pennington Formation paleosols at Pound Gap, Kentucky, USA: Implications for high-frequency climate variations: Palaeogeography, Palaeoclimatology, Palaeoecology, v. 259, p. 357-381.

Kemp, R.A., and Zárate, M.A., 2000, Pliocene pedosedimentary cycles in the southern Pampas, Argentina: Sedimentology, v. 47, p 3-14.

Königer, S., and Stollhofen, H., 2001, Environmental and tectonic controls on preservation potential of distal fallout ashes in fluvio-lacustrine settings: the Carboniferous-Permian Saar-Nahe Basin, south-west Germany: Special Publication of the International Association of Sedimentologists, v. 30, p. 263-284.

Kraus, M. J., 1986, Integration of channel and floodplain suites, II. Vertical relations of alluvial paleosols: Journal of Sedimentary Petrology, v. 57, No. 4, p. 602-612.

Kraus, M. J., 1998, Development of potential acid sulfate paleosols in Paleocene floodplains, Bighorn Basin, Wyoming, USA: Paleogeography, Paleoclimatology, Paleoecology, v. 144, p. 203-224.

Kraus, M. J., 1999, Paleosols in clastic sedimentary rocks: their geologic applications: Earth Science Reviews, v. 47, p. 41-70.

Kraus, M.J., and Aslan, A., 1993, Eocene hydromorphic paleosols: Significance for interpreting ancient floodplain processes: Journal of Sedimentary Petrology, v. 63, No. 3, p. 453-463.

Kraus, M.J., and Hasiotis, S.T., 2006, Significance of different methods of rhizolith preservation to interpreting paleoenvironmental and paleohydrologic settings: Examples from Paleogene paleosols, Bighorn Basin, Wyoming, U.S.A.: Journal of Sedimentary Research, v. 76, p. 633-646.

Krull, E.S., and Retallack, G.J., 2000, $\delta^{13}C$ depth profiles from paleosols across the Permian-Triassic boundary: Evidence for methane release: Geological Society of America Bulletin, v. 112, No. 9, p. 1459-1472.

La Porte, L.F., and Behrensmeyer, A.K., 1980, Tracks and substrate reworking by terrestrial vertebrates in quaternary sediment of Kenya: Journal of Sedimentary Petrology, v. 50, No. 4, p. 1337-1346.

Law, K.R., Nesbitt, H.W., and Longstaffe, F.J., 1991, Weathering of granitic tills and the genesis of a Podzol: American Journal of Science, v. 291, p. 940-976.

Leckie, D., Fox, C., and Tarnocai, C., 1989, Multiple paleosols of the Late Albian Boulder Creek Formation, British Columbia, Canada: Sedimentology, V. 36, p. 307-323.

Lin, C., Melville, M.D., and Hafer, S., 1995, Acid sulphate soil-landscape relationships in an undrained, tide-dominated estuarine floodplain, Eastern Australia: Catena, v. 24, p. 177-194.

Loope, D.B., 1986, Recognizing and utilizing vertebrate tracks in cross section: Cenozoic hoofprints from Nebraska, Palaios, v. 1, p. 141-151.

Ludvigson, G.A., González, L.A., Metzger, R.A., Witzke, B.J., Brenner, R.L., Murillo, A.P., and White, T.S., 1998, Meteoric sphaerosiderite lines and their use for paleohydrology and paleoclimatology: Geology, v. 26, No. 11, p. 1039-1042.

Madsen, H.B., and Jensen, N.H., 1988, Potentially acid sulfate soils in relation to landforms and geology: Catena, v. 15, p. 137-145.

McCarthy, P.J., 2002, Micromorphology and development of interfluve paleosols: a case study from the Cenomanian Dunvegan Formation, NE British Columbia, Canada: Bulletin of Canadian Petroleum Geology, v. 50, No. 1, p. 158-177.

McCarthy, P.J., and Plint, A.G., 1998, Recognition of interfluve sequence boundaries: Integrating paleopedology and sequence stratigraphy: Geology, v. 26, p. 387-390.

McCarthy, P.J., Martini, P.I., and Leckie, D.A., 1997, Pedosedimentary history and floodplain dynamics of the Lower Cretaceous upper Blairmore Group, southwestern Alberta, Canada: Canadian Journal of Earth Sciences, v. 34, p. 598-617.

McCarthy, P.J., Martini, P I., and Leckie, D.A., 1998, Use of micromorphology for paleoenvironmental interpretation of complex alluvial paleosols: an example from the Mill Creek Formation (Albian), southwestern Alberta: Palaeogeography, Palaeoclimatology, Palaeoecology, v. 143, p. 87-110.

McCarthy, P.J., Ubiratan, F.F., and Plint, G., 1999, Evolution of an ancient coastal plain: paleosols, interfluves and alluvial architecture in a sequence stratigraphic framework, Cenomanian Dunvegan Formation, NE British Columbia, Canada: Sedimentology, v. 46, p. 861-891.

McCarthy, P.J., and Plint, A.G., 2003, Spatial variability of paleosols across Cretaceous interfluves in the Dunvegan Formation, NE British Columbia, Canada: paleohydrological, paleogeomorphological, and stratigraphic implications: Sedimentology, v. 50, p. 1187-1220.

McSweeney, K., and Fastovsky, D.E., 1987, Micromorphological and SEM analysis of Cretaceous-Paleogene petrosols from eastern Montana and western North Dakota: Geoderma, v. 40, p. 49-63.

Molenaar, C.M., 1985, Subsurface correlations and depositional history of the Nanushuk Group and related strata, North Slope, Alaska, *in* Huffman, A.C., ed., Geology of the Nanushuk Group and Related Rocks, North Slope, Alaska: United States Geological Survey Bulletin 1614, p. 37-60.

Molenaar, C.M., Bird, K.J., and Kirk, A.R., 1987, Cretaceous and Tertiary stratigraphy of northeastern Alaska, *in* Tailleur, I.L., and Weimer, P., eds., Alaskan North Slope Geology: Society of Economic Paleontologists and Mineralogists, Pacific Section, Book 50, v. 1, p. 513–528.

Moore, S.E., Ferrell, R.E. Jr., and Aharon, P., 1992, Diagenetic siderite and other ferroan carbonates in a modern subsiding marsh sequence: Journal of Sedimentary Petrology, v. 62, No. 3, p. 357-366.

Moore, T.E., Wallace, W.K., Bird, K.J., Karl, S.M., Mull, C.G., and Dillon, J.T., 1994, Geology of northern Alaska, *in* Plafker, G, and Berg, H.C., eds., The Geology of Alaska: Geological Society of America, The Geology of North America, Boulder, Colorado v. G-1, p. 49-140.

Mull, C.G., 1985, Cretaceous tectonics, depositional cycles, and the Nanushuk Group, Brooks Range and Arctic Slope, Alaska, *in* Huffman, A.C. Jr., ed., Geology of the Nanushuk Group and related rocks, North Slope, Alaska: United States Geological Survey Bulletin 1614, p. 7-36.

Mull, C.G., Houseknecht, D.W., and Bird, K.J., 2003, Revised Cretaceous and Tertiary stratigraphic nomenclature in the Colville Basin, northern Alaska: United States Geological Survey Professional Paper 1673, p. 1-51.

Munsell Colour Company, 1984, Munsell Soil Colour Charts, Munsell Colour Company, Baltimore, MD.

Nesbitt, H.W., and Young, G.M., 1982, Early Proterozoic climates and plate motions inferred from major element chemistry of lutites: Nature, v. 299, p. 715-717.

Oboh-Ikuenobe, F.E., Obi, C.G., and Jaramillo, C.A., 2005, Lithofacies, palynofacies, and sequence stratigraphy of Paleogene strata in Southeastern Nigeria: Journal of African Earth Sciences, v. 41, p. 79-101.

Parrish, J.T., and Spicer, R.A., 1988, Late Cretaceous terrestrial vegetation: A near-polar temperature curve: Geology, v. 16, p. 22-25.

Parrish, J.M., Parrish, J.T., Hutchison, J.H., and Spicer, R.A., 1987. Late Cretaceous vertebrate fossils from the North Slope of Alaska and implications for dinosaur ecology. Palaios v. 2, p. 377-389.

Phillips, R.L., 2003, Depositional environments and processes in Upper Cretaceous nonmarine and marine sediments, Ocean Point dinosaur locality, North Slope, Alaska: Cretaceous Research, v. 24, p. 499-523.

Pons, L.J., and van Breemen, N., 1981, Factors influencing the formation of potential acidity in tidal swamps, *in* Dost, H., and van Breemen, N. eds., Proceedings of the Bangkok symposium on acid sulphate soils: Second International Symposium on Acid Sulphate soils, Bangkok, Thailand, p. 37-51.

Postma, D., 1977, The occurrence and chemical composition of recent Fe-rich mixed carbonates in a river bog: Journal of sedimentary Petrology, v. 47, No. 3, p. 1089-1098.

Postma, D., 1982, Pyrite and siderite formation in brackish and freshwater swamp sediments: American Journal of Science, v. 282, p. 1151-1183.

Quattrocchio, M.E., Martínez, M.A., Carpinelli Pavisich, A., and Volkheimer, W., 2006, Early Cretaceous palynostratigraphy, palynofacies, and paleoenvironments of well sections in northeastern Tierra del Fuego, Argentina: Cretaceous Research, v. 27, p. 584-602.

Retallack, G.J., 1983, Late Eocene and Oligocene paleosols from Badlands National Park, South Dakota: Geological Society of America Special Paper 193, 82 p.

Retallack, G.J., 1991, Untangling the effects of burial alteration and ancient soil formation: Annual Review of Earth and Planetary Sciences, v. 19, p. 183-206.

Retallack, G.J., 1997, A colour guide to paleosols: John Wiley and Sons, West Sussex, England, 175 p.

Retallack, G.J., 1999 Postapocalyptic greenhouse paleoclimate revealed by earliest Triassic paleosols in the Sydney Basin, Australia: Geological Society of America Bulletin, v. 111, p. 52–70.

Retallack, G.J., 2001, Soils of the Past, an Introduction to Paleopedology, Second Edition: Oxford, United Kingdom, Blackwell Science, 404 p.

Retallack, G.J., and Alonso-Zazra, A. M., 1998, Middle Triassic Paleosols and paleoclimate of Antarctica: Journal of Sedimentary Research, v. 68, No. 1, p. 169-184.

Retallack, G.J., and Krull, E.S., 1999, Landscape ecological shift at the Permian-Triassic boundary in Antarctica: Australian Journal of Earth Sciences, v. 46, No. 4, p. 786-812.

Retallack, G.J., Bestland, E.A., and Fremd, T.J., 1999, Eocene and Oligocene Paleosols of central Oregon: Geological Society of America Special Paper 344, 192 p.

Rich, T.H., Gangloff, R.A., and Hammer, W.H., 2002, Polar Dinosaurs: Science, v. 295, p. 979-980.

Richardson, J.L., and Daniels, R.B., 1993, Stratigraphic and hydraulic influences on soil color development, *in* Bigham, J.M and Ciolkosz, E. J. eds., Soil Color: Soil Science Society of America Special Publication Number 31, p.109-125.

Ritsema, C.J., and Groenberg, J.E., 1993, Pyrite oxidation, carbonate weathering, and gypsum formation in a drained potential acid sulfate soil: Soil Science Society of America Journal, v. 57, p. 968-976.

Robinson, M.S., 1989, Kerogen microscopy of coal and shales from the North Slope of Alaska: Alaska Division of Geological and Geophysical Surveys Public Data File 89–22, 19 p.

Roehler, H.W., 1987, Depositional environments of the coal-bearing and associated formations of Cretaceous age in the National Petroleum Reserve in Alaska: United States Geological Society Bulletin 1575, 16 p.

Sheldon, N.D., 2006, Abrupt chemical weathering increase across the Permian–Triassic boundary: Palaeogeography, Palaeoclimatology, Palaeoecology, v. 231, p. 315– 321.

Sheldon, N.D., Retallack, G. J., and Geochemical Climofunctions from North American Soils and Tanake, S., 2002, Application to Paleosols across the Eocene-Oligocene Boundary in Oregon: The Journal of Geology, v. 110, p. 687-696.

Smith, N.D., Cross, T.A., Dufficy, J.P., and Clough, S.R., 1989, Anatomy of an avulsion: Sedimentology, v. 36, p. 1-23.

Smith, R., 1990, Alluvial paleosols and pedofacies sequences in the Permian Lower Beaufort of the southwestern Karoo Basin, South Africa: Journal of Sedimentary Petrology, v. 60, p. 258-276.

Soil Survey Staff, United States Natural Resources Conservation Service 1999, Soil taxonomy: A basic system of soil classification for making and interpreting soil surveys: United States Department of Agriculture, Natural Resources Conservation Service, 869 p.

Spicer, R.A., 2003, Changing climate and biota, *in* Skelton, P., ed., The Cretaceous World: Cambridge, U.K., Cambridge University Press, p. 85-162.

Spicer, R.A., and Parrish, J.T., 1987, Plant megafossils, vertebrate remains, and paleoclimate of the Kogosukruk Tongue (Late Cretaceous), North Slope, Alaska: U. S. Geological Survey Circular, Report: C 0998, p. 47-48.

Spicer, R.A., and Parrish, J., 1990, Late Cretaceous-early Tertiary paleoclimates of northern high latitudes: a quantitative view: Journal of the Geological Society, London, v. 147, No. 6, p. 329-341.

Spicer, R.A., and Herman, A.B., 2010, the Late Cretaceous environment of the Arctic: A quantitative reassessment based on plant fossils: Palaeogeography, Palaeoclimatology, Palaeoecology, doi: 10.1016/j.palaeo.2010.02.025

Spicer, R.A., Parrish, J.T., and Grant, P.R., 1992, Evolution of vegetation and coal-forming environments in the Late Cretaceous of the North Slope of Alaska, *in* McCabe, P.J., and Parrish, J.T., eds., Controls on the Distribution and Quality of Cretaceous Coals: Geological Society of America Special Paper 267, p. 177-192.

Stiles, C.A., Mora, C.I., and Driese, S.G., 2003, Pedogenic processes and domain boundaries in a Vertisol climosequence: evidence from titanium and zirconium distribution and morphology: Geoderma, v. 116, p. 279-299.

Sweeney, R.E., and Kaplan, I.R., 1973, Pyrite framboid formation: Laboratory synthesis and marine sediments: Economic Geology, v. 68, p. 618-634.

Tanner, L.H., and Lucas, S.G., 2006, Calcareous paleosols of the Upper Triassic Chinle Group, Four Corners region, southwestern United States: Climatic implications, *in* Alonso-Zarza, A.M., and Tanner, L.H., eds., Paleoenvironmental Record and Applications of Calcretes and Palustrine Carbonates: Geological Society of America Special Paper 416, p. 53–74.

Tomsich, C.S., McCarthy, P.J., Fowell, S.J., and Sunderlin, D., 2010, Paleofloristic and paleoenvironmental information from a late Cretaceous (Maastrichtian) flora of the lower Cantwell Formation near Sable Mountain, Denali National Park, Alaska: Palaeogeography, Palaeoclimatology, Palaeoecology, doi: 10.1016/j.palaeo.2010.02.023

Turner, B.R., 1993, Paleosols in Permo-Triassic continental sediments from Prydz Bay, East Antarctica: Journal of Sedimentary Petrology, v. 63, No. 4, p. 694-706.

Ufnar, D.F., González, L.A., Ludvigson, G.A., Brenner, R.L., and Witzke, B.J., 2001, Stratigraphic implications of meteoric sphaerosiderite $\delta^{18}O$ values in paleosols of the Cretaceous (Albian) Boulder Creek Formation, N.E. British Columbia foothills, Canada: Journal of Sedimentary Research, v. 71, p. 1017-1028.

Ufnar, D.F., Ludvigson, G.A., González, L.A., Brenner, R.L., and Witzke, B.J., 2004, High latitude meteoric $\delta^{18}O$ compositions: Paleosol siderite in the Middle Cretaceous Nanushuk Formation, North Slope, Alaska: Geological Society of America Bulletin, v. 116, No. 3/4, p. 463-473.

Ufnar, D.F., González, L.A., Ludvigson, G.A., Brenner, R.L., Witzke, B.J., and Leckie, D., 2005, Reconstructing a mid-Cretaceous landscape from paleosols in western Canada: Journal of Sedimentary Research, v. 75, No. 6, p. 984-996.

Ufnar, D.F., 2007, Clay coatings from a modern soil chronosequence: a tool for estimating the relative age of well-drained paleosols: Geoderma, v. 141, p. 181-200.

Vanstone, S.D., 1991, Early Carboniferous (Mississippian) paleosols from southwest Britain: Influence of climatic change on soil development: Journal of Sedimentary Petrology, v. 61, No. 4, p. 445-457.

Veneman, P.L.M., Vepraskas, M.J., and Bouma, J., 1976, the physical significance of soil mottling in a Wisconsin toposequence: Geoderma, v. 15, p. 103-118.

Wanas, H.A., and Abu El-Hassan, M.M., 2006, Paleosols of the Upper Cretaceous-Lower Tertiary Maghra El-Bahari Formation in the northeastern portion of the Eastern Desert, Egypt: Their recognition and geological significance, Sedimentary Geology, v.183, p. 243-259.

Witte, K.W., Stone, D.B., and Mull, C.G., 1987, Paleomagnetism, paleobotany, and paleogeography of the Cretaceous, North Slope, Alaska, *in* Tailleur, I., and Weimer, P., eds., Alaska North Slope Geology: The Pacific Section, Society of Economic Paleontologists and Mineralogists and the Alaska Geological Society, v. 1, p. 571-579.

Wright, V.P., 1986, Pyrite formation and the drowning of a paleosol: Geological Journal, v. 21, p. 139-149.

Wright, V.P. 1992, Paleopedology: stratigraphic relationships and empirical models, *in* Martini, I.P., and Chesworth, W. eds., Weathering, Soils and Paleosols: Elsevier, Amsterdam, p. 475–499.

Wu, G., Qin, J., Deng, B., and Li, C., 2002, Palynomorphs in the first layer of the Yangtze Delta and their paleoenvironmental implication: Chinese Science Bulletin, v. 47, No. 21, p. 1837-1841.

Chapter 4 Muddy Hyperconcentrated Flows: Dinosaur Killer Crevasse Splays of the Cretaceous Arctic (Prince Creek Formation, northern Alaska)*

Peter P. Flaig, Paul J. McCarthy, and Anthony R. Fiorillo

*Flaig, P. P., McCarthy, P. J., and Fiorillo, A. R., 2010, Muddy hyperconcentrated flows: Dinosaur killer crevasse splays of the Arctic (Prince Creek Formation, northern Alaska). Prepared for submission to the journal *Palaios* in 2010. A shortened version will be submitted to the Geological Society of America journal *Geology* in late 2010 or early 2011

ABSTRACT

The Cretaceous (Early Maastrichtian) Prince Creek Formation, northern Alaska, contains the richest concentration of high-latitude dinosaur remains on Earth. The bulk of these dinosaurs are found in several high-density bonebeds encased in muddy alluvium. $^{40}Ar/^{39}Ar$ incremental-heating analysis of a tuff stratigraphically above a bonebed in the Sling Point outcrop belt returned an age of 69.2 ± 0.5 Ma.

Rare individual bones and bone fragments are found in fluvial channels but the highest bone concentrations are consistently found outside of channel margins in laterally-extensive, fine-grained overbank deposits overlying organic-rich floodplain facies. Three bonebeds encased in alluvium, the Sling Point, Liscomb, and Byers bonebeds, are overwhelmingly dominated by partially articulated to associated juvenile hadrosaurian dinosaurs. All bones are in hydraulic disequilibrium with the clay-rich matrix and exhibit little evidence of rounding, weathering, predation or trampling, suggesting short-distance transport and rapid burial. Muddy overbank deposits encasing these dinosaur death assemblages exhibit a bipartite division of flow and display a facies association that suggests deposition by fine-grained hyperconcentrated flows.

In all three bonebeds, current ripple cross-laminated siltstone containing well-sorted dinosaur bone above a sharp base fine-upward into a distinctive, massive mudstone lacking sedimentary structures but including rare dinosaur bone and flow-parallel plant fragments that appear to "float" in a matrix of mud. Laterally, the graded siltstone beds may be absent and bone is instead encased directly within the massive

mudstone. These massive mudstones overlying normally-graded siltstone beds form a depositional couplet similar to deposits expected for two-phase hyperconcentrated flows. The existence of hyperconcentrated flows in the Prince Creek Fm. is not unexpected considering that these muddy, bone-bearing facies were deposited on a low-gradient coastal plain far from the mountain front. Exceptional floods, probably driven by seasonal snowmelt in the ancestral Brooks Range, likely entrained abundant fine-grained sediments stored on muddy point bars and on floodplains, increasing suspended sediment concentrations and generating hyperconcentrated overbank flows that killed and buried scores of juvenile dinosaurs occupying this high-latitude coastal plain. This unique killing mechanism for polar dinosaurs likely resulted from seasonal discharge resulting from the near polar latitude of northern Alaska in the Late Cretaceous.

INTRODUCTION

One of the more remarkable aspects of the fossil record is the occurrence of densely-packed remains of fossil organisms. With respect to fossil vertebrates, these occurrences are termed bonebeds (see Rogers et al. 2007 for a recent overview). Depositional mechanisms deemed responsible for emplacement of bonebeds in or near fluvial channels include but are not limited to streamflows (Wood et al. 1988, Trueman 1999, Ryan et al. 2001, Bandyopadhyay et al. 2002), debris flows (Fastovsky et al. 1995, Trueman 1999, Rogers 2005, Eberth et al. 2006, Britt et al. 2009), and a combination of debris flows and coarse-grained hyperconcentrated flows (Myers and Storrs 2007,

Lauters et al. 2008). Never has the depositional mechanism for bonebed emplacement been attributed primarily to fine-grained hyperconcentrated flows.

Bonebeds encased in debris flows are typically found close to orogenic belts, topographic highs, steep gradients, and sources of coarse-grained clastics (Fastovsky et al. 1995, Eberth et al. 2006, Britt et al. 2009). Bonebeds in more distal environments are commonly deposited by streamflows in channel-fills or as channel-lags (Fiorillo 1991, Trueman 1999, Ryan et al. 2001) or contain facies successions and sedimentary structures that indicate depositional mechanisms other than fine-grained hyperconcentrated flow. These mechanisms include but are not limited to deposition of bloated carcasses on floodplains by streamflow, burial of carcasses on floodplains by overbank deposits after catastrophic drought, and reworking of previously deposited bone on channel margins and proximal floodplains by streamflow (Wood et al. 1988, Smith 1993, Gates 2005, Suarez et al. 2007). Many of these bonebeds were deposited at mid-paleolatitudes in warm, temperate climates (e.g. Wood et al. 1988, Ryan et al. 2001, Rogers 2005, Gates 2005, Eberth et al. 2006, Suarez et al. 2007, Lauters et al. 2008, Britt et al. 2009). Bonebeds deposited at near-polar latitudes under cooler temperatures in environments affected by high-latitude seasonality are much less common in the rock record (Currie et al. 2008, Fiorillo et al. 2010b, Gangloff and Fiorillo, 2010).

Three high-density dinosaur bonebeds of the Cretaceous (Early Maastrichtian) Prince Creek Formation (Fm.), the Sling Point, Byers, and Liscomb bonebeds (Fiorillo and Gangloff 2000; Fiorillo et al. 2009, 2010b), are preserved in bluffs along the Colville

River, northern Alaska (Fig. 4.1). These bluffs contain alluvial sediments of tidally influenced suspended-load trunk channels, muddy suspended-load distributary channels, and clay- and organic-rich floodplains deposited on a high-latitude, low-lying, low-gradient coastal plain (Phillips 2003, Flaig et al. 2010). All bonebeds are dominated by juveniles and sub-adults (Fiorillo et al. 2010b). Bones are associated to semi-articulated, not in hydraulic equilibrium with the enveloping fine-grained matrix, and exhibit little evidence of rounding, weathering, predation, or trampling suggesting short distance transport and rapid burial (Fiorillo et al. 2010b). Bonebed emplacement probably resulted from flooding driven by seasonal snowmelt in the ancestral Brooks Range to the south (Fiorillo et al. 2010a, 2010b). Although seasonal flooding is interpreted as the driving force behind bonebed emplacement, the local depositional mechanism has remained a mystery.

Determining the precise mechanism for bonebed emplacement requires, in part, analyzing local facies, correlating local stratigraphy, determining the relative position of bonebeds within the local stratigraphy, and reconciling local stratigraphy with the regional depositional model (Eberth et al. 2007). The purpose of this paper is to describe and correlate facies of the Prince Creek Fm., in bluffs that include the Sling Point, Byers, and Liscomb bonebeds, in order to establish the environment(s) of bonebed deposition on the Cretaceous coastal plain and determine the depositional mechanism responsible for bonebed emplacement.

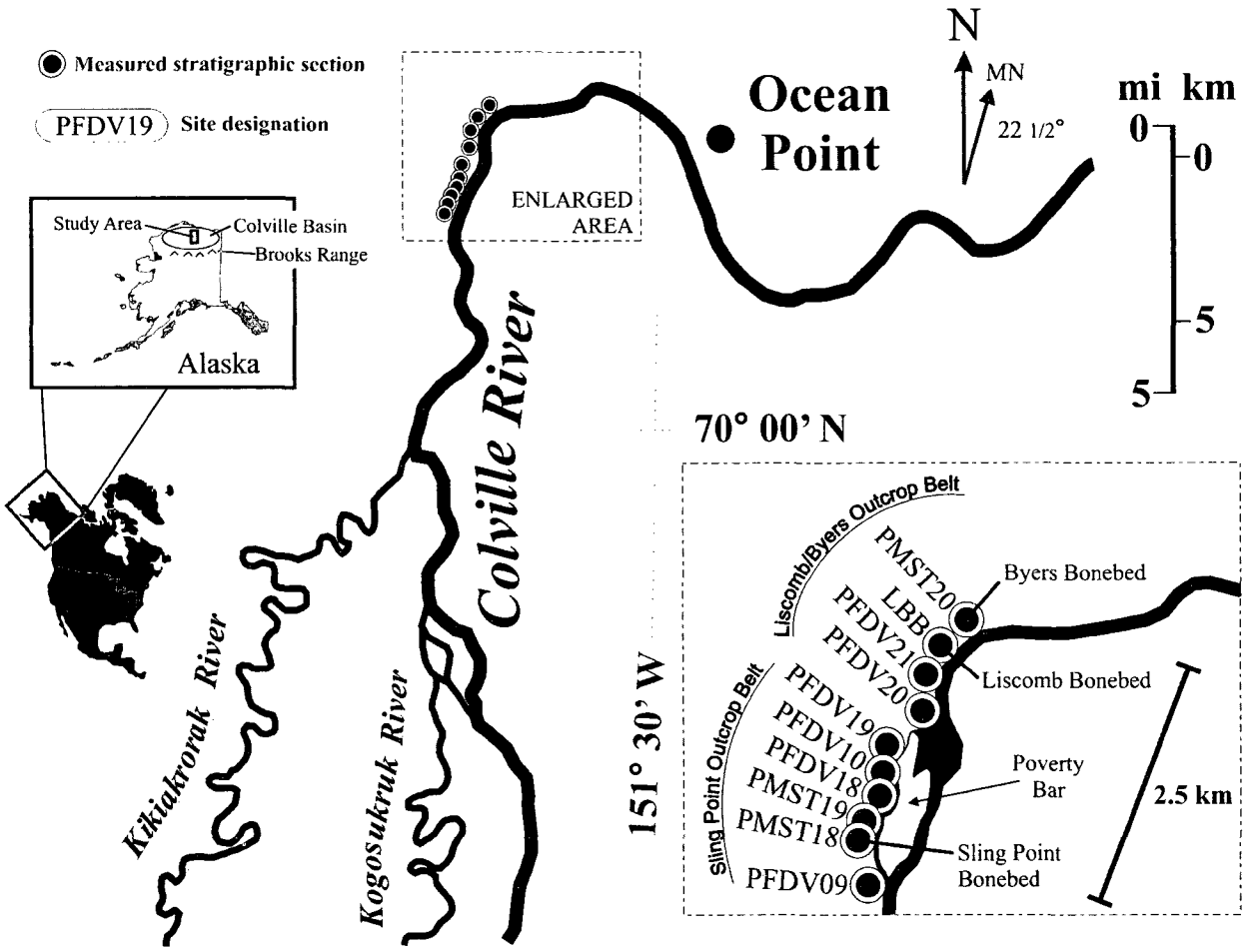

Figure 4.1. Study area along the Colville River, North Slope of Alaska including locations of the Sling Point outcrop belt, Liscomb/Byers outcrop belt, and ten measured stratigraphic successions described in this study. MN=magnetic north.

REGIONAL GEOLOGY

The Colville Basin of northern Alaska (Fig. 4.1) formed as a result of subsidence to the north of the Brooks Range orogenic belt (Moore et al. 1994, Cole et al. 1997). Uplift and erosion of the Brooks Range drove sediments into the basin, filling it both axially and transversely during the Late Cretaceous and Tertiary (Molenaar 1985, Mull 1985, Molenaar et al. 1987, Moore et al. 1994, Mull et al. 2003, Decker 2007). The Prince Creek Fm. (Fig. 4.2), exposed for ~ 60 km in bluffs along the Colville River, contains northeastward-dipping strata (< 3°) composed predominantly of alluvial sandstone, siltstone, mudstone, carbonaceous shale, coal, bentonite, and tuff (Roehler 1987, Mull et al. 2003; Fiorillo et al. 2009, 2010b, Flaig et al. 2010). These facies are the most proximal in a Late Cretaceous to Paleocene, continental to marine succession that also includes the shallow marine Schrader Bluff Fm. and the slope to deepwater Canning Fm. and Hue Shale (Fig. 4.2).

The base of the Prince Creek Fm. along the Colville River is comprised of fluvial sandstones and conglomerates incised into shallow-marine sandstones of the lower Schrader Bluff Fm. (Mull et al. 2003, Flores et al. 2007b) interpreted as an incised paleovalley (Flores et al. 2007a, 2007b). At Ocean Point (Fig. 4.1), the contact between the top of the Prince Creek Fm. and the overlying upper Schrader Bluff Fm. is transgressive between alluvial and interdistributary bay facies of the Prince Creek Fm. and shoreface deposits of the upper Schrader Bluff Fm. (Phillips 2003). Pollen (Frederiksen et al. 1986, 1988, 2002; Frederiksen 1991; Frederiksen and McIntyre 2000; Flores et al. 2007b; Brandlen, 2008; Fiorillo et al. 2010a), flora and fauna

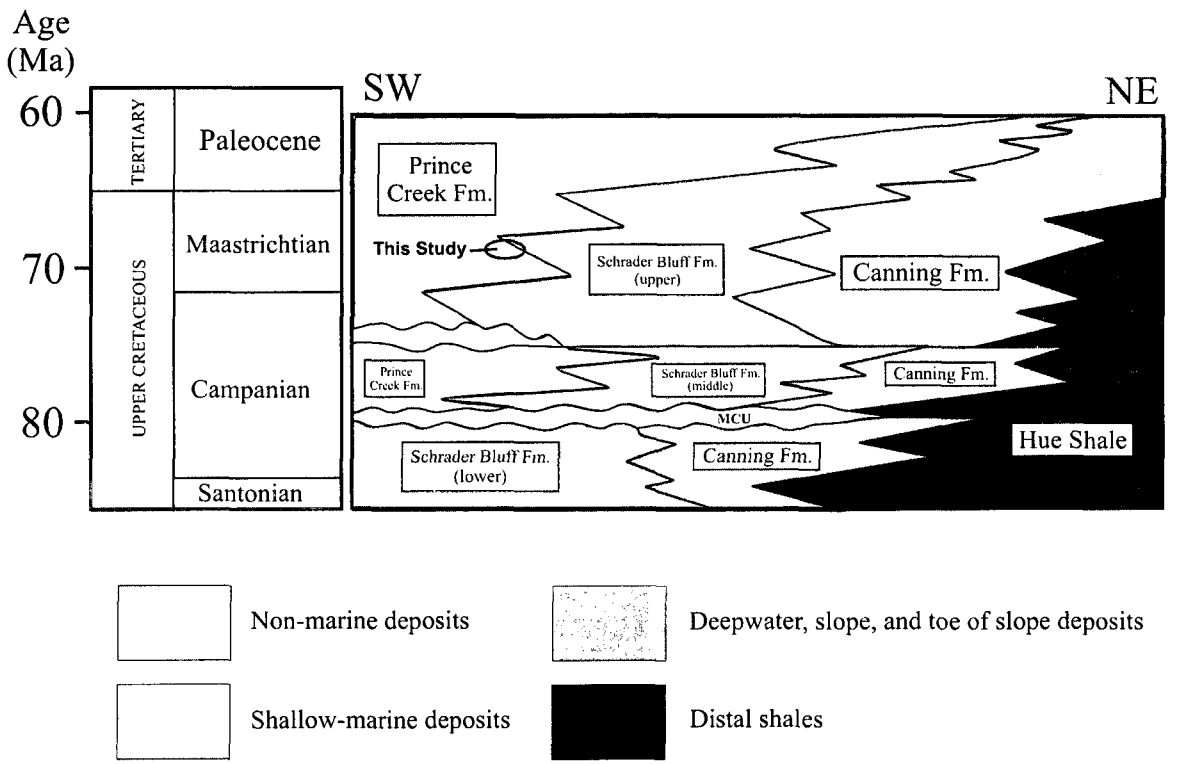

Figure 4.2. Generalized chronostratigraphic column for the central North Slope, Alaska. MCU=mid-Campanian unconformity. Revised from Mull et al. (2003), Garrity et al. (2005), and Decker et al. 2009.

(Parrish and Spicer 1988, Brouwers and de Deckker 1993), and K/Ar and $^{40}Ar/^{39}Ar$ analyses (Conrad et al. 1990) indicate that the Prince Creek Fm. ranges from Campanian to Paleocene in age. Recent work (Fiorillo et al. 2010a, Flaig et al. 2010) demonstrates that all of the deposits in the study area are Early Maastrichtian.

The Prince Creek Fm. is thought to have been deposited at paleolatitudes of 82°-85° N (Brouwers et al. 1987, Witte et al. 1987, Besse and Courtillot 1991, Rich et al. 2002, Spicer and Herman 2010) under Cretaceous greenhouse conditions (Fischer 1981, Parrish et al. 1987, Spicer et al. 1992, Zakharov et al. 1999, Deconto et al. 2000, Spicer 2003, Nordt et al. 2003, Gallagher et al. 2008). Arctic Alaska temperature estimates based on megaflora indicate Maastrichtian mean annual temperatures (MAT) of ~5° C (Spicer and Parrish 1987; Parrish and Spicer 1988; Spicer 2003; Fiorillo et al. 2009, 2010a, 2010b) with a warmest month mean temperature of 10-12 ° C and a coldest month mean temperature of 2-4 ° C (Brouwers et al. 1987, Tomsich et al. 2010). Mean annual precipitation is estimated at 500-1500 mm a^{-1} (Spicer and Parrish 1990, Brandlen 2008). Abundant charcoal indicates that forest fires were common during periodic dry periods (Spicer and Parrish 1987, Spicer 2003). No evidence of cryoturbation or ground ice exists in sediments of the Prince Creek Fm., however, false rings in fossil wood suggest at least periodic freezes may have occurred (Spicer and Parrish 1990, Spicer et al. 1992, Spicer 2003). Elevations in the nearby Brooks Range likely ranged from 1500-5000 m with MAT at high elevations below 0^0 C (Spicer 2003), implying probable snow and ice fields at higher elevations (Spicer and Parrish 1990, Fiorillo et al. 2009, Fiorillo et al. 2010b).

The Prince Creek Fm. has been interpreted as an alluvial-coastal plain succession (Roehler 1987, Mull et al. 2003; Flores et al. 2007a, 2007b; Fiorillo et al. 2009, 2010a, Flaig et al. 2010). The Prince Creek Fm. contains three distinct channel forms along with copious floodplain facies (Fiorillo et al. 2009, 2010, Flaig et al. 2010). Channels include suspended-load meandering trunk channels, suspended-load meandering distributary channels and associated mud-filled abandoned channels occupying crevasse splay-complexes, and fixed ribbon sandbodies similar to anastomosed channels also on crevasse splay-complexes. All channels contain inclined heterolithic stratification (IHS) with thick muddy members suggesting tidal influence. Fine-grained, organic-rich facies are abundant. Fine-grained facies include sheet-like sandstones and siltstones interpreted as deposits of crevasse splays and levees; siltstones and mudstones, rarely containing brackish-water clams (*Nucula* aff. *N. percrassa* Conrad, pers. comm. Robert Blodgett) and indeterminate gastropods, interpreted as deposits of floodplain lakes and ponds; organic-rich mudstone, carbonaceous shale, and coal interpreted as deposits of swamps; drab-colored, ubiquitously rooted and mottled siltstones and mudstones interpreted as paleosols (Brandlen 2008, Fiorillo et al. 2010a, Flaig et al. 2010); and numerous tuffs and bentonites. Irregular, undulating basal contacts at the base of many fine-grained facies are likely the result of trampling by dinosaurs (Flaig et al. 2010). Evidence for marine influence on pore waters in sediments and soils in distal parts of the Prince Creek Fm. include brackish-water clams, jarosite, and rare pyrite and gypsum (Flaig et al. 2010).

VERTEBRATE PALEONTOLOGY

Dinosaur body fossils (Fig. 4.3) were first collected from exposures of the Prince Creek Fm. by Dr. Robert Liscomb along the Colville River in 1961 during a survey for hydrocarbons (Clemens 1994). The fossils were not recognized as dinosaurian until 1983 when the specimens became available to Charles Repenning, a vertebrate paleontologist with the U.S. Geological Survey (Fiorillo 2004). Starting in the mid-1980s, several institutions including the United States Geological Survey; the University of California at Berkeley; the University of Alaska-Fairbanks; and the Museum of Nature and Science in Dallas began fieldwork in bluffs along the Colville River. As a result of these paleontological excavations, several thousand skeletal elements from the Prince Creek Fm. are now housed in various museums. The Prince Creek Fm. is unique in its paleontological productivity, having produced an abundance of specimens that remain a rich source of paleontologic insight into the dynamics of an ancient high-latitude terrestrial ecosystem (Brouwers et al. 1987; Parrish et al. 1987; Clemens and Nelms 1993; Currie 1989; Fiorillo and Gangloff 2000, 2001; Rich et al. 2002; Gangloff et al. 2005; Fiorillo 2008a, 2008b; Fiorillo et al. 2009, 2010a, 2010b).

These Alaskan Cretaceous dinosaurs are scientifically significant for several reasons: (1) Alaskan populations lived at the northern ecological extreme of latitudinal gradients (67-85^0 N) for North America during the Cretaceous (Fiorillo and Gangloff 2001), (2) unprecedented faunal and floral exchanges took place between Asia and North America during the Cretaceous with northern Alaska functioning as the biological dispersal path between these two landmasses (Russell 1993, Sereno 2000, Fiorillo 2008a)

Figure 4.3. Semi-articulated juvenile duck-billed dinosaur bones from the Liscomb quarry site along the Colville River. Pocket knife is 9 cm long.

and (3) by virtue of being at the opposite end of the continent from the reputed terminal Chicxulub Crater impact site in Mexico, the Prince Creek Fm. fossil vertebrate assemblage offers insight into an Arctic paleoenvironment prior to dinosaur extinction.

The discoveries of dinosaur remains from high paleolatitudes of North America have provided insights into ancient ecosystem dynamics. For example, these remains proved to be ecologically problematic given current models of dinosaur physiology. Several workers (Hotton 1980, Brouwers et al. 1987, Parrish et al. 1987, Currie 1989) support the hypothesis that dinosaurs were long distance, seasonal migrants, with a migratory range of several thousand kilometers, typically using a modern analog, caribou (*Rangifer tarandus*) to support their conclusions. The preserved cell structure of juvenile hadrosaurian fossil bones from the Prince Creek Fm. suggests that juveniles were greater than one year in age (Fiorillo and Gangloff 2001). Comparison between the relative size of juvenile vs. adult hadrosaurs and juvenile vs. adult caribou indicates (based on qualitative energetics) that juvenile hadrosaurs were too small for long-distance migration and therefore must have been year-round residents of the Cretaceous high-latitudes (Fiorillo and Gangloff 2001).

The annual low level of light, rather than temperature, may have been the primary determinant of vertebrate productivity in Cretaceous northern high latitudes (Fiorillo and Gangloff 2000). *Troodon formosus*, a relatively small dinosaur known for its exceptionally large eyes compared to skull size, was the most abundant predatory dinosaur in northern Alaska (Fiorillo and Gangloff 2000). *Troodon* is known from

northern Alaska south to west Texas, but is more common in the north. Although its geographic range was extensive, *Troodon* was preadapted to the low light conditions of the Arctic where it thrived (Fiorillo and Gangloff 2000, Fiorillo 2008a, Fiorillo et al. 2009). This adaptation gave *Troodon* a competitive edge over other predatory dinosaurs, allowing it to achieve a larger body size relative to its more southerly counterparts (Fiorillo 2008a).

A popular model for dinosaur extinction predicts that there was a short-term period of darkness and cold, and it was this period of implied poor environmental conditions that was the primary cause for extinctions at the end of the Cretaceous (e.g. Alvarez 1986, Officer 1992, Pope et al. 1994). Alaskan non-avian dinosaurs, as shown from remains in the Prince Creek Fm., thrived under the profound seasonality of the ancient Arctic (Clemens and Nelms 1993), yet they too died at the end of the Cretaceous. Clemens and Nelms (1993) used this fact to argue against short-term climatic change as the cause for non-avian dinosaur extinction.

This brief overview of the significance of vertebrate fossils from the Prince Creek Fm. shows that Alaskan dinosaurs provide paleontologists with a unique opportunity to understand polar dinosaur paleobiology and inferences regarding the global extinction of non-avian dinosaurs. The polar world of the Cretaceous, as with the modern Arctic (Hardy 1996, Hodgkins et al. 2003, Pavelsky and Smith 2004), contained many unique attributes and environments, some of which may have contributed to the unique

depositional mechanism responsible for killing and preserving these polar dinosaurs in the Prince Creek Fm.

METHODS

Fieldwork was conducted from 2005-2007 along the Colville River (Fig. 4.1) in bluffs adjacent to Poverty Bar (Sling Point outcrop belt, Fig. 4.1) and bluffs north of Poverty Bar and west of Ocean Point (Liscomb/Byers outcrop belt, Fig. 4.1). These bluffs were selected for extensive study because they include the Sling Point, Liscomb, and Byers dinosaur quarries. A total of 75 sections were measured in total and detailed descriptions of 10 measured sections (Figs. 4.4, 4.5) from this local study area, including descriptions of grain size, lithology, contacts, sedimentary structures, flora, fauna, and vertical and lateral facies relationships, form the data set for this paper (Figs. 4.4, 4.5). Petrographic features in thin section were examined in plane and polarized light using a Nikon Eclipse LV 100 POL petrographic microscope (1x-50x magnification).

$^{40}Ar/^{39}Ar$ analysis of a single tuff sample (07PFDVDK-09-14.9) was conducted at the Geochronology Laboratory, University of Alaska-Fairbanks. The sample was crushed, washed in de-ionized water, rinsed in acetic acid, and sieved to preserve the 250-500 micron size fraction. The remaining material was hand-picked for glass-rich separates. The monitor mineral MMhb-1 (Samson and Alexander 1987) with an age of 513.9 Ma (Lanphere and Dalrymple 2000) was used to monitor the neutron flux and calculate the irradiation parameter "J". The sample and standard were wrapped in

aluminum foil and loaded into aluminum canisters. The sample was irradiated for 20 megawatt-hours in position 5c of the uranium enriched research reactor at McMaster University in Hamilton, Ontario, Canada. After irradiation the sample and monitor were placed into a 2 mm diameter hole in a copper tray and loaded into an ultra-high vacuum extraction line. The monitor was fused and the sample was heated using a 6-watt argon-ion laser following the technique described in York et al. (1981), Layer et al. (1987), and Layer (2000). Argon purification was achieved using a liquid nitrogen cold trap and a SAES Zr-Al getter at 400°C. The sample was analyzed in a VG-3600 mass spectrometer at the Geophysical Institute, University of Alaska-Fairbanks. Argon isotope measurements were corrected for system blank and mass discrimination as well as calcium, potassium, and chlorine interference reactions following the procedures outlined in McDougall and Harrison (1999). System blanks were measured at $2x10^{-16}$ mol ^{40}Ar and $2x10^{-18}$ mol ^{36}Ar which are 10-50 times smaller than fraction volumes. Mass discrimination was monitored by running both calibrated air shots and a zero-age glass sample. Measurements were made on a monthly basis to check for changes in mass discrimination. The age is quoted to the ± 1 sigma level and is calculated using the constants of Steiger and Jaeger (1977). The integrated $^{40}Ar/^{39}Ar$ age is given by the total gas measured and is equivalent to a K-Ar age. The spectrum was deemed to provide a plateau age if (1) three or more consecutive gas fractions represented at least 50% of the total gas release and (2) those gas fractions were within two standard deviations of each other (Mean Square Weighted Deviation less than ~2.7).

Figure 4.4 (Following Page.) Stratigraphic correlations for six measured sections at the Sling Point outcrop belt including lithology, contacts, sedimentary structures, flora, fauna, overall depositional environment, dinosaur bonebeds, and dinosaur quarries. MDC= Meandering distributary channel, FDC=Fixed distributary channel, FP=Floodplain sediments.

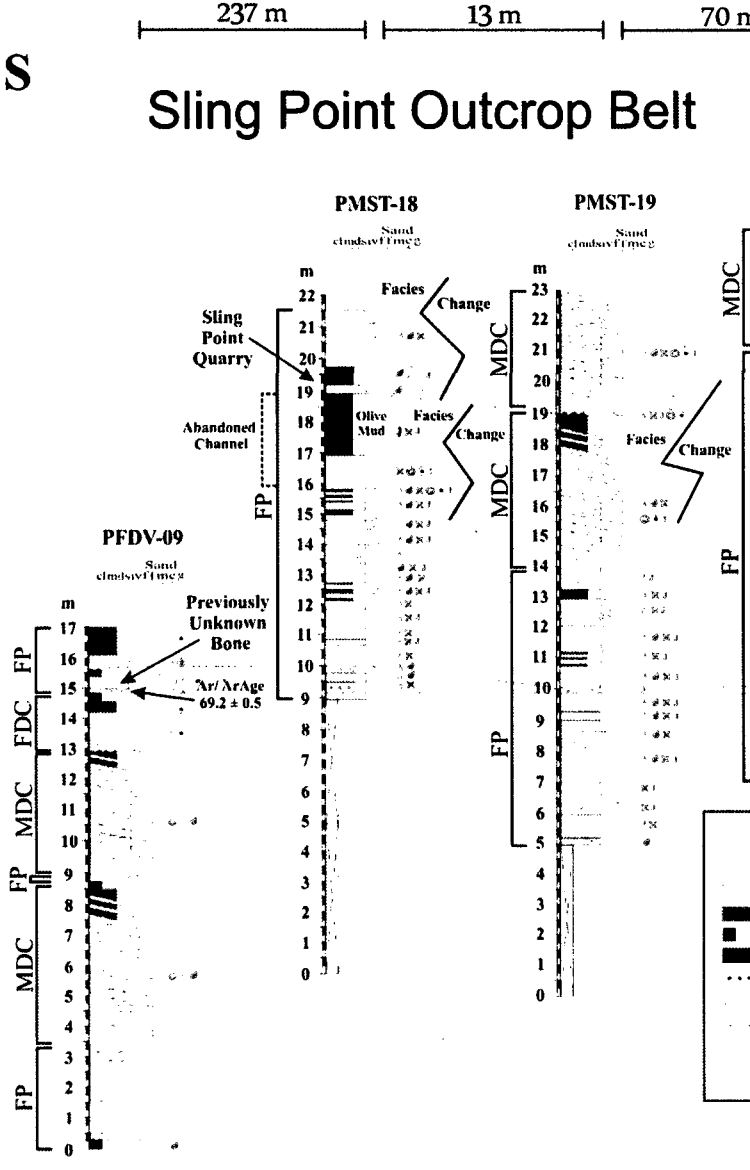
237 m
13 m
70 m
S
Sling Point Outcrop Belt
PMST-18
PMST-19
PFDV-09
Sand
clmdsiv f f mcg
m
Facies
Change
Sling
Point
Quarry
Abandoned
Channel
Olive
Mud
Facies
Change
Facies
Change
Previously
Unknown
Bone
Ar/ ArAge
69.2 ± 0.5
FP
FDC
MDC
FP
MDC
FP
MDC
MDC
FP
FP

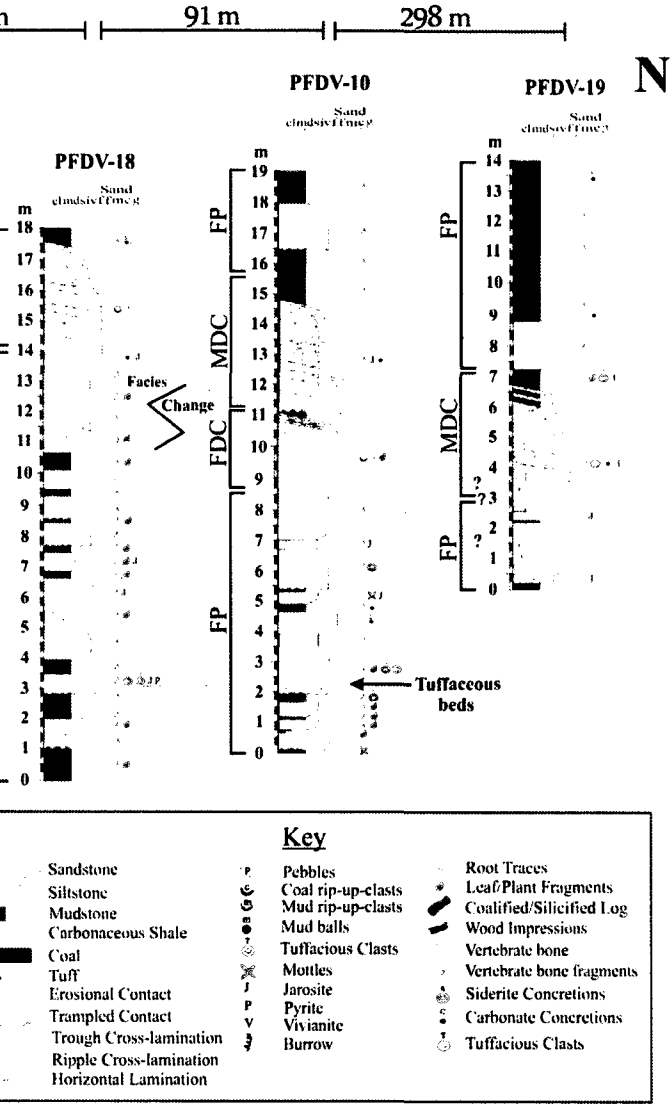
91 m
298 m
N
PFDV-18
PFDV-10
PFDV-19
Sand
Facies
Change
FP
MDC
FDC
Tuffaceous
beds
m
Key
Sandstone
Siltstone
Mudstone
Carbonaceous Shale
Coal
Tuff
Erosional Contact
Trampled Contact
Trough Cross-lamination
Ripple Cross-lamination
Horizontal Lamination
Pebbles
Coal rip-up-clasts
Mud rip-up-clasts
Mud balls
Tuffacious Clasts
Mottles
Jarosite
Pyrite
Vivianite
Burrow
Root Traces
Leaf/Plant Fragments
Coalified/Silicified Log
Wood Impressions
Vertebrate bone
Vertebrate bone fragments
Siderite Concretions
Carbonate Concretions
Tuffacious Clasts

Figure 4.5 (Following Page). Stratigraphic correlations for four measured sections at the Liscomb/Byers outcrop belt including lithology, contacts, sedimentary structures, flora, fauna, overall depositional environment, dinosaur bonebeds, and dinosaur quarries. MDC= Meandering distributary channel, FDC=Fixed distributary channel, FP=Floodplain sediments.

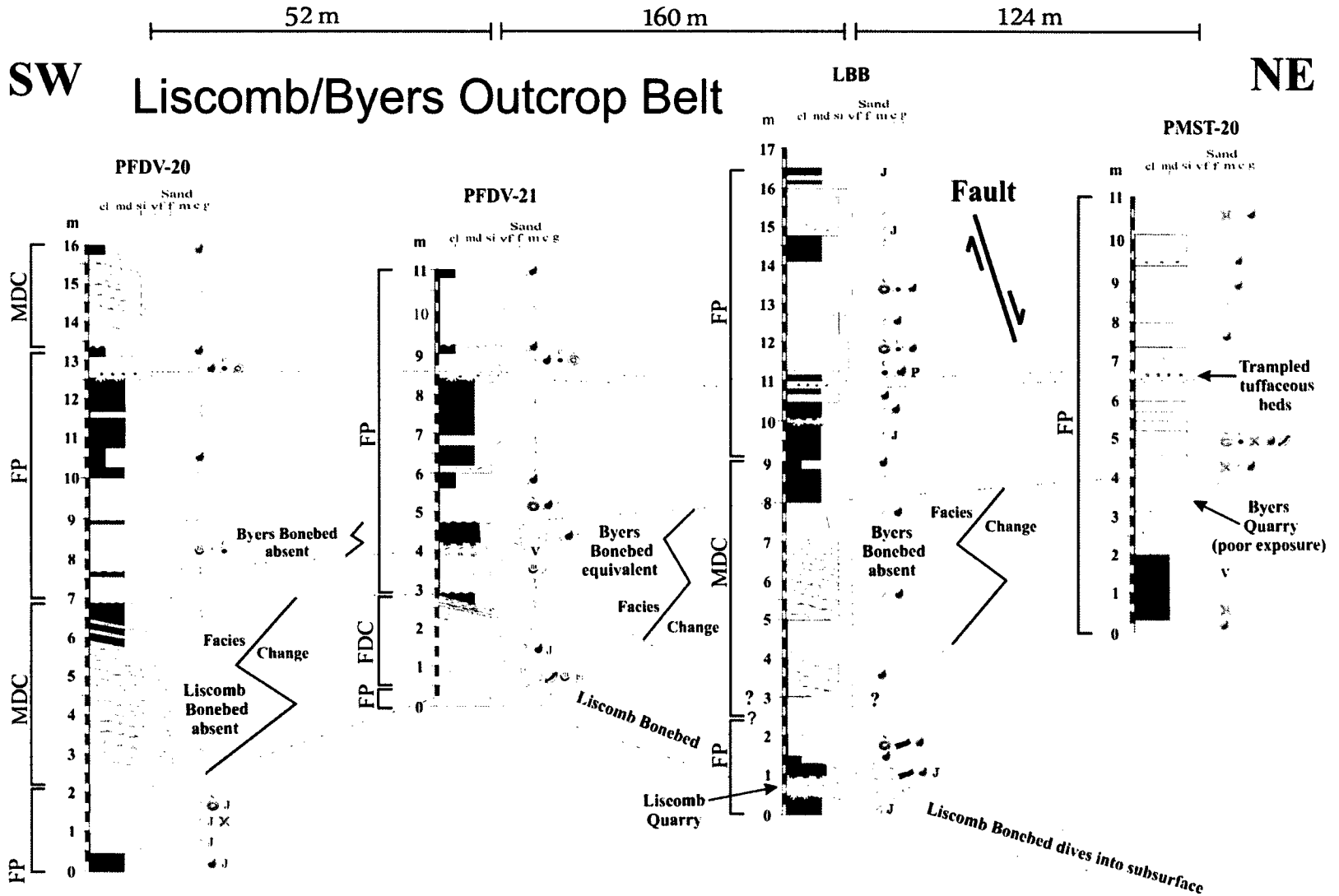
52 m
160 m
124 m
SW
Liscomb/Byers Outcrop Belt
NE
PFDV-20
PFDV-21
LBB
PMST-20
Sand
cl md si vf f m c g
m
MDC
FP
FDC
Byers Bonebed absent
Facies Change
Liscomb Bonebed absent
Byers Bonebed equivalent
Facies Change
Liscomb Bonebed
Liscomb Quarry
Fault
Byers Bonebed absent
Facies Change
Trampled tuffaceous beds
Byers Quarry (poor exposure)
Liscomb Bonebed dives into subsurface

SLING POINT OUTCROP BELT

Stratigraphy

The Sling Point outcrop belt (Fig. 4.4) is comprised of 15-30 m-high bluffs that extend laterally for 800 m before dipping below tundra cover. The top of the bluffs are erosionally truncated by the Pleistocene Gubik Formation (Black 1964) or the Holocene unconformity. Depositional environments include meandering and fixed distributary channels, lakes, ponds, swamps, paleosols, and ashfall deposits (Flaig et al. 2010). Trampled sediments (dinoturbation) are common (Flaig et al. 2010). Muddy IHS suggests tidal influence on sedimentation while abundant jarosite suggests marine influence on pore waters in sediments. Six measured stratigraphic sections were correlated using tuffs and basal erosion surfaces of laterally-extensive distributary channels as marker horizons (Fig. 4.4).

Bonebeds

Two concentrations of dinosaur bone (Fig. 4.4) are found in fine-grained floodplain sediments, outside of channel margins at the Sling Point quarry (~19-20 m in PMST-18) and at an additional, previously unidentified location (~15-15.5 m in PFDV-09).

Dinosaur bone at the Sling Point quarry (Fig. 4.6) is preserved within a 20 cm-thick, organic-rich, ripple cross-laminated siltstone that grades upward into a 60 cm-thick

Figure 4.6 (Following Page). Outcrop exposure of the Sling Point dinosaur bonebed showing the stratigraphic relationships between an olive mudstone filling an abandoned channel and a fining-upward depositional couplet including a bone-bearing siltstone and massive mudstone containing flow-parallel plant fragments. Hammer is 30 cm long.

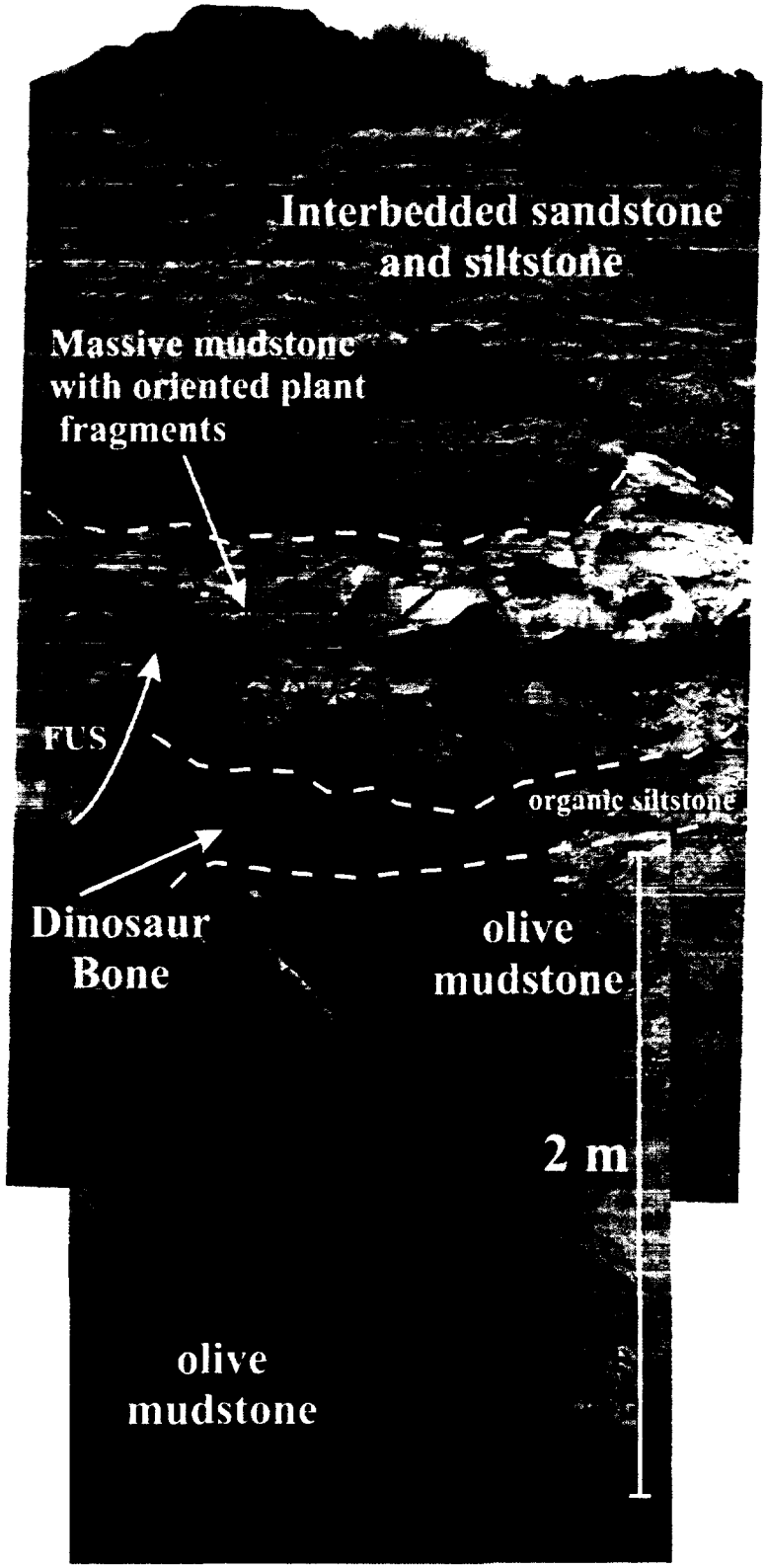
Interbedded sandstone and siltstone
Massive mudstone with oriented plant fragments
FUS
organic siltstone
Dinosaur Bone
olive mudstone
2 m
olive mudstone

Figure 4.8 (Following Page). Images showing facies of the Liscomb Bonebed including (A) contact between a dinosaur bone-bearing ripple cross-laminated organic siltstone and brown mudstone lacking dinosaur bone below, (B) massive mudstone with flow-parallel plant fragments encasing dinosaur bone, (C) close-up of dinosaur bone encased in massive mudstone with flow-parallel plant fragments, (D) massive mudstone with flow-parallel plant fragments, sand inclusion, and dinosaur bone, (E) photomicrograph of massive mudstone taken under polarized light, image shows sub-parallel alignment of plant fragments encased in a muddy matrix. Fieldbook is 20 cm long, hammer is 30 cm long.

massive mudstone containing flow-parallel oriented plant fragments and conifer needles(?) (Phillips 2003) (Fig. 4.4, (PMST-18 19.0-19.75m)). The bone-bearing siltstone and massive mudstone form a depositional couplet observed throughout the quarry. These two facies overlie a bone-free 2 m-thick olive mudstone that vertical and lateral facies relationships demonstrate to be a muddy abandoned channel fill (Figs. 4.4, 4.6). Well-sorted dinosaur bone is found immediately above a sharp basal contact between the organic-rich siltstone and the olive mudstone filling the muddy channel plug. The siltstone and massive-mudstone couplet is sharply overlain by a 2 m-thick succession of interbedded sandstone, siltstone, and mudstone interpreted as a levee or splay. The Sling Point bonebed extends laterally for tens of meters and is smaller in extent than either the Liscomb or Byers bonebed. Bone is absent in laterally equivalent strata to the north of the quarry due to a facies change to within-channel deposition in a distributary channel (Fig. 4.4). Bone-bearing facies are lost to the modern unconformity immediately to the south of the quarry.

An additional concentration of previously unknown dinosaur bone was discovered encased in organic-rich siltstone to the south of the Sling Point quarry in bluffs along the Colville River (Fig. 4.4). The siltstone contains abundant carbonaceous root traces, has a sharp basal contact with a rooted tuff, and fines-upward into carbonaceous shale. Stratigraphic relationships suggest that the bone is contained within a paleosol that formed on a distal crevasse splay (Flaig et al. 2010). $^{40}Ar/^{39}Ar$ analysis of tuff sample 07PFDVDK-09-14.9 from directly below the bonebed provided an integrated age of 68.9

± 0.4 Ma and a plateau age of 69.2 ± 0.5 Ma (Fig. 4.7), indicating an Early Maastrichtian age for the tuff.

LISCOMB/BYERS OUTCROP BELT

Stratigraphy

An extensive tundra-covered interval separates the Liscomb/Byers and Sling Point outcrop belts (Fig. 4.1) making direct stratigraphic correlation impossible. However, the north-to-northeast structural dip of bedding indicates that sediments of the Liscomb/Byers outcrop belt are probably stratigraphically higher and younger than those at the Sling Point outcrop belt.

The Liscomb/Byers outcrop belt (Fig. 4.5) is also comprised of 15-20 m high bluffs that extend laterally for 340 m and are erosionally truncated by the Gubik Formation. Depositional environments again include meandering and fixed distributary channels, lakes, ponds, swamps, paleosols, and ashfall deposits (Phillips 2003, Flaig et al. 2010). Some distributary channel lags contain quartz pebbles (up to 3 cm in diameter), reworked dinosaur bone, brackish-water clams (*Nucula* aff. *N. percrassa* Conrad, pers. comm. Robert Blodgett), and indeterminate gastropods. Muddy IHS, jarosite, pyrite, gypsum, and brackish-water invertebrates suggest tidal influence in channels and marine influence on pore waters in sediments. Trampled sediments (dinoturbation) are again common. Four measured stratigraphic sections were correlated using laterally-extensive

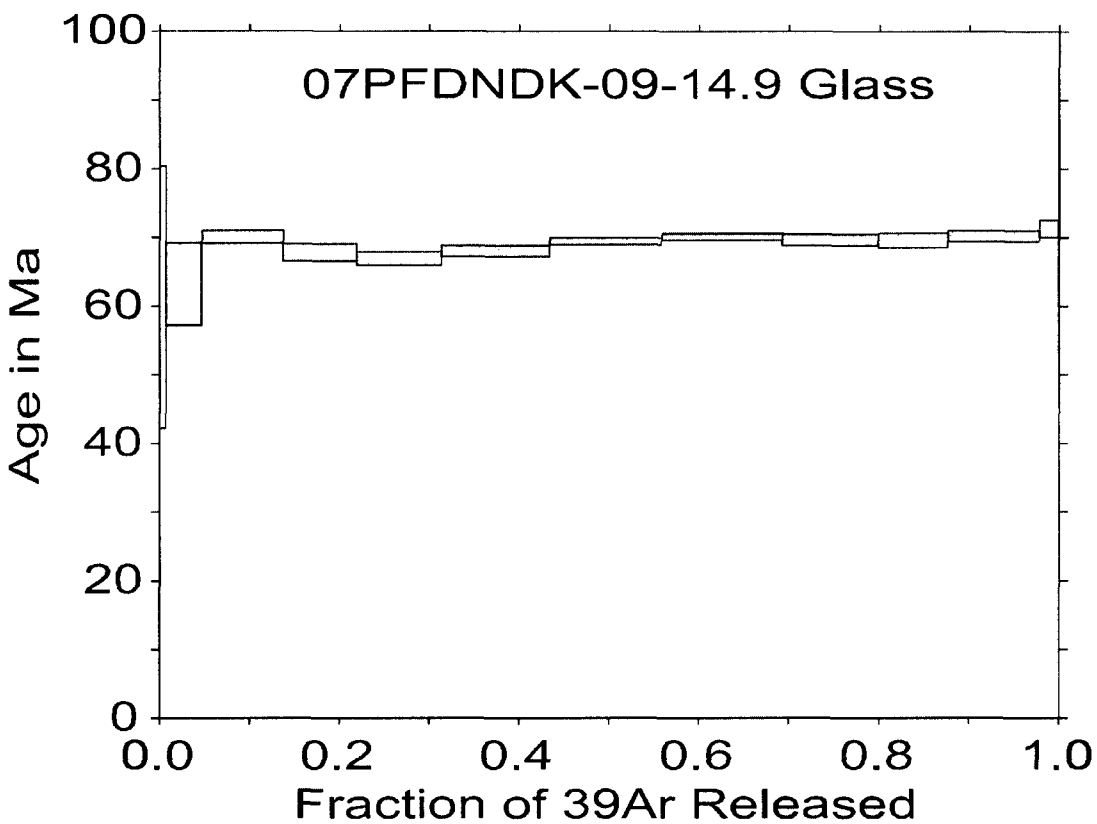

Figure 4.7. Argon-release spectra from incremental heating of tuff sample 07PFDVDK-09-14.9. Sample returned an integrated age of 68.9 ± 0.4 Ma and a plateau age of 69.2 ± 0.5 Ma. Uncertainties in age are indicated by the vertical width of bars.

tuffs, trampled beds, and high-density bone-accumulations as marker horizons (Fig. 4.5). A normal fault with small displacement is found in the northeast corner of the bluffs (Fig. 4.5).

Bonebeds

Although some channel lags include sparse reworked dinosaur bone, bonebeds are again found exclusively in fine-grained floodplain facies outside of channel margins. Bonebeds at the Liscomb/Byers outcrop belt extend laterally for hundreds of meters and typically pinch-out into organic-rich floodplain facies or are lost laterally to distributary channel facies (Fig. 4.5). Two separate horizons were chosen as representative examples of bonebed stratigraphy (0.5-1.5 m in LBB and 4.0-4.75 m in PFDV-21, Fig. 4.5).

Dinosaur bone at the Liscomb bonebed is preserved within a 50 cm-thick organic-rich, ripple cross-laminated siltstone that grades upward into a 20 cm-thick massive mudstone (Fig. 4.5 (LBB 0.5-1.25 m), 4.8A, 4.8B). Well-sorted dinosaur bone is found at the base of the siltstone above a sharp to irregular basal contact with a 50 cm-thick brown mudstone (Fig. 4.8A). The siltstone initially coarsens-upward, but ultimately fines-upward into the massive mudstone containing carbonized wood, rare dinosaur bone, convolute bedding and flow-parallel oriented plant fragments and conifer needles(?) (Phillips 2003) (Figs. 4.8B, 4.8C, 4.8D). The bone-bearing siltstone and massive mudstone again form a depositional couplet observed within the bonebed horizon. Microscopic examination of the couplet-capping mudstone reveals comminuted

Figure 4.8 (Following Page). Images showing facies of the Liscomb Bonebed including (A) contact between a dinosaur bone-bearing ripple cross-laminated organic siltstone and brown mudstone lacking dinosaur bone below, (B) massive mudstone with flow-parallel plant fragments encasing dinosaur bone, (C) close-up of dinosaur bone encased in massive mudstone with flow-parallel plant fragments, (D) massive mudstone with flow-parallel plant fragments, sand inclusion, and dinosaur bone, (E) photomicrograph of massive mudstone taken under polarized light, image shows sub-parallel alignment of plant fragments encased in a muddy matrix. Fieldbook is 20 cm long, hammer is 30 cm long.

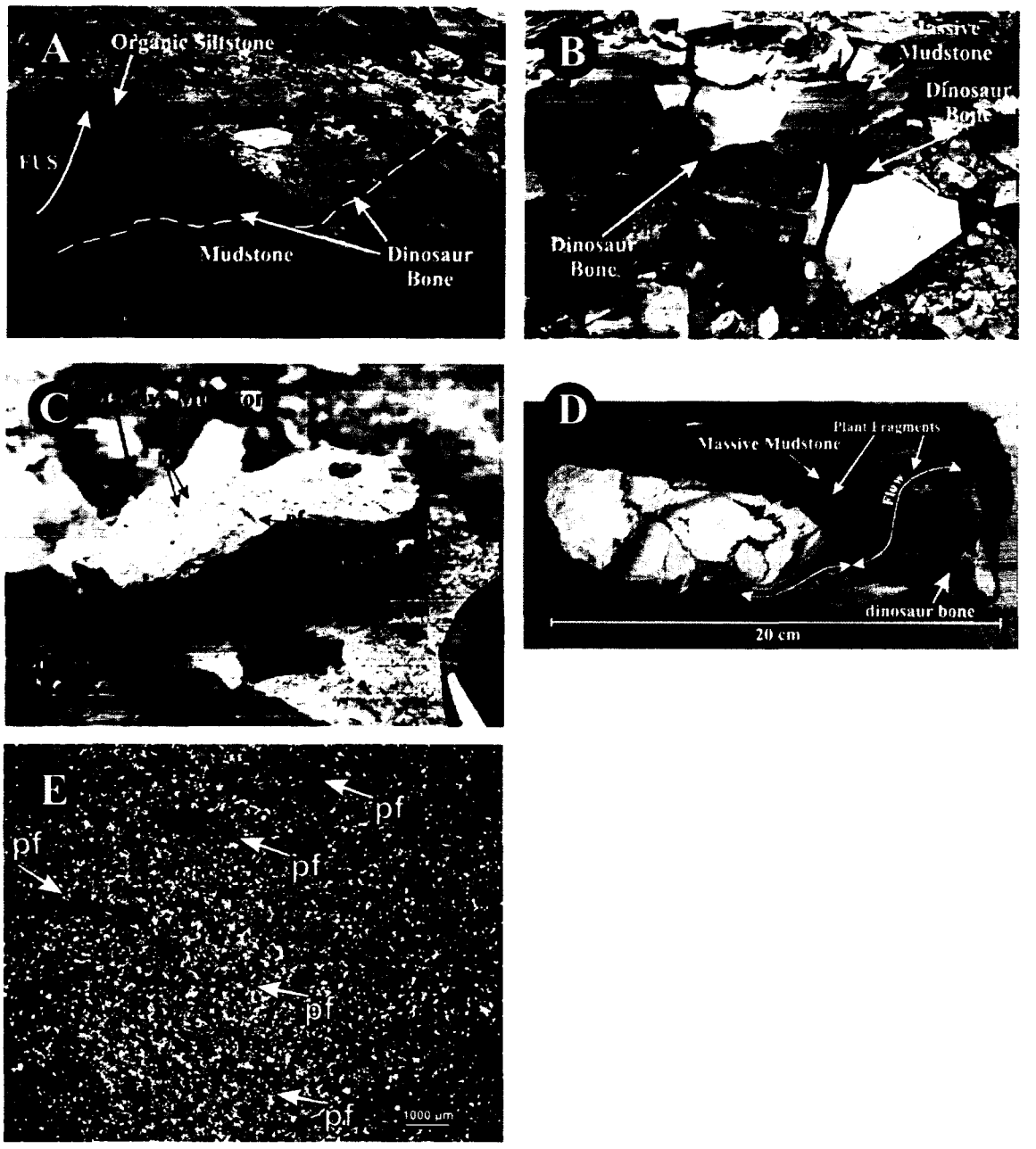
A
Organic Siltstone
FLS
Mudstone
Dinosaur Bone
B
Mudstone
Dinosaur Bone
Dinosaur Bone
C
D
Massive Mudstone
Plant Fragments
Flow
dinosaur bone
20 cm
E
pf
pf
pf
pf
pf
1000 um

carbonaceous plant fragments and rare bone fragments aligned sub-parallel to each other in a muddy matrix (Fig. 4.8E). The contact at the base of the mudstone may be irregular. In some laterally equivalent strata, the basal siltstone bed is absent and bone is instead encased directly within the massive mudstone (Figs. 4.8B, 4.8C, 4.8D). The mudstone is sharply overlain by 20 cm of carbonaceous shale.

The Byers bonebed is typically scree covered and at a location that is prone to bluff collapse and seasonal flooding. As a result, bonebeds are described in sediments that stratigraphic correlations indicate are laterally-equivalent to Byers bonebed sediments (Fig. 4.5 PFDV-21 4-4.75 m). Stratigraphic relationships also demonstrate that the Byers bonebed and Liscomb bonebed lie at two discreet horizons and are, therefore, interpreted as separate event beds (Fig. 4.9). Dinosaur bone in the Byers bonebed is preserved within a 25 cm-thick organic-rich, ripple cross-laminated siltstone that grades upward into 50 cm-thick massive mudstone overlying the siltstone (Fig. 4.10). The bluish-grey siltstone has a sharp to irregular basal contact with a very-fine sandstone and fines-upward into the massive mudstone containing carbonaceous root-traces, soft sediment deformation, dinosaur bone, and flow-parallel oriented plant fragments and conifer needles(?) (Phillips 2003). The bone-bearing siltstone and massive mudstone are consistently observed together in the bonebed horizon (Fig. 4.10). The basal contact of the massive mudstone may be irregular and the upper contact of the mudstone is truncated by the base of a 75 cm-thick splay sand.

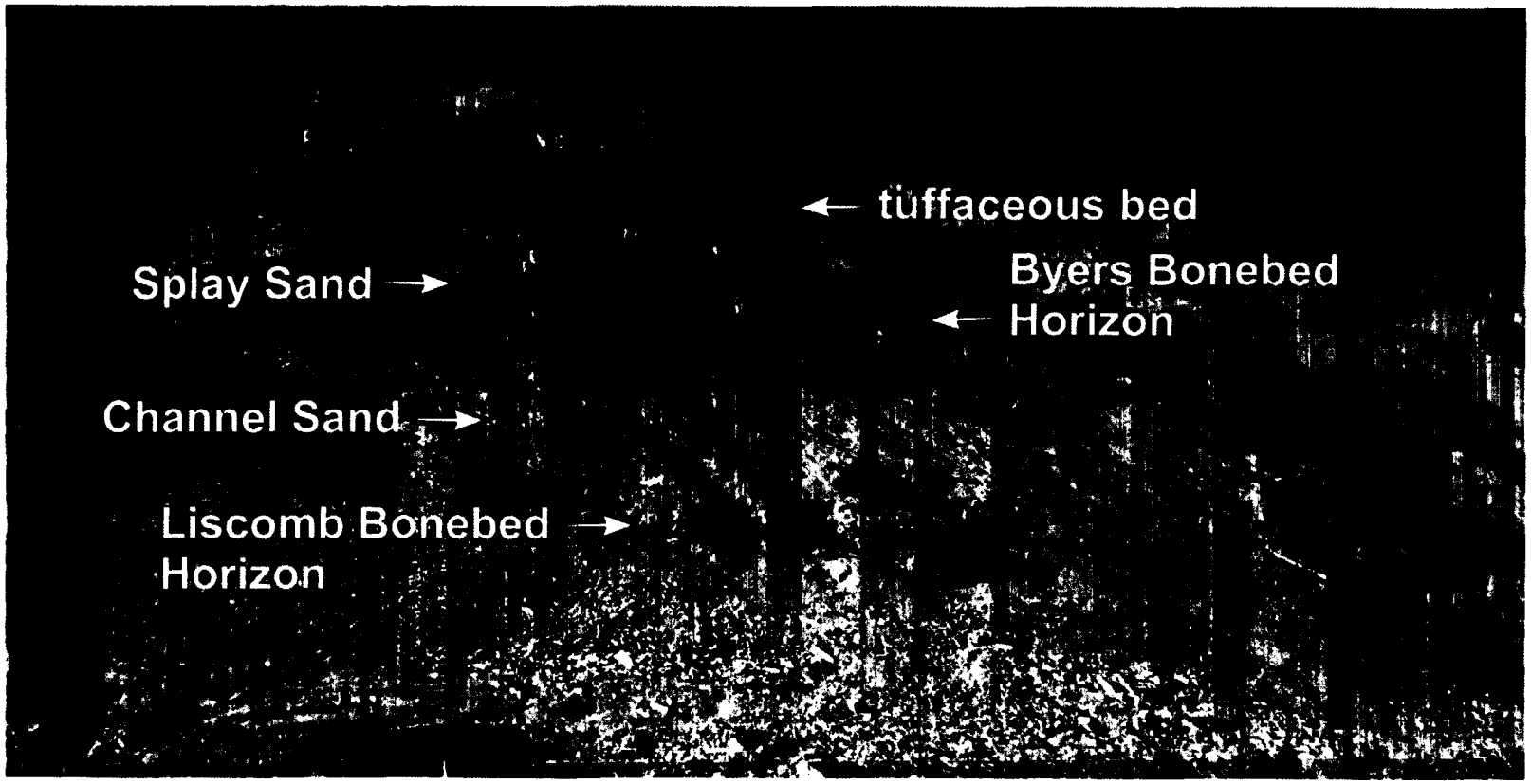

Figure 4.9. Outcrop exposure at the Liscomb/Byers outcrop belt. Image shows the distinctly separate Liscomb bonebed horizon And Byers bonebed horizon along with tuffaceous bed used for correlation of stratigraphy. Person for scale.

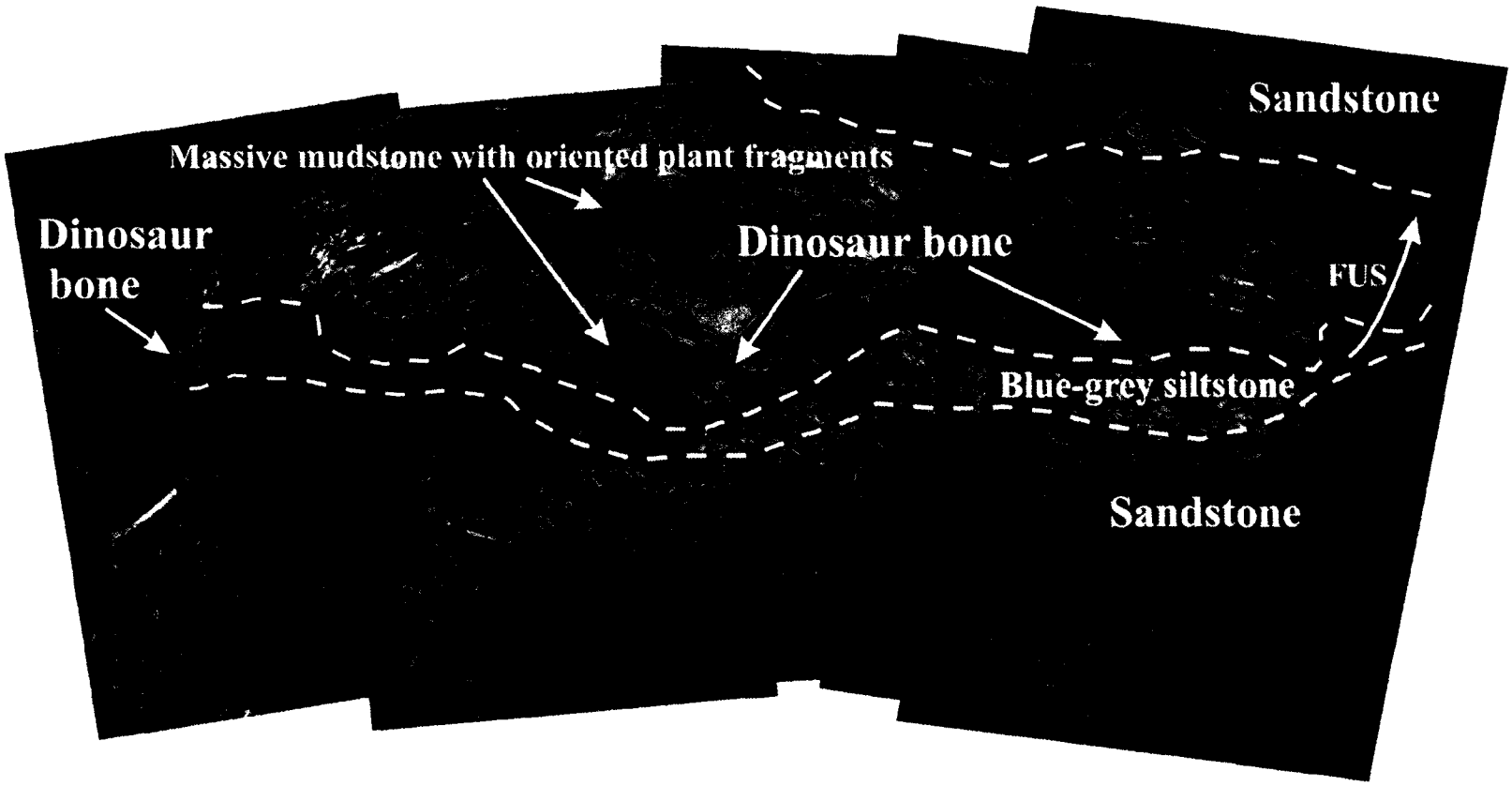

Figure 4.10. Outcrop exposure of the Byers bed horizon including fining-upward succession including blue-grey dinosaur bone-bearing siltstone and massive mudstone with flow-parallel plant fragments. Pocket knife is 9 cm long, hammer is 30 cm long.

DISCUSSION

Streamflow, Debris Flow & Hyperconcentrated Flow

In order to determine the depositional mechanism responsible for bonebed emplacement it is necessary to investigate facies (successions) expected for deposits of streamflow, debris flow, and hyperconcentrated flow. Although there are a continuum of physical processes at work between the three types of flow, and although a single bed may exhibit characteristics of more than one type of flow (Sohn et al. 1999, Pierson 2005, Hessel 2006), deposits of each flow-type are unique.

Streamflows are traction dominated turbulent flows that behave as Newtonian fluids with no internal strength to resist flow (Smith 1986, Benvenuti and Martini 2002, Pierson 2005). Streamflows transport fine-grained suspended sediments in small quantities relative to the total flow volume via turbulence, and these suspended sediments (usually < 4% by volume) have little overall effect on flow behavior (Smith 1986, Pierson 2005). Because streamflows are Newtonian fluids, grains are deposited individually during or after flow, typically resulting in well-sorted, well-stratified deposits with sedimentary structures that include current ripples, planar laminations, or trough cross-laminations (Sohn et al. 1999, Pierson 2005, Zaleha and Wiesemann 2005, Hessel 2006).

In contrast to streamflows, debris flows are highly concentrated flows composed of a mixture of sediment and water (Pierson 2005) and typically require steeper slopes to continue moving (Hampton 1975, Sohn et al. 1999, Hungr et al. 2001, Lorenzini and

Mazza 2004). Debris flows generally contain < 30% suspended fine-grained particles and > 50% coarser–grained material (Varnes 1978, Hungr et al. 2001, Lorenzini and Mazza 2004). Debris flows are highly viscous, exhibit non-Newtonian plastic behavior, and can fully suspend large particles (e.g. cobbles or boulders) even after the flow stops (Pierson 2005). In contrast to streamflow deposits, debris flow deposits are emplaced *en masse,* are poorly sorted, contain larger clasts encased in a finer-grained matrix, and rarely exhibit sedimentary structures typical of streamflows (Pierson 1981, Smith 1986, Major and Pierson 1992, Sohn et al. 1999, Hungr et al. 2001, Lorenzini and Mazza 2004). In addition, because debris flows are non-Newtonian, non-turbulent, shearing laminar flows, elongate clasts suspended in the matrix may be preferentially oriented in the direction of flow (Elston and Smith 1970, Smith 1986, Karátson et al. 2002, Lorenzini and Mazza 2004).

Hyperconcentrated flows are turbid, two-phase flows intermediate in suspended sediment concentration between streamflows and debris flows (Sohn et al. 1999, Pierson 2005). The addition of even a small amount of clay (e.g. 1-4 weight %) into a streamflow permits electrostatic forces acting between clay particles to increase the viscosity and transform a streamflow into a non-Newtonian hyperconcentrated flow with measurable yield strength (Hampton 1975, Pierson and Costa 1987, O'Brien and Julien 1988, Costa 1988, Lorenzini and Mazza 2004, Pierson 2005, Zaleha and Wiesemann 2005, Hessel 2006). Because properties such as suspended sediment concentration, viscosity, and rheology cannot be measured in ancient sediments, the existence of hyperconcentrated flows must be inferred from their deposits (Sohn et al. 1999).

Hyperconcentrated flows differ from streamflows and debris flows because they are two-phase flows (Smith 1986, Sohn et al. 1999, Karátson et al. 2002, Lorenzini and Mazza 2004, Pierson 2005). The transporting fluid and solid particles behave independently (Sohn et al. 1999, Hessel 2006). The largest particles, too large to be suspended in the flow, are transported as bedload (Pierson 2005, Zaleha and Wiesemann 2005). However, unlike a streamflow, clay-flocculation allows some coarser-grained sediment to remain in suspension during hyperconcentrated flow, and unlike a debris flow these larger particles eventually settle out of suspension when the flow stops, and some level of stratification and sorting is achieved (Pierson 2005). Coarser-grained suspended sediments are deposited first, above bedload, while finer-grained sediments and rare coarse particles remain in suspension to be deposited as a layer of finer-grained muddy material at the top of the deposit (Sohn et al. 1999, Pierson 2005, Zaleha and Wiesemann 2005). Ultimately, deposits of hyperconcentrated flows are better sorted and stratified than the suspensions from which they settle out of (Pierson 2005) and can be recognized by their bipartite division of flow (Sohn et al. 1999, Zaleha and Wiesemann 2005). This bipartite facies succession typically includes (1) a coarser-grained basal layer composed of bedload and coarser-grained suspended load below normally-graded beds, and (2) a dilute, finer-grained upper layer (Smith 1986, Sohn et al. 1999, Cronin et al. 2000, Pierson 2005, Zaleha and Wiesemann 2005).

Depositional Mechanism for Sling Point, Liscomb, and Byers Bonebeds

Alluvium encasing the Sling Point, Liscomb, and Byers bonebeds exhibits characteristics of all three types of flow: streamflow, debris flow, and hyperconcentrated flow. In each bone-bearing succession a coarser-grained basal layer containing well-sorted bone encased in ripple cross-laminated siltstone underlies a fining-upward succession (Fig. 4.4 PMST-18 (19.0-19.75 m), Fig. 4.5 PFDV-21(4.0-5.0 m), Fig. 4.5 LBB (0.5-1.5 m), Figs. 4.6, 4.8A, 4.10), a facies succession expected for waning streamflow. Massive mudstone lacking sedimentary structures but containing flow-parallel oriented plant fragments and outsized bone "frozen" in a muddy matrix, similar to debris flow deposits, caps these bone-bearing successions (Figs. 4.6, 4.8B, 4.8C, 4.8D, 4.8E, 4.10). If these deposits are, however, interpreted as a single event-bed rather than two separate events, then the facies succession forms a depositional couplet similar to that expected for two-phase hyperconcentrated flows (Figs. 4.6, 4.10).

Observations suggest that the Sling Point, Liscomb, and Byers bonebeds are neither exclusively the deposits of streamflows nor solely those of debris flows, but are instead two-phase hyperconcentrated overbank flows. Evidence for this includes: (1) all bonebeds contain fining-upward successions, similar to streamflows that include a basal bone-bearing siltstone and uppermost massive mudstone, suggesting a genetic relationship between the two facies (Fig. 4.4 PMST-18 (19.0-19.75 m), Fig. 4.5 PFDV-21(4.0-5.0 m), Fig. 4.5 LBB (0.5-1.5 m), and Figs. 4.6, 4.8A, 4.10); (2) massive mudstones encase bone at locations where the basal siltstone is absent, indicating that these mudstones are an integral part of bonebed deposition (Fig 4.8B, 4.8C, 4.8D); (3)

massive mudstones with flow-parallel oriented elongate clasts "frozen" in a muddy matrix (Figs. 4.6, 4.8C, 4.8D, 4.8E, 4.10) are similar to debris flow deposits (Elston and Smith 1970, Smith 1986, Karátson et al. 2002, Lorenzini and Mazza 2004) suggesting that bonebeds are not simple streamflow deposits; (4) bonebeds are laterally and areally extensive (Figs. 4.4, 4.5), appearing similar over hundreds of meters (Fiorillo et al. 2010b) similar to deposits of hyperconcentrated flow and unlike streamflow deposits that can exhibit abrupt changes in grain size and stratification over even short distances (Pierson 2005); (5) bonebeds consistently exhibit sharp basal contacts and overlie organic floodplain facies (Figs. 4.4, 4.5, 4.6, 4.8A, 4.10), indicating deposition as unconfined flows on floodplains, outside of channel margins; and (6) the regional paleoenvironment, a low-gradient distal coastal plain (Phillips 2003, Fiorillo et al. 2010b, Flaig et al. 2010), precludes deposition of bonebeds by classic debris flows that require steep topography to flow (Hampton 1975, Sohn et al. 1999, Hungr et al. 2001, Lorenzini and Mazza 2004, Zaleha and Wiesemann 2005).

Steep slopes are not required to maintain hyperconcentrated flows and they can travel for long distances on low gradients (Jiongxin 1993, Hessel 2006). In fact, ancient hyperconcentrated flows are documented on a low relief alluvial-delta plain hundreds of miles from an orogenic belt (Zaleha and Wiesemann 2005), an environment similar to the low-lying, low-gradient coastal plain of the Prince Creek Fm. (Phillips 2003, Fiorillo et al. 2010b, Flaig et al. 2010). Hyperconcentrated flows are observed in modern rivers with banks composed of easily erodible material (Jiongxyn 1999, Pierson 2005, Hessel 2006). Abundant tephra on floodplains can accelerate the transformation of a

streamflow into a hyperconcentrated flow (Pierson 2005). Paleoenvironmental reconstructions for the Prince Creek Fm. include high suspended-load rivers with muddy point bars and clay- and ash-rich floodplains (Phillips 2003, Flaig et al. 2010), an ideal environment for the generation of hyperconcentrated flows.

At high sediment concentrations rigid plugs can form at the top of hyperconcentrated flows as the flows slow and dewater (Pierson 2005, Hessel 2006). If clay-concentrations are high and the flow is viscous, settling of particles stops when the flow stops (Hessel 2006). The massive mudstones with flow parallel oriented plant fragments "floating" in a muddy matrix that we observe (Figs. 4.6, 4.8B, 4.8C, 4.8D, 4.8E, 4.10) may be rigid plugs formed at the top of hyperconcentrated flows. Reduced settling velocities in sheared viscous fluid may be responsible for the "frozen" appearance of the massive mudstone with plant fragments (Smith 1986, Karátson et al. 2002, Lorenzini and Mazza 2004). Although convolute bedding in these massive mudstones has typically been attributed to trampling by dinosaurs (Flaig et al. 2010); soft sediment deformation features are also associated with dewatering in hyperconcentrated flows (Zaleha and Wiesemann 2005). Dewatering may be responsible for some of the deformation features in these mudstones..

Dinosaur bone in all bonebeds is encased in a hydraulically incompatible matrix of siltstone and mudstone (Fiorillo et al. 2010b). For example, the diameter of hydraulically equivalent quartz grains for bones larger than 5 cm long is 21 mm (*sensu* Behrensmeyer 1975, Korth 1979) indicating that bones should be found in pebble

conglomerate if they were in equilibrium with flow velocities and pebbles were present (Wentworth 1922). Semi-articulated to associated dinosaur bones are instead found encased in silt and mud suggesting that these dinosaurs lived close to where they were buried (Fiorillo et al. 2010b) and that carcasses or parts of carcasses did not travel far. In addition, bones are not well rounded suggesting short distance transport (Fiorillo et al. 2010b) or transport in suspension. Bones also show little evidence of weathering, predation, or trampling, suggesting rapid burial (Fiorillo et al. 2010b). Copious evidence suggests that herds of juvenile to sub-adult dinosaurs were engulfed by overbank floods close to distributary channels and were either buried immediately or transported in suspension over relatively short distances.

Our favored interpretation for the emplacement of bonebeds on this Cretaceous coastal plain is by muddy hyperconcentrated flows. Hyperconcentrated flows such as these are most common where fine-grained sediment is repeatedly incorporated into a fluvial system (Smith 1986) often via extreme discharge events fed by intense rainfall or snowmelt (Smith 1986, Julien and O'Brien 1997, Pierson 2005). Regular floods generated by seasonal snowmelt in the nearby Brooks Range generated hyperconcentrated overbank mudflows that killed and entombed scores of juvenile dinosaurs occupying floodplains, resulting in the formation of these extraordinary, world-class bonebeds. We further suggest that a killing mechanism such as this is likely to be more prevalent in high-latitude settings where regular seasonal melting of snow and ice would have generated large floods necessary for the development of hyperconcentrated flows.

CONCLUSIONS

Dinosaurs of the Prince Creek Fm. are found in several world-class, high-density bonebeds encased in muddy alluvium. The bulk of dinosaur bone is found outside of channels in laterally extensive, fine-grained overbank deposits overlying floodplain facies. $^{40}Ar/^{39}Ar$ analysis of a tuff above a bonebed in the Sling Point outcrop belt returned an age of 69.2 ± 0.5 Ma. The Sling Point, Liscomb, and Byers bonebeds are overwhelmingly dominated by partially-articulated to associated juvenile dinosaurs with bones in hydraulic *dis*equilibrium with the clay-rich matrix. Bones exhibit little evidence of rounding, weathering, predation, or trampling suggesting short-distance transport and rapid burial.

To the best of our knowledge bonebeds attributed to deposition by hyperconcentrated overbank flows are previously unrecognized. In all three bonebeds alluvium exhibits a bipartite division of flow and massive mudstone facies that suggest deposition by fine-grained hyperconcentrated flows. Ripple cross-laminated siltstone consistently fines-upward into a distinctive mudstone lacking sedimentary structures but containing rare dinosaur bone and flow-parallel oriented plant fragments that appear to "float" in a matrix of mud. Fining-upward successions reminiscent of streamflow underlie sheared mudstone facies suggestive of debris flow. Together these facies form a depositional couplet in a single event-bed that exhibits a facies succession expected for two-phase hyperconcentrated flow.

Exceptional discharge events generated by seasonal snowmelt from the ancestral Brooks Range in this ancient high-latitude environment, likely entrained abundant clay and ash, increased suspended sediment concentrations and generated hyperconcentrated flows, killing and burying scores of juvenile dinosaurs close to where they lived on this high-latitude Alaskan coastal plain.

ACKNOWLEDGMENTS

This project was funded through the National Science Foundation Office of Polar Programs grants #OPP-425636 to Paul McCarthy and # OPP-424594 Anthony Fiorillo. Additional funding was provided by the Geist Fund at the University of Alaska Museum of the North, the Alaska Geologic Society, the University of Alaska-Fairbanks Graduate School Fellowship Program, the Geological Society of America, the Evolving Earth Foundation, and BP America. Logistical support was provided by the Barrow Arctic Science consortium (BASC), CH2M Hill (formerly Veco Polar Resources), Wrights Air, Air Logistics, Alaska Air Taxi, Evergreen Helicopters, and the support staff at Umiat, Alaska. The authors graciously thank Dolores van der Kolk, Thomas Adams, David Norton, Roland Gangloff, Douglas Hissom, Susan Tomsich, and Jason Addison for diligent assistance in the field. In addition we thank Paul Layer, Jeffrey Benowitz, David LePain, Paul Decker, Marwan Wartes, David Houseknecht, and Charles "Gil" Mull for discussions regarding $^{40}Ar/^{39}Ar$ dating techniques, the evolution of the Colville Basin, and regional Cretaceous stratigraphy. This manuscript benefitted greatly from constructive reviews by _____ and _____.

REFERENCES

Alvarez, W., 1986, Toward a theory of impact crisis: EOS Transactions, American Geophysical Union, v. 67, p. 649, 653-658

Bandyophadhyay, S., RoyChowdhury, T.K., and Sengupta, D.P., 2002, Taphonomy of some Gondwana vertebrate assemblages of India: Sedimentary Geology, v. 147, p. 219-245.

Behrensmeyer, A.K., 1975, The taphonomy and paleoecology of the Plio-Pleistocene vertebrate assemblages east of Lake Rudolf, Kenya: Bulletin of the Museum of Comparative Zoology, v. 146, p. 474–578.

Benvenuti, M., and Martini, I.P., 2002, Analysis of terrestrial hyperconcentrated flows and their deposits, *in* Martini, I.P., Baker, V.R., and Garzon, G., eds., Flood and Megaflood Processes and Deposits: Recent and Ancient Examples: International Association of Sedimentologists Special Publication, v. 32, p. 167–193.

Besse, J., and Courtillot, V., 1991, Revised and synthetic apparent polar wander paths of The African, Eurasian, North American and Indian plates, and true polar wander since 200 Ma: Journal of Geophysical Research, v. 96, p. 4029-4050.

Black, R.F., 1964, Gubik Formation of Quaternary age in northern Alaska: US Geological Survey Professional Paper 302-C, p. 59–91.

Brandlen, E., 2008, Paleoenvironmental reconstruction of the Late Cretaceous (Maastrichtian) Prince Creek Formation, near the Kikak-Tegoseak dinosaur quarry, North Slope, Alaska: Unpublished Master's Thesis, University of Alaska-Fairbanks, Fairbanks, Alaska, 225 p.

Britt, B.B., Eberth, D.A., Scheetz, R.D., Greenhalgh, B.W., and Stadtman, K.L., 2009,Taphonomy of debris-flow hosted dinosaur bonebeds at Dalton Wells, Utah (Lower Cretaceous, Cedar Mountain Formation, USA): Palaeogeography, Palaeoclimatology, Palaeoecology, v. 280, p. 1-22.

Brouwers, E.M., Clemens, W.A., Spicer, R.A., Ager, T.A., Carter, L.D., and Sliter, W.V., 1987, Dinosaurs on the North Slope, Alaska: High latitude, latest Cretaceous environments: Science, v. 25, p. 1608-1610.

Brouwers, E.M., and de Deckker, P., 1993, Late Maastrichtian and Danian ostracod faunas from northern Alaska: Reconstructions of environment and paleogeography: Palios, v. 8, p. 140-154.

Clemens, W.A., 1994, Continental vertebrates from the Late Cretaceous of the North Slope, Alaska, *in* Thurston, D.K., Fujita, K., eds., 1992 proceedings International Conference on Arctic Margins, Outer Continental Shelf Study: Mineral Management Service 94-0040, p. 395–398.

Clemens, W.A., and Nelms, L.G., 1993, Paleoecological implications of Alaskan terrestrial vertebrate fauna in latest Cretaceous time at high paleolatitudes: Geology, v. 21, p. 503–506.

Cole, F., Bird, K.J., Toro, J., Roure, F., O'Sullivan, P.B., Pawlewicz, M., and Howell, D.G., 1997, An integrated model for the tectonic development of the frontal Brooks Range and Colville Basin 250 km west of the Trans-Alaska Crustal Transect: Journal of Geophysical Research, v. 102, No. B9, p. 20,685–20,708.

Conrad, J.E., McKee, E.H. and Turrin, B.D., 1990, Age of tephra beds at the Ocean Point Dinosaur Locality, North Slope, Alaska, based on K-Ar and $^{40}Ar/^{39}Ar$ Analyses: United States Geological Survey Bulletin 1990-C, p. 1–12.

Costa, J. E., 1988, Rheology, geomorphic and sedimentologic differentiation of water floods, hyperconcentrated flows and debris flows, *in* Baker, V.R., Kockel, R.C., Patton, P.C. eds., Flood Geomorphology: John Wiley and Sons, Inc., New York, p. 113–122.

Cronin, S.J., LeCointre, J.A., Palmer, A.S., and Neall, V.E., 2000, Transformation, internal stratification and depositional processes within a channelized, multi-peaked lahar flow: New Zealand Journal of Geology and Geophysics, v. 43, p. 117-128.

Currie, P.J. 1989, Long-distance dinosaurs: Natural History, p. 59-65.

Currie, P.J., Langston, W., and Tanke, D.H. 2008. A new species of Pachyrhinosaurus (Dinosauria, Ceratopsidae) from the Upper Cretaceous of Alberta, Canada, *in* Currie, P.J., Langston, W., and Tanke, D.H. 2008, A New Horned Dinosaur from an Upper Cretaceous Bone Bed in Alberta: NRC Research Press, Ottawa, Ontario, Canada p. 1-108.

Decker, P. L., 2007, Brookian Sequence stratigraphic correlations, Umiat Field to Milne Point Field, west-central North Slope, Alaska: Preliminary Interpretive Report 2007-2, Alaska Department of Natural Resources, Fairbanks, Alaska, 21 p., 1 map.

Decker, P.L., LePain, D.L., Wartes, M.A., Gillis, R.J., Mongrain, J.R., Kirkham, R.A., and Schellenbaum, D.P., (in press), Sedimentology, stratigraphy, and subsurface expression of Upper Cretaceous strata in the Sagavanirktok River area, east central North Slope, Alaska, *in* Wartes, M.W., and Decker, P.L., eds., Preliminary results of recent geologic field investigations in the Brooks Range foothills and North Slope, Alaska: Alaska Division of Geologic & Geophysical Surveys Preliminary Interpretive Report 2009-1C, 3 sheets.

Deconto, R.M., Brady, E.C., Bergengren, J., and Hay, W.W., 2000, Late Cretaceous climate, vegetation, and ocean interactions, *in* Huber, B.T., MacLeod, K.G., and Wing, S.L., eds. 2000, Warm Climates in Earth History: Cambridge University Press, Cambridge, UK, p. 275-296.

Eberth, D.A., Britt, B.B., Scheetz, R., Stadtman, K.L., Brinkman, D.B., 2006, Dalton Wells: geology and significance of debris-flow-hosted dinosaur bonebeds in the Cedar Mountain Formation (Lower Cretaceous) of eastern Utah, USA. Palaeogeography, Palaeoclimatology, Palaeoecology v. 236, p. 217–245.

Eberth, D.A., Rogers, R.R., and Fiorillo, A.R., 2007, A practical approach to the study of bonebeds, *in* Rogers, R. R., Eberth, D. A., and Fiorillo, A. R. eds., Bonebeds, Genesis, Analysis, and Paleobiological Significance: The University of Chicago Press, Chicago, IL, p. 265-331.

Elston, W. E., and Smith, E. I., 1970, Determination of flow direction of rhyolitic ash-flow tuffs from fluid textures: Geological Society of America Bulletin, v. 81, p. 3393-3406.

Fastovsky, D.E., Clark, J.M., Strater, N.H., Montellano, M.R., Hernandez, R., and Hopson, J.A., 1995, Depositional environments of a middle Jurassic terrestrial vertebrate assemblage, Huizachal Canyon, Mexico: Journal of Vertebrate Paleontology, v. 15, No. 3, p. 561-575.

Fiorillo, A.R., 1991, Taphonomy and depositional setting of Careless Creek Quarry (Judith River Formation), Wheatland County, Montana, U.S.A.: Palaeogeography, Palaeoclimatology, Palaeoecology, v. 81, p. 281–311.

Fiorillo, A.R., 2004, The dinosaurs of arctic Alaska: Scientific American, v. 291, p. 84-91.

Fiorillo, A.R. 2008a, Cretaceous dinosaurs of Alaska: Implications for the origins of Beringia, *in* Blodgett, R.B. and Stanley, G., eds., The Terrane Puzzle: new perspectives on paleontology and stratigraphy from the North American Cordillera: Geological Society of America Special Paper, v. 442, p. 313-326.

Fiorillo, A. R. 2008b, On the occurrence of exceptionally large teeth of Troodon (Dinosauria: Saurischia) from the Late Cretaceous of northern Alaska. Palaios, v. 23, p. 322–328.

Fiorillo, A.R., and Gangloff, R.A, 2000, Theropod teeth from the Prince Creek Formation (Cretaceous) of northern Alaska, with speculations on arctic dinosaur paleoecology: Journal of Vertebrate Paleontology, v. 20, p 675–682.

Fiorillo, A.R., and Gangloff, R.A., 2001, The caribou migration model for Arctic hadrosaurs (Ornithischia: Dinosauria): a reassessment: Historical Biology, v. 15, p. 323-334.

Fiorillo, A.R., Tykoski, R.S., Currie, P.J., McCarthy, P.J., and Flaig, P. P., 2009, Description of two Troodon partial braincases from the Prince Creek Formation (Upper Cretaceous), North Slope, Alaska: Journal of Vertebrate Paleontology, v. 29, No. 1, p. 178-187.

Fiorillo, A.R., McCarthy, P.J., Flaig, P.P., Brandlen, E., Norton, D., Jacobs, L., Zippi, P., and Gangloff, R.A., 2010a, Paleontology and paleoenvironmental interpretation of the Kikak-Tegoseak dinosaur quarry, (Prince Creek Formation: Late Cretaceous), northern Alaska: A multi-disciplinary study of an ancient high-latitude, ceratopsian dinosaur bonebed, *in* Ryan, M.J., Chinner-Algeier, B.J., and Eberth, D.A., eds., New Perspectives on Horned Dinosaurs: The Royall Tyrell Museum Ceratopsian Symposium: Indiana University Press, Bloomington, IN, p. 456-477.

Fiorillo, A.R., McCarthy, P.J., and Flaig, P.P., 2010b, Taphonomic and Sedimentologic Interpretations of the Dinosaur-Bearing Upper Cretaceous Strata of the Prince Creek Formation, Northern Alaska: Insights from an Ancient High-Latitude Terrestrial Ecosystem: Palaeogeography, Palaeoclimatology, Palaeoecology, doi:10.1016/j.palaeo.2010.02.029

Fischer, A.G., 1981, Climatic oscillations in the biosphere, *in* Nitecki, M.H., ed., Biotic Crisis in Ecological and Evolutionary Time: New York, NY, Academic Press, p. 103-132.

Flaig, P.P., McCarthy, P.J., and Fiorillo, A.R., 2010, A tidally-influenced coastal plain: The Prince Creek Formation, North Slope, Alaska: SEPM Special Publication, From River to Rock Record: The Preservation of Fluvial Sediments and their Subsequent Interpretation

Flores, R.M., Stricker, G.D., Decker, P.L., and Myers, M.D., 2007a, Sentinel Hill Core Test 1:Facies descriptions and stratigraphic reinterpretations of the Prince Creek and Schrader Bluff Formations, North Slope, Alaska: United States Geological Survey Professional Paper 1747, 31 p.

Flores, R.M., Myers, M.D., Houseknecht, D.W., Stricker, G.D., Brizzolara, D.W., Ryherd, T.J., and Takahashi, K.I., 2007b, Stratigraphy and facies of Cretaceous Schrader Bluff and Prince Creek Formations in Colville River Bluffs, North Slope, Alaska: United States, Geological Survey Professional Paper 1748, 52 p.

Frederiksen, N.O., Ager, T.A., and Edwards, L.E., 1986, Comment on "Early Tertiary marine fossils from northern Alaska: Implications for Arctic Ocean paleogeography and faunal evolution": Geology, v. 14, p. 802-803.

Frederiksen, N.O., Ager, T.A., and Edwards, L.E., 1988, Palynology of Maastrichtian and Paleocene rocks, lower Colville River region, North Slope, Alaska: Canadian Journal of Earth Sciences, v. 25, p. 512-527.

Frederiksen, N.O, 1991, Pollen zonation and correlation of Maastrichtian marine beds and associated strata, Ocean Point dinosaur locality, North Slope, Alaska: United States Geological Survey Bulletin 1990-E, 24 p.

Frederiksen, N.O., and McIntyre, D.J., 2000, Palynomorph biostratigraphy of mid(?) Campanian to upper Maastrichtian strata along the Colville River, North Slope of Alaska: United States Geological Survey Open-File Report 00-493, 36 p.

Frederiksen, N.O., McIntyre, D.J., and Sheehan, T.P., 2002, Palynological dating of some Upper Cretaceous to Eocene outcrop and well samples from the region extending from the easternmost part of NPRA in Alaska to the western part of ANWR, North Slope of Alaska: U.S. Geological Survey Open-File Report 02-405, 37 p.

Gallagher, S.J., Wagstaff, B.E., Baird, J.G., Wallace, M.W., and Li, C.L., 2008, Southern high latitude climate variability in the Late Cretaceous greenhouse world: Global and Planetary Change, v. 60, p. 351-364.

Gangloff, R.A., Fiorillo, A.R., and Norton, D.W., 2005, the first Pachycephalosaurine (Dinosauria) from the paleo-arctic of Alaska and its paleogeographic implications: Paleontology, v. 79, No. 5, p. 997-1001.

Gangloff, R.A., and Fiorillo, A.R., 2010, Taphonomy and paleoecology of a bonebed from the Prince Creek Formation, North Slope, Alaska, Palaios, v. 25, No. 5, p.

Garrity, C.P., Houseknecht, D.W., Bird, K.J., Potter, C.J., Moore, T.E., Nelson, P.H., and Schenk, C.J., 2005, U.S. Geological Survey 2005 oil and gas resource assessment of the central North Slope, Alaska: Play maps and results: U.S. Geological Survey Open-File Report 2005-1182, 29 p.

Gates, T.A., 2005, The Late Jurassic Cleveland-Lloyd Dinosaur Quarry as a Drought-Induced Assemblage: Palaios, v. 20, p. 363–375.

Hampton, M.A., 1975, Competence of fine-grained debris flows: Journal of Sedimentary Petrology, v. 45, No. 4, p. 834-844.

Hardy, D.R., 1996, Climatic influences on streamflow and sediment flux into Lake C2, northern Ellesmere Island, Canada: Journal of Paleolimnology, v. 16, p. 133-149.

Hessel, R., 2006, Consequences of hyperconcentrated flow for process-based soil erosion modeling on the Chinese Loess Plateau: Earth Surfaces Processes and Landforms, v. 31, p. 1100-1114.

Hodgkins, R., Cooper, R., Wadham, J., and Tranter, M., 2003, Suspended sediment fluxes in a high-Arctic glacierised catchment: implications for fluvial sediment storage: Sedimentary Geology, v. 162, No. 1-2, p. 105-117.

Hotton, N., 1980, An alternate to dinosaur endothermy; the happy wanderers, *in* Thomas, R.D.K., and Olson, E.C. eds., A Cold Look at the Warm-blooded Dinosaurs: American Association for the Advancement of Science Selected Symposia Series, No. 28, p. 311-350.

Hungr, O., Evans, S G., Bovis, M.J., and Hutchinson, J.N., 2001, A review of the classification of landslides of the flow type: Environmental and Engineering Geoscience, v. 7, No. 3, p. 221-238.

Jiongxin, X., 1993, Meanders caused by hyperconcentrated water flow: An example from the Loess Plateau, China: Earth Surface Processes and Landforms, v. 18, No. 8, p 687-702.

Jiongxin, X., 1999, Erosion caused by hyperconcentrated flow on the Loess Plateau of China: Catena, v. 36, p. 1-19.

Julien, P., Y., and O'Brien, 1997, Selected notes on debris flow dynamics, *in* Armanini, A., and Michiue, M., eds., Recent Developments on Debris Flows, Lecture Notes in Earth Sciences, Springer-Verlag, Berlin, p. 144-162.

Karátson, D., Orsolya, S., and Telbisz, T., 2002, Preferred clast orientation in volcaniclastic mass-flow deposits: Application of a new photo-statistical model: Journal of Sedimentary Research, v. 72, No. 6, p. 823-835.

Korth, W.W., 1979, Taphonomy of microvertebrate fossil assemblages: Annals of the Carnegie Museum, v. 48, p. 235–284.

Lanphere, M.A., and Dalrymple, G.B., 2000, First principles calibration of ^{38}Ar tracers: Implications for the ages of $^{40}Ar/^{39}Ar$ fluence monitors: United States Geological Survey Professional Paper 1621, 10 p.

Lauters, P., Bolotsky, Y.L., van Itterbeeck, J., and Godefroit, P., 2008, Taphonomy and age of a latest Cretaceous dinosaur bone bed in far eastern Russia: Palaios, v. 23, p. 153-162.

Layer, P.W., 2000, $^{40}Ar/^{39}Ar$ age of the El'gygytgyn impact event, Chukotka, Russia: Meteroitics and Planetary Science, v. 35, p. 591-599.

Layer, P.W., Hall, C.M., and York, D., 1987, the derivation of $^{40}Ar/^{39}Ar$ age spectra of single grains of hornblende and biotite by laser step heating: Geophysical Research Letters, v. 14, p. 757-760.

Lorenzini, G., and Mazza, N., 2004, Debris flow, phenomenology and rheological modeling, WIT Press, Southampton, UK, 202 p.

Major, J.J., and Pierson, T.C., 1992, Debris Flow Rheology: Experimental Analysis of Fine-Grained Slurries: Water Resources Research, v. 28, No. 3, p. 841-857.

McDougall, I., and Harrison, T.M., 1999, Geochronology and Thermochronology by the $^{40}Ar/^{39}Ar$ method: Second edition, Oxford University Press, New York, 269 p.

Molenaar, C.M., 1985, Subsurface correlations and depositional history of the Nanushuk Group and related strata, North Slope, Alaska, *in* Huffman, A.C., ed., Geology of the Nanushuk Group and Related Rocks, North Slope, Alaska: United States Geological Survey Bulletin 1614, p. 37-60.

Molenaar, C.M., Bird, K.J., and Kirk, A.R., 1987, Cretaceous and Tertiary stratigraphy of northeastern Alaska, *in* Tailleur, I. L., and Weimer, P., eds., Alaskan North Slope Geology: Society of Economic Paleontologists and Mineralogists, Pacific Section, Book 50, v. 1, p. 513–528.

Moore, T.E., Wallace, W.K., Bird, K.J., Karl, S.M., Mull, C.G., and Dillon, J.T., 1994, Geology of northern Alaska, *in* Plafker, G, and Berg, H. C., eds., The Geology of Alaska: Geological Society of America, The Geology of North America, Boulder, Colorado, v. G-1, p. 49-140.

Mull, C.G., 1985, Cretaceous tectonics, depositional cycles, and the Nanushuk Group, Brooks Range and Arctic Slope, Alaska, *in* Huffman, A.C. Jr., ed., Geology of the Nanushuk Group and related rocks, North Slope, Alaska: United States Geological Survey Bulletin 1614, p. 7-36.

Mull, C.G., Houseknecht, D.W., and Bird, K.J., 2003, Revised Cretaceous and Tertiary stratigraphic nomenclature in the Colville Basin, northern Alaska: United States Geological Survey Professional Paper 1673, p. 1-51.

Myers, T.S., and Storrs, G.W., 2007, Taphonomy of the Mother's Day Quarry, Upper Jurassic Morrison Formation, south central Montana, USA: Palaios, v. 22, p. 651-666.

Nordt, L., Atchley, S., and Dworkin, S., 2003, Terrestrial evidence for two greenhouse events in the latest Cretaceous: GSA Today, v. 13, No. 12, p. 4-9.

O'Brien, J.S. and Julien, P.Y., 1988, Laboratory analysis of mud flow properties: Journal of Hydrologic Engineering, v. 114, No. 8, p 877-887.

Officer, C.B., 1992, The relevance of iridium and microscopic dynamic deformation features toward understanding the Cretaceous/Tertiary transition: Terra Nova, v. 4, p. 394-404.

Parrish, J.M., Parrish, J.T., Hutchison, J.H., and Spicer, R.A., 1987, Late Cretaceous vertebrate fossils from the North Slope of Alaska and implications for dinosaur ecology: Palaios, v. 2, p. 377-389.

Parrish, J.T., and Spicer, R.A., 1988, Late Cretaceous terrestrial vegetation: A near-Polar temperature curve: Geology, v. 16, p. 22-25.

Pavelsky, T.M., and Smith, L.C., 2004, Spatial and temporal patterns in Arctic river ice breakup observed with MODIS and AVHRR time series: Remote Sensing of Environment, v. 93, p. 328–338.

Phillips, R.L., 2003, Depositional environments and processes in Upper Cretaceous nonmarine and marine sediments, Ocean Point dinosaur locality, North Slope, Alaska: Cretaceous Research, v. 24, p. 499-523.

Pierson, C.T., 1981, Dominant particle support mechanisms in debris flows at Mt Thomas, New Zealand, and implications for flow mobility: Sedimentology, v. 28, p. 49-60.

Pierson, C.T., 2005, Hyperconcentrated flow – transitional processes between water flow and debris flow, *in* Jakob, M., and Hungr, O. eds., Debris-flow Hazards and Related Phenomenon: Springer-Verlag, Berlin, p. 159-202.

Pierson, T.C., and Costa, J.E., 1987, A rheologic classification of subaerial sediment-water flows: *in* Costa, J. E., and Wieczorek, G. F., eds., Debris Flows/avalanches: Process, Recognition, and Mitigation: Geological Society of America, Reviews in Engineering Geology, v. 7, p. 1-12.

Pope, K.O., Baines, K.H., Ocampo, A.C., and Ivanov, B.A., 1994, Impact winter and the Cretaceous/Tertiary extinctions: Results of a Chicxulub asteroid impact model: Earth and Planetary Science Letters 128, p. 719-725.

Rich, T.H., Gangloff, R.A., and Hammer, W.H., 2002, Polar Dinosaurs: Science, v. 295, p. 979-980.

Roehler, H.W., 1987, Depositional environments of the coal-bearing and associated formations of Cretaceous age in the National Petroleum Reserve in Alaska: United States Geological Society Bulletin 1575, 16 p.

Rogers, R.R., 2005, Fine-grained debris flows and extraordinary vertebrate burials in the Late Cretaceous of Madagascar: Geology, v. 33, No. 4, p. 297-300.

Rogers, R.R., Eberth, D.A., and Fiorillo, A.R., 2007, Bonebeds, Genesis, Analysis, and Paleobiological Significance: The University of Chicago Press, Chicago, IL, 512 p.

Russell, D.A. 1993, The role of central Asia in dinosaurian biogeography: Canadian Journal of Earth Sciences, v. 30, p. 2002–2012.

Ryan, M.J., Russell, A.P., Eberth, D.A., and Currie, P.J., 2001. The Taphonomy of a *Centrosaurus* (Ornithischia: Certopsidae) Bone Bed from the Dinosaur Park Formation (Upper Campanian), Alberta, Canada, with Comments on Cranial Ontogeny: Palaios, v. 16, p. 482-506.

Samson, S.D., and Alexander, E.C., 1987, Calibration of the interlaboratory $^{40}Ar/^{39}Ar$ dating standard, MMhb1: Chemical Geology, v. 66, p. 27-34.

Sereno, P.C., 2000, The fossil record, systematics and evolution of pachycephalosaurs and ceratopsians from Asia, *in* Benton, M.J., Shishkin, M.A., Unwin, D.M., and Kurochkin, E.N., eds., The age of dinosaurs in Russia and Mongolia: Cambridge, U.K., Cambridge University Press, p. 480-516.

Smith, G.A., 1986, Coarse-grained nonmarine volcaniclastic sediment: Terminology and depositional processes: Geological Society of America Bulletin, v. 97, p. 1-10.

Smith, R.M.H., 1993, Vertebrate Taphonomy of Late Permian floodplain deposits in the southwestern Karoo basin of South Africa: Palaios, v. 8, p. 45-67.

Sohn, T.K., Rhee, C.W., and Bok, C.K., 1999, Debris flow and hyperconcentrated flood-flow deposits in an alluvial fan, northwestern part of the Cretaceous Yongdong Basin, Central Korea. Journal of Geology, v. 107, p. 111-132.

Spicer, R.A., 2003, Changing climate and biota, *in* Skelton, P., ed., The Cretaceous World: Cambridge, U.K., Cambridge University Press, p. 85-162.

Spicer, R.A., and Parrish, J.T., 1987, Plant megafossils, vertebrate remains, and paleoclimate of the Kogosukruk Tongue (Late Cretaceous), North Slope, Alaska: U. S. Geological Survey Circular, Report: C 0998, p. 47-48.

Spicer, R.A., and Parrish, J., 1990, Late Cretaceous-early Tertiary paleoclimates of northern high latitudes: a quantitative view: Journal of the Geological Society, London, v. 147, No. 6, p. 329-341.

Spicer, R.A., and Herman, A.B., 2010, the Late Cretaceous environment of the Arctic: A quantitative reassessment based on plant fossils: Palaeogeography, Palaeoclimatology, Palaeoecology, doi: 10.1016/j.palaeo.2010.02.025.

Spicer, R.A., Parrish, J.T., and Grant, P.R., 1992, Evolution of vegetation and coal-forming environments in the Late Cretaceous of the North Slope of Alaska, *in* McCabe, P.J., and Parrish, J.T., eds., Controls on the Distribution and Quality of Cretaceous Coals: Geological Society of America Special Paper 267, p. 177-192.

Steiger, R.H., and Jaeger, E., 1977, Subcommission on geochronology: Convention in the use of decay constants in geo and chosmochronology: Earth and Planetary Science Letters, v. 36, p. 359-362.

Suarez, M.B., Suarez, C.A., Kirkland, J.I., González, L.A., Grandstaff, D.E., and Terry, D.O. Jr., 2007, Sedimentology, stratigraphy, and depositional environment of the Crystal Geyser Dinosaur Quarry, east-central Utah: Palaios, v. 22, p. 513-527.

Tomsich, C.S., McCarthy, P.J., Fowell, S.J., and Sunderlin, D., 2010, Paleofloristic and paleoenvironmental information from a late Cretaceous (Maastrichtian) flora of the lower Cantwell Formation near Sable Mountain, Denali National Park, Alaska: Palaeogeography, Palaeoclimatology, Palaeoecology, doi: 10.1016/j.palaeo.2010.02.023.

Trueman, C.N., 1999, Rare Earth Element Geochemistry and Taphonomy of Terrestrial Vertebrate Assemblages: Palaios, v. 14, p. 555-568.

Varnes, D.J., 1978, Slope movement types and processes, *in* Schuster, R.L., and Krizek, R.J., eds., Landslides: Analysis and control: Transportation Board Special Report 176, National Academy of Sciences, Washington, D. C., p. 11-33.

Wentworth, C.K., 1922, A scale of grade and class terms for clastic sediments: Journal of Geology, v. 30, No. 5 p. 377–392.

Witte, K.W., Stone, D.B., and Mull, C.G., 1987, Paleomagnetism, paleobotany, and paleogeography of the Cretaceous, North Slope, Alaska, *in* Tailleur, I., and Weimer, P., eds., Alaska North Slope Geology: The Pacific Section, Society of Economic Paleontologists and Mineralogists and the Alaska Geological Society, v. 1, p. 571-579.

Wood, J.M., Thomas, R.G., and Visser, J., 1988, Fluvial processes and vertebrate taphonomy: the upper Cretaceous Judith River Formation, south-central Dinosaur Provincial Park, Alberta, Canada: Palaeogeography, Palaeoclimatology, Palaeoecology, v. 66, p. 127-143.

York, D., Hall, C.M., Yanse, Y., Hanes, J.A., and Kenyon, W.J., 1981, $^{40}Ar/^{39}Ar$ dating of terrestrial minerals with a continuous laser: Geophysical Research Letters, v. 8, p. 1136-1138.

Zaleha, M.J., and Wiesemann, S.A., 2005, Hyperconcentrated flows and gastroliths: sedimentology of diamictites and wackes of the Upper Cloverly formation, Lower Cretaceous, Wyoming, U.S.A.: Journal of Sedimentary Research, v. 75, No. 1, p. 43-54.

Zakharov, Y.D., Boriskina, N.G., Ignatyev, A.V., Tanabe, K., Shigeta, Y., Popov, A.M., Afanasyeva, T.B., and Maeda, H., 1999, Paleotemperature curve for the Late Cretaceous of the northwestern circum-Pacific: Cretaceous Research, v. 20, p. 685-697.

Chapter 5 Conclusions

(1) The Late Cretaceous (Early Maastrichtian) Prince Creek Formation in the Colville River Region is an alluvial succession on a coastal plain containing erosionally-based, fining-upward successions interpreted as (1) large, sinuous first-order meandering trunk channels; (2) small, sinuous second-order meandering distributary channels; and (3) small, low sinuosity third-order fixed (anastomosed?) distributary channels. Finer-grained, non-channelized interbedded sandstone, siltstone, and mudstone were deposited on organic-rich floodplains.

(2) Larger trunk channels are regionally-restricted, are the thickest channel deposits, contain the largest sediment sizes/clasts and exhibit physical sedimentary structures indicative of the highest flow velocities. IHS in these channels indicates lateral accretion of channels.

(3) Smaller meandering distributaries are thinner, lack conglomerates, and are composed predominantly of IHS with thick mud drapes. Mud-filled abandoned channels are commonly associated with these channels.

(4) Fixed anastomosed(?) distributaries are the thinnest channel deposits, are composed predominantly of ripple cross-laminated sandstone, lack prominent his except at the very top of fining-upward successions, and are filled primarily by vertical as opposed to lateral accretion. Both types of smaller distributaries contain carbonaceous root-traces throughout the channel–fill succession while larger trunk channels lack roots.

(5) Thinner, non-channelized sheet sandbodies are interpreted as deposits of small-scale crevasse splays and levees. Organic siltstone, organic mudstone, carbonaceous shale, coal, bentonite, and tuff are interpreted as deposits of lakes formed after channel abandonment, smaller lakes, ponds, swamps, paleosols, and ashfall deposits. Trampling of fine-grained floodplain sediments by dinosaurs is common.

(6) Meandering distributaries appear lenticular along strike, erode into pre-existing distributary deposits, and interfinger with and incise into floodplain facies. Fixed (anastomosed?) distributaries either incise into meandering distributary deposits or into organic-rich floodplain facies. Multiple fixed (anastomosed?) distributaries may be preserved in tiers at the same stratigraphic level.

(7) Spatial relationships between channels and floodplain facies indicate that the bulk of deposition occurred on crevasse splay-complexes

adjacent to trunk channels. Splay-complexes were constructed by the lateral migration of meandering distributaries and the vertical filling of anastomosed distributaries. Flow within meandering and fixed (anastomosed?) distributaries may have been contemporaneous or, alternatively, fluctuating discharge through the main crevasse channel and peat compaction may have controlled the type of system occupying the splay-complex.

(8) IHS is found at some stratigraphic level within all three orders of channels. Thick mud drapes on point bars and rhythmically-repeating coarse-to fine-grained couplets in the IHS suggest that flow within all channels was likely influenced by tidal effects.

(9) A multifaceted approach to paleosol analysis including field observations, soil micromorphology, geochemistry, and biological analyses can provide unparalleled detail when reconstructing ancient paleoenvironments from paleosol profiles.

(10) Paleosols of the Prince Creek Fm. formed as vertically stacked successions that alternate with overbank alluvium, or are truncated by distributary channels on crevasse splay complexes or individual channels on floodplains.

(11) Weakly-developed cumulative to compound paleosols similar to modern aquic subgroups of *Entisols*, *Inceptisols*, and potential acid

sulfate soils formed on a low-lying, muddy, frequently-wet coastal plain on levees, point bars, crevasse splays, and on the margins of floodplain lakes and swamps.

(12) Soil profiles experienced repeated alluviation from overbank flooding of distributary channels. Evidence for this includes thin layers of silt and sand dispersed throughout paleosol profiles, common pedorelicts and papules, and fluctuations with depth in the molecular ratios of Ti/Zr, Ba/Sr, Fe/Al, Al/Si, and Al/(Na+K+Ca+Mg). Overbank floods also introduced additional iron into some soil profiles.

(13) Macroscopic and micromorphological features in paleosols suggesting water-saturated, anoxic conditions include drab colors, carbonaceous organic material including carbonaceous root-traces, siderite, depletion coatings on ped surfaces, and zoned peds. In contrast, Fe-rich mottled soil aggregates, ferruginous and manganiferous nodules, ferruginous void and grain coatings, ferruginous void infillings, burrows, and rare illuvial clay coatings and clay infillings suggest oxidizing conditions and drying out of some soils. Repeated wetting and drying in paleosol profiles is likely tied to fluctuating discharge resulting from seasonal variations in light, temperature, and precipitation due to the high-paleolatitude of Alaska in the Late Cretaceous.

(14) Marine influence on sedimentation and pedogenesis is evidenced by jarosite mottles, jarosite halos surrounding rhizoliths, microscopic pyrite, and euhedral gypsum which become increasingly evident to the north in stratigraphically higher strata of the Prince Creek Fm. near the contact with the overlying shallow-marine Schrader Bluff Fm.

(15) The biota of the Prince Creek Fm. includes Peridinioid dinocysts; brackish and freshwater algae; projectate pollen; age diagnostic *Wodehouseia edmontonicola*; pollen from lowland trees, shrubs and herbs; *Bisaccate* pollen; fern and moss spores; and fungal hyphae. The overall assemblage indicates that all strata in the study area are Early Maastrichtian and that sediments become progressively younger from measured section NKT in the south to measured section LBB in the north.

(16) Biota adjacent to swamps included algae (*Pediastrum, Botryococcus braunii, Leiospheres*), angiosperms (*Aquilapollenites quadrilobus, Aquilapollenites scabridus*) and ferns (*Psilatriletes*). Lakes were covered in algae (*Pediastrum, Pterospermella*) with lowland trees (*Taxodiaceaepollenites*) on their margins. Point bars supported thriving fern communities (*Laevigatosporites*). Biota on splays included fungi (*fungal hyphae*) ferns (*Laevigatosporites*), lowland trees (*Taxodiaceaepollenites*), and algae (*Sigmapollis psilatus*).

Levees sustained communities of herbaceous shrubs and ferns. Pollen from hinterland conifers (*bisaccate)* and older, reworked Peridinioid dinocysts were incorporated into levees, crevasse splays, and point bars by channels. The most distal areas of the coastal plain supported rich and varied biota that included algae (*Botryococcus braunii*, *Pediastrum*, *Sigmapollis psilatus)*, ferns (*Laevigatosporites*) and lowland trees (*Taxodiaceaepollenites*). *Bisaccate* pollen and reworked Peridinioid dinocysts were brought to the distal coastal plain by distributary channels and were incorporated into soils during pedogenesis along with *in situ* Peridinioid dinocysts from marine waters.

(17) The integration of pollen/biota analyses with paleopedology can provide clues to regional biomass, paleo-topography, clastic input from channels (e.g. influx of hinterland pollen and reworked pollen and Peridinioid dinocysts), and the location of pedogenesis relative to the paleo-coastline.

(18) Dinosaurs of the Prince Creek Fm. are found in several world-class, high-density bonebeds encased in muddy alluvium. The bulk of dinosaur bone is found outside of channels in laterally extensive, fine-grained overbank deposits overlying floodplain facies. No large concentration of bone is found in channels. The Liscomb/Byers and

Sling Point bonebeds are laterally extensive except where bonebed horizons transition into distributary channel facies.

(19) The Sling Point Bonebed was deposited above a mud-filled abandoned channel on the floodplain. Dinosaur bone is absent in a laterally equivalent horizons to the north because a distributary channel occupies that location within the bluffs. A previously unknown concentration of bone was discovered in bluffs along the Colville River in the Sling Point outcrop belt that is laterally equivalent to facies near the base of the outcrop belt to the northwest. $^{40}Ar/^{39}Ar$ analysis of a tuff directly below the bone accumulation returned an integrated age of 68.9 ± 0.4 Ma and a plateau age of 69.2 ± 0.5 Ma

(20) The Byers bonebed is a separate, unique, stratigraphically higher and younger deposit than the Liscomb bonebed horizon. The Liscomb bonebed horizon descends into the subsurface near the middle of the Liscomb/Byers outcrop belt.

(21) In all three bonebeds (Sling Pont, Liscomb, Byers) alluvium encasing dinosaur bone exhibits a bipartite division of flow and a massive mudstone facies that suggest deposition by fine-grained hyperconcentrated flows. Siltstone consistently fines-upward into a distinctive mudstone lacking sedimentary structures but containing rare dinosaur bone and flow-parallel oriented plant fragments that

appear to "float" in a matrix of mud. Fining-upward successions suggestive of streamflow underlie sheared mudstone facies similar to debris flow deposits. Together these facies form a depositional couplet in a single event-bed that exhibits a facies succession expected for two-phase hyperconcentrated flow.

(22) Exceptional floods, likely driven by seasonal snowmelt in the ancestral Brooks Range, entrained abundant fine-grained sediments stored on muddy point bars and on floodplains, increasing suspended sediment concentrations and generating hyperconcentrated overbank flows that killed and buried scores of juvenile dinosaurs occupying this high-latitude coastal plain. This unique killing mechanism for these polar dinosaurs likely resulted from seasonally fluctuating discharge brought about by the near polar latitude (82-85°N) of northern Alaska in the Late Cretaceous.

(23) Compared to northern Alaska today, the Late Cretaceous coastal plain was warmer, wetter, and shows no evidence of snow or ice. The region supported diverse vegetation, including ferns, shrubs, angiosperms and swamp cypress. Herds of dinosaurs including *Hadrosaurs* and *Pachyrhinosaurs* occupied the region

(24) Tides affected sedimentation in both trunk channels and distributaries. Ash repeatedly fell on the coastal plain. Seasonality at high paleo-

latitudes produced flashy, possibly ephemeral rivers with discharge linked to melting snow and ice at higher elevations. Soil experienced repeated episodes of wetting and drying and soil formation was constantly interrupted by sediment influx from flooding of channels. The coastal plain could be a dangerous place for dinosaurs as viscous, muddy floodwaters eroded riverbanks, overtopped levees and buried herds of dinosaurs close to where they lived.

Chapter 6 Future Work

Considering the remote location of Alaska's North Slope, and the relatively few individuals who have studied the area in detail, much work remains to be done on the Prince Creek Formation (Fm.) and other Cretaceous and Tertiary continental and shoreface successions. Some suggestions for future work include:

- A Fourier analysis should be performed on the rhythmically-repeating tidal signature within the inclined heterolithic stratification of Prince Creek Fm. channel sandbodies. This Fourier analysis could potentially reveal the frequency of the tidal signal preserved in the channels, exposing the driving mechanism(s) behind the signal. The frequency of the signal in the Prince Creek Fm. should be compared to similar signals found within IHS in other coastal plain/deltaic successions along the Cretaceous Western Interior Seaway. This comparison will aid in our understanding of the frequency and magnitude of Cretaceous tides in the Seaway and could reveal variations in the signal with latitude and between basins.

- The base of the Prince Creek Fm. along the Colville River near the confluence of the Colville, Anaktuvuk, and Chandler Rivers is composed of fluvial sandstone

and conglomerate interpreted as the deposits of braided streams (Mull et al. 2003; Flores et al. 2007b). All channels encountered in this investigation are interpreted as meandering or fixed (anastomosed?). This change in morphology up-section from braided systems at the base of the Prince Creek Fm. to meandering and fixed (anastomosed?) in the bulk of the Prince Creek Fm. along the Colville River should be further investigated and tied to tectonism, sediment supply, sea level fluctuations or other mechanisms.

- Although not discussed in this study due to insufficient data, a change in sandstone composition from quartz and chert rich sandstones to lithic rich sandstones was noted in the uppermost strata of the Prince Creek Fm. near the contact with the overlying shallow marine Schrader Bluff Formation near Ocean Point. Changing sandstone composition between the two formations should be further investigated in a provenance analysis with the goal of identifying the relationship between large-scale facies changes and shifting provenance. Additional paleocurrent orientations should be recorded from all Prince Creek Fm. outcrops encountered for comparison with data from this study. Additional paleoflow orientations should be recorded from the Schrader Bluff Fm

- A detailed survey of Prince Creek Fm. and Schrader Bluff Fm. ichnofacies would provide details on the characteristics and habitats of high latitude fauna found in these formations. A study that focused on the transition zone between these

formations could provide valuable insight into salinity variations with distance from the paleo-shoreline.

- Most coals encountered in the course of this study were thin and of poor quality. Potentially thicker coals were observed just outside of the study area to the west. An investigation of coal quality and coal thickness at more proximal locations further from the paleo shoreline is warranted. The high-latitude Prince Creek Fm. may prove to be an ideal laboratory for studying the relationship between coal quality and distance from the paleo-shoreline on a coastal plain. Paleosols found at more proximal locations should also be compared to those investigated here.

- A LiDAR survey of the Prince Creek Formation along the Colville River would help to quantify sandbody geometries in outcrops that are inaccessible. This LiDAR survey would also enhance surface to subsurface correlations in the region and help to produce a more precise 3-D subsurface model for petroleum exploration of the West Sak and Ugnu formations.

- Coals and lake deposits are thicker in the Paleocene Prince Creek formation (Coals > 5 m-thick, lacustrine deposits > 20 m thick). A comparison of the facies, petrography, and stacking pattern between the Cretaceous Prince Creek Formation along the Colville River with the Paleocene Prince Creek Fm. and Sagwon

member of the Sagavanirktok Fm. along the Toolik, Sagavanirktok, and Canning Rivers would provide insight into transforming basin geometries from the Cretaceous into the Tertiary.

- A similar comparison between the Cretaceous Prince Creek Formation and the continental facies of the Nanushuk Fm., and between the Schrader Bluff Formation and the shoreface deposits of the Nanushuk Fm. could provide additional insight into the dynamics of an evolving Cretaceous basin.

- A paleopedological analysis coupled with a biofacies analysis similar to the study in Chapter 3 should be applied to the Paleocene Prince Creek Fm. and the Nanushuk Fm. Inconsistencies in paleoenvironmental interpretations between the three data sets should be investigated to reveal changes in parent material, climate, accommodation, organisms, and sea level over time.

- The discovery of additional accumulation of bone in the Prince Creek Fm appears likely. Every opportunity should be taken to identify the frequency and extent of bonebed deposition.

- A centimeter-scale, high-resolution study of the hyperconcentrated flow deposits at the Liscomb, Byers, Sling Point, and Kikak-Tegoseak bonebeds would provide a more detailed model for recognition of muddy hyperconcentrated flows in ancient sediments and would provide paleontologists with a test for this previously unrecognized killing mechanism.

- Evidence for hyperpycnal fluid muds in prodeltaic settings and hyperpycnal flows in shelf facies "coeval" to hyperconcentrated flows on the Prince Creek coastal plain should be sought out to test our model of hyperconcentrated flows generated by extreme discharge events, as these fluid muds and hyperpycnites could be distal facies equivalents generated by the same processes.

REFERENCES

Flores, R.M., Myers, M.D., Houseknecht, D.W., Stricker, G.D., Brizzolara, D.W., Ryherd, T.J., and Takahashi, K.I., 2007b, Stratigraphy and facies of Cretaceous Schrader Bluff and Prince Creek Formations in Colville River Bluffs, North Slope, Alaska: United States Geological Survey Professional Paper 1748, 52 p.

Mull, C.G., Houseknecht, D.W., and Bird, K.J., 2003, Revised Cretaceous and Tertiary stratigraphic nomenclature in the Colville Basin, northern Alaska: United States Geological Survey Professional Paper 1673, p. 1-51.